

***IN SILICO* DRUG DESIGN AND CHARACTERIZATION OF SELECTED ACTIVE  
COMPOUNDS FROM *Sapium* AND *Salvia* GENUS AS ANTI-CANCER AGENTS  
USING MOLECULAR DOCKING AND MOLECULAR DYNAMICS SIMULATIONS**

**OUMA RUSSELL BEN OMONDI**

**A Research Thesis Submitted to the Graduate School in Partial Fulfilment for the  
Requirements for the Award of the Degree of Doctor of Philosophy in Chemistry of  
Egerton University**

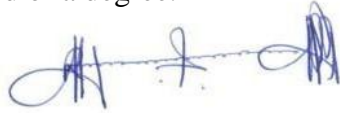
**EGERTON UNIVERSITY**

**OCTOBER 2025**

## DECLARATION AND RECOMMENDATION

### Declaration

This thesis is my original work and has not been presented in this University or any other for the award of a degree.



Signature..... Date...05/10/2025.....

Ouma Russell Ben Omondi

SD11/18507/17

### Recommendation

This thesis has been submitted for examination with our approval as university supervisors.



Signature... Date...06/10/2025.....

Prof. Mwaniki Silas Ngari, PhD

Department of Chemistry

Egerton University



Signature... Date...06/10/2025.....

Prof. Joshua K. Kibet, PhD

Department of Chemistry

Egerton University

## **COPYRIGHT**

© 2025, Ouma Russell Ben Omondi

All rights are reserved. No part of this thesis or information herein may be reproduced, scanned, photocopied, stored in a retrievable system or transmitted in any form without the permission of Egerton University on behalf of the author.

## **DEDICATION**

This thesis is dedicated to my parents, Apollo Ouma and Eunice Ouma, my mother-in-law, Anne Ntwiki, my uncle Willis Adero, his wife Consolata Otieno and their children. The thesis is also dedicated to my wife, Grace and children Davis, Tariya, Raymond and Edith.

## **ACKNOWLEDGEMENTS**

First and foremost, I thank the Lord God Almighty for his care, provision and protection throughout my studies. Secondly, I am grateful to my supervisors, Prof Joshua K. Kibet and Prof. Mwaniki Silas Ngari, for their guidance, encouragement, and positive constructive criticism on my work. I highly appreciate the financial support received from HELB and friends toward financing my studies. I also acknowledge the support offered to me by my employer, Mount Kenya University, and colleagues, especially the Chairman of the BOD, Prof. Simon Gicharu, for sponsoring me with a state-of-the-art laptop and positive encouragement from Dr Nahashon Mwirigi, PhD, my then immediate supervisor at work. Lastly, I want to acknowledge my colleagues and fellow students: Benjamin Korir, Samuel Kirkok (PhD), Njema, Eric Akimenti (PhD), Festus, and other colleagues abroad in Pakistan, India, South Africa, and Bangladesh, who contributed immensely toward the success of this work.

## ABSTRACT

Extensive research projects have been performed to better understand the genetic landscape and tumour development of localized and metastatic breast cancer (BC) and prostate cancer (Pca). In this study, computational studies and *in vitro* analysis were conducted before *in vivo* analysis to provide predictive insights into potential mechanisms and mitigate risks and hazards associated with animal experiments. Through molecular dynamics, ligand binding within the binding pocket of a ligand-protein was investigated using parameters such as root mean square deviation (RMSD) and root mean-square fluctuation (RMSF), along with molecular dynamics simulations that tracked ligand-receptor interactions over a 200-nanosecond (ns) simulation trajectory. This study presents studies of a far less explored ellagic acid (EA), [20-<sup>3</sup>H] phorbol-12, 13-dibutyrate ([<sup>3</sup>H] PDBu), and [20-<sup>3</sup>H]-12-deoxyphorbol-13-isobutyrate ([<sup>3</sup>H] DPB) key metabolites from the genus *Sapium* and compares with the widely studied salvianolic acid B (Sal B) from *Salvia*. The molecular interactions of these compounds with the proteins were determined using molecular docking and molecular dynamics simulation. The molecular dynamics simulations revealed that salvianolic acid B exhibited binding affinities of -38.49 kJ/mol, -28.87 kJ/mol, and -33.05 kJ/mol when targeting DNA lyase, topoisomerase II alpha, and mTOR, respectively. These docking scores were comparable to those of EA, exhibiting a binding affinity of -36.40 kJ/mol, -27.20 kJ/mol, and -31.80 kJ/mol when targeting DNA lyase, topoisomerase II alpha, and mTOR, respectively. Based on this, Sal B showed greater negative binding affinity indicating kinetically stable ligand-protein interactions. The dominance of the ligand- protein interactions indicate the significance of synergies such as the electrostatic interactions, Van der Waals forces and hydrogen bonds. Sal B had docking scores of - 46.86 kJ/mol and -27.24 kJ/mol respectively when docking NUDT5 and androgen receptor (AR). The findings of the molecular dynamics simulation also showed that the interaction of Sal B-protein had a stable RMSD with an average of 1.5- 2.0 Angstroms (Å). These *in-silico* results are indicative of biologic potential of Sal B as an anticancer agent. Evaluation of the RMSD values indicated that there were structural changes with time before reaching a plateau. This indicated a fixed ligand binding site. The RMSF plot also provided information regarding the flexibility of the protein residues. In the studied ligand-receptor complexes, the RMSF values fluctuation did not exceed 2 Å, showing that the protein residues remained relatively rigid.

## TABLE OF CONTENTS

<b>COPYRIGHT</b> .....	<b>iii</b>
<b>DEDICATION</b> .....	<b>iv</b>
<b>ACKNOWLEDGEMENTS</b> .....	<b>v</b>
<b>ABSTRACT</b> .....	<b>vi</b>
<b>LIST OF FIGURES</b> .....	<b>xi</b>
<b>LIST OF TABLES</b> .....	<b>xiv</b>
<b>LIST OF ABBREVIATIONS AND ACRONYMS</b> .....	<b>i</b>
<b>CHAPTER ONE</b> .....	<b>1</b>
<b>INTRODUCTION</b> .....	<b>1</b>
1.1 Background information .....	1
1.2 Statement of the problem .....	5
1.3 Objectives.....	5
1.3.1 General objective .....	5
1.3.2 Specific objectives .....	6
1.4 Research questions .....	6
1.5 Justification .....	6
<b>CHAPTER TWO</b> .....	<b>8</b>
<b>LITERATURE REVIEW</b> .....	<b>8</b>
<b>A REVIEW OF THE CURRENT TRENDS IN COMPUTATIONAL APPROACHES IN DRUG DESIGN AND METABOLISM</b> .....	<b>8</b>
2.1 Introduction .....	9
2.2 Methodology .....	14
2.2.1 Systematic approach to data synthesis.....	16
2.3 Breast cancer and prostate cancer overview, potential treatments, and perspectives ....	16
2.3.1 Prostate cancer diagnosis and treatment .....	16
2.3.2 Current therapies deployed in localized and systemic BC .....	17
2.3.3 Limitations of the current treatment options for BC and PCa.....	19
2.3.4 The potential of natural plant extracts for BC and PCa treatment.....	19
2.4 Fundamentals of drug discovery and development using computational tools and software .....	21
2.4.1 <i>In Silico</i> approaches in pre-clinical drug design.....	22
2.4.2 Applications of molecular dynamics in drug design .....	23

2.4.3 Application of molecular docking in drug design .....	26
2.4.4 Docking algorithms .....	30
2.5 Hybrid quantum mechanical/molecular mechanics in drug design .....	36
2.5.1 Subtractive and additive QM/MM coupling.....	38
2.6 Drug metabolism predictions for drug design.....	39
2.6.1 The role of machine learning algorithms in drug metabolism prediction .....	41
2.7 Case example of drug pharmacokinetics with cancer cells.....	42
2.8 The accuracy of DFT in drug design.....	44
2.8.1 Deficiencies of computational methods in pre-clinical drug design .....	46
2.9 Use of artificial intelligence in drug design .....	48
2.9.1 Limitations of the AI approach in pre-clinical drug research.....	51
2.10 Conclusions and outlook .....	51
<b>CHAPTER THREE.....</b>	<b>53</b>
<b>COMPUTATIONAL SIMULATION OF THE BIOACTIVITY OF SELECTED</b>	
<b>COMPOUNDS DERIVED FROM <i>SAPIUM</i> AND <i>SALVIA</i> GENUS AS ANTI-CANCER</b>	
<b>AGENTS .....</b>	<b>53</b>
Abstract .....	53
3.1 Introduction .....	53
3.2 Materials and methods .....	57
3.2.1 Molecular docking studies.....	57
3.2.2 <i>In vitro</i> enzyme inhibition analysis .....	59
3.2.3 <i>In vitro</i> anti-cancer activity on cell lines .....	61
3.3. Results and discussions .....	62
3.3.1 Molecular docking studies of DNA lyase.....	62
3.3.2 Molecular docking studies on topoisomerase II alpha .....	67
3.3.3 Molecular docking studies on serine-threonine kinase mTOR .....	69
3.3.4 Docking validation protocol .....	71
3.4 Chemical descriptors .....	74
3.4.1 <i>In vitro</i> enzyme inhibition assay.....	75
3.4.2 <i>In vitro</i> anti-cancer assay .....	78
3.5 Conclusions .....	83
<b>CHAPTER FOUR.....</b>	<b>84</b>

<b>EXPERIMENTAL AND THEORETICAL ASSESSMENT OF SALVIANOLIC ACID B, ELLAGIC ACID, AND PHORBOL ESTERS AS DRUG CANDIDATES AGAINST BREAST AND PROSTATE CANCER .....</b>	<b>84</b>
Abstract .....	84
4.1 Introduction .....	84
4.2 Methodology .....	88
4.2.1 Molecular dynamics simulations .....	88
4.2.2 Properties of drugs and ADMET .....	90
4.2.3 Statistical analysis.....	91
4.3 Results and discussions .....	91
4.3.1 Assessment of drug-likeness and ADME investigation .....	91
4.3.2 Excretion and toxicity profiles .....	94
4.3.3 Bioavailability radar and boiled egg models .....	96
4.3.4 Molecular dynamics simulation.....	99
4.3.5 Statistical analysis.....	107
4.4 Conclusions .....	110
<b>CHAPTER FIVE .....</b>	<b>112</b>
<b><i>IN-SILICO</i> STUDIES OF MOLECULAR PROPERTIES AND BIOACTIVITY OF POTENTIAL DRUG LEADS USING MOLINSPIRATION AND AUTODOCK VINA SOFTWARE: UNVEILING THE COMPETENCY OF BIOACTIVE COMPOUNDS FROM THE GENUS <i>SALVIA</i> AND <i>SAPIUM</i> .....</b>	<b>112</b>
Abstract .....	112
5.1 Introduction .....	113
5.2 Methodology and methods.....	116
5.2.1 Crystalline structures of compounds using molinspiration software.....	116
5.2.2 Protein and ligand preparation.....	116
5.2.3 Cavity detection and docking .....	117
5.2.4 Filtering and selection of optimal complexes.....	118
5.2.5 Visualizations .....	118
5.2.6 Molecular dynamics simulations .....	119
5.2.7 Trajectory analysis and post-simulation assessment .....	119
5.3 Results and discussions.....	120
5.3.1 3D Modelling of target protein .....	120

5.3.2 Assessment of drug likeness.....	121
5.3.3 Bioactivity scores of the lead compounds .....	122
5.3.4 Docking and molecular dynamics.....	122
5.4 Conclusions .....	133
<b>CHAPTER SIX .....</b>	<b>134</b>
<b>SUMMARY, CONCLUSIONS AND RECOMMENDATIONS .....</b>	<b>134</b>
6.1 General discussion.....	134
6.1.1 Rationale of the study .....	134
6.1.2 Findings of the study .....	135
6.2 Conclusions .....	136
6.3 Recommendations .....	137
<b>REFERENCES.....</b>	<b>139</b>
<b>APPENDICES.....</b>	<b>195</b>
<b>Appendix A:</b> Copyright of paper published in the journal of discover public health .....	195
<b>Appendix B:</b> Abstract of paper published in the journal of discover public health.....	196
<b>Appendix C:</b> Supplementary information on excretion and toxicity profile of EA.....	197
<b>Appendix D:</b> Supplementary information on excretion and toxicity profile of phorbol dibutyrate.....	198
<b>Appendix E:</b> Supplementary information on excretion and toxicity profile of 12 deoxy-phorbol 13-isobutyrate .....	199
<b>Appendix F:</b> Supplementary information on one-way ANOVA on $\log_{10}(\text{IC}_{50})$ within each cell line and Dunnett vs control.....	200
<b>Appendix G:</b> Supplementary information on selected Tukey all-pairs comparisons among test compounds (p-adj) .....	201
<b>Appendix H:</b> NACOSTI Research permit .....	202
<b>Appendix I:</b> Certificate of training in drug design and molecular docking .....	203

## LIST OF FIGURES

<b>Figure 2.1:</b> Drug discovery process and identification using various computational methods .....	12
<b>Figure 2.2:</b> The computation resources used in predicting molecules with potential therapeutic effects.....	13
<b>Figure 2.3:</b> Schematic representation of molecular dynamics simulations.....	24
<b>Figure 2.4:</b> Active site determination of 3D-receptors, protein-ligand docking simulation (blind and site-specific docking), and analysis of docking complex.....	27
<b>Figure 2.5:</b> Two models of molecular docking - (a) rigid-body and (b) flexible (induced-fit model).....	28
<b>Figure 2.6:</b> Rigid-body, flexible-rigid, and flexible docking methods.....	29
<b>Figure 2.7:</b> Applications of molecular docking in drug discovery and development.....	33
<b>Figure 2.8:</b> Molecular docking steps: conformation generation and scoring.....	34
<b>Figure 2.9:</b> The partitioning of the protein-ligand complex into the MM applied region, QM applied region, and QQ/MM applied regions.....	37
<b>Figure 2.10:</b> Phase I and phase II drug metabolism.....	40
<b>Figure 2.11:</b> The structure of CAP and metabolic conversion of CAP to 5-FU.....	44
<b>Figure 2.12:</b> The DFT method (B3LYP and CAM-B3LYP) in drug design.....	46
<b>Figure 2.13:</b> Application of AI in various aspects of the pharmaceutical industry in the context of drug design.....	50
<b>Figure 3.1:</b> 2D interactions of Sal B interacting with DNA lyase.....	63
<b>Figure 3.2:</b> 2D interactions of the EA-DNA lyase complex.....	65
<b>Figure 3.3:</b> 2D interactions of [ <sup>3</sup> H] PDBu -DNA lyase complex.....	66
<b>Figure 3.4:</b> 2D structure of [ <sup>3</sup> H] DPB -DNA lyase complex.....	67
<b>Figure 3.5:</b> 2D interactions of Sal B and topoisomerase II alpha.....	69
<b>Figure 3.6:</b> 2D structure of Sal B and mTOR interactions.....	70
<b>Figure 3.7:</b> 3D ribbon structure (a) and (b) 2D structure of EA and mTOR interactions.....	71
<b>Figure 3.8:</b> 2D interaction diagram of methoxyamine on active site residues of DNA lyase (a) and (b) superimposition of original pose (yellow) and re-dock pose (cyan).....	71
<b>Figure 3.9:</b> 2D interaction diagram of etoposide on active site residues of topoisomerase alpha II alpha (a) and (b) superimposition of original pose (orange) and re-dock pose (pink).....	72

<b>Figure 3.10:</b> 2D interaction diagram of etoposide on active site residues of topoisomerase alpha II (a) and (b) superimposition of original pose (orange) and re-dock pose (pink) .....	73
<b>Figure 3.11:</b> Percentage inhibition of ligands on selected protein targets.....	78
<b>Figure 3.12:</b> Cell viability of compounds on different cell lines.....	79
<b>Figure 3.13:</b> Microscopic images of anticancer effect of compounds and standards.....	82
<b>Figure 4.1:</b> Radar plots and BOILED-egg diagrams for (a) Sal B acid, (b) EA, (c) [ <sup>3</sup> H] PDBu, and (d) [ <sup>3</sup> H] DPB.....	98
<b>Figure 4.2:</b> Root mean square deviation (a) Sal B acid B, (b) EA, (c) [ <sup>3</sup> H] PDBu, and (d) [ <sup>3</sup> H] DPB ligands.....	100
<b>Figure 4.3:</b> Absolute free energy for the four ligands studied.....	102
<b>Figure 4.4:</b> Root mean square deviation (a) Sal B acid B, (b) EA, (c) [ <sup>3</sup> H] PDBu, and (d) [ <sup>3</sup> H] DPB ligands.....	103
<b>Figure 4.5:</b> Absolute free energy of (a) Sal B acid B, (b) EA, (c) [ <sup>3</sup> H] PDBu and (d) [ <sup>3</sup> H] DPB ligands.....	104
<b>Figure 4.6:</b> Root mean square deviation of (a) Sal B acid, (b) EA, (c) [ <sup>3</sup> H] PDBu, and (d) [ <sup>3</sup> H] DPB ligands.....	105
<b>Figure 4.7:</b> Absolute free energy of (a) Sal B, (b) EA, (c) [ <sup>3</sup> H] PDBu, and (d) [ <sup>3</sup> H] DPB ligands .....	106
<b>Figure 4.8:</b> Error bars mean IC <sub>50</sub> values (μM) and standard deviation (SD) of lead compounds in PCa and BC cell lines.....	108
<b>Figure 5.1:</b> Chemical structures of potential lead drugs.....	117
<b>Figure 5.2:</b> 3D ribbon structure of mutant androgen receptor (a) and (b) NUDT5 oncology proteins.....	120
<b>Figure 5.3:</b> 3D ligand interaction (a) and (b) of Sal B with androgen receptor.....	123
<b>Figure 5.4:</b> 3D interactions (a) and (b) 2D interactions of salvianolic acid-NUDT5 complex .....	124
<b>Figure 5.5:</b> Root mean square fluctuation plot for (a) salvianolic acid-androgen receptor and (b) salvianolic acid-NUDT5.....	126
<b>Figure 5.6:</b> Root mean square deviation plot for (a) salvianolic acid-androgen receptor and (b) salvianolic acid-NUDT5.....	127
<b>Figure 5.7:</b> Radius of gyration plot for (a) salvianolic acid-androgen receptor and (b) salvianolic acid-NUDT5.....	128

<b>Figure 5.8:</b> Principal component analysis plot for (a) salvianolic acid-androgen receptor and (b) salvianolic acid-NUDT5.....	129
<b>Figure 5.9:</b> Principal component analysis trajectories for (a) salvianolic acid-androgen receptor and (b) salvianolic acid-NUDT5 complexes.....	130
<b>Figure 5.10:</b> DCCM plot for (a) salvianolic acid-androgen receptor and (b) salvianolic acid-NUDT5.....	131
<b>Figure 5.11:</b> (a) 3D free energy landscape for Sal B -androgen receptor complex and (b) 3D free energy landscape for Sal B -NUDT5 complex, (c) 2D free energy landscape of two central components (PC1 and PC2) for Sal B -androgen receptor complex and (d) 2D free energy landscape of two central components (PC1 and PC2) for Sal B -NUDT5 complex.....	132

## LIST OF TABLES

<b>Table 2.1:</b> Force fields employed in MD simulations.....	25
<b>Table 2.2:</b> Docking software and their corresponding algorithms.....	31
<b>Table 2.3:</b> Software tools that have been used to predict sites of metabolism and their corresponding methods.....	41
<b>Table 3.1:</b> Docking scores of ligands in comparison with reference drugs.....	74
<b>Table 3.2:</b> Chemical descriptor data.....	74
<b>Table 3.3:</b> Inhibitory potential of ligands.....	76
<b>Table 3.4:</b> Percentage of inhibition of compounds at different concentrations.....	77
<b>Table 3.5:</b> Cell viability of compounds on different cell lines.....	79
<b>Table 4.1:</b> Assessment of drug-likeness of the potential lead compounds.....	93
<b>Table 4.2:</b> Excretion and toxicity profile of Sal B.....	96
<b>Table 4.3:</b> IC <sub>50</sub> (μM, 48 h) for test compounds and standards — mean ± SD (95% CI).....	109
<b>Table 5.1:</b> Drug likeness scores of potential lead compounds.....	121
<b>Table 5.2:</b> Molinspiration bioactivity score of lead compounds.....	122
<b>Table 5.3:</b> Binding affinities and interactions of top scorers of oncoproteins.....	125

## LIST OF ABBREVIATIONS AND ACRONYMS

<b>[<sup>3</sup>H] PDBu</b>	[20- <sup>3</sup> H] phorbol-12, 13-dibutyrate
<b>[<sup>3</sup>H] DPB</b>	[20- <sup>3</sup> H]-12-deoxyphorbol-13-isobutyrate
<b>ADF</b>	Amsterdam Density Functional
<b>ADMET</b>	Absorption, distribution, metabolism, excretion and toxicity
<b>CADD</b>	Computer-aided drug design
<b>CoMFA</b>	Comparative molecular field analysis
<b>CoMSIA</b>	Comparative molecular similarity indices analysis
<b>DFT</b>	Density function theory
<b>DNA</b>	Deoxyribonucleic acid
<b>MD</b>	Molecular Dynamics
<b>MDGs</b>	Millennium Development Goals
<b>MM</b>	Molecular Mechanics
<b>PDB</b>	Protein Data Bank
<b>QM</b>	Quantum Mechanics
<b>SDGs</b>	Sustainable Development Goals
<b>WHO</b>	World Health Organisation
<b>VS</b>	Virtual screening
<b>VHTS</b>	Virtual high-throughput screening

# CHAPTER ONE

## INTRODUCTION

### 1.1 Background information

Globally, cancer continues to be a major health burden that has been directly linked to increased mortality rates (Han et al., 2024). Research has revealed that the etiology of cancer tumour is complex, recurrence is high, it is resistant to chemotherapy and metastatic. Therefore, cancer is becoming a challenge to the world health care system. The ongoing research efforts are aimed at designing and developing effective treatments of breast cancer (BC) and prostate cancer (PCa). All of these efforts have led to development of various forms of treatment of these malignancies including surgery, radiotherapy, and chemotherapy (Bauso et al., 2024; Zafar et al., 2025). Scientific studies reveal that these methods are effective in the therapy of BC and PCa, but are directly related to other complications, such as lack of accuracy and specificity of tumour cells and drug resistance (Garg et al., 2024). Research has also shown that the existing treatment modalities are not responding to metastatic cancer and this signifies the challenges in the treatment of advanced stages of cancer. Additionally, the poor and middle-income countries lack adequate healthcare facilities, and this does not allow access to cancer treatment (Bukke et al., 2024). These challenges indicate that more effective and safe treatment options to cancer are required. In view of this, the strategy of plant-based therapeutic means has become the future of cancer treatment (Saadh et al., 2024). It is known to medicinal plants that they have diverse phytochemical profiles and pharmacological properties including antioxidant properties, anti-inflammatory properties, and direct cytotoxicity. Thus, they have the potential to satisfy the present demand of cheap, effective, and less toxic medical plant-based therapeutic strategies (Saadh et al., 2024). In this regard, the scientific challenges that are related to the available pharmacological treatment methods could be solved by exploring the possibilities of using plant-based therapies in treating these malignancies

Cancer has been the major cause of high mortality rate in men and women across the world in the recent past leading to the quest of innovative ways of treating it to improve treatment outcome. Effective therapy and management of BC and PCa is in line with Sustainable Development Goals (SDGs) on sustainable and equitable future to everyone (Bukke et al., 2024). However, the burden on the low- and middle-income economies is disproportionately high, as the rise in cancer prevalence is threatening the accomplishment of SDG 1 on reduction of poverty, SDG 3 on healthy living, SDG 4 on quality education, and SDG 10 on reduction of

inequality (Bukke et al., 2024). In addition, the 2030 agenda also recognized the severe impacts of the chronic disease prevalence, including cancer on the SDGs. According to Kumar et al in 2021, it is important to note that the ethnobotanical knowledge must be identified as a feasible approach in achieving SDGs. The ethnobotanical knowledge, which is conventional, along with modern science, has played a major role in enriching the comprehension of how a specific compound is able to acquire its pharmacological profile (Kumar et al., 2021). Thus, as the gifts of nature, the medicinal plants have been directly linked to SDGs through the restoration of health and wellbeing of each individual.

Drug performance that is focused on different diseases has recently attracted great attention due to its efficacy as the theoretical models simulate the manner in which a drug may behave in the contact with a disease-causing pathogen. This has helped to address the challenge that the design of therapeutic drugs is a more complex task (Klipp et al., 2010; Wang et al., 2023). To reduce the search process of finding potent medicinal drugs, computational chemists have been combining their understanding of molecular interaction and drug activity with visualization tools, detailed computational energy, geometries and with enormous databases (Huggins et al., 2012). Computer-aided drug design is a significant component of rational drug design and is becoming increasingly relevant as our understanding of molecular activity deepens. The volume of available experimental data for processing continues to proliferate (Eweas et al., 2014). It has made drug discovery one of the most promising processes in recent years. It begins with target and lead discovery, followed by lead optimization and preclinical *in vitro* and *in vivo* studies to identify the potent compounds that meet the primary criteria for drug development (Niazi & Mariam, 2023). Drug development through *in vitro* and *in vivo* means is conventionally expensive, tedious, and time-consuming (Garg et al., 2024). Therefore, drug design through molecular docking in conjunction with molecular modelling is essential for predicting the active compounds and also provides insight into the drug discovery process (Kiewisch et al., 2013; Van Gisbergen et al., 1999). Molecular recognition, including enzyme-substrate, toxin-nucleic acid, toxin-protein, and protein-protein interactions, plays essential roles in biological processes such as signal transduction and cell regulation, cancer development, and the formation of other macromolecular assemblies (Egorova et al., 2017; Horne, 2017).

Molecular modelling involves applying computational methodologies, such as energy computation of a molecular system, energy minimization, Monte Carlo methods, or molecular

dynamics, to evaluate or describe the properties of a drug candidate's molecular structure (Fourches, 2017; Pearlman et al., 1995). From a pharmaceutical standpoint, drug design refers to the generation, manipulation, or representation of three-dimensional structures of molecules and their associated physicochemical properties. It involves a range of computerized techniques based on theoretical chemistry methods and experimental data to predict molecular and biological properties. On the other hand, molecular docking is a method that predicts the favourable orientation of one molecule over another when they bind to, for instance, a protein or ligand molecule to form a stable complex structure (Eldridge et al., 1997; Gioia et al., 2017). Docking directs ligand binding to its receptor or target protein (Evangelista et al., 2019). It also predicts stable drug interactions by inspecting and modeling the interactions between a drug candidate and target receptor molecules. This leads to the development of several ligand conformations and orientations, which in turn determine the affinity and activity of a complex formed by two or more constituent molecules with known structures (Yuan et al., 2013).

It is scientifically challenging to model how a drug (ligand) interacts with the protein (receptor) (Hann et al., 2001). The intermolecular interactions that are involved in drug-protein interactions are varied and include van der Waals forces, electrostatic forces, dispersion, and hydrophobic forces (Horne, 2017). Hydrophobic interactions are the primary force for binding, although the binding specificity appears to be influenced by hydrogen bonding and electrostatic interactions. Therefore, the process of docking a ligand to a binding site attempts to simulate the natural interaction course between the ligand and its receptor via the lowest energy pathway (Gioia et al., 2017). Extracts (alkaloids) from *Sapium ellipticum* and other natural plants in the same family contain bioactive molecules that could serve as lead compounds in drug development (Williamson, 2017). Studies have shown that cancer cell proliferation and inflammation can be suppressed by key metabolites from the genus *Sapium*, such as EA, [20-<sup>3</sup>H] phorbol-12, 13-dibutyrate ([<sup>3</sup>H] PDBu), and [20-<sup>3</sup>H]-12-deoxyphorbol-13-isobutyrate ([<sup>3</sup>H] DPB) are key metabolites of *Sapium ellipticum* that have been known to inhibit the growth of cancer cells and reduce inflammation. The emerging scholarly evidence shows that [<sup>3</sup>H] PDBu and [<sup>3</sup>H] DPB activate protein kinase C, which has been used to investigate cell processes such as differentiation, proliferation, and immunological responses (Cheshomi et al., 2021; El-Fakahany, 2020; El Omari et al., 2021). The potential of EA compound as an antioxidant that neutralizes free radicals and prevent the damage of deoxyribonucleic acid (DNA) (Kanthé et al., 2021; Wang et al., 2022). Nevertheless, the molecular characteristics of these compounds have not been studied widely. On the other hand they have they have served

as vital pointers of diverse chemical molecules, such as analgesics. They are commonly defined as biological, chemical, and physical molecular properties (Egorova et al., 2017). The properties are simulated through three computational algorithms, that is, molecular mechanics, molecular dynamics, and quantum mechanics.

Molecular mechanics (MM) is a formalism that recreate the geometries of molecules, its energies among other features by changing bond lengths, bond angles, and torsion angles to equilibrium values that depend on the hybridization of an atom and a bonding scheme (Raabe, 2017). Based on this, MM can simulate macromolecules like enzymes in a faster and easier manner. On the contrary, Sonawane and Dhanavade (2018) state that molecular dynamics (MD) is a method of calculation that mimics the movement of the molecules by determining the movement of every atom using the equation of Newton. This enables the velocity and the location of every atom to be increased by a minute time interval. The method generates the 3-dimensional (3D) structure of molecules including proteins and peptides. It is worth mentioning that this method has played the key role in the determination of the binding affinities, mobility, stability, and structural-functional connections of proteins, nucleic acids, and other macromolecules which are not available through the static models (Sonawane & Dhanavade, 2018).

Quantum mechanics (QM) is a mathematical model of theoretical chemistry (Csizi & Reiher, 2023; Raabe, 2017). Xu et al. (2018) point out that QM calculations can be employed to characterize electronic behaviour mathematically. Nonetheless, no chemical system has ever had its QM equations precisely solved except for the hydrogen atom (Jedwabny et al., 2017). Typically, first-principles calculations or ab initio techniques can be employed to replicate the laboratory measurements of molecular characteristics, including ionization potential, molecular geometry, UV/visible spectra, and heat of formation can reproduce laboratory measurements of molecular properties, such as the heat of formation, ionization potential, UV/Visible spectra, and molecular geometry. According to Quertinmont et al. (2017), it has been found to be a reliable method of handling small compounds because it can provide highly accurate results and determine reaction processes.

It has been established in the literature that the process of drug design and development is very time-consuming, complicated and costly. But in the development and optimization of new drug compounds, *in vitro* experimentation and computer methods have been essential in speeding up the process. It is astonishing that the structural interactions of drug-protein complex can be

comprehended more clearly through utilized methods like a simulation of a molecular docking. Platforms like SwissADME enable the early prediction of pharmacokinetics, drug-likeness, and medicinal chemistry friendliness. These approaches reduce the risk of late-stage drug development failures and help prioritize promising compounds for further evaluation. Natural and synthetic compounds, including [<sup>3</sup>H] PDBu, [<sup>3</sup>H] DPB, Sal B, and EA, have shown potential biological activities. However, their pharmacokinetic behaviour, structural binding characteristics, and in vitro anticancer properties require systematic investigation to establish their relevance as potential drug candidates for breast and prostate cancer treatment.

## **1.2 Statement of the problem**

Given the increased levels of carcinogen infections in Africa and Latin America, herbal medicine has been used for cancer treatment. However, herbal medicines suffer from several shortcomings, including insufficient and unacceptable evidence of safety, efficacy, and standardization, as well as inconsistent production practices. While phytochemistry and the pharmacology of the genera *Sapium* and *Salvia* have piqued researchers' interest in studying various factors involved in cancer progression and development, there is a scarcity of literature on their pharmacological properties. In addition to the qualitative and quantitative analysis of selected phytochemicals in the aqueous and solvent extracts, the efficacy of herbal preparations from these plants has not been adequately investigated to provide a scientific basis for their use as drugs to treat cancerous infections. Furthermore, the active principles of these drugs have not been identified. Molecular modelling simulation platforms are accurate, fast, and robust computational tools capable of studying chemical reactivity, bond elaboration, and spectroscopic properties from simple to complex compounds. Therefore, drug design will help generate a possible active lead molecule from the preclinical discovery stage to late-stage clinical development, utilizing selected active metabolites of the *Sapium* and *Salvia* genera, i.e., EA, (PDBu), (3H DPB), and Sal B. The lead molecules developed will be fundamental in selecting only potent leads to cure particular diseases.

## **1.3 Objectives**

### **1.3.1 General objective**

To contribute to the drug design and characterization of the active extracts ([<sup>3</sup>H] PDBu), ([<sup>3</sup>H] DPB), Sal B, and EA in combating cancer pathogens using Molecular Docking and Molecular Dynamics at the level of theories.

### 1.3.2 Specific objectives

- i. To characterize the drug-like properties of selected drug candidates for the prediction of pharmacokinetics and drug-likeness using SwissADME (Absorption, Distribution, Metabolism and Excretion Swiss software).
- ii. To determine the structural and molecular characteristics of [20-<sup>3</sup>H] phorbol-12, 13-dibutyrate (<sup>3</sup>H-PDBu), and [20-<sup>3</sup>H]-12-deoxyphorbol-13-isobutyrate (<sup>3</sup>H-DPB), Sal B, and EA using molecular docking simulation.
- iii. To determine the binding affinities between disease-causing cancer proteins and selected drug candidates using molecular docking simulation.
- iv. To conduct in vitro analysis of [20-<sup>3</sup>H] phorbol-12, 13-dibutyrate (<sup>3</sup>H-PDBu), salvianolic acid, [20-<sup>3</sup>H]-12-deoxyphorbol-13-isobutyrate (<sup>3</sup>H-DPB) and EA.
- v. To determine the most effective drug candidates for treating breast and prostate cancers.

### 1.4 Research questions

- i. Is the SwissADME suitable for predicting the pharmacokinetics and drug-likeness of selected drug candidates?
- ii. How do [20-<sup>3</sup>H] phorbol-12,13-dibutyrate (<sup>3</sup>H-PDBu), [20-<sup>3</sup>H]-12-deoxyphorbol-13-isobutyrate (<sup>3</sup>H-DPB), salvianolic acid, and EA interact structurally and molecularly with their target proteins as predicted by molecular docking simulations?
- iii. What are the binding affinities and interaction profiles of selected drug candidates on disease-causing proteins?
- iv. Do [20-<sup>3</sup>H] phorbol-12,13-dibutyrate (<sup>3</sup>H-PDBu), salvianolic acid, [20-<sup>3</sup>H]-12-deoxyphorbol-13-isobutyrate (<sup>3</sup>H-DPB), and EA exert biological activities on selected disease-related targets?
- v. What is the most effective drug candidate for treating breast and prostate cancers?

### 1.5 Justification

According to the World Health Organization's (WHO) traditional medicine program, it is estimated that nearly 80% of the world's population relies on phyto-products and phyto-constituents from wild plants, which play a vital role in the treatment of diseases among rural communities worldwide. In third-world countries, plants play a crucial role in the healthcare of the majority of the population. Since these plant concoctions have not been evaluated to determine their side effects, efficacy, and toxicities, it is necessary to conduct model drug

design experiments to establish their credibility. The major plant targeted for this study is *Sapium ellipticum*, which is believed to cure cancer, malaria, and typhoid among the Tugen community (Kalenjin sub-tribe) who live in Baringo County. Remarkably, the attainment of the Millennium Development Goals (MDGs) on better health and poverty reduction, as well as the Sustainable Development Goals (SDGs) on wellbeing and reduction of poverty, depends on better management and treatment of cancers. Also, the design and development of innovative cancer therapies align with the Kenyan government's Universal Health Coverage (UHC) program, which aims to collaborate with other organizations to create life-saving cancer medications and provide cancer care through the Social Health Insurance Fund (SHIF).

## CHAPTER TWO

### LITERATURE REVIEW

#### A REVIEW OF THE CURRENT TRENDS IN COMPUTATIONAL APPROACHES IN DRUG DESIGN AND METABOLISM

##### **Abstract**

In the recent past, the design and development of novel small compounds with desirable therapeutic profiles has largely relied on computer-aided drug design and discovery techniques. Herein, this review offers comprehensive research findings and pertinent literature on drug discovery processes using computational resources. Reliable databases such as the WHO Global Health Library, Scopus, Cochrane, Google Scholar, ProQuest Dissertations and Theses, Worldwide Pharmaceutical Abstracts (Ovid), ScienceDirect, and Web of Science were used extensively in the searches. Accordingly, a standardized template was used to ensure the chosen articles were pertinent to the review and satisfied the inclusion requirements. As a result, this review article offers practical applications of *in silico* and *ab initio* methodologies and algorithms, as well as the application of artificial intelligence in drug research. Computational tools and methods for drug design and development, such as molecular dynamics (MD), molecular docking, quantum mechanics (QM), hybrid quantum mechanics/molecular mechanics (QM/MM), and Density functional theory (DFT), have been reviewed. Accordingly, the emerging approach of synergistically employing these methods addresses the fundamental challenges of conventional medicines for complex diseases. Herein, we discuss ligand-based and structure-based drug discoveries, force field models in MD simulations, docking algorithms, and subtractive and additive QM/MM coupling. Nonetheless, as computer-aided drug (CADD) approaches continue to evolve with significant improvements, the focus areas will be on docking and virtual screening, scoring functions, optimization of hits, and assessment of adsorption, distribution, metabolism, excretion, and toxicity (ADMET) properties. With the current success, the present computational resources will aid in the future discovery of novel compounds with high therapeutic performance. The ongoing oncology research efforts will also significantly contribute to the UN Sustainable Development Goals, specifically good health and wellbeing, as well as sustainable innovation and industrialization.

## 2.1 Introduction

For a long time, plants have been recognized for their therapeutic properties, and many plant-derived medicines have been utilized to manage various pathological conditions (Alotaibi et al., 2021; Ebrahimi et al., 2019). While these medicines have been effective when used as concentrated plant extracts or concoctions, modern medicine requires the isolation and purification of active compounds (Ge et al., 2023). Despite the identification of drugs for treating hypertension, malaria, HIV/AIDS, cancer, and diabetes, these diseases continue to pose global health concerns, with modern medicine struggling to find sustainable cures. Research activities on medicinal chemistry show that antimalarial drugs such as Artemisinin (*Artemisia annua*), quinine (*Cinchona* spp.), and anticancer drugs such as Vinblastine (*Catharanthus roseus*) and Taxol (*Taxus brevifolia*) were discovered from natural products and were effective in managing and treating serious health problems and diseases (Gusain et al., 2021; Moraes et al., 2017). Similar reports show that natural products are relevant in drug discovery for communicable and non-communicable diseases (Alotaibi et al., 2021). Modern drug discovery methods in the realm of natural products represent a significant breakthrough in achieving the United Nations Sustainable Development Goals (SDGs) related to health (Nedungadi et al., 2023). In particular, aspects of drug discovery and development are essential translational science activities that contribute to SDG 3 (good health and wellbeing) and SDG 9 (sustainable innovation and industrialization) (Sorooshian, 2024). The urgency of providing affordable essential vaccines and medicine in accordance with the Doha Declaration on the Trade-Related Aspects of Intellectual Property Rights (TRIPS) Agreement and Public Health cannot be overstated within the context of sustainable healthcare (Solovy, 2021).

Cancer is a serious illness that poses a significant concern to the global population's health (Xi & Xu, 2021; Xu et al., 2023). Academic series have described cancer as a cell growth that forms abnormal tissue masses in the body. The National Cancer Institute (NCI) defines cancer as “a disease in which some parts of the body's cells grow uncontrollably and spread to other parts of the body” (Brown et al., 2023). Cancer first arises from changes in cells (the growth of tissue mass) to form a tumor. It was first recognized as “a disease of the genes,” where normal cells transform into malignant cells (Brown et al., 2023). The cancer cells undergo epigenetic and genetic changes, adopting a tumorigenic process (metastasis). The more resilient and aggressive cells drive the disease progression and multi-drug resistance. Considering the evolutionary nature of cancer cells by natural selection and genetic and epigenetic changes,

Brown et al. (2023) define cancer as “a disease of uncontrolled proliferation by transformed cells subject to evolution by natural selection”. The underlying mechanism of heterogeneous prostate cancer (PCa) and breast cancer (BC), both genetically and histopathologically, is still uncertain. The mono-therapeutic treatment selection for these malignancies includes chemotherapy, hormonal therapy, surgery, and radiotherapy (Cai & Liu, 2021).

Notwithstanding the success of mono-therapeutic selection for cancer treatment, the success of mono-therapies is limited by drawbacks associated with an increase in resistance and damage to the healthy growing cells. Therefore, the current research programs focus on targeted therapy by leveraging the existing and vast knowledge in structural and functional characteristics with high specificity on the target protein. Current advances in cancer research aim to overcome chemoresistance mechanisms, improve the delivery of treatment regimens that selectively target cancer cells without damaging the microenvironment, and reduce the toxicity profiles of anticancer agents (Marey et al., 2024). Accordingly, there is a need to leverage the synergistic potential of next-generation technologies and the extensive knowledge in structural biology to enhance the early detection of biomarkers, optimize treatment delivery, and develop personalized treatment plans for cancer patients (Marey et al., 2024).

Conventional drug design and discovery methods are well known to be cost-intensive and time-consuming, taking an average of 10 to 15 years and costing more than US\$2 billion before they reach the market (Berdigaliyev & Aljofan, 2020). The long-standing impediment in drug design and discovery is the reproducibility of the experimental designs (Brown et al., 2020; Korshunova et al., 2021; Schaduangrat et al., 2020). Drug development has also benefited greatly through the massive computational techniques that have been brought about by the rapid advancement of computer algorithms, computer hardware, and computer software. This has significantly decreased the time needed to discover a drug. The investigation of biological systems requires methods that will yield significant information in a short time. More notably, the computational tools have gained prominence as valuable and necessary to aid in the discovery of chemical compounds which had the potential to have therapeutic properties (Garg & Dewangan, 2022; Hasan et al., 2022; Prieto-Martínez et al., 2019). Various computational packages have significantly helped scientists to detect and screen new drug targets and forecast the possible interactions. It has allowed researching thermodynamic and structural properties of the target proteins at various levels, which are useful in the study of drug mechanisms of action and drug targets (Decherchi & Cavalli, 2020).

The failure of classical pathways of drug discovery and design has led the scientific community to apply computer-aided drug discovery (CADD), that implies system-based approaches, structure-based approaches, and ligand-based approaches to drug discovery (del Carmen Quintal Bojórquez & Campos, 2023; Niu & Lin, 2023). The scientific investigation on CADD starts with wet-lab experiments that entail the discovery of the hit or target compound, and then high-throughput screening (HTS). Hussein et al. (2023), Kommalapati et al. (2023), and Komura et al. (2023), consider that the adverse effects associated with medication need to be evaluated with early measurement of absorption, distribution, metabolism, excretion, and toxicity (ADMET) profiles. As a result, computational screening of compounds with the help of CADD decreases the number of drug candidates, enhances the success rates, and reduces the time required to screen potential bioactive compounds with desirable pharmaceutical profiles. Despite the remarkable success of using CADD, it is linked with high costs and high-resource requirements (Moinul et al., 2022), driving the need for virtual screening techniques such as molecular docking, which involves screening known proteins against a virtual library of compounds (Barge et al., 2022; Yadav et al., 2021). The first step in drug design usually identifies the target molecule (a protein of a biochemical pathway associated with the disease). The lead compounds are then designed or identified to promote or inhibit the biochemical pathway (Deore et al., 2019). Another crucial step in drug design and discovery is lead optimization to achieve maximum interaction between the target molecules. Consequently, CADD plays a central role in lead optimization (Verma & Pathak, 2022).

As noted in Figure 2.1, CADD is broadly classified into ligand-based and system-based approaches. The ligand-based approach leverages the experimental distinction between inactive/active molecules. This strategy needs only bioactivity data and the structural information of small molecules rather than prior knowledge of mechanisms of action. In a ligand-based approach, similar molecules likely have similar properties (Vemula et al., 2023). Numerous studies have reported that when the experimental three-dimensional (3D) structure is unavailable, a ligand-based approach is used to understand the physicochemical and structural properties of the ligand associated with the desired pharmacological activity (Acharya et al., 2011; Fadaka et al., 2022). Acharya et al. (2011) state that ligand-based methods do not restrict themselves to known ligand molecules but can also be natural products or substrate analogs that react with target molecules to produce the desirable therapeutic effect. The same studies have indicated that, in case the 3D structures are known, structure-based methods have been used to optimize leads such as in silico chemical modification or molecular

docking (Fadaka et al., 2022). To maximize the interaction, structure-based methods help in identifying the kind of the protein-ligand interactions (Acharya et al., 2011). Figure 2.1 presents a description of drug discovery processes and tools involved in the process of computation.

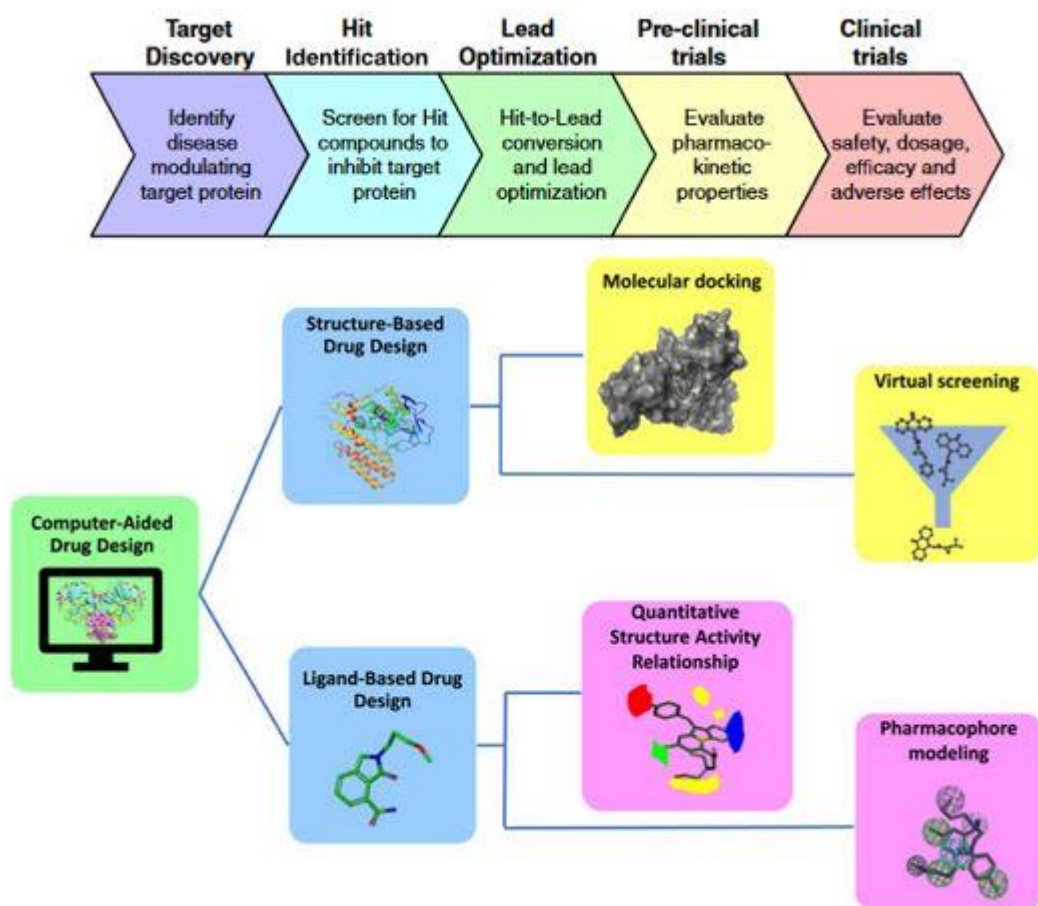


**Figure 2.1:** Drug discovery process and identification using various computational methods (Schaduangrat et al., 2020; Vemula et al., 2023)

Multiscale simulations of biomolecular systems can be done in preclinical drug discovery depending on the biological issue being studied. Dempan et al. (2022) and Saura et al. (2019) state that both molecular mechanics (MM) and the quantum mechanics (QM) (QM/MM) have become popular in the calculation of spectra, simulation of chemical reactions, and the study of electronic properties in a single simulation. Such a combination assists in comprehending the processing of drug actions (Kulkarni et al., 2022; Raghavan et al., 2023). Structural biology has also extensively employed the use of molecular dynamics (MD) in order to investigate the binding free energies of possible drug binding areas and their mode of action. Typically, MD is grounded in classical Newtonian physics and employs mechanical force fields (Lin et al.,

2020; Salo-Ahen et al., 2020). Figure 2.2 presents the computational resources used in the virtual screening of drug compounds.

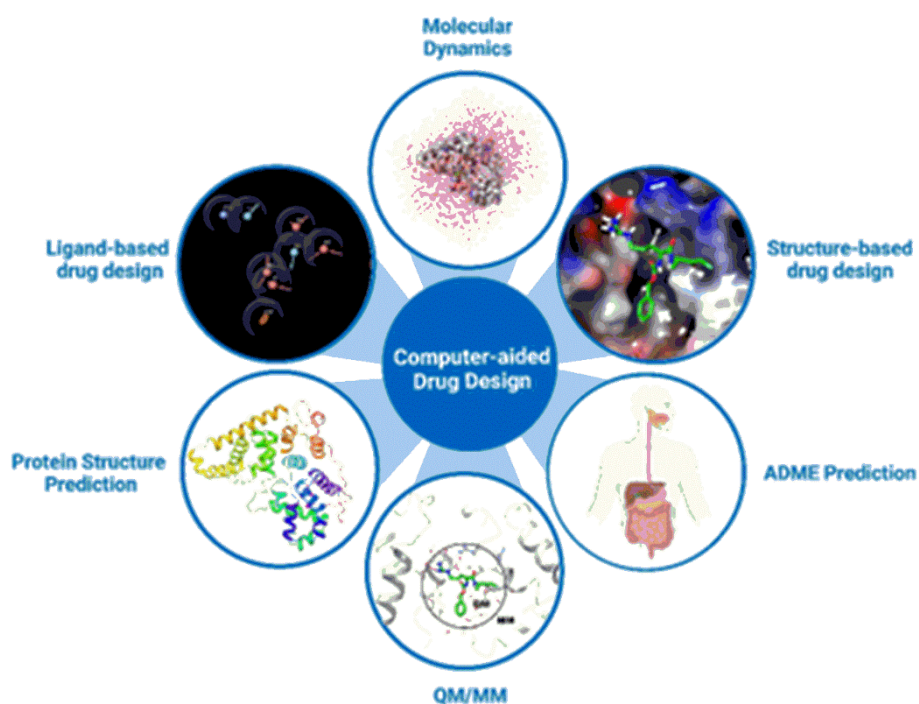


**Figure 2.2:** The computation resources used in predicting molecules with potential therapeutic effects (Chang et al., 2023)

Further to this, depending on different accuracy requirements, coarse-grained (CG), united-atom (UA), and all-atom (AA) MD simulations, as well as implicit/explicit solvent models, have been used in simulations of spatial and temporal scales in drug design ( Ma et al., 2023). Various biomolecular simulation methods are required to work on a specific problem. Accordingly, each of these methods is associated with practical limitations, disadvantages, and advantages in terms of the type of phenomena that can be modelled, the size of the biomolecular system that can be modelled, and the length of simulation required (Aminpour et al., 2019). In drug design and discovery, understanding the action mechanism of a drug, the dynamics of drug targets, and elucidating binding sites on the target protein require multiple simulation methods to analyze cross-scale connections. Figure 2.2 shows computational strategies, including MADE prediction, QM/MM, structure and ligand-based structure designs, protein structure design, and MD.

A significant thrust in most preclinical drug discovery research activities is the identification of drug candidates that are orally efficacious and safe, and amenable to low daily dosing. In this pursuit, drug metabolism has played a crucial role in identifying chemical compounds with optimal ADMET characteristics (Borah et al., 2020; Sohlenius-Sternbeck & Terelius, 2022). Minimizing drug metabolism is the focus of research efforts not only through the introduction of conformational constraints, modification of stereochemistry, modulation of electronic and steric factors, and decreasing lipophilicity (van der Kolk et al., 2022). Computational resources are certainly relevant to drug discovery, and scientists will never fail to investigate new forms of interactions (Sabe et al., 2021). Based on this, docking with the help of such software as AutoDock, Glide, and GOLD is initially performed, and MD simulations are conducted to obtain information about the implications of interactions over time (Adelusi et al., 2022; Badar et al., 2022; Taldaev et al., 2022). Free energy perturbation (FEP), as an alternative method of calculations applied along with Monte Carlo (MC) and MD, is one of the most interesting options in the literature because the approach provides a stable theoretical framework to calculate changes in binding free energy (Cournia et al., 2021; Wang et al., 2019).

A combination of several computational resources has been utilized in the case of preclinical research of drugs. For instance, density functional theory (DFT) and Amsterdam Density Functional (ADF) have been employed together to identify the reactivity, electronic properties and molecular properties of lead compounds (Ji et al., 2020; Islam et al., 2023; Sajid and Addicoat, 2023). Shukla and Tripathi (2021) claim that MD models play a crucial role in the thermodynamic stability of ligand-protein complexes. They also play a central role in defining the binding modes of the ligands to the target proteins (Guterres & Im, 2020). Based on this, hybrid approaches such as QM/MM are used to combine accuracy and effective promises in the study of enzyme-catalyzed reactions (Sharma et al., 2023). The primary aim of the review article is to give a brief overview of the application of computational methods in drug studies. It also attempts to review the relevant literature on the application of hybrid techniques (QM/MM and Quantum MC), DFT, MD and MM (Monte Carlo Simulations and MD) in evaluating the pharmacological properties of compounds. The domain of this paper is also not restricted on the use of artificial intelligence (AI) in drug research. The results of this paper offer a basis on which the application of computational methods is sought in the discovery of new therapeutic agents that can be used to treat different categories of cancer.

## 2.2 Methodology

The methodology used in this paper involves a thorough analysis of pertinent literature and research studies on drug research and development. By combining systematic literature and various viewpoints, this paper summarizes the ever-evolving computational techniques in search for compounds with medicinal properties. A summary of numerous research findings on artificial intelligence (AI), deep learning, and machine learning in medicinal chemistry has been highlighted. Extensive searches were performed using Scopus, International Pharmaceutical Abstracts (OvidSP), WHO Global Health Library, Cochrane, Google Scholar, Web of Science, ScienceDirect, ProQuest Dissertations & Theses, Worldwide Political Science Abstracts (CSA), and PubMed. The identified studies were cross-checked to ensure that they were peer-reviewed, written in English, and published in scientific journals. Due to the long history of drug design and development, search strategies combining keywords “drug discovery and development” with concepts of “drug metabolism”, “artificial intelligence”, “machine learning”, “computational”, “*in silico* methods”, or “theoretical” were used; nevertheless, elaborate details of the search strategies were available on request. The search keywords and terms were also not restricted to “docking”, “therapeutic agents”, and “virtual screening”.

Over 800 scientific papers in the medical field, published between 1990 and 2024, were identified for this review, but only 263 were deemed relevant. Papers were selected in two phases using pre-defined inclusion and exclusion criteria. Oftentimes, the titles of literature studies are vague; thus, in the first phase, we selected studies by reading abstracts and titles. Abstracts and titles that mentioned drug design and development, *in silico* methods, metabolism, and pharmacokinetics, were included. Studies that combined drug discovery, computational drug design, drug metabolism, AI-assisted drug design, and other aspects of drug design were included. If the abstract was not available electronically, the articles were passed along to the second phase of full-text review. A standardized template was used to ensure that the selected papers met the inclusion criteria. Due to the long history of medicinal chemistry and the development of computational tools, the year of publication was not strictly adhered to. The template collected data on drug discovery studied using theoretical/computational methods, years of publication, and drug classes. Studies focused solely on protein structure prediction or traditional medicines without drug development projects, as well as those examining wet laboratory approaches and describing drug discovery

projects, also met the inclusion criteria. The search results were then imported into EndNote X8, a product of Clarivate Analytics, USA.

### **2.2.1 Systematic approach to data synthesis**

Two authors extracted data from the publications that met the inclusion criteria. The data included the first author, year of publication, computational method used in drug discovery, molecular docking tool, metabolism in drug design, potential therapeutic candidates, the visualization tool used, *in silico* approach employed in pre-clinical drug design trials, drug pharmacokinetics, and the use of AI in drug discovery. In the event of any discrepancies or disagreements, the two authors discussed and sought to reach a consensus.

## **2.3 Breast cancer and prostate cancer overview, potential treatments, and perspectives**

### **2.3.1 Prostate cancer diagnosis and treatment**

Prostate cancer (PCa) is a malignant growth that affects middle-aged men aged 45 and older (Kraujalis et al., 2022) and accounts for the increased mortality rates globally. The diseases arise from the lining of the epithelium of the prostate gland, ranging from indolent to lethal tumours (Hashemi et al., 2024). Nevertheless, the biology underlying the existence of low-grade tumours that require no treatment for highly lethal cancers is not well understood. The increased mortality rates are due to PCa diagnosis at advanced stages and failure of the therapy. Conventionally, PCa diagnosis by digital rectal examination (DRE) involves the assessment of the size of the prostate gland by inserting a gloved finger into the patient's rectum (Andrews et al., 2024). In addition to DRE, health screening, magnetic resonance imaging (MRI), prostate-specific antigen (PSA) testing, and prostate biopsy and analysis have been proposed as PCa screening techniques (Hugosson et al., 2022). Advanced imaging techniques include multi-parametric MRI (mp-MRI), the PCa gene 3 (PCA3) test, which measures the PCA3 gene level, and the prostate health index (PHI), which combines various forms of PSA (Li et al., 2024). Other additional tests may include the Gleason score to determine the aggressive nature of PCa (Godtman et al., 2022), bone scan to monitor cancer cells in bones (Han et al., 2022), and computed tomography (CT) scan to accurately detect PCa (de Feria Cardet et al., 2021).

The frequently cited risk factors for PCa include obesity, age, ethnicity, and family history, among other environmental factors (Lynch et al., 2020; Zhang & Zhang, 2023). However, there is documented proof that gene mutations are the prevalent cause of cancer (Mendiratta et al., 2021). Men younger than 40 have low risks of developing PCa, but risks increase as an

individual approaches 50 (Huynh-Le et al., 2020). Academic series show that six out of 10 PCa incidences are men aged over 65 (Jha et al., 2014). It is also well-established in the literature that African-American men face a high risk of PCa compared to other racial groups (Murphy et al., 2024). Genetic and family history are additional risk factors, particularly if one or more family members have been affected. Individuals may inherit gene mutations, including those related to BRCA1/BRCA2, and the risk is even higher for men with Lynch syndrome (Cheng et al., 2024). The Westernized lifestyles include consuming high-content red meat and high-fat dairy products, which are associated with PCa (Castelló et al., 2023). Conversely, diets rich in vegetables or fruits may lower the risk of prostate cancer (PCa). People with obesity and high smokers are also likely to develop aggressive PCa. Research has been ongoing on various treatment options for PCa, including hormonal therapy, active surveillance, radiation therapy, chemotherapy, cryotherapy, and surgery (Sekhoacha et al., 2022). The treatment option delivered to PCa patients depends on various factors, including the potential for recurrence of the malignancy, PSA level, nature of the tumor, grade, and stage—whether localized or metastatic (Sekhoacha et al., 2022). For instance, hormonal therapy is recommended for treating cancers that have reoccurred or have spread beyond the prostate (Merseburger et al., 2022). For low-risk PCa, radiation therapy in conjunction with radical prostatectomy (surgical option) is recommended (Moris et al., 2020).

### **2.3.2 Current therapies deployed in localized and systemic BC**

The available systemic and local treatment options for BC include immunotherapy, hormone therapy, radiotherapy, HER2 targeted therapy, surgery, endocrine therapy, and chemotherapy (Mir & Mir, 2023; Wang & Wu, 2023). The treatment option depends on the patient's age, medical condition, and physical condition. The treatment for the localized BC is delivered to prevent metastatic disease recurrence and eliminate the tumour (Gote et al., 2021). However, for metastatic BC, the goal of the treatment option is to prolong the patient's life and reduce the severity of the symptoms (Yu et al., 2022). It is well-established in the literature that treating BC becomes more difficult after recurrence and metastasis (Afifi & Barrero, 2023). The disease relapse is associated with multi-drug resistance (MDR) characteristics, including the activation of transcription factor genes and the increased expression of efflux transporters, which lead to gene mutations and the proliferation of cancer cells (Gote et al., 2021). According to Afifi and Barrero (2023), studies on addressing BC MDR are in progress, including the use of nanomedicine chemotherapy for BC management.

Studies by Christiansen et al. (2022) reveal that breast-conserving procedures of BC local therapy are lumpectomy and mastectomy. Other similar reports demonstrate that tumour recurrence and overall survival rates of breast-conserving procedures followed by surgery are equal (Kim et al., 2021). Compared to sentinel lymph node biopsy (SLNB), axillary lymph node dissection (ALND) is directly linked to complications such as paresthesia and lymphedema. In view of this, Pesapane et al. (2023) note that ALND has become a better alternative for assessing the axilla in the early cancer stages. For several decades, radiotherapy has emerged as another therapeutic option for cancer management. Accordingly, this therapeutic option targets and eliminates tumour cells using high-energy radiation. According to Yang et al. (2023), there are two radiotherapy options: internal radioisotope therapy (RIT) and external beam radiotherapy (EBRT). To suppress cancer cells and reduce recurrence, radiotherapy is typically administered in the chest walls and regional lymph nodes; breast-conserving surgery is delivered in conjunction with radiotherapy (da Luz et al., 2022).

In systemic treatment of BC, chemotherapy has been extensively used to suppress the rapid division and proliferation of cancer cells (An et al., 2021). This method targets cancer cells at different stages of the cell cycle by administering common chemotherapy agents, including cyclophosphamide, platinum agents (carboplatin, cisplatin), taxanes (paclitaxel, docetaxel), and anthracyclines (doxorubicin, epirubicin), among others (Ferrari et al., 2022). The multi-drug combination in chemotherapy improves the anti-tumour effect compared to administering a single chemotherapy drug. There are two types of chemotherapy – neoadjuvant and adjuvant chemotherapy. Neoadjuvant chemotherapy refers to the chemotherapy administered to patients prior to surgery (An et al., 2021). In contrast, adjuvant chemotherapy is chemotherapy delivered after surgery for BC, particularly for cancer tumours that may recur or BC patients with lymphatic metastases (Yu et al., 2020).

Immunotherapy is also used in BC treatment, whereby the patient's immunity is strengthened to identify and destroy the tumours precisely (Anayyat et al., 2023; Dvir et al., 2024). Immunotherapeutic agents have also been shown to help minimize recurrence rates and prevent distant metastasis. Patients with TNBC benefit from this treatment option due to tumor-infiltrating lymphocytes, mutations, and increased levels of programmed death ligand 1 (Ribeiro et al., 2022). HER2 therapy is also a treatment option recommended for patients with HER2-enriched subtypes (Shen et al., 2021). The characteristics of the HER2 subtype are more aggressive development and rapid tumour growth, and have been managed by the use of drugs

such as tyrosine kinase inhibitors (lapatinib, neratinib, among others), monoclonal antibodies (pertuzumab and trastuzumab), and antibody-drug conjugate (trastuzumab emtansine) (Le Du et al., 2021; Li et al., 2023).

### **2.3.3 Limitations of the current treatment options for BC and PCa**

Chemotherapy is a conventional treatment option for BC but has been associated with suppression of normal cells due to its non-specific tumour targeting (Brianna & Lee, 2023). Therefore, chemotherapeutic agents may lead to inevitable adverse effects, such as mouth ulcers, increased susceptibility to infections, diarrhea, vomiting, nausea, anemia, leukopenia, myelosuppression, and others (Poulopoulos et al., 2017). There are also side effects related to drugs, such as cisplatin-induced ototoxicity, nephrotoxicity, and anthracycline-induced cardiotoxicity (Yang et al., 2023). Another scientific challenge is the drug resistance of commonly used chemotherapeutic agents, which reduces their efficacy in treatment (Yang et al., 2023). Drug resistance is also a significant setback in immunotherapy and hormone therapies (Magee et al., 2015). The widely cited adverse effects of endocrine treatment include a high risk of bone-related adverse events, thromboembolic events, vaginal dryness, night sweats, and hot flashes (Dent et al., 2011; Jackson et al., 2021). Furthermore, radiation therapy has been linked to radiation-induced malignancy, radiation pneumonia, lymphedema, fatigue, swelling, myelosuppression, cardiac and pulmonary injury, and radiation dermatitis (Sung et al., 2024).

The available chemotherapeutic drugs deployed in PCa include cyclophosphamide, Cabazitaxel, docetaxel, and paclitaxel (Carpenter et al., 2020; Jiang et al., 2024). Unfortunately, these drugs have clinical challenges linked to high drug resistance, short-circulation time, therapy side effects (renal, hepatic, bone marrow, and cardiac toxicity), and impact on the normal cells, affecting the quality of life of patients (Liu et al., 2023; Zhao et al., 2022). Furthermore, immunotherapy agents such as programmed cell death protein 1 (PD-1) and its ligand (PD-L1) have shown promise in slowing PCa progression or managing its symptoms. Still, there exists no treatment that can be deployed to prolong the survival of patients (Kgatle et al., 2021).

### **2.3.4 The potential of natural plant extracts for BC and PCa treatment**

Over the last decades, considerable research has been undertaken in developing biological and chemical analytical techniques that link pharmacology with phytochemistry. Combined with

the emerging technologies in lead identification implemented in clinical research, these have driven the rapid development of natural drugs from plant extracts to complement the treatment of various disorders and diseases (Singh et al., 2025). The growing body of scientific publications on prescriptions of Traditional Chinese Medicine has demonstrated the potential of *Dan-Shen* (*Salvia miltiorrhiza*, DS) to complement the different types of cancers (Lai et al., 2024). According to Gu et al. (2024), herbal medications from natural products have bioavailability and efficacy similar to those reported in chemotherapy or radiation therapy. They are also associated with very few adverse effects and low toxicity profiles. Phenolic compounds extracted from Danshen have shown remarkable anti-cancer effects, and their derivatives may also be used as lead compounds in the search for novel anti-cancer agents (Zhang et al., 2024). Studies by Lai et al. (2024) have shown the potential of active compounds extracted from traditional Chinese medicine, such as Danshen, in the management of various pharmacological conditions, depending on their structural and chemical properties. Danshen bioactive compounds are reported to be water-soluble phenolic acid or lipid-soluble tanshinones. Salvianolic acid B (Sal B) is a water-soluble phenolic compound, and tanshinones are lipid-soluble (tanshinones I and II, cryptotanshinone, and dihydrotanshinone) (Xing et al., 2025). Based on this, Sal B is identified to possess the best antioxidant activity of the bioactive compounds of *Salvia miltiorrhiza* (Danshen). Sal B, is chemically, (2*R*)-2-[(*E*)-3-[(2*S*,3*S*)-3-[(1*R*)-1-carboxy-2-(3,4-dihydroxyphenyl) ethoxy] carbonyl-2-(3,4-dihydroxyphenyl)-7-hydroxy-2,3-dihydro-1-benzofuran-4-yl]prop-2-enoyl]oxy-3-(3,4-dihydroxyphenyl) propanoic acid. It has a relative molecular weight of 718.62 Daltons and the chemical formula is C<sub>36</sub>H<sub>30</sub>O<sub>16</sub>. It has also been reported in other studies that Sal B has the potential of boosting apoptosis, reducing inflammation, oxidative stress, and angiogenesis (Zhang et al., 2024). Hence, with the numerous clinical uses of Sal B in the Asia region and other parts of the world, it is wise to understand the mechanisms of action to maximize the benefits of its clinical usage and mitigate the undesirable side effects of the traditional management methods.

Whereas *Sapium ellipticum* is not recognized as a TCM herb, it has been widely used in African traditional medicine to treat inflammation, infections, diabetes, and malaria. Organic chemists have discovered that *Sapium ellipticum* and other plants of the same family contain extracts (alkaloids) with active compounds that may serve as lead compounds for drug development (Williamson, 2017). Previous studies have highlighted the phenolic antioxidants, such as astragalins, gallic acid, and kaempferol, underlying the pharmacological benefits of *Sapium sebiferum* leaf extract (Yadav et al., 2025). The current pharmacological and phytochemical

findings of the genus *Sapium* indicate that EA has been successfully used in managing various conditions, including dermatitis (Al Muqarrabun et al., 2014). Although polyphenols are known to be structurally similar, EA has been proclaimed to be effective in the regression of various kinds of cancer, including prostate cancer and breast cancer (Vanella et al., 2013). Ellagic acid (EA) in *Sapium ellipticum* exists in free form as an aglycone form extracted using methanol and acetone, as well as ellagitannins and polyphenols found in leaves and barks that hydrolyze to release EA. EA glycosides, which are sugar-bound forms, exist in trace amounts. Many *in vivo* and *in vitro* investigations have established the promising effects of EA as an antitumorigenic compound (directly killing cancer cells), an inhibitor of metastasis and angiogenesis, and an antiproliferative agent that arrests carcinogenesis (Ceci et al., 2018; Čižmáriková et al., 2023). This bioactive compound exhibits selective cytotoxicity towards carcinoma cells without harming normal cells. Little is known about improving the oral availability of EA. This naturally occurring bioactive substance has attracted numerous studies in *in vivo* pharmacokinetics and *in vitro* cellular uptake to enhance its antitumor efficacy (Čižmáriková et al., 2023).

#### **2.4 Fundamentals of drug discovery and development using computational tools and software**

There are two drug discovery strategies: drug repositioning and *de novo* drug discovery. Drug repurposing refers to the approach of identifying new uses for existing products (Xia et al., 2024). Drug repurposing (also called drug repositioning) has various inherent advantages, including cost-efficient and faster drug development time due to prior knowledge of toxicity profiles, dosage, and safety of existing medications (Pinzi et al., 2024). Drug repositioning has gained more interests in the recent times. Thalidomide, a drug has been repurposed to treat multiple myeloma and leprosy after being officially known to cause birth defects (Fadnis et al., 2023; Wimmelbücker and Kar, 2023). Bulfude (alkylating agent) and chlorambucil are the examples of alkylating agents that have been reevaluated to treat leukemia (Xia et al., 2024). Therefore, repositioning of drugs can be an effective and attractive approach in improving the treatment of different diseases. On the other hand, *de novo* drug design refers to the design of a collection of drug candidates to be analyzed sequentially to generate something new, something newly, or something fresh, i.e. therapeutically interesting molecules, directly (Devi et al., 2015).

Drug research and development pursue three directions of experiments *in silico*, *in vivo*, and *in vitro* (Jean-Quartier et al., 2018). *In silico* is defined as the studies done on a computer simulation, while *in vitro* refers to studies conducted with biological molecules, cells, or microorganisms in flasks and test tubes (Kashkooli et al., 2021). These experimentations are performed outside living organisms. On the other hand, *in vivo* experimentations are mainly involved in clinical trials and animal studies (Mukherjee et al., 2022). Accordingly, an *in-silico* study is easily facilitated by the rapid development of numerical algorithms, the ability of pharmaceutical companies to reproduce human environments, advancements in computational power, and medical imaging.

Novel computational drug design methods, better machine algorithms, and faster architectures of Graphic Processing Unit (GPU)-based clusters that have been developed recently have significantly helped researchers perform high-level computations, aiding in the discovery of promising drug candidates by improving areas such as scoring functions (Banegas-Luna et al., 2019; Vitali et al., 2024). Undoubtedly, computational strategies in drug discovery have uncovered numerous therapeutic undertakings. In particular, advances in nuclear magnetic resonance spectroscopy, protein purification and structural analysis, and crystallography have stood out as successes that have scaled the drug-discovery process. Despite the extensive research undertaken in the academic environment for concept validation, various obstacles limit the application of these concepts. Accordingly, this work compiles a concise discussion on the developments and challenges of *in silico* approaches in drug discovery, as well as hybrid methods based on QM/MM, drug metabolism, machine learning, and AI in pre-clinical drug research.

#### **2.4.1 *In Silico* approaches in pre-clinical drug design**

*In Silico* approaches have been successfully applied to the *in vivo* prediction of ADMET and have been developed to replace *in vivo* models in the study of pharmacokinetics (Wu et al., 2020). Molecular modelling and data modelling are two popular techniques of *in silico* ADMET prediction (Wu et al., 2020). The 3D protein structures form the basis of molecular modelling which involves 3D simulations of QM, MD simulations, pharmacophore modelling, molecular docking calculations (Hu et al., 2019; Jayaraj et al., 2019; Panwar and Singh, 2021). To an extent, it is shown that the computational capacity of molecular modelling can supplement or even outperform the quantitative structure-activity relationship (QSAR) as more 3D protein structures can be obtained (Belfield et al., 2023). It will also be useful to mention

that the molecular modeling of the ADMET properties of small bioactive compounds is scientifically problematic because of the flexibility of receptors and large binding cavities (Ferreira & Andricopulo, 2019).

#### **2.4.2 Applications of molecular dynamics in drug design**

Typically, molecular dynamics performs simulations using Newton's second law of motion. These simulations have been used to study complex water systems, the motions of small molecules, and water or ions that represent biological environments, such as water molecules and lipid membranes (Huggins et al., 2019; Salo-Ahen et al., 2020). Therefore, MD simulations have been widely used to study drugs against specific proteins, considering the movement of proteins in a solvated environment (Salo-Ahen et al., 2020). These simulations generate data on conformational, energetic, and binding free energy changes, proving useful in drug design (Huggins et al., 2019).

The MD simulations have been paired with experiments to understand the underlying behavior of biological and chemical systems, which play an increasingly important role in drug discovery (Cournia et al., 2021). Notably, MD simulations appear destined to impact drug discovery significantly (Bera & Payghan, 2019; Salo-Ahen et al., 2020; Shukla & Tripathi, 2021). MD simulations follow virtual screening simulations. It is considered an advanced technique that complements docking, and most research scholars have used it in conjunction with virtual screening. MD employs Newtonian mechanics to improve the efficacy and binding properties of lead compounds (Sabe et al., 2021). For this reason, researchers have popularly used MD to confirm the validity of the docked results. Figure 2.3 presents the steps involved in MD simulations.

The computational chemistry methods based on MD are used to study various types of macromolecules – carbohydrates, nucleic acids, proteins – of medicinal or biological interest (Nian et al., 2021). They are well-suited to the study of membrane proteins and their behaviour. In MD simulations, dihedral angles are depicted using a sinusoidal function, while bond angles and chemical bonds are handled using simple virtual springs. MD applications, including free energy perturbation methods (FEP), linear interaction energy (LIE), and molecular mechanics Poisson-Boltzmann surface area (MM/PBSA), are used to calculate free energy to correlate calculated and experimental binding affinities of small molecules of proteins (King et al., 2021; Wang et al., 2019).

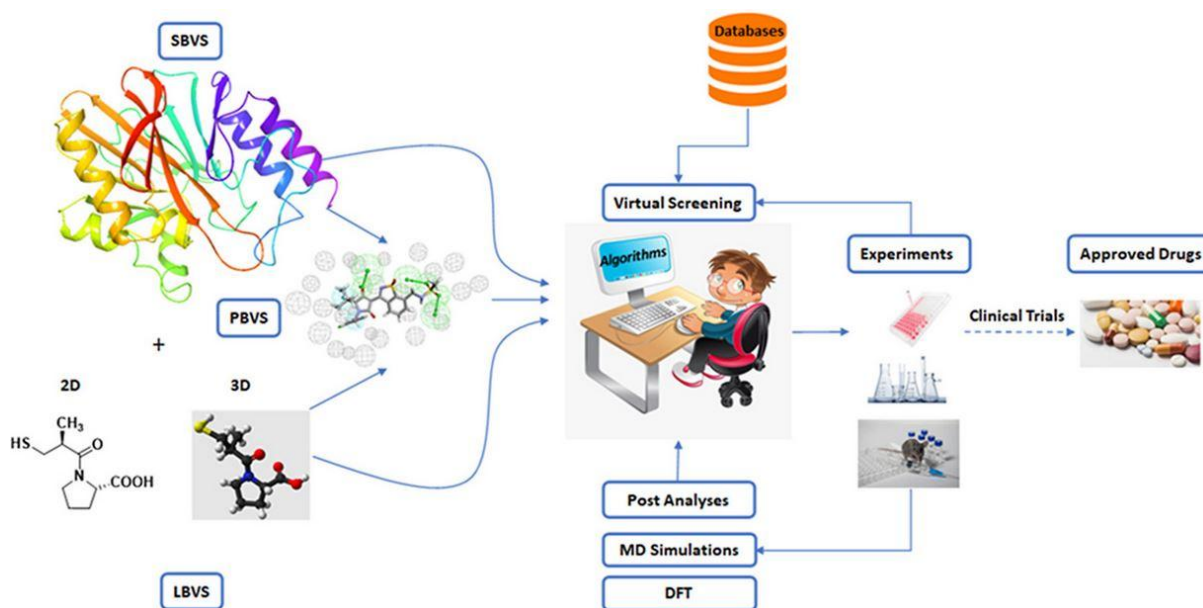


**Figure 2.3:** Schematic representation of molecular dynamics simulations (Sabe et al., 2021)

MD simulations employ force fields like CHARMM, GROMOS, Amber, OPLS, and coarse-grained (CG) (Vemula et al., 2023). According to Wang et al. (2004), Assisted Model Building with Energy Refinement (AMBER) is one of the force field models developed by Peter Kollman and colleagues at the University of California. Among other macromolecules, AMBER has been used mainly to study the dynamic behaviour of organic compounds, carbohydrates, lipids, proteins, DNA, and ribonucleic acid (RNA) AMBER, with respect to prediction of the environment of solvents, models the water, such as TIP3P, SPC/E, PIP4PEW, and OPC, in biomolecular simulations (Vemula et al., 2023). At Harvard University, Martin Karplus and co. developed CHARMM (Chemistry at Harvard Macromolecular Mechanics), which has been a major workhorse in MD simulations. Another accurate force field model in the prediction of structural and thermodynamic parameters by MC computations compared to experimental results is this model (Ghahremanpour et al., 2022), which is called optimized potentials for liquid simulations (OPLS) (Leonard et al., 2019). Table 2.1 provides a summary of various force fields that have been reported.

**Table 2.1:** Force fields employed in MD simulations

<b>Force field</b>	<b>Proteins</b>	<b>Carbohydrates</b>	<b>Nucleic acids (DNA/RNA)</b>	<b>Lipids</b>	<b>Organic molecules</b>
CHARMM	CHARMM 36, CHARMM 36 & CHARMM 22/CMAP	CHARMM 36	C27 RNA (Denning et al., 2011; Foloppe & MacKerell, 2000; Hart et al., 2012), C36 RNA, and C36 DNA, AND DNA	CHARMM36 lipids, CHARMM22 & CHARMM27 lipids (Feller et al., 1997; Schlenkrich et al., 1996)	CHARMM General FF (CGenFF)
AMBER	Ff19SB (Tian et al., 2019), ff14Bonlysc, ff14SB, ff15ipq-m, ff15ipq	GLYCAM-06j (Kirschner et al., 2008)	OL15 (Galindo-Murillo et al., 2016), OL3 (Bergonzo & Cheatham III, 2015)	LIPID14, LIPID21	gaff2
GROMOS	GROMOS87 & GROMOS96	GROMOS53A6, GLYC (Pol-Fachin et al., 2012), GROMOS45A4	GROMOS43A1, GROMOS45A3 & GROMOS55A1	GROMOS 54A8 (Marzuoli et al., 2019)	GROMOS96, GROMOS53A5 & GROMOS 53A6 (Oostenbrink et al., 2005)
OPLS	OPLS-UA, OPLS-AA, OPLS3, OPLS3e, OPLS4	OPLS-AA-SEI (Kony et al., 2002)	OPLSAA/M (Robertson et al., 2019)	OPLS-AA/Berger (Maciejewski et al., 2014)	OPLS-AA, OPLS3, OPLS3e, OPLS4 (Dodda et al., 2017)
Coarse-grained	MARTINI OPEP (Kalimeri et al., 2015), UNRES (Liwo et al., 1997) & PaLaCe (Pasi et al., 2013)	MARTINI (Gautieri et al., 2010)	SIRAH (Uusitalo et al., 2015)	MARTINI and ELBA (Siani et al., 2016)	Martini 3 (Alessandri et al., 2022)

Notably, optimized potentials for liquid simulations – all-atom (OPLS-AA) were created to replicate QM conformational energy profiles of small molecules. On the other hand, Groningen Molecular Simulation (GROMOS) has proven to be a versatile computational technique for studying biomolecular systems such as nucleotides, sugars, and proteins (Nian et al., 2021). Research groups have prevalently used GROMOS to model biomolecule solutions, liquid crystals, polymers, and glasses. A common computational technique known as coarse-grained (CG) makes computational simulations easier by reducing the degrees of freedom. Similarly, CGMartini possesses the computational ability to simulate large-scale systems (Nian et al., 2021; Vemula et al., 2023).

### **2.4.3 Application of molecular docking in drug design**

Molecular docking encompasses three key objectives: binding affinity estimation, pose prediction, and virtual prediction (Singh et al., 2022). Reliable molecular docking techniques must be able to differentiate between non-binding sites and binding sites, as well as their corresponding molecular interactions (Adelusi et al., 2022). Additionally, these techniques must also classify molecules as either non-binding or binding, and rate binding molecules among the best compounds when dealing with large compound libraries. The success of virtual screening relies on the accuracy and the amount of structural information known about the ligand and the target protein being docked. The first step in molecular docking is the analysis of protein-ligand to identify novel binding pockets using *in silico* methods such as PATCH-SURFER (Sael & Kihara, 2012), AFT, POCKET SURFER Catalytic Site Atlas (Kumar et al., 2011), and SURFACE. Molecular docking, based on virtual screening, is the most preferred and helpful technique when the binding site of the target biomolecule is known (Mohammad et al., 2021; Patel et al., 2021). Therefore, ligands with inhibitory potential against the target protein could be docked against the target protein in search of novel therapeutic candidates. Furthermore, blind docking techniques can also be employed when the binding site in a protein is unknown (Grasso et al., 2022). However, blind docking is associated with downsides, such as low success rates and high computational time requirements, compared to docking into a known binding pocket (Adelusi et al., 2022). Figure 2.4 represents the scheme of molecular docking techniques

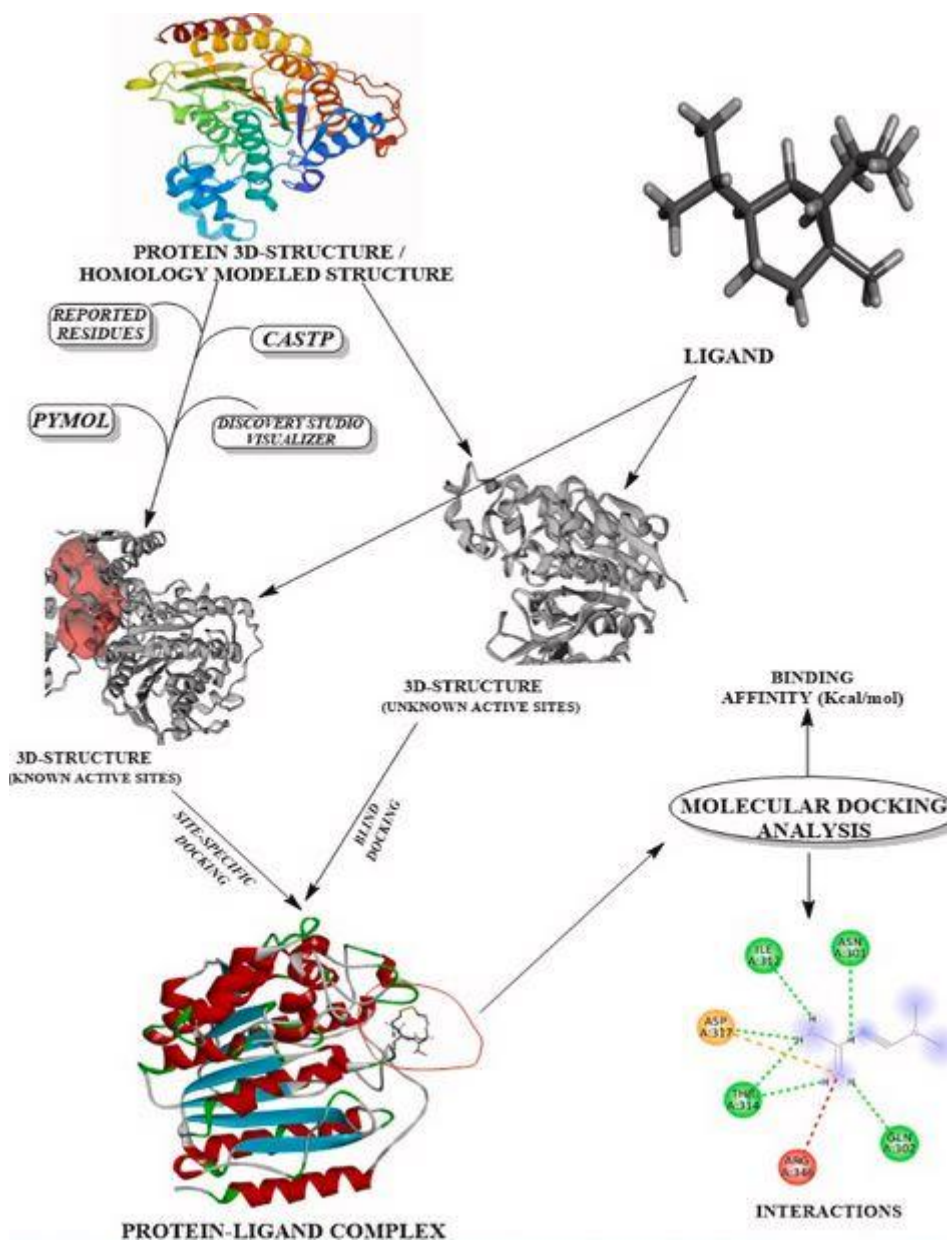


**Figure 2.4:** Active site determination of 3D-receptors, protein-ligand docking simulation (blind and site-specific docking), and analysis of docking complex (Adelusi et al., 2022)

Accuracy and speed are key features required for a successful molecular docking simulation. Typically, docking algorithms are developed to accelerate the discovery of novel lead compounds in virtual screening or to validate experimental data with higher accuracy (Hu et al., 2021; Jin et al., 2020; Patel et al., 2021). There are various docking programs: Zdock (Pierce et al., 2014), GOLD (Wang et al., 2016), MSDOCK (Sauton et al., 2008), FLEXX (Taylor et al., 2003), AUTODOCK (Goodsell & Olson, 1990), MOE-DOCK (Corbeil et al., 2012), FRED (Mcgann et al., 2003), Surflex (Jain, 2003), among others. These computational packages have specific search algorithms such as MC, genetic algorithm, incremental construction, and cavity

detection algorithm (Adelusi et al., 2022). These algorithms have their specific search method and specific parameters. Docking has computational capabilities of searching for the best fit between molecules, considering various parameters obtained from ligand and receptor input coordinates, such as ligand or receptor structure flexibility, interatomic interactions such as hydrophobic contacts and hydrogen bonds, and geometric complementarity (Adelusi et al., 2022; Singh & Pathak, 2020; Stanzione et al., 2021). Docking applications usually return the pose (predicted predictions) of a ligand in the binding site of the target.

Docking applications can be classified based on defined parameters and rules used to predict the conformations of molecules. For instance, the flexibility of receptor and/or ligand docking algorithm can be classified as flexible or rigid-body docking (Agnihotry et al., 2020; Kumar & Kumar, 2019). Rigid-body docking does not account for the flexibility of either the receptor or the ligand, which limits the accuracy and specificity of the results, particularly in considering the geometrical complementarities between two molecules (Kumar & Kumar, 2019). However, rigid-body docking is still capable of predicting the correct position of ligands when compared with crystallographic structures. It has also been used to perform a rapid initial screening of a small molecule database. Conversely, flexible docking considers several possible conformations of both the receptor and ligand simultaneously, albeit with a higher computational time (Stanzione et al., 2021). In flexible docking, the process must be flexible so that ligands and receptors can change their conformations to fit each other well, thus forming an "induced-fit model" (c.f. Figure 2.5) (Fan et al., 2019).

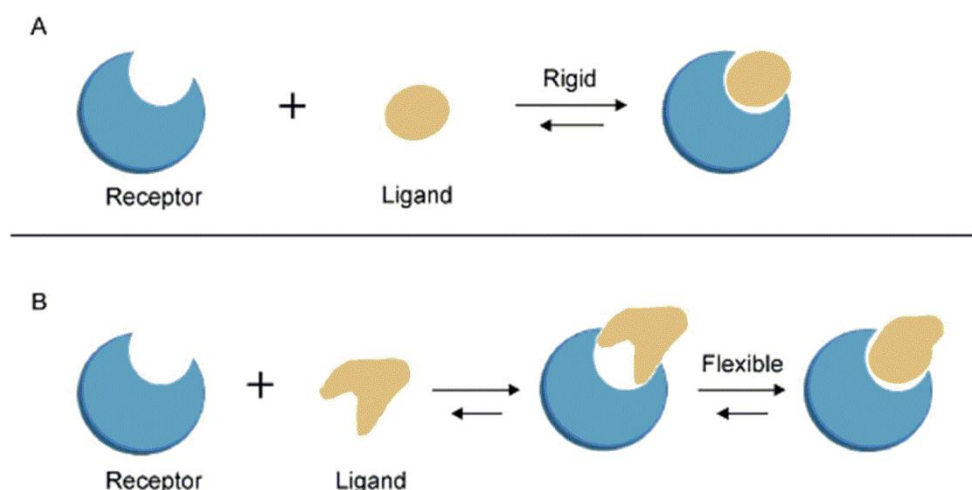


**Figure 2.5:** Two models of molecular docking - (a) rigid-body and (b) flexible (induced-fit model) (Fan et al., 2019)

Rigid-body, also called the "lock-and-key model", emphasizes the importance of geometric complementarity.

As shown in Figure 2.5, rigid-body docking is a traditional docking technique that assumes the ligand and receptor are rigid. It thus relies on the scoring function to determine the optimal binding orientation of the ligand to the receptor pockets (Chen et al., 2003). The scoring function is based on the geometric complementarity of the electrostatic and steric interaction of the ligand and the receptor (Chen et al., 2003; Fan et al., 2019). This method is less complicated and more effective in the cases where production of multiple docking is challenging. The disadvantages of the rigid-body docking are that it does not consider changes in conformation that could happen upon the binding of two molecules, the ligand and the receptor (Fan et al., 2019). Fan et al. (2019) state that receptors change their conformational changes to increase the drug-receptor interactions, which would hamper the validity of the computational resources in predicting the docking scores of ligands. With this consideration, the computational models of flexible-rigid docking are already under development to consider the conformational change of receptors (Surana et al., 2021). In this docking method, particular, preconceived conformational alterations of the receptors are taken into account. These receptor-specific rotatable bonds can be redefined and the algorithm is used to describe different conformational variations of these bonds in order to improve docking prediction. It also gives a correct prediction of the binding affinity (Agnihotry et al., 2020). (Singh et al., 2022). Figure 2.6 illustrates three docking methods, i.e. rigid-body, flexible-rigid, and flexible docking methods.

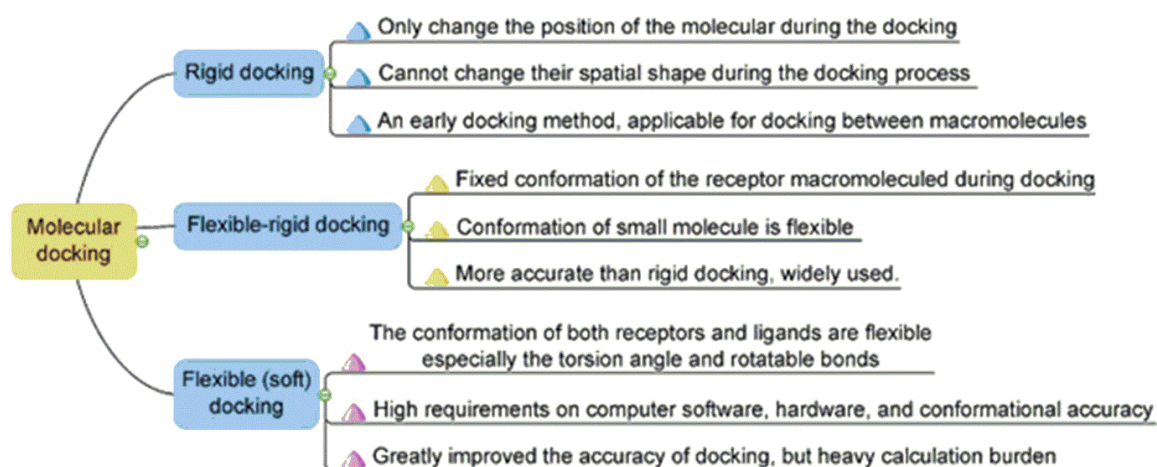


**Figure 2.6:** Rigid-body, flexible-rigid, and flexible docking methods (Fan et al., 2019)

Flexible (soft) docking is also an advanced docking technique that explores the full flexibility of both the ligand and receptor structures. Its dynamic nature accounts for the receptor and docking flexibility to investigate possible conformations, making it more accurate than flexible-rigid and rigid-docking methods (Fan et al., 2019). Docking programs are known to use one or a combination of the following ways: MC, distance geometry, incremental construction, simulated annealing, geometric algorithms, etc.

#### **2.4.4 Docking algorithms**

Various docking algorithms are used depending on the features of the optimization problem and the problem domain. For instance, the genetic algorithm (GA) uses a population-based approach inspired by biological evolution, where chromosomes evolve over generations (Duela et al., 2023). According to Steinmann and Jensen (2021), Darwin's theory of evolution influences GA. The solutions of these methods are primarily implemented in GOLD 3.1 and AUTODOCK 4.0, and they are selected and combined with other solutions to develop new ones (Vemula et al., 2023). Stochastic or MC is another significant method of calculating numerical problems where random sampling is employed (Luengo et al., 2020). It therefore calculates numerical integrals using a probability distribution. Balandat et al. (2020) reports reveal that MC algorithm finds the global optima by probabilistic selection. Colossal construction (IC) is another important computational technique that is used to build solutions by adding small changes to the solutions and analyzing them to generate new solutions (Torres et al., 2019).

According to Vemula et al. (2023), conformational selection is critical in biomolecular systems since it entails the study of the conformation of biomolecules, in which cases the lowest energy is identified by the degrees of freedom in a system. Conformational sampling is used together with energy minimization in order to compute the global minimal energy conformation of a system. Recent results by Ghosh et al. (2022) indicate that the tools of mathematics, such as derivatives and gradients, are applied in the search process by non-stochastic methods instead of randomness or probability. Cavity detection is another method that begins with randomness or probability and solves the problem through the iterative approach. Table 2.2 presents the docking algorithm used by docking software.

**Table 2.2:** Docking software and their corresponding algorithms

<b>Docking software</b>	<b>Algorithm</b>	<b>Protein flexibility model</b>	<b>Ref.</b>
AUTODOCK 4.0	Genetic algorithm	Rigid	(Morris et al., 1998)
ROSETTALIGAND	Stochastic algorithm (Monte Carlo)	Induced-fit	(Meiler & Baker, 2006)
ICM	Stochastic algorithm (Monte Carlo)	rigid	(Totrov & Abagyan, 1997)
DARWIN	Genetic information	rigid	(Taylor & Burnett, 2000)
GOLD 3.1	Genetic algorithm	Induced-fit	(Jones et al., 1997)
YUCCA	Stochastic algorithm (Monte Carlo)	Rigid	(Choi, 2005)
PRODOCK	Stochastic algorithm (Monte Carlo)	Induced-fit	(Trosset & Scheraga, 1999)
FRED	Non-stochastic method	Ensemble	(Mcgann et al., 2003)
GLAMDOCK	Stochastic algorithm (Monte Carlo)	Rigid	(Tietze & Apostolakis, 2007)
FLOG	Incremental construction	Rigid	(Miller et al., 1994)
EUDOC	Conformation selection-based algorithm	Rigid	(Pang et al., 2001)
Surflex	Incremental construction	Induced-fit	(Jain, 2003)
PSI-DOCK	Genetic algorithm	Rigid	(Pei et al., 2006)
FITTED	Genetic algorithm	Rigid	(Corbeil et al., 2007)
GAMBLER	Genetic algorithm	Rigid	(Charifson et al., 1999)
Hammerhead	Incremental construction	Induced-fit	(Welch et al., 1996)
ProPose	Incremental construction	Induced-fit	(Seifert et al., 2004)
Schrödinger's Glide	Hierarchical method	Induced-fit	(Friesner et al., 2004)

For nearly five decades, molecular algorithms have evolved due to rapid advancements in computer systems, which have led to applications in studying the docking of nucleic acids (NA) as potential drug targets (Tessaro & Scapozza, 2020). The druggability of specific ribonucleic acid (RNA) has sparked research activities on RNA-ligand binding, with a particular focus on docking and scoring methods. With the ever-increasing findings on powerful methods of RNA structure determination, RNA-based therapeutics have become a promising approach to treating human diseases such as cancer and human immunodeficiency virus (HIV) (Parikesit et al., 2022; Valeska & Parikesit, 2022). Typically, there are two types of RNA-based therapeutics: (1) RNA molecule serves as the target for the drug binding, which is analogous to protein-targeted drug discovery, and (2) the therapeutic RNAs (i.e. guide RNAs, small interfering RNAs, RNA aptamers, antisense oligonucleotides) bind to target (protein targets, DNA targets, and RNA transcripts) to induce or inhibit targeted biochemical reactions (Tessaro & Scapozza, 2020). Studies show that genes that are difficult to target with drugs or undruggable by targeting their associated proteins may be inhibited by drugs targeting the corresponding messenger (coding) RNA sequence (Berdasco & Esteller, 2022; Sztuba-Solinska et al., 2019). Unlike proteins, RNAs show broader druggability, garnering tremendous interest in gene therapy (Tessaro & Scapozza, 2020).

Computational approaches based on small-molecule docking are aimed at predicting the binding poses of biomacromolecules and small molecules such as NA or protein targets such as RNA or DNA (Nithin et al., 2018; Umare et al., 2022). Various docking algorithms help in predicting and understanding binding modes (molecular recognition) and estimating scoring (binding energy). While the molecular methods for proteins are well-developed, docking methods for NA are comparatively underdeveloped (Luo et al., 2019). Researchers in medicinal chemistry have used docking programs such as GRAMM, ZDOCK, HDOCK, and FTDOCK, initially developed for protein-ligand docking, to RNA-ligand docking and developed new scoring functions and methods for NA-docking (He et al., 2019). Emerging transcriptomics studies, particularly studies on non-coding RNA such as small interfering RNA (siRNA) and microRNAs (miRNA) in the development of anti-cancer drugs (Parikesit et al., 2022). Machine learning (ML) and algorithms, such as HNADOCK for RNA-ligand docking, although still in their infancy, have shown promising performance. The improvement in *in vivo* efficacy would accelerate RNA-targeted drug discovery (Sato & Hamada, 2023). A noteworthy interdisciplinary collaboration and the application of cutting-edge scientific knowledge in medicinal chemistry have led to the development of these powerful docking software programs,

which are currently in use (Muhammed & Aki-Yalcin, 2024). However, no single docking algorithm is suitable for every system, and thus using multiple software programs increases the quality of the output (Muhammed & Aki-Yalcin, 2024).

While molecular docking has been used in the study of interactions between targets and ligands, its application scope is currently broader, encompassing drug repurposing, polypharmacology, virtual screening, drug side effect prediction, target profiling, and discovery (cf. Figure 2.7) (Mathur et al., 2024; Mullins, 2010). Remarkably, there exist vast opportunities provided by molecular docking in the drug discovery process. It has typically been integrated into a workflow that includes a variety of experimental and *in silico* techniques. Wet lab experiments and computational methods, in conjunction with docking, may be utilized to elucidate drug metabolism and gain meaningful insights from the cytochrome P450 system. They are also useful for the development of new antibacterial agents, such as those targeting DNA gyrase (Kumar & Kumar, 2024). Typically, the protein-ligand docking algorithm involves two steps: conformation generation and scoring. During conformation generation, different ligand orientations are generated at various positions inside the protein binding pocket (Amit, 2019). Consequently, these conformations are evaluated by a scoring function, as illustrated in Figure 2.7.

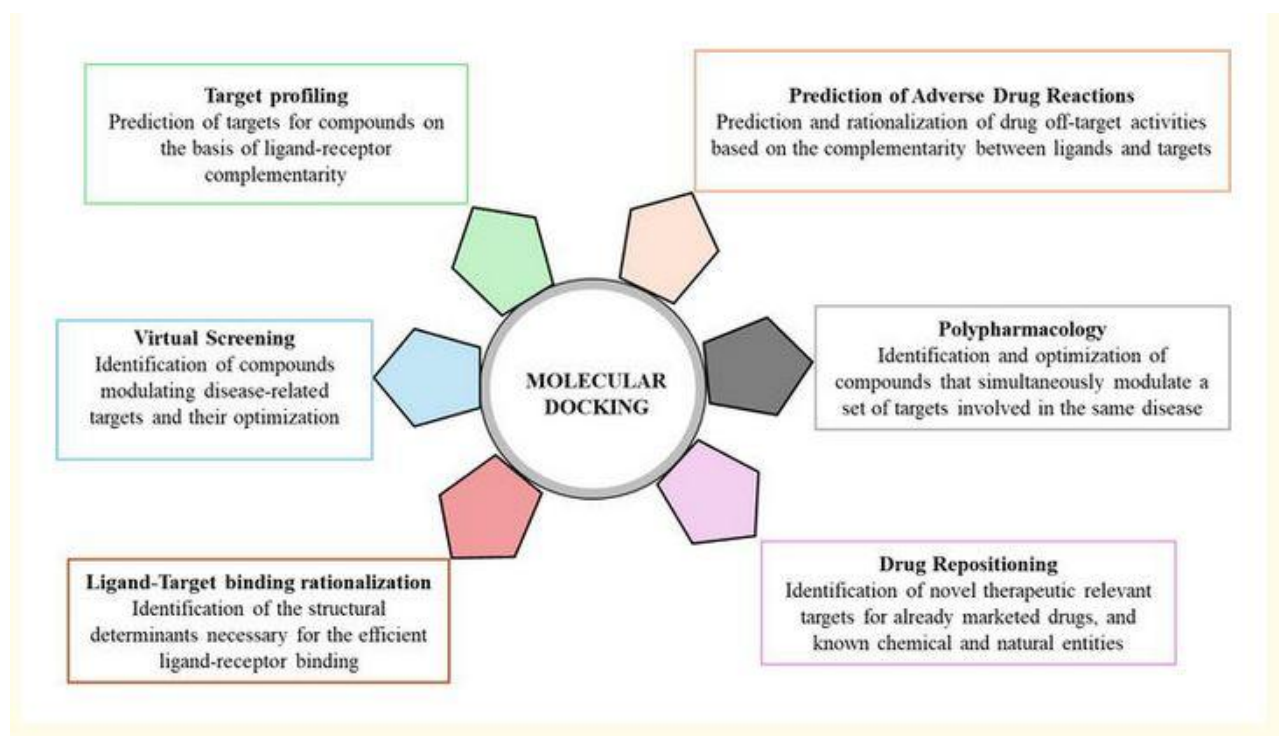


**Figure 2.7:** Applications of molecular docking in drug discovery and development

Besides the various applications of docking in drug discovery, they have also been used in target fishing and target (identifying a series of targets for which the ligands exhibit desirable complementarity, drug repositioning (identifying uses of novel pharmaceutical products with already optimized profiles), and in polypharmacology (identification of ligands that simultaneously bind to a pool of selected targets of interest (Mathur et al., 2024). Docking involves a combination of a search algorithm and a scoring function. Molecular docking is a method that employs various docking algorithms based on molecular dynamics, Monte Carlo, fragment-based, and genetic algorithms (Amit, 2019). The methodology used in molecular docking is as presented in Figure 2.8.

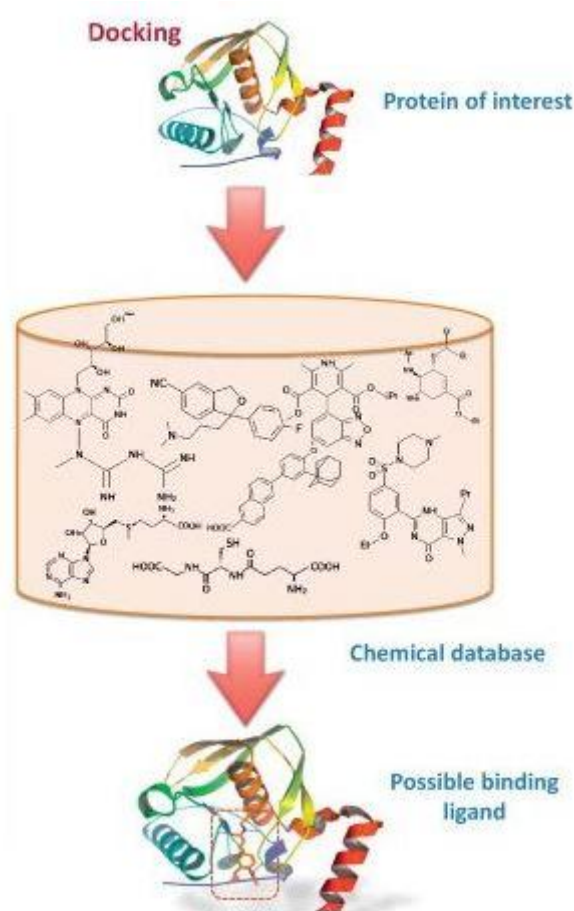


**Figure 2.8:** Molecular docking steps: conformation generation and scoring

Nevertheless, the shortcomings of docking are well-documented in the literature (Jakhar et al., 2020). Docking is associated with challenges, such as receptor flexibility, because a protein/biomolecule typically adopts a variety of conformations depending on the ligand with which it binds (Mathur et al., 2024; Zhang et al., 2024). Conformational states of proteins contribute to the better affinity achieved between the target and the drug (Friedman, 2022).

Another scientific challenge directly linked to docking is the imperfect scoring function, as scoring schemes often disregard electrostatic interactions and entropy, among other physical phenomena (Jakhar et al., 2020). Other studies have also reported that the success of molecular docking is hindered by an incomplete understanding of the underlying molecular protein-ligand binding mechanism, which involves various classes of ligands and modelling receptor flexibility (Mathur et al., 2024). Most docking software employs force field calculations that estimate binding energy guided by experimental data and quantum mechanics. Molecular dynamics (MD) and MM simulate motions of molecules and atoms in a complex (Badar et al., 2022). The binding affinity is estimated by computing the energy of the systems using force fields like GROMOS, CHARMM, or AMBER (Çınaroğlu & Biggin, 2021; Plazinska & Plazinski, 2021). However, it is known that accurate binding energies can only be obtained from *ab initio* methods such as MM simulations and DFT (Haikuo Zhang et al., 2021). Most docking programs remove protons (hydrogens) of inhibitors or enzymes under study, potentially excluding important information and leading to inaccuracies (Kaya et al., 2022). MD simulations have been coupled with docking to obtain important information on solvation and protonation on docking preliminary results (Santos et al., 2019). Remarkably, the cutting-edge advancement in force fields and MD simulations has improved the accuracy of these simulations.

The significance of bioinformatics within the context of drug discovery and development cannot be overstated. Enormous volumes of biological data from experimental studies, as well as genomic and proteomic data, have been studied and analyzed in bioinformatics. Molecular docking allows for the prediction of the interactions between the drug and the ligand. Additionally, structural biology and preclinical drug research have tremendously benefited from a combination of bioinformatics and docking algorithms (Noor et al., 2022). Also, in network pharmacology, these computational methods have been incorporated to improve hit identification, enhance docking results accuracy, and identify multi-target drug candidates. Also, machine learning and AI methods have been incorporated in drug research to study protein-ligand interactions (Okpo et al., 2024).

Nevertheless, bioinformatics and docking algorithms have drawbacks that demand careful attention in pre-clinical drug research. The scientific challenges of these methods extend beyond the widely reported conformational challenges because docking assumes the orientation of the protein, and the dynamic nature of ligand-receptor interactions makes it

difficult to achieve the desired accuracy. Furthermore, these simulations require high computational demands, which hinder large-scale virtual screening undertakings (Okpo et al., 2024). The frequently cited shortcomings of docking techniques include assumptions and simplifications in scoring functions that lead to inaccuracies; the programs fail to account for entropic, solvent, directional, and hydrogen bonding interactions (Mathur et al., 2024). Other limitations include issues related to conformational flexibility and structural flexibility, as well as inadequate resolution of crystallographic targets (Mathur et al., 2024).

## **2.5 Hybrid quantum mechanical/molecular mechanics in drug design**

QM method is a computational technique that models covalent and non-covalent intermolecular interactions (Aucar & Cavasotto, 2020). Computer experiments based on QM methods, such as *ab initio* molecular orbital or DFT, have been used to explore interactions of molecular systems of up to hundreds of atoms (Dawson et al., 2022). They have also been used to relate the structure of proteins and enzymes to their biological function. Reports by Chen et al. (2023) suggest that substrate-protein binding has been modelled by employing MM techniques. Successful preclinical research relies on the ability of computational methods to precisely and accurately model bond formation and breakdown, a capability that MM simulations lack. (Ye et al., 2022). Remarkably, QM is associated with widely reported scientific challenges prompting the researchers to combine MM and QM methods in the QM/MM model (Giese et al., 2022; Kar, 2023; Magalhães et al., 2020; Vennelakanti et al., 2022). Kar (2023) notes that integrating QM and MM simulations is invaluable for studying electrostatic interactions over time, which influence the electronic structures of biological macromolecules.

There are various computational tools that can be used for QM/MM simulations. For instance, AMBER and CHARMM are used for MM simulations while Gaussian is used for QM calculations (Tian et al., 2019). However, an effective way to perform QM/MM calculations is to jointly use the existing MM and QM packages with an interface program such as PUPIL, QoMMM, and ChemShell (Kang & Tateno, 2012). The hybrid QM/MM method enables a combination of computational abilities that each package possesses (e.g., algorithms for obtaining stationary points and optimal reaction paths on potential energy surfaces, implemented in QM packages, and algorithms for expanding conformational spaces sampled in MD simulations, executed in MM packages). The hybrid QM/MM approach is suitable for biophysical and biochemical mechanisms, as it combines the low computational cost of MM

(with additive classical force fields) with the high accuracy obtained from the QM part (with first-principles methods) (Kar, 2023).

Hybrid methods based on QM/MM have allowed researchers to study enzyme catalysis in drug discovery (Sharma et al., 2023; Sousa et al., 2017). They have also been used to gain meaningful insights into the binding between drug candidates and target proteins. The hybrid QM/MM calculations have also facilitated the determination of binding pathways, individual interactions, and the investigation of the ligand binding (Kumar et al., 2023). Furthermore, it has also been addressed how protein and solvent dynamics can affect the behaviour of drugs. As an example, Alonso-Cotchico et al. (2020) applied hybrid QM/MM to study the metalloenzymes during drug reactions. QM/MM hybrid methods can be used to study the influence of metal ions in enzymes, which can provide valuable information on the subject regarding metal-related toxicity (Kang & Tateno, 2012). Besides, tautomerization, protein design, and electron transfer during drug research (Kang & Tateno, 2012). Notably, QM/MM has been prevalently used to expedite the drug discovery process and to describe the ligand-receptor interactions (cf. Figure 2.9).

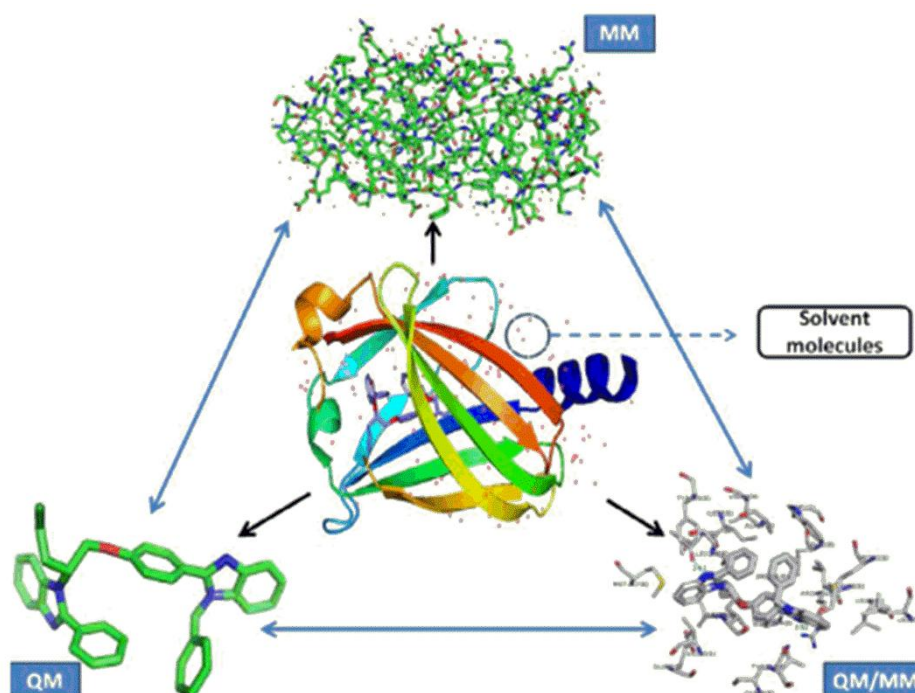


**Figure 2.9:** The partitioning of the protein-ligand complex into the MM applied region, QM applied region, and QM/MM applied regions (Omer et al., 2015)

The Hamiltonian operator is essential for quantum calculations and corresponds to the total energy of the system (Omer et al., 2015; Schwinn et al., 2020). Equation 2.1 is the Hamiltonian of the system.

$$H = H_{QM} + H_{MM} + H_{QM/MM} \quad 2.1$$

Here,  $H_{QM}$ ,  $H_{MM}$ , and  $H_{QM/MM}$  are the Hamiltonians accounting for all QM particles of the ligand, MM particles of the protein, and the interactions between QM and MM particles within the system, respectively. Simple functions, such as the Leonard-Jones potential, describe van der Waals forces at the MM level. Conversely, the electrostatic term enters the Fock Matrices as a self-consistent field method. The hybrid QM/MM calculations are divided into additive QM/MM coupling and substantive QM/MM coupling (Omer et al., 2015).

### 2.5.1 Subtractive and additive QM/MM coupling

Subtractive QM/MM coupling includes three steps in calculating the energy of systems: calculation of the total energy at the MM level, the addition of QM energy of the isolated system, and calculating the energy value of the MM system and subtracting this value (Yusef Buey et al., 2022). It is a simple method that mainly uses the ONION method in calculations. However, it is limited by the need for a flexible force field to describe the effects of chemical changes during reactions. Moreover, modelling biological charge transfer is challenging due to the absence of polarization by the MM environment on QM electron density (Omer et al., 2015).

Generally, the QM system is within the MM system; thus, the sum of MM, QM, and QM/MM energy terms gives the total energy of the system. The expression for additive QM/MM coupling is as shown in Equation 2.2.

$$\frac{V_{QM}}{MM} = V_{QM}(QM) + V_{MM}(MM) + \frac{V_{QM}}{MM}(QM + MM) \quad 2.2$$

According to Pérez-Barcia et al. (2023), various interactions have been described by these methods, including electrostatic, mechanical, and polarization embedding. It is worthwhile to note that mechanical embedding enhances QM/MM methods by accounting for mechanical degrees of freedom. Pérez-Barcia et al. (2023) point out that mechanical embedding also enhances the capability of QM/MM methods by treating electronic interactions quantum mechanically and describing molecular deformations and vibrations. However, mechanical embedding has limitations: it requires accurate MM parameters for MM and QM systems and

ignores the perturbation of the electronic structure of the MM system (Omer et al., 2015). According to Rivera et al. (2019), polarization embedding accounts for the influence of the surrounding polarizable environments on the quantum regions. Electrostatic embedding is used within the ONIOM framework. It does not require MM or QM electrostatic parameters as in mechanical embedding and offers a more sophisticated treatment of electrostatics (Rivera et al., 2019). The hybrid QM/MM methods have been employed in drug design. For instance, Tuttle (2012) used this approach to investigate the binding modes of Latrunculin A, Latrunculin B (a naturally occurring analogue), and synthetic L32 to G-actin. The research group concluded that L32 exhibits biological activity similar to that of naturally occurring latrunculins.

## **2.6 Drug metabolism predictions for drug design**

Drug metabolism scientists have been able to control the pharmacokinetic profiles of drugs, such as half-life, through metabolism-guided drug design, thereby reducing attrition rates (Hwang et al., 2023; Kramlinger et al., 2022; Wang et al., 2023). The well-established *in vivo* and *in vitro* methods, along with the *in silico* computational predictions, have been fundamental in reducing toxicological factors at early stages. Studies have shown that drug toxicity is mainly due to their metabolites, either as a result of free radicals or reactive electrophiles (NASSAR, 2022). Therefore, identifying potential liabilities in new chemical series is arguably one of the critical roles of preclinical drug metabolism prediction. To date, many chemical compounds with therapeutic effects have been identified from quantum chemical, docking, and MD calculations. Pharmaceutical companies have leveraged *in silico* tools, such as Autodock, combined with other methods to introduce drugs to the market (Agamah et al., 2020). Lead optimization for optimal pharmacodynamics (PD) and pharmacokinetics (PK), along with the comparison of preclinical metabolism in animals to humans to support human dose prediction, are the main breakthroughs in medicinal chemistry to date (Yadav et al., 2021).

The two phases of drug metabolism – phase I and phase II metabolism are well documented in the literature (de Bruyn Kops et al., 2020; Eddershaw & Dickins, 2021; Farrukh et al., 2024; Guo et al., 2021; Hassenberg et al., 2020). Typically, phase I metabolism involves hydrolysis, reduction, and oxidation of the drug, which produces metabolites that can be toxic, active, or inactive (Eddershaw & Dickins, 2021). On the other hand, phase II metabolism involves the conjugation of the modified drug with another molecule, such as an amino acid, sulfate, and glucuronic acid (Farrukh et al., 2024). Phase II metabolism increases the water solubility of the drug, easing its excretion. Various enzymes are responsible for these phases of metabolism.

The cytochrome P450 (CYP) family of enzymes carries out phase I metabolism. In contrast, a variety of enzymes, such as glutathione S-transferases (GSTs), sulfotransferases, and UDP-glucuronosyltransferases (UGTs), carry out phase II metabolism (cf. Figure 2.10) (Tran et al., 2023). Various factors, including disease status and individual characteristics such as age, genetics, and sex, influence drug metabolism (Valodara & SR, 2019).

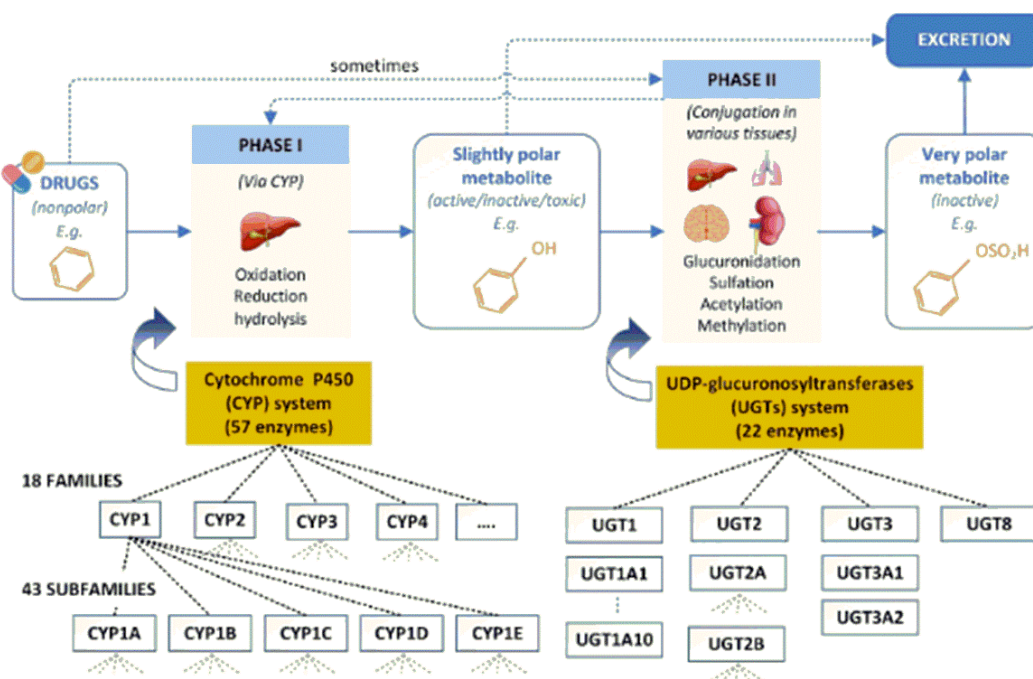


**Figure 2.10:** Phase I and Phase II drug metabolism (Tran et al., 2023)

Figure 2.10 depicts CYP-mediated metabolism, which accounts for 75% of the overall metabolism. The human CYP family comprises 57 isoenzymes, and CYP-mediated metabolism plays a significant role in drug discovery and development, as it significantly affects the safety profile, desired activity, and bioavailability (Jamwal & Barlock, 2020; Tran et al., 2023). These enzymes are highly concentrated in the liver, where the majority of drug metabolism occurs (Jamwal & Barlock, 2020; Zhao et al., 2021). Evidence in the literature suggests that a drug-drug interaction, resulting from the co-uptake of two drugs, where one is an inducer and the other is an inducer of drug metabolism, may have adverse pharmacological effects on the body (Bettonte et al., 2022; Malki & Pearson, 2020). For this reason, enzymatic metabolic studies are crucial for identifying and quantifying primary metabolites, assessing potential drug-drug interactions, and determining metabolic stability (Krishna et al., 2021).

The prediction of sites of metabolism and metabolite structures in CYP-mediated reactions is primarily employed in silico, with AI approaches serving as the starting point of the metabolic research pathway leading to lead optimization (Tran et al., 2023). There exist vast software tools to predict sites of metabolism, including BioTransformer, FAME 3, GLORYx, CypReact, PreMetabo, virtual Rat, FP-ADMET, and Cyproduct (Tran et al., 2023). These software employ various methods, including rule-based, machine learning (ML), knowledge-based, and Random Forest, among others. Table 2.3 summarises the public metabolism tools and their corresponding methods (Tran et al., 2023).

**Table 2.3:** Software tools that have been used to predict sites of metabolism and their corresponding methods

Name	Metabolism prediction	Methods	Ref.
Biotransformer 3.0	Metabolic transformation	Knowledge-based/rule-based ML	(Djoumbou-Feunang et al., 2019)
Cyproduct (CypReact, CypBom, MetaboGen)	Reactant, CYP, structure	BoM for metabolic ML	(Tian et al., 2021)
PreMetabo	Phase I and II sites of metabolism for CYP, UGT, and SULT	Arrhenius equation and EaMEAD model	(Hwang et al., 2020)
GLORYx	Metabolite structure	ML	(de Bruyn Kops et al., 2020)
FAME 3	Phase I and II sites of metabolism for CYP	ML	(Šícho et al., 2019)
Virtual Rat	CYP inhibitors	Random Forest	(Hsiao et al., 2021)
FP-ADMET	CYP inhibitors and substrates	GCNN	(Venkatraman, 2021)

### 2.6.1 The role of machine learning algorithms in drug metabolism prediction

The metabolic reactions mediated by enzymes in the human body can transform the administered drug into metabolites that exhibit different biological activities (Zhao et al.,

2021). The effect of metabolic reactions in deactivating the administered drug cannot be overlooked (Litsa et al., 2021). At the same time, metabolism is essential for the formation of active substances in prodrugs (biologically inactive compounds). To this end, the metabolic fate of drug candidates requires thorough investigation. The growing body of literature on drug metabolism has made data available, and machine learning (ML) models, such as Random Forests and Support Vector Machines, have become the primary choices for faster inference (Litsa et al., 2021). Rule-based methods have been used in conjunction with ML models to predict drug metabolism, thereby reducing false positives and filtering out unlikely predictions. The recent ML models are trained on data to cover the entire human metabolism, including endogenous compounds. For instance, researchers have utilized Graph Convolutional Neural Networks to gain insights into molecule interactions with the enzyme (Jiménez-Luna et al., 2020). These models also predict reaction outcomes and provide valuable insights into reaction mechanisms (Schwaller et al., 2021).

However, Litsa and others (Litsa et al., 2021) reported that current ML approaches used in metabolism prediction of drug candidates are based on shallow ML models and primarily classification models for distinguishing between sites of metabolism and non-sites of metabolism, as well as enzyme binders and non-binders. Additionally, existing ML models often fail to provide valuable insights into why and how a prediction is made, similar to computational approaches. ML models also suffer from limitations related to inconsistent labeling of the sites of metabolism due to various factors. Additionally, these models are unable to distinguish between primary and secondary metabolites (Litsa et al., 2021). These issues often deter medicinal chemists from taking an active role not only in developing novel models for predicting drug metabolism but also in the comparative assessment and evaluation of methods.

## **2.7 Case example of drug pharmacokinetics with cancer cells**

Cancer is the most challenging and devastating disease, threatening the health and life of millions of people. It is the prominent cause of high mortality rates in the world. Cancer develops when abnormal cells proliferate and invade surrounding tissues, eventually spreading to body organs and other parts of the body through the lymphatic and circulatory systems (Sriharikrishnaa et al., 2023). Several strategies, including hormonal therapy, radiation therapy, chemotherapy, immunotherapy, and surgery, have been employed in the fight against cancer (Sriharikrishnaa et al., 2023). Despite these strategies being effective in fighting cancer cells,

they are known to have potential toxicity, accompanied by adverse drug reactions, pain, and cost, limiting their application in clinical settings and public health in general (Anand et al., 2023). Furthermore, the risk of tumours acquiring multidrug resistance prompts medicinal chemists to develop efficient, safer, and novel antitumor agents for fighting cancer (Nussinov et al., 2021). Pharmacokinetic (PK) studies are often conducted to determine the optimal schedule and dose of treatment for a drug, the relationship between drug concentrations and functional or biochemical effects, the route of administration, and potential drug interactions when more than one drug is administered (Ge et al., 2023).

In the current drug development paradigm, animal studies provide a framework for human clinical trials (Ma et al., 2021). However, a drug that works in animals may be ineffective in humans due to the inappropriate translation of a drug dose from animals to humans (Ge et al., 2023). Scientific experts in the pharmaceutical industry utilize pharmacodynamics (PD, effect vs. time) and pharmacokinetics (PK, concentration vs. time) to design optimal drug therapies and discover new treatments for combating cancer cell growth (Ge et al., 2023). While PD has been defined as “how the drug affects the body”, PK has been described as “how the body handles the drug”. Accordingly, PK/PD data are becoming more available in the literature and, consequently, have piqued significant scholarly attention from industry, academia, and regulatory authorities as an advanced method for exposure-response analysis (Zhu et al., 2023). Often, a combination of therapies is used to treat cardiovascular diseases, cancer, and infectious diseases.

Research activities in developing anticancer treatments have yielded desirable outcomes, but many of these drugs have been reported to have significant systemic toxicity (Aggarwal et al., 2023). This challenge is attributed to the drug’s lack of selectivity, which affects healthy tissues and cells that undergo rapid turnover, resulting in toxicity. For instance, approximately 30% of colorectal cancer patients develop tumour metastasis, therefore posing a significant challenge in diagnosis and treatment (Ge et al., 2023). Whereas chemotherapy is known to be a conventional treatment for patients with this type of cancer, the therapeutic benefits are limited by toxicity to standard drugs and drug-drug resistance (Knezevic & Clarke, 2020; Roy et al., 2020; Sharma et al., 2022). Capecitabine (CAP) is a tumour-selective pro-drug which has been approved by the Food and Drug Administration (FDA) for the management of pancreatic cancer, breast cancer, gastric cancer, and colorectal cancer, tumours known to be resistant to 5-fluorouracil (5-FU) among other malignancies (Courtin et al., 2013; Ge et al., 2023). CAP is

an oral chemotherapy, tumor-selective pro-drug that is preferentially converted to 5-FU (the most active compound) in targeting tumor tissues via three metabolic steps (Zhang et al., 2021). After oral administration, CAP is absorbed in the intestine and metabolized to 5'-deoxy-5-fluorocytidine (5'-5'-DFCR) by the carboxylesterase (CES) enzyme, which is located in the liver (Ge et al., 2023). The ubiquitous enzyme cytidine deaminase (CyD) then converts 5'-DFCR to 5'-deoxy-5-fluorouridine (5'-DFUR). Finally, 5'-DFUR is then converted to the toxic and active metabolite 5-FU by thymidine phosphorylase (TP) (Figure 2.11), which is more concentrated in solid tumours than normal adjacent tissues, decreasing the effect of 5-FU on normal cells.

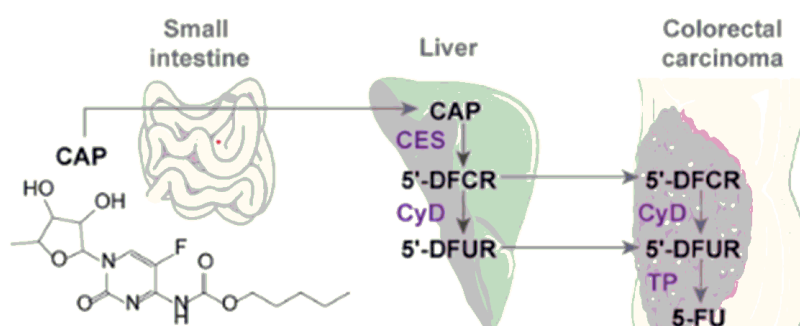


**Figure 2.11:** The structure of CAP and metabolic conversion of CAP to 5-FU (Ge et al., 2023)

Previous scholars conducted a pharmacology study on CAP to assess the clinical pharmacokinetics and disposition of CAP and its metabolites, 5'-DFUR, 5'-5'-DFCR, and 5-FU. The objective of their research was to establish the first and steady-state PK values, such as area under the curve, maximum plasma concentrations ( $C_{max}$ ), volume of distribution ( $V_d$ ), and clearance (Cl) of CAP and its metabolites (Alqahtani et al., 2022). The authors indicated that CAP and the metabolite PK were linear and time-dependent in the range of dosage (500–3500 mg/m<sup>2</sup>/day) of cancer patients. The paper also concluded that low CAP represented a tolerable response rate, which could also indicate that there is no always a need to use high doses of CAP to reach the therapeutic effect (Alqahtani et al., 2022).

There is a growing body of literature in the oncology field indicating that PK-PD studies have played a critical role in personalizing the drug dosage regimen to reduce toxicity and to elicit desirable pharmacodynamic conditions (Cardoso et al., 2018; Crombag et al., 2016; Ioele et al., 2022). Rodríguez-Gascón et al. (2021) and Yu et al. (2020) state that the impediments

directly associated with PK-PD studies include the complexity of PK-PD data, variability of drug metabolism, response, and distribution (Rodríguez-Gascón et al., 2021; Yu et al., 2020). These inhibit the extrapolation of experimental to real life applications. Moreover, the interpretation of anticancer drugs based on PK-PD data is not straightforward and is costly, which hinders the extrapolation of PK-PD investigations in the preclinical drug development.

## **2.8 The accuracy of DFT in drug design**

Hartree-Fock (HF) approach does not consider electron correlations and can thus not be effective in describing the properties of drug candidates in particular (Tandon et al., 2019). On the same note, configuration interaction (CI) and Møller-Plesset perturbation (MPn) theory which belongs to the post-Hartree-Fock methods is flawed by being too expensive to be calculated considering electron interactions. Compared to CI, HF, and MPn methods, DFT has been cheap and highly accurate in its computation (Tandon et al., 2019). Consequently, DFT has gained a massive academic attention among the researchers (Bakheit et al., 2023; Noureddine et al., 2020). Tandon et al. (2019) identify that DFT has proven to be effective in the study of geometries of smaller drug molecules, which makes it appropriate in drug design.

The energetic properties including ionization energies and the strength of metal ligand bonds are also part of the energetic features that are to be studied in DFT studies (Mollaamin & Monajjemi, 2023; Tandon et al., 2019). The chemical structures of the lead candidates dictate the interactions of the compounds with the receptors. DFT, therefore, has been effective in the prediction of the relative conformational energies in drug research (Bursch et al., 2021). As has been reported in many studies, potential interactions between a drug and a receptor are charge transfer, dipole-dipole interactions, ionic interactions, ion-dipole interactions, covalent bonds, hydrophobic interactions, and hydrogen bonding (Chandrasekar et al., 2020; Jayashankar et al., 2022; Srivastava, 2021). The covalent, ionic and hydrogen bonding are reasonably predicted with DFT method (cf. Figure 2.12), but interaction of weaker bonds is difficult to predict (Huang et al., 2022).

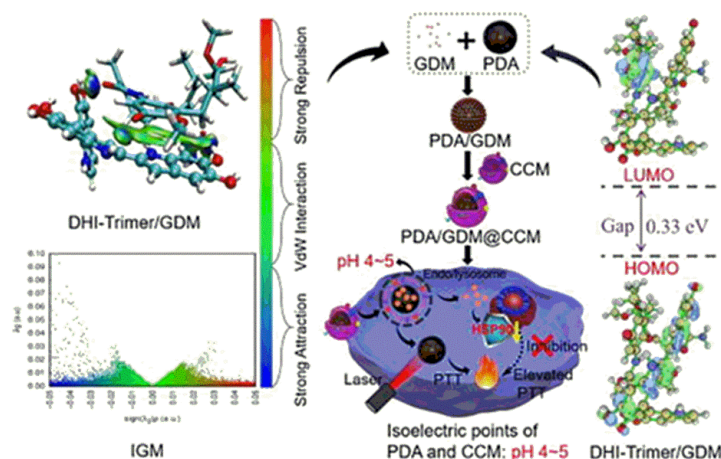


**Figure 2.12:** The DFT method (B3LYP and CAM-B3LYP) in drug design (Huo et al., 2021)

Quantum chemistry software packages such as ADF employ DFT in electronic structure calculations and elucidate spectroscopic properties such as nuclear magnetic resonance (NMR), infrared (IR), and vibrational frequency spectra (Ji et al., 2020; Sajid & Addicoat, 2023). Furthermore, ADF can also be used for molecular geometry optimization, to explore the role of catalysis in reactions, and to study the reaction channels and activation energies of the systems being studied (Vermeeren et al., 2020). A significant number of research reports have demonstrated that DFT has been utilized for structure elucidation and modelling the interactions between the drug and the receptor (Akkoc et al., 2023; Rajee et al., 2023; Sabe et al., 2021).

Remarkably, B3LYP and CAM-B3LYP are two DFT-based energy functionality, which are employed in the prediction of the lead-candidates (Huo et al., 2021). Huo et al. (2021) also state that the experimental value of the binding affinity is placed on the x-axis and the calculated values of the binding affinity are obtained on the y-axis to the aid of the two DFT methods. The more the figures are close to the diagonal line, the more accurate their structures and prediction of binding affinity as they are more closely approximated to experimental data. Both approaches, as identified in the graph, are marked by high-performance, when it comes to predicting the structural accuracy, as well as binding affinity (Huo et al., 2021). The CAM-B3LYP approach however is marginally losing its performance to the B3LYP as far as results are concerned. The efficiency of DFT techniques and their use in drug design is measured by the correct binding affinity of the ligand, which determines its ability to predict the correct binding affinity (Tandon et al., 2019; Ye et al., 2022). This is a necessary prediction in the new and efficient drug development. The image is also a pointer to the saving in time and cost that

is entailed in the traditional method of designing the drug through DFT. Huo et al. (2021) stated that it could be achieved with the help of adequate computational predictions.

### **2.8.1 Deficiencies of computational methods in pre-clinical drug design**

It is well-established in the literature that each *in silico* method has its application scope and features (Brogi et al., 2020; Shaker et al., 2021). Therefore, in drug design and development, it is essential to select appropriate methods for accurate prediction; however, some methods have limitations that may impact the accuracy of the predicted results. Theoretical limitations associated with various approaches, including ADMET, QSAR, cavity prediction, pharmacophore building, modeling, and structure optimization, have been reported (Gramatica, 2020). Molecular modeling has been widely used in identifying possible interactions between metabolic enzymes and compounds, as well as predicting metabolism (Raunio et al., 2015). However, it is known that the scoring function in molecular docking affects the accuracy of ADMET prediction (Hasan et al., 2022).

On the other hand, the accuracy of data modeling methods such as QSAR depends on the quantity and quality of data (Gramatica, 2020). These models cannot predict chemicals outside the chemical space in which they were developed. Furthermore, the simplistic nature of data models limits their ability to predict drug interactions and behavior in a whole system. QSAR prediction methods assume that similar molecules have similar properties; however, in other instances, such as CYP metabolism, similar molecules exhibit different activities (Sheridan et al., 2004). Accordingly, ADMET software has been widely used in predicting multiple properties and qualitative analysis of compounds (Cheng et al., 2013). However, it cannot give an accurate prediction of quantitative values (Gola et al., 2006).

DFT, on the other hand, has been important in drug design and development but has its limitations. The DFT computation approach introduces errors for systems with dispersion interactions and electron correlation (Gräfenstein & Cremer, 2009). DFT, in particular, diffusion quantum Monte Carlo (DQMC) is also associated with high computational requirements in terms of time and cost; thus, medicinal chemists often prefer lower-level computational methods (Kent et al., 2020; Malone et al., 2020). Incorrect choices of binding sites for ligands can lead to false DFT results, thereby affecting the accuracy of the approach. Another notable challenge is that for a drug candidate to be licensed as an effective drug or lead, it has to satisfy various therapeutic necessities. CADD relies on predefined codes, algorithms, and theoretical parameters/principles (Chandershekar et al., 2020). Therefore, all

CADD tools used for pharmacophore modeling, QSAR, virtual screening, molecular modelling, and MD have both limitations and merits (Chandershekar et al., 2020). These models are supported by knowledge and experimental data to ensure the accuracy of the models (Rajkishan et al., 2021). Khandelwal et al. (2005) feel that the hybrid QM/MM procedures are limited by the lack of novel approaches of virtual screening and costly computing support. Such methods are also believed to be effective in the study of the multidrug-protein interactions as well as large scale molecular dynamics. It has also been mentioned that these hybrid techniques do not have the capability of resolving conformational changes and binding modes (Ahmadi et al., 2018). However, it is known to be accurate where QM calculations using large-scale conformational sampling at large systems are costly to calculate (Vennelakanti et al., 2022).

## **2.9 Use of artificial intelligence in drug design**

It should be mentioned that the aspects of drug research have changed considerably due to the emergence of artificial intelligence (AI). Computational resources have been used along with AI to aid in the process of lead identification. Drug research has been cost effective, precise and more efficient today due to the use of technologies. To this extent, AI will allow researchers to have the ability to validate their findings without having to go to the wet lab. The studies by Brown et al. (2020), Jimenez-Luna et al. (2021), and Lin et al. (2020) hypothesize that the conventional drug discovery process is a time-consuming and expensive one. Nevertheless, AI is innovative because it can effectively filter a substantial number of compounds and analyze their structural and chemical features to research the relationship between them and their respective targets (Brown et al., 2020). This will allow the researcher to narrow the list of compounds, and develop the most important ones. The main mode of analyzing chemical substances with the application of AI is by using algorithms and computer simulation. Using these methodologies, scientists can also test a large number of potential medicines more precisely than the traditional ones (Jiménez-Luna et al., 2021). Jiménez-Luna et al. (2021) also clarify that this has the ability to assess the performance of bioactive compounds and give more precise predictions that have saved resources and avoided potential risks. Using AI in computational drug design enables the access to a state of a considerable chemical space that hosts various compounds and elements. Schneider et al. (2020) explain that the high cost and time-consuming nature of developing and testing a single drug led to the fact that the drug research processes been focused on researching a few substances. However, with the

combination of AI and computer technology, today, the number of compounds that can be tested is unlimited, which raises the chances of discovering a powerful and safe prospect of a drug (Schneider et al., 2020).

Prediction of chemical and physical properties of a lead compound are of paramount importance by AI during preclinical research. Some of the properties that should be measured clearly and subsequently submit the compound to subsequent studies are its safety, possible interactions, and solubility in water (Schneider et al., 2020). The scientists utilize this information to make changes in the composition of the compound so that it can perform better and have better changes of achieving the required outcomes. Jiménez-Luna et al. (2021) claimed that researchers can design and optimize drug delivery systems with the help of AI taking into account the particle size, the degree of its surface charge, and the release rate dynamics. The personalization of the drug delivery system i.e. particular pharmacological condition, could also be facilitated through the aid of the AI and computational tools that would allow the researcher to tailor a drug delivery system. The articles by Schneider et al. (2020) demonstrate that pharmacogenomics is a practice implemented by utilizing the genetic information of a patient and assessing the response of the patient to the drug and the ability of the drug to act on the existent patient. The fact that AI and computational approaches can help in finding disease-specific biomarkers and, as a result, develop a particular treatment method is impressive (Jiménez-Luna et al., 2021; Patel et al., 2020; Schneider et al., 2020).

Along with the mentioned advantages of AI and computational resources that have become widely reported, there are also challenges. According to reports by Panwar et al. (2019) and Patel et al. (2020), the techniques are reliant on the accuracy of the data applied in the programming of the AI. Another drawback is the limitations linked to the bias in data, or incomplete data may lead to wrong model projections (Panwar et al., 2019; Patel et al., 2020). Even though these technologies are able to forecast the performance of a lead compound prior to the preclinical trial, researchers should ensure that the information is not biased (Patel et al., 2020). Moreover, AI and computations explain certain chemical reactions and biological pathways. Although such techniques are capable of forecasting the behaviour of a compound, in some conditions, they do not provide details about the behaviour of such drugs in a live system. Nevertheless, these issues can be solved through conducting experimental validation to obtain more precise results (Panwar et al., 2019).

According to Batool et al. (2021), *in silico* studies have been successfully applied in drug design, which has numerous successful applications of AI. Indicatively, Batool et al. (2021) find that during the discovery of an HIV protease inhibitor darunavir, computational technology was employed to design and screen a library of compounds that could be used as potential inhibitors. Chuntakaruk et al. (Chuntakaruk et al., 2024) used computational techniques to study the ligand-protein interaction of darunavir with HIV-1 protease. Protease inhibitors are feasible; 19-0-14-3, 19-8-10-0 and 19-8-14-3 were three analogues of darunavir, they indicated. Consequently, we have discovered darunavir which is currently frequently used to treat HIV. On the same note, a vaccine known as Relenza, which helps prevent influenza, was developed with the help of computational techniques, which assisted in determining the binding affinity of the medicine with the viral protein (HIV-1 protease) (Batool et al., 2021). Figure 2.13 illustrates the integration of AI in drug research, and the different emerging uses of AI in the pharmacology studies. The drug discovery process can be divided into four main components: drug design, polypharmacology, drug repurposing, and drug screening (Patel & Shah, 2022).

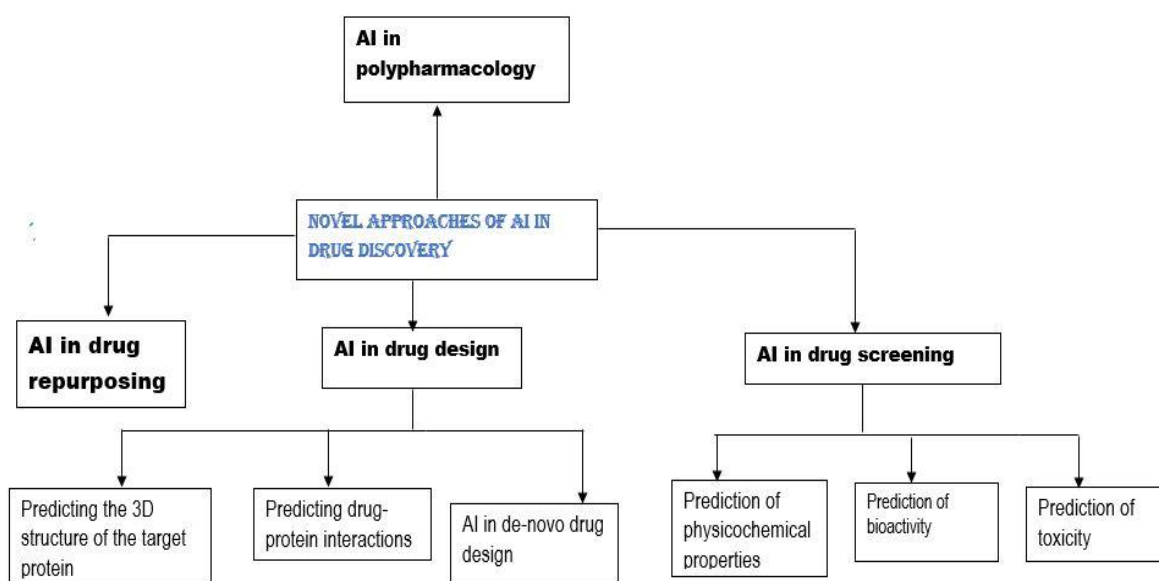


**Figure 2.13:** Application of AI in various aspects of the pharmaceutical industry in the context of drug design (Patel & Shah, 2022)

A review of literature shows that AI finds major applications in the identification of lead candidates, as well as their properties. Accordingly, this can reduce the need for clinical trials and the involvement of live study participants. Such a development would bring benefits from both financial and ethical perspectives. This section discusses the studies identified in this

review that support the integration of AI into the drug discovery procedure. These studies highlight how AI can improve efficiency, accuracy, and productivity (Patel & Shah, 2022).

### **2.9.1 Limitations of the AI approach in pre-clinical drug research**

There is a significant advancement in *de novo* drug design attributed to the emergence of computing technologies and AI, according to Gupta et al. (2021) and Vijayan et al. (2022). QSAR modeling, and synthesis planning, among other crucial pre-clinical research activities, have benefited from AI and computational techniques. However, the efficiency of AI in accelerating drug research is yet to be reported. There are associated problems that impede the integration and implementation of these technologies in search of compounds with therapeutic properties. One of them is inefficient data integration due to the diversity of datasets, which comprise raw data, metadata, candidate data, race data, or processed data (Patel and Shah, 2022). To be analyzed in an efficient way, such datasets should be collated or collected, and at present, there is no means of doing so. Schneider et al. (2020) are able to conclude that the existing AI systems tend to provide misleading outcomes without properly structured data. Second, the inability of occupational specialists to move because many scientists in the medicine chemistry field do not possess the skills and competencies to operate and interpret AI systems (Patel and Shah, 2022). The second issue is a significant problem is the insufficiency of funding to develop innovative AI systems in drug discovery and development (Belousova et al., 2020). The reluctance to invest in AI can be explained by the doubts in the outcomes of machine learning and AI in drug research that stalls the AI-relevant developments (Patel & Shah, 2022). A lack of understanding of the methodology in AI systems leads to distrust, and researchers may be skeptical about using this technology, which could hinder the industry's progress over the next few years (Patel & Shah, 2022; Starke & Ienca, 2022).

### **2.10 Conclusions and outlook**

Over the past decade, the rate of identifying disease-associated targets has been higher than that of identifying novel compounds with promising therapeutic effects. There is a drastic increase in computational methods, such as docking or virtual screening, and MD, that have accelerated drug design and discovery methods in the pharmaceutical industry. Well-developed computational tools have been utilized in the pharmaceutical industry and academia, demonstrating success and offering remarkably promising prospects for providing a faster and more cost-effective approach in the drug discovery landscape. Nowadays, structure-based

methods are widely used in studying protein targets. Molecular docking and MD simulations are prominent examples of these methods, which have been applied in characterizing binding sites and determining the thermodynamics and kinetics involved in ligand-target recognition. The biological activity of active compounds has been identified and enhanced by the use of ligand-based techniques like QSAR. Remarkably, CADD has various applications, including the identification of hit compounds, lead optimization, and the investigation of the ADME (absorption, distribution, metabolism, and excretion) profile of drug candidates. Considering optimization of drug candidates as a consequence of decisions made in identifying the potential target and dosing regimen, AI and computational techniques can help with these choices.

The field of medicinal chemistry will continue to advance in drug design and development, making the complex and tedious process effective and affordable. There is an increase in the number of pharmaceutical companies using these approaches, and plenty of opportunities exist for more research activities. Notably, drug discovery and design rely on human expertise and the combination of CADD and human intelligence for success. CADD approaches are known to have vast computational capabilities in conducting unsupervised analysis of databases; human judgment and input are necessary to consider ethical concerns related to drug research. Human expertise is also required to validate real-world clinical studies and wet-lab experiments. All classical and new methods, when combined with existing computational disciplines, are given an advantage at nearly every stage of drug discovery and development. With the required expertise in biophysics, biochemistry, and biology, significant investment in time and resources, and the availability of necessary computational software and hardware, drug discovery has become a more affordable task in the pharmaceutical industry and research institutions. Accordingly, we foresee the impact of computational chemistry in the form of accelerated drug discovery and the reduction of attrition rates due to negative ADMET results.

With the entry of AI in the field of drug design and development, the drug industry will be inspired to develop drugs not only in a faster manner but also drugs that can target complex diseases with high accuracy. The synergistic application of computational tools and AI technologies has contributed to public health improvement and alignment with the United Nations' SDG 3 on good health and well-being. The AI-driven predictions have enabled medicinal chemists to tailor cancer management regimens to patient characteristics, such as drug response patterns and tumor heterogeneity, thereby reducing potential adverse reactions and promoting global access and equity.

## CHAPTER THREE

### COMPUTATIONAL SIMULATION OF THE BIOACTIVITY OF SELECTED COMPOUNDS DERIVED FROM *SAPIUM* AND *SALVIA* GENUS AS ANTI- CANCER AGENTS

#### **Abstract**

Research on cancer management is rapidly progressing and geared towards natural products. This research presents studies of bioactive compounds from *Salvia miltiorrhiza* Bunge and *Sapium ellipticum*. *In-silico* and *in vitro* analysis of ellagic acid (EA), [20-<sup>3</sup>H] phorbol-12, 13-dibutyrate ([<sup>3</sup>H] PDBu), and [20-<sup>3</sup>H]-12-deoxyphorbol-13-isobutyrate ([<sup>3</sup>H] DPB) have been performed. The molecular docking simulations showed that salvianolic acid B (Sal B) had a docking score of -39.75 kJ/mol, -28.87 kJ/mol, and -33.05 kJ/mol when targeting DNA lyase, topoisomerase II alpha, and mTOR, respectively. The findings of the study show that these docking scores were also similar to those of EA, exhibiting a docking score of -36.40 kJ/mol, -27.20 kJ/mol, and -31.80 kJ/mol when targeting DNA lyase, topoisomerase II alpha, and mTOR, respectively. Accordingly, Sal B has higher potency, approaching the docking score of rapamycin (-46.86 kJ/mol). Similarly, the *Sapium* bioactive compounds show moderate and limited interactions. Notably, Sal B is a potential anticancer agent with an IC<sub>50</sub> of 12-18 μM in PC-3 and DU145 prostate cancer (Pca) lines and 14-20 μM in MCF-7 and MDA-MB-231 breast cancer (BC) lines. Inhibitory potential was also promising in this compound and 95% inhibition was observed at 50 μM and an IC<sub>50</sub> of 14.8 μM. Sal B had high potency with the IC<sub>50</sub> of 11.6 μM which is almost equal to that of the standard inhibitor, rapamycin (IC<sub>50</sub> of 5.2 μM). With a similar IC<sub>50</sub> of 21.9 μM, ellagic acid (EA) was moderately inhibited. It is likely that the results obtained in this research provide a great lead to the development of therapeutic medicine against breast cancer (BC) and prostate cancer (PCa). Based on potential preventive and therapeutic effects of these bioactive compounds, there is an urgent need to undertake accurate clinical trials and *in vivo* studies to substantiate the effects.

#### **3.1 Introduction**

Recent research has also revealed that early diagnosis, the establishment and use of new medicines are critical in ensuring that cancer patients have desirable health outcomes (Dubey & Sikarwar, 2025). The management of breast cancer (BC) and prostate cancer (PCa) has

controversies and questions, which directly affect everyday practice. However, existing modalities of detection and intervention, which include magnetic resonance imaging (MRI), mammography, and ultrasound, are linked to specificity and sensitivity limitations, which makes the timely and precise diagnosis even more challenging (Abeelh & AbuAbeileh, 2024; Grasso et al., 2025). Biomarker abnormalities, enzyme proteins, and nucleic acids (microRNAs) (miRNAs), androgen receptor (AR), and Apurinic/Apyrimidinic Endonuclease 1 (APE1) (Antanciali et al., 2017; Malfatti et al., 2023; Sun et al., 2019). Pharmacological inhibition of DNA repair holds great promise in targeting genetic differences between tumours and normal tissues. Recent scientific reports have also suggested that pharmacological inhibition of deoxyribonucleic acid (DNA) repair spares normal cells while targeting the genetic vulnerabilities of cancer cells (Perurena et al., 2024). DNA base excision repair (BER) is involved in repairing DNA base damage induced by alkylating agents, including dacarbazine and temozolomide, as well as oxidative damage, spontaneous hydrolysis, and deamination (Alyafeai et al., 2024). DNA glycosylases are very important in base excision repair (BER), which detects and eliminates damaged bases, forming an apurinic/apyrimidinic site (AP site). Lee and Lee (2025) and Piscone et al. (2025) describe that apurinic/apyrimidinic endonuclease (APE1) subsequently introduces a nick of the DNA backbone at the AP site of the DNA by short-patch or long-patch BER cellular events, which recruit particular enzymes. APE1 has been found to perform other functions besides DNA repair, which are mitochondrial metabolism, biological functions that regulate redox homeostasis, and neo-vascularization. According to Hartman et al. (2021) and Mijit et al. (2021), APE1 is a promising target in diabetic macular edema (DME), inflammatory bowel disease (IBD), retinal ocular disease, cancer and chemotherapy-induced peripheral neuropathy.

By analogy, the contemporary methods of drug discovery have applied the molecular docking approach to predict the interactions of ligands (small molecules) with their target in order to help identify modulators or inhibitors of their activity (Nada et al., 2024; Siddiqui et al., 2025). The algorithms of molecular docking can be useful in the study of the repurposing of the available drugs, the search of the prospective drugs, the explanation of the drug-target interaction, and the design of the highly-active enzymes (Adelusi et al., 2022; Nada et al., 2024). The huge uses of molecular docking are essential to the ever-growing generation of reliable ligand-receptor modelling applications and scoring functionality. Apurinic/Apyrimidinic Endonuclease 1 (APE1) has also become a treatment modality in the

inhibition of breast and prostate tumour cells (Hartman et al., 2021). It is commonly observed to be overexpressed, and it also plays an important role in tumour regression, therapy resistance, and unfavourable clinical outcomes (Caston et al., 2021; Logsdon et al., 2018). The APE1 overexpression in BC is linked to the DNA repair of reactive oxygen species that enable the tumour cells to grow under oxidative stress environments that induce apoptosis in normal cells. This resistance ability of cancer cells to anti-cancer agents is associated with the increased DNA repair ability of APE1 (Ma et al., 2025). According to Caston et al. (2021) and Shah et al. (2017), secondary role of APE1 as transcription factor (TF) redox regulator facilitates cancer cell survival, cell metastasis, and angiogenesis.

According to research, topoisomerase II alpha is a key target for chemotherapy drugs that inhibit the proliferation of cancer cells. The clinically approved topoisomerase I alpha target includes belotecan, topotecan, and camptothecin analogue irinotecan (Martín-Encinas et al., 2022; Thomas & Pommier, 2019), while topoisomerase II alpha inhibitors comprise doxorubicin, pixantrone, etopophos, epirubicin, daunorubicin, amrubicin, idarubicin, amsacrine, and mitoxantrone (Maurya et al., 2025). Topoisomerase II alpha has major roles in the many physiological activities, such as DNA replication, transcription, and recombination, and helps release overwound DNA, which causes torsional tensions when strands separate (Maurya et al., 2025). Topoisomerase I alpha as well as topoisomerase II alpha (particularly, topoisomerase II alpha isoform) are both involved in cancer development because of their involvement in the maintenance of DNA topology during transcription and replication. According to Maurya et al. (2025) and Zerfas et al. (2019), serine/threonine protein kinases have been shown to control various cellular activities such as cell apoptosis, cell proliferation, cell survival, and cell activity. Over the past few years, this protein has already received a significant amount of academic interest as a possible therapeutic target in autoimmune diseases, viral infections, inflammation and neurological diseases, as well as in cancer of any type. Nonetheless, in spite of the growing body of evidence of both computational and experimental work, there is no universal recipe that helps to create new protein inhibitors. Therefore, many research projects are aimed at the creation of new key inhibitors. The importance of proteins in the diagnosis, treatment and prevention of cancer has been realized because they play a role in repairing DNA, cell growth as well as cancer survival. Other past scientific investigations have focused on enzymes in DNA repair such as mTOR (Fu et al. and Wu, 2023; Ihlamur and others, 2024; Son et al., 2024), topoisomerase II alpha (Kanagasabai et al., 2024; Matias-

Barrios et al., 2021; Swedan et al., 2023), and the DNA lyase have been used in cancer therapies.

In other pre-clinical trials, antioxidant activity of ellagic acid (EA) has been also reported; it inhibited the damages of DNA and counteracted free radicals, and can be considered as a potential agent which can be utilized in *Sapium ellipticum* as a natural analog in the treatment of cancer (Kanthé et al., 2021; Wang et al., 2022). It also inhibits topoisomerase II alpha, intercalates with DNA and indicates the possibility of being an anti-cancer agent which can interfere with the enzymes involved in the processing of DNA, including DNA lyase, and control the expression of APE1. Sal B is an anti-cancer agent that has potential to be used because of its capability to react with DNA, as well as possessing antioxidant properties. Sal B was also reported to prevent oxidative DNA damage and decrease the activity of DNA repair proteins like poly (adenosine diphosphate-ribose) polymerase 1 (PARP1), and x-ray repair cross-complementing (XRCC) protein (Lu et al., 2022). Tang and Zhao (2024) note that Sal B is a polyphenolic molecule that is extracted out of the roots of *Salvia miltiorrhiza* (also called Danshen). Sal B, chemically, is identified as (2*R*)-2-[(*E*)-3-[(2*S*,3*S*)-3-[(1*R*)-1-carboxy-2-(3,4-dihydroxyphenyl) ethoxy] carbonyl-2-(3,4-dihydroxyphenyl)-7-hydroxy-2,3-dihydro-1-benzofuran-4-yl] prop-2-enoyl] oxy-3-(3,4-dihydroxyphenyl) propanoic acid. It has multiple hydroxyl groups, which enable it to form metal ion chelation and hydrogen bonding, thereby interfering with the magnesium-ion-dependent catalytic activity of DNA lyases and enhancing apoptosis. Considering the widespread clinical use of Sal B in Asia and beyond, it is crucial to understand its mechanism to prevent complications and maximize its therapeutic benefits. These molecular properties of various bioactive molecules are characterized as biological, chemical, and physical (Egorova et al., 2017). The properties are determined and calculated using three computational methods: molecular mechanics, molecular dynamics, and quantum mechanics.

The current study aims to perform *in silico* and *in vitro* studies by examining the four drug candidates– EA, Sal B, [<sup>3</sup>H] DPB, and [<sup>3</sup>H] PDBu. Accordingly, they are promising candidates that can interact with APE1, topoisomerase II alpha, and serine/threonine-protein kinase mTOR in combating cancer-causing agents. Studies have shown that the topoisomerase II alpha enzyme is linked to the AR in PCa and is associated with tumour progression. Also, in BC chemotherapy, topoisomerase II alpha inhibitors are employed. PCa progression is also associated with the DNA lyase enzyme, particularly edenylosuccinate lyase (ADSL), and

oxidative DNA damage repair enzymes are linked to BC aggression (Li et al., 2021). Conversely, mTOR is targeted in BC management to overcome resistance (Li et al., 2021) and is known to drive the growth of prostate cancer (PCa) (Chen et al., 2024). In this coupled theoretical and experimental study, molecular docking and *in vitro* studies were performed to elucidate the docking scores and the inhibitory potential of the ligands against PCa and BC cell lines. In this study, *in vitro* analysis has been used to study the anti-cancer activity of all compounds and validate the molecular dynamics and docking findings. The cell inhibitory effects of all ligands on cell lines were also investigated to identify the bioactive compound with potential anti-cancer effects targeting BC and PCa, as well as their efficacy against standard drugs.

## **3.2 Materials and methods**

### **3.2.1 Molecular docking studies**

#### **3.2.1.1 Ligand and protein preparation**

Ligands were retrieved from the PubChem database. The compounds from these medicinal plants, Sal B (CID: 119177), EA (CID: 5281855), [3H] PDBu (CID: 3778), and [3H] DPB (CID: 107855), were obtained from the PubChem database in .sdf format and then converted to mol2 using Open Babel version 3.1.1 before applying MMFF94 force field by Avogadro software (version 1.2.0) for geometry optimization. The optimized energy values of the ligands were -766.51 kJ/mol for Sal B, -638.90 kJ/mol for EA. [3H] PDBu had an optimized energy value of -582.41 kJ/mol, and [<sup>3</sup>H] DPB had an energy value of -564 kJ/mol. The minimized structures were converted to PDBQT format using AutoDock tools version 1.5.7 and then docked using AutoDock Vina version 1.2.3. The ligand structures were subjected to docking by setting the grid box on the coordinates of identified catalytic residues using AutoDockVina. The target enzyme structures with PDB ID: 1DE8 for APE1, implicated in DNA base excision, topoisomerase II alpha DNA complexed with etoposide with PDB ID: 5GWK, and serine/threonine protein kinase, mTOR with PDB ID: 4JSV were retrieved from Research Collaboratory for Structural Bioinformatics-Protein Data Bank (RCSB-PDB) (Ahmad et al., 2025; Burley et al., 2019; Burley et al., 2024) and subjected to pre-processing for docking. The three-dimensional (3D) structure of the protein was retrieved from PDB, downloaded in a .pdb file, and pre-processed. The preparation of the protein was performed using AutoDock Tools v1.5.7, where crystallographic water molecules were removed, polar hydrogen atoms were

added, and Kollman charges were assigned. Nitrogen atoms in their  $sp^3$  hybridization state were then protonated (made positive) and carboxyl groups were also deprotonated (made negative). The aim of this was to stabilize the charges and fill in the missing residues and produce the side chains based on the parameters that were available in the computing suite. After preparing a disease-causing protein, the active site of the protein was predicted. The receptor may possess numerous active sites, but only one significant pose was selected for analysis.

In most cases, water molecules and heteroatoms, if present, were removed to enhance the scoring measurements. To ensure accurate tautomeric configurations, the ligands were protonated at pH 7.4 before molecular docking. The grid box coordinates were set for x, y, and z axis as (127.768545, 28.633364, and 109.181545, respectively with center box 15 Å for DNA lyase ligand and a grid setting with dimensions of -18.968439 (x), -32.923976 (y), and -56.432976 (z), centered on the adenosine triphosphate (ATP) binding domain of the kinase, with a box size of 15 Å was used for mTOR protein. For the topoisomerase II alpha protein, the coordinates of etoposide and the amino acids involved in catalysis, with x, y, and z dimensions, are 23.790037, -37.327815, -55.582123, respectively. For all the docking calculations, the grid box coordinates were user-driven, relying on structural biology data. Exhaustiveness was set to 8 to obtain 10 poses per ligand. The AutoDockVina version 1.2.3 performed the docking and generated the results, which included the docking score expressed as kilojoules per mole (kJ/mol) with the corresponding 2D and 3D atomic structures. In addition, to ensure the reliability of the docking protocol, we tested the binding site determination by re-docking the co-crystallized ligands into their original binding pockets. The low RMSD values (less than 2.0 Å) obtained with the help of these controls provide evidence that the binding sites were correctly defined. The interaction analysis was visualized using Discovery Studio software version 21.1.0 to depict compound-protein interactions that involved pi-pi stacking, water-mediated interactions, hydrophobic contacts, and hydrogen bonds (Baroroh et al., 2023; Rustagi et al., 2025).

### **3.2.1.2 Calculation of chemical reactivity descriptor**

The optimizations of geometries, energies, and cocrystal structures were computed using Gaussian 09w software with density functional theory (DFT) and the Becke three-parameter Lee, Yang, and Parr (B3LYP) functional, along with a 3-21G basis set. Several suitable calculation formulas were employed to determine reactivity and chemical descriptors. The

optimization potential,  $I$ , was calculated using the formula,  $I = -\epsilon_{\text{HOMO}}$ , energy gap  $\Delta E_{\text{Gap}}$  from  $\Delta E_{\text{Gap}} = \epsilon_{\text{HOMO}} - \epsilon_{\text{LUMO}}$ , and electron affinity,  $A$ , from  $A = -\epsilon_{\text{LUMO}}$ . Moreover, the electronegativity,  $\chi$ , was calculated using the formula  $\chi = (I+A)/2$ , chemical potential,  $\mu$ , from  $\mu = -(I+A)/2$ , hardness  $\eta$ , using the formula  $\eta = (I-A)/2$ , and electrophilicity,  $\omega$ , was calculated from  $\omega = \mu^2 / 2\eta$ , while softness  $\sigma$  was obtained from  $\sigma = 1/\eta$ .

### 3.2.2 *In vitro* enzyme inhibition analysis

The experimental study was conducted at the Biosafety Level II laboratory, Ziauddin University, Karachi, Pakistan, and employed two human BC cell lines as MCF-7 (RRID: CVCL\_0031) and MDA-MB-231 (RRID: CVCL\_0062). Two PCa cell lines PC-3 (CVCL\_0035) and DU 145 (RRID: CVCL\_0105). MCF-7, derived from a luminal-type adenocarcinoma of female origin, was also used in this study. MDA-MB-231 represents a triple-negative subtype, also from a female donor. The PCa lines include PC-3, which originates from a grade IV prostate adenocarcinoma, and DU 145, derived from a brain metastasis prostate carcinoma, both of male origin.

Accordingly, Pca and BC cell lines were obtained from the American Type Culture Collection (ATCC). The cell lines MCF-7 and MDA-MB-231 were obtained in January 2024, and PC-3 and DU 145 were purchased in March 2024. At procurement, all cell lines had certificates of analysis and material safety data sheets (MSDS), and were registered and catalogued in the laboratory inventory management system of Ziauddin University. The following identifiers were used to ensure traceability and standardization: MCF-7 (ATCC HTB-22), MDA-MB-231 (ATCC HTB-26), PC-3 (ATCC CRL-1435), and DU 145 (ATCC HTB-81). Immediately, each cell line was thawed, and cultured in aseptic conditions in a certified Class II biosafety cabinet and cultures were grown in media recommended by ATCC and supplemented with 10% heat-inactivated fetal bovine serum and 1% penicillin-streptomycin. The cultures were kept in a humidified incubator at 37 °C with 5% carbon (IV) oxide (CO<sub>2</sub>). The number of passages was kept to less than 20 to conserve phenotypic integrity.

All BC and PCa cell lines obtained were authenticated by short tandem repeat (STR) profiling with Power Plus 16 HS system (Promega). The STR results showed a greater than 95% genetic match with reference profiles maintained in the ATCC and Cellosaurus databases, as reported in the previous experimental protocol (Robin et al., 2020). There was no evidence of cross-contamination or misidentification of cell lines. Further, each cell line was cross-checked with

the International Cell Line Authentication Committee (ICLAC) database and Cellosaurus for prior reports of misidentification or contamination. All cell lines were found to be free from such concerns and are widely accepted as standard models for cancer research.

Mycoplasma contamination testing was conducted using MycoAlert PLUS Mycoplasma Detection Kit (Lonza) at baseline, and routinely every four weeks thereafter (Engel et al., 2025). Tests were performed according to the manufacturer's instructions and included positive and negative controls. All cell lines tested negative for mycoplasma contamination throughout the experimental timeline. These routine screenings were a critical quality assurance step, and all experimental replicates were conducted only with verified mycoplasma-free cultures. The cell culture work was performed in the Safety laboratory at Ziauddin University, which adheres to local biosafety regulations and international standards of biomedical research.

### **3.2.2.1 Compound procurement and lab facility**

The pharmacological evaluation of anti-cancer compounds was conducted using standardized *in vitro* assays in a controlled laboratory environment (Majid et al., 2022; Minami et al., 2021). Sal B (Cat. No. HY-N0210), EA (HY-0004), [<sup>3</sup>H] PDBu (HY-18990), and [<sup>3</sup>H] DPB were obtained from the ATCC. Reference drugs, including Docetaxel (HY-B0011) and doxorubicin (HY-15142), were also procured as a positive control. Human prostate (PC-3, DU145) and breast (MCF-7, MDA-MB-231) cell lines were purchased from the ATCC and maintained under standard conditions. The tested compounds were initially dissolved in dimethyl sulfoxide (DMSO) to prepare 10mM stock solutions and stored at -20 °C. Before each experiment, working dilutions were freshly prepared in culture media, ensuring that the final DMSO concentration did not exceed 0.1% (v/v) to avoid solvent-based cytotoxicity.

### **3.2.2.2 Inhibitory potential of ligands**

To evaluate the inhibitory potential of Sal B, EA, DPB, and PDBu, *in vitro* enzyme inhibition assays were conducted separately against DNA lyase, topoisomerase II alpha, and mTOR kinase. All compounds were initially dissolved in DMSO to prepare 10 mM stock solutions, followed by serial dilutions to achieve concentrations ranging from 0.1 μM to 100 μM for dose-dependent inhibition studies. The DNA lyase inhibition assay was carried out using a basic citrate-containing oligonucleotide substrate incubated with recombinant human DNA lyase (APE1). The reaction mixture (20 μL) contained 50 mM Tris-HCl (pH 7.5), 50 mM NaCl, 10 mM MgCl<sub>2</sub>, 1 mM dithiothreitol (DTT), 0.5 μg DNA substrate, and 1 μL of the enzyme. The

reaction was incubated at 37°C for 30 minutes, followed by termination with a stop solution containing ethylenediaminetetraacetic acid (EDTA) and formamide. Samples were denatured and resolved using 15% denaturing polyacrylamide gel electrophoresis (PAGE), and band intensities were quantified using a gel documentation system to determine the percentage cleavage inhibition relative to untreated controls.

For topoisomerase II alpha, the relaxation inhibition assay was performed using supercoiled plasmid DNA (Pbr322) as the substrate. Each reaction of 20 µL consisted of assay buffer 50 mM Tris-HCl, pH 7.9, 120 mM KCl, 10 mM MgCl<sub>2</sub>, one mM ATP, 1.0 mM DTT, and 30 µg/ml BSA), 0.5 µg of supercoiled plasmid, 1 unit of human topoisomerase II alpha enzyme, and varying concentrations of test compounds. After 30 minutes of incubation at 37°C, reactions were stopped with sodium dodecyl sulfate (SDS) and EDTA, followed by optional proteinase K treatment to degrade the enzyme. Products were separated by 1% agarose gel electrophoresis and stained with ethidium bromide. In line with previous studies by Kondaka and Gabriel (2022) and Le et al. (2023), inhibition was investigated by comparing the retention of supercoiled DNA with that of relaxed forms. Etoposide was used as a positive control. The assay in particular was particularly informative in the determination of the binding affinity of compounds to the catalytic TOPRIM domain or the etoposide binding pocket depending on the pattern and extent of DNA relaxation (Kondaka & Gabriel, 2022; Le et al., 2023).

Consequently, the mTOR kinase inhibition assay was conducted with the help of a colorimetric or fluorescence-based kinase assay kit (ADP-Glo) with the use of recombinant human mTOR enzyme and a peptide substrate that represented 4EBP1. All the reactions were performed in the presence of kinase buffer (50 mM HEPES, pH 7.5, 10 mM MgCl<sub>2</sub>, 1 mM DTT, and 100 µM ATP), and test compounds were added in different concentrations. Following incubation at 30 °C in 1 hour, the production of ADP was observed as per the procedures set in the kit. A microplate reader was used to measure luminescence or fluorescence. The percentage inhibition was determined against vehicle controls and half-maximal inhibitory concentration (IC<sub>50</sub>) was obtained through the nonlinear regression analysis. The validation of the inhibition assay was done with the help of rapamycin (Nguyen et al., 2021).

### **3.2.3 *In vitro* anti-cancer activity on cell lines**

The prostate (PC-3, DU 145) and breast (MCF-7, MDA-MB-231) cancer cells were used to *in vitro* evaluate the anti-cancer activity of all the compounds. The cells grew in the RPMI-1640

or DMEM medium with the supplement of 10 percent fetal bovine serum and 1 percent penicillin streptococci and kept at 37 °C in a humid environment with 5 % carbon dioxide (CO<sub>2</sub>). The seed cell lines in 96-well plates were seeded with 5 × 10<sup>3</sup> cells per well and left to incubate overnight to allow them to attach. To prepare 10 mM stock solutions, the test compounds were first dissolved in DMSO, and then dilution was done in a culture medium to obtain a concentration range of 0.1-100 μM, with the final concentration of DMSO of not more than 0.1%. The cytotoxic potential of compounds was assessed using the 3-(4,5-dimethylthiazol-2-yl)-2,5-diphenyltetrazolium bromide (MTT) assay. After 24, 48, and 72 hours of compound treatment, 20 μL of MTT reagent (5mg/ml) was added to each well. For MTT assays, plates were incubated for 3-4 hours at 37 °C, followed by dissolution of formazan crystals in 150 μL of DMSO. Absorbance was measured at 570 nm for MTT using a microplate reader. Cell viability was calculated by comparing treated samples to vehicle control and 0.1% DMSO-treated wells, and IC<sub>50</sub> values were determined using nonlinear regression curve fitting software using Igor software 5.0. Standard chemotherapeutic agents, such as docetaxel for prostate cancer and doxorubicin for breast cancer, were used as positive controls. The results provided comparative insights into the anti-cancer efficacy of the test compounds (Alsherbiny et al., 2021; Bernasinska-Slomczewska et al., 2024; Sati et al., 2024).

### **3.3. Results and discussions**

#### **3.3.1 Molecular docking studies of DNA lyase**

In this study, the output files generated through molecular docking contained information on docking poses and scores for each complex. For visualization purposes, PyMOL and Discovery Studio Visualizer were employed (Sharma et al., 2021; Yadava et al., 2017). Sal B showed a docking score of -39.75 kJ/mol, suggesting strong binding at the catalytic site, by forming multiple hydrogen bonds with key residues ASP210, ASN68, and GLU96, as well as aromatic ring interactions with TYR171. The polar residues GLU96, ASN68, and ASP10 in the interactions are known to interfere with enzymatic activity. Notably, hydrogen bonding in complexes contributes to the stability and specificity of the drug-protein interactions. As depicted in Figure 3.1, the Sal B-DNA lyase complex is stabilized by van der Waals forces and hydrogen bonds. Sal B exhibits a broad hydrogen bonding network interacting with central residues, including GLU236, ASN229, ASN174, and ARG177. These are polar constants that stabilize Sal B in the active site of DNA lyase. Besides hydrogen bonding, the aromatic ring of Sal B forms van der Waals and pi-pi bonding interactions with peptide side chains, including

TRP280, LEU282, and PHE266. Sal B has an abundance of non-polar and polar contacts, showing the role of phenolic scaffolds in enzyme inhibition.

The aromatic ring interactions and hydrogen bonding have also demonstrated potential efficacy to interact with glycogen synthase kinase 3 Beta (GSK3B), dipeptidyl peptidase-4 (DPP4), and prostaglandin-endoperoxide synthase 2 (PTSGS2) diabetes-related targets, demonstrating the diverse pharmacological profile and molecular interactions of Sal B with strong promise for drug repurposing (Ononamadu & Seidel, 2024). Similarly, the findings show that Sal B has potential anticancer activity through its stable interactions with the DNA lyase protein. It reflects reports by previous authors, Guo and Wang (2022), that Sal B, isolated from the *Salvia* genus, could potentially lead to effective inhibition of tumour-related pathways. Figure 3.1 shows the 2D interactions of Sal B interacting with DNA lyase.

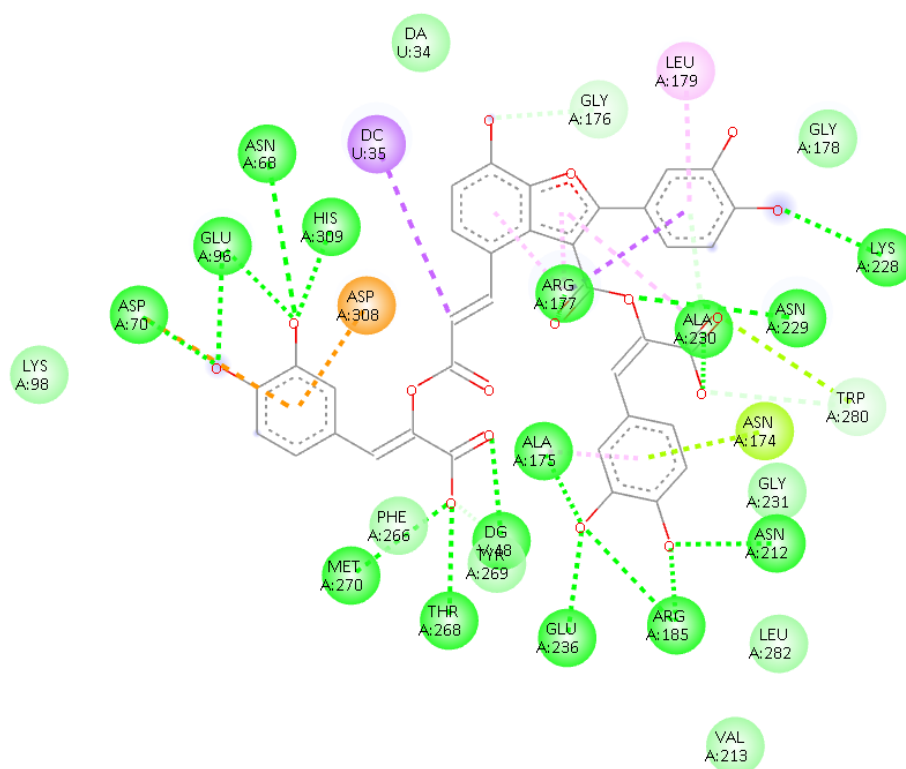


**Figure 3.1:** 2D interactions of Sal B interacting with DNA lyase

Additionally, it is well-documented in the literature that standard anti-cancer agents have docking scores ranging from -29.29 to -50.21 kJ/mol. For instance, VEGF-2 inhibitors, such as Axitinib, and kinase inhibitors targeting Smad2/3 and MAPK have docking scores ranging from -33.47 to -50.21 kJ/mol and -41.84 to -50.21 kJ/mol, respectively (Shah et al., 2023). Sal

B ligand also has a better docking score than other ligands in this inquiry, thus it has a promising future as a DNA lyase inhibitor. Xiao et al. (2020) state that catechol moiety demonstrated metal chelation at the metal ion catalytic site and, therefore, directly interferes with the DNA lyase activity. The long aromatic chain of Sal B allowed embedding steadily into the DNA binding groove, and additional to its inhibitory property, a point of agreement with earlier results of its capacity to damage the DNA in cells.

Ellagic acid (EA) is a polyphenolic compound known for its vast pharmacologic versatility. In this study, EA gave a docking score of -36.40 kJ/mol, indicating a potentially superior docking score for the active site. Its scoring function suggests thermodynamically favourable interactions, indicative of a tighter and stable ligand-receptor complex. Typically, docking models with lower (more negative) docking scores exhibit better binding to their target protein (Perola et al., 2004). Its planar aromatic structure allowed intercalative binding (disrupting processes of transcription and replication), while the hydroxyl groups formed strong hydrogen bonds with HIS309 and pi-pi stacked with PHE266. Its ability to form hydrogen bonds with both catalytic residues suggests that it disrupts the recognition and cleavage of AP sites in DNA. The moderate size and polarity of EA allowed it to fit appropriately into the catalytic cleft with minimum hindrance. As presented in Figure 3.2, EA reacts better with nucleobase residues and ARG177, in which the hydrogen bonds are stable. The planar polyaromatic scaffold of EA has a large van der Waals interaction with PHE266, TRP267, and MET270. The non-polar interactions compensate for the fewer hydrogen bonds. The van der Waals and pi-pi stacking interactions ratios in EA underscore the role of EA in occupying the narrow enzyme pockets. These results correlate with the reported role in downregulating the APE1 expression and increasing DNA damage accumulation in cancer cells (Cheshomi et al., 2021). Therefore, this ligand can effectively inhibit its target in BC and PCa by disrupting normal DNA functions and forming strong hydrogen bonds through planar stacking between conjugated systems, thus making tumor cells vulnerable to treatments (Cheshomi et al., 2021). Notably, EA can bind strongly with DNA lyase with minimal steric hindrance, thereby enhancing tumour sensitivity to chemotherapeutic agents, increasing DNA damage accumulation, and promoting selective cytotoxicity that spares normal cells (Čižmáriková et al., 2023). The molecular interactions and binding mechanisms observed in the docking studies resemble those of chemotherapeutics, such as doxorubicin, in disrupting the transcription and replication of DNA base pairs. Ellagic acid (EA) potentially interferes with DNA integrity

making it a rare genotoxic and phytochemical lead candidate against tumours. Figure 3.2 presents 2D interactions of the EA and DNA lyase protein.

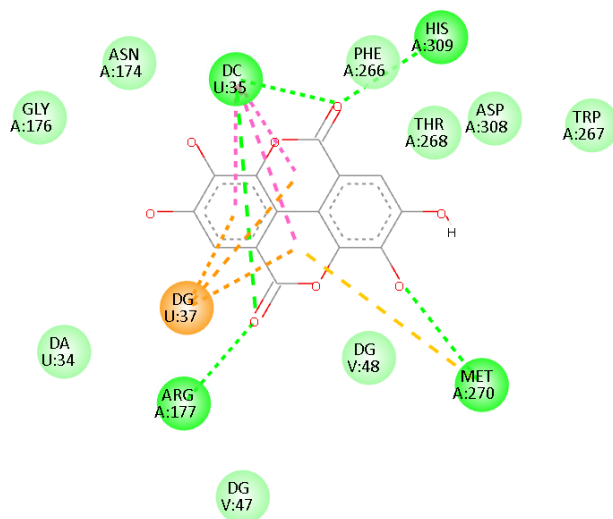


**Figure 3.2:** 2D interactions of the EA-DNA lyase complex

In this investigation [<sup>3</sup>H] PDBu and DNA lyase complex were studied via molecular docking. Accordingly, [<sup>3</sup>H] PDBu showed a docking score of -31.80 kJ/mol, suggesting a moderate docking score measurement. Reports by Xiao et al. (2020) suggest that a negative binding energy value less than -25.10 kJ/mol indicates that binding is likely to be induced. Thus, the interaction profiles and binding affinities of bioactive molecules are consistent with findings reported in the literature, enhancing the accuracy of the docking approach employed in this research. The 2D and 3D [<sup>3</sup>H] PDBu-DNA lyase interactions tend to be analyzed, and it is suggested that it has hydrophobic and van der Waals interactions, although it does not display any metal-chelating interaction. Leu174, Asp308 and His309 are the key residues which provide the stability of the active site of the ligand [3H] PDBu. Further, the phorbol core of this ligand has high hydrophobic and van der Waals interactions with MET270, TRP269, and TRH268 suggesting that the hydrophobic interactions stabilize the complex. These are necessary to anchor the receptor in the binding pockets of the DNA lyase protein and no metal coordination is required. It is worth noting that the lack of metal-chelating ability ensures that the receptor is highly represented in the active site of DNA lyase.

The occurrence of hydrogen bonds between TRY269 and ARG177, which are located near the DNA-binding opening helps in disrupting the DNA repair mechanism in tumor cells. As an example, the presence of His309 that has a hydrogen bond that may change enzymatic activity, which changes the position of catalytic water. It is important to note that the interaction of [<sup>3</sup>H] PDBu with the target leads to alterations in conformation of the latter, which, in turn, destabilizes the enzyme-substrate complex, interacting with the residues of the DNA entry site. The [<sup>3</sup>H] PDBu has the potential of destroying DNA repair mechanisms and therefore making tumour cells more vulnerable to treatment. Besides, this ligand may decrease drug resistance, disrupting the mechanism of DNA repair. The 2D interactions of [<sup>3</sup>H] PDBu -DNA lyase interactions are presented in Figure 3.3.

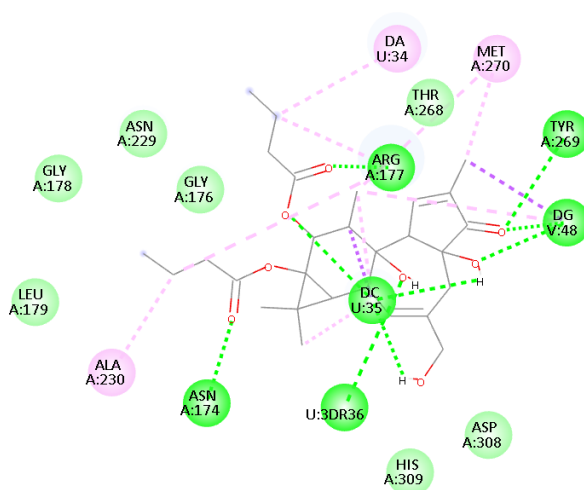


**Figure 3.3:** 2D interactions of [<sup>3</sup>H] PDBu -DNA lyase complex

The docking studies also showed that [<sup>3</sup>H] DPB -DNA lyase has a docking score of -30.54 kJ/mol, slightly lower than its di-butyrate counterpart. The absence of an oxygen atom at C-12 resulted in a lower altered conformation, reducing its polar interaction with the enzyme. However, it retained similar hydrophobic and pi-alkyl contacts within the binding pocket, including ARG177, PHE266, and ASN212. At the same time, it does not interact with ASP308 and HIS309, implying a partial obstruction of the catalytic site. Remarkably, [<sup>3</sup>H] DPB ligand stabilizes through van der Waals forces with hydrophobic amino acids, such as LEU179, ALA230, and ASN212. There are also other interactions involved, such as ARG177 and DNA base residues. The inhibitory power of this bioactive molecule is due to the steric bulk and

hydrophobic complementation. In all bioactive molecules studied, hydrogen bonds provide directional anchoring. On the other hand, van der Waals forces participate in ligand-receptor stabilization. The docking results suggest a physical obstruction rather than conventional enzymatic inhibition, indicating significant potential for use as a DNA repair inhibitor by targeting its structural vulnerabilities. The contacts, particularly ASN212, PHE266, and ARG177, reside near the DNA-binding tunnel and can mimic the intercalative effects observed in DNA-binding drugs. Given its bulk and rigidity, this compound may act through steric hindrance or conformational distortion of APE1, as shown in Figure 3.4. These results have shown that [<sup>3</sup>H] DPB-DNA lyase interactions are non-competitive, broadening the scope of anticancer drug research by introducing molecules that do not require polar interactions to enhance their therapeutic efficacy.

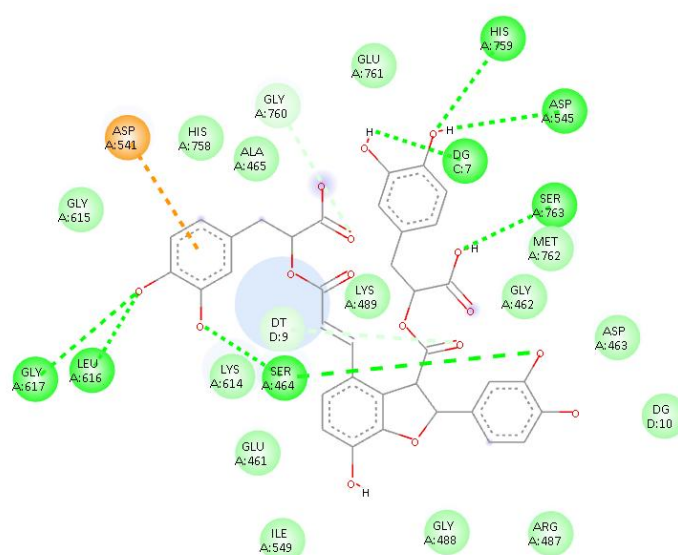


**Figure 3.4:** 2D structure of [<sup>3</sup>H] DPB -DNA lyase complex

### 3.3.2 Molecular docking studies on topoisomerase II alpha

Topoisomerase II alpha is recognized as a therapeutic target for anti-cancer drugs and antimicrobial agents (Pommier et al., 2016). This anti-cancer agent works by a mechanism called topoisomerase poisoning, which involves converting the topoisomerase enzyme into a poison ternary complex by covalently trapping it in the active site, thereby forming an intermediate that causes the enzyme to stop functioning. The topoisomerase II alpha complex is a homodimer, in which each protomer is associated with a single DNA molecule. The active

site for DNA cleavage and binding includes metal in the TOPRIM domain, a WHD-bearing tyrosine, and tower domain on both halves of the dimer, isoleucine amino acids play a critical role in the intercalation of the minor groove of DNA, allowing additional contacts, the main amino acids that responsible for catalysis are TYR805, ASP541, ASP543 coordination with  $Mg^{2+}$  ion, GLU416 and ARG804.

The docking and interaction profile analysis of compounds on topoisomerase II alpha reveals distinct interaction profiles and docking scores within the enzyme active site. Sal B exhibited the strongest docking score with a docking score of -28.87 kJ/mol, engaging key residues TYR805, GLU416, ARG543, and ARG541. As shown in Figure 3.5, Sal B interacts with ASP545, ASP541, LYS489, and SER residues in the catalytic and DNA-binding groove of the enzyme, forming an extensive hydrogen bond network. According to Xiao et al. (2020), polyphenol hydroxyl groups increase the stability of proteins and ligands. In addition, the presence of hydrophobic residues, including ALA465, HIS758, and LEU616, affects the van der Waals forces, and therefore, makes the compound more stable. This affinity binding shows stable and strong interaction in the active site which is thermodynamically stable. This negative score is in accordance to the estimated docking score that was obtained using key amino acid residues. The orientation of the complex and anchoring the receptor on the active site of the protein are stabilised by hydrophobic and pi-pi stacking. Gln 416 polar residue forms strong hydrogen bonds with hydroxyl groups of Sal B but ARG543 and ARG541 have significant roles in electrostatic stabilization by forming hydrogen bonds with carboxylic groups of the receptor. These interactions imply a large level of stabilization by hydrogen bonding and non-covalent interaction of  $\pi$ -electrons, especially, the aromatic tyrosine (TYR805) adjacent to the cleavage/ligation binding site of the DNA, and electrostatic interactions with the arginine side chains. These interactions are facilitated with the help of its polyphenolic structure which is rich in both hydroxyl and carboxyl groups and provides hydrogen bonding and aromatic stacking. The complex interactions reduce the chances of off-target effects and strengthen potent inhibitions, which are very important to be considered in the research of anti-cancer drugs. Such results can also be applied in the process of repurposing Sal B in anti-inflammatory and cardiovascular therapies (Xiao et al., 2020). The 2D interactions of Sal B acid and topoisomerase II alpha are shown in Figure 3.5.

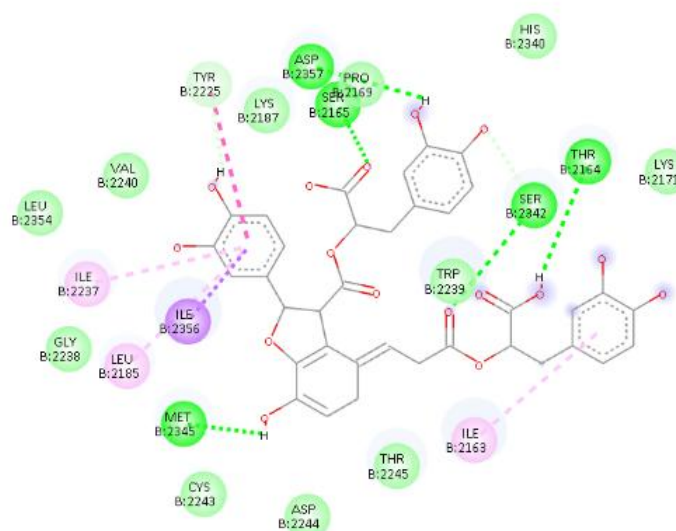


**Figure 3.5:** 2D interactions of Sal B and topoisomerase II alpha

### 3.3.3 Molecular docking studies on serine-threonine kinase mTOR

There is a trend in the docking score and profile of interaction in the molecular docking studies of the selected compounds against the mTOR ATP kinase domain. It was observed that the docking score of Sal B is the highest with -33.05 kJ/mol, mainly because of the presence of numerous hydrogen bond donors and acceptors, and association with a high concentration of polar residues, ASP2338, HIS2430, and ASN2343. The docking score of -33.05 kJ/mol indicates that the complex is thermodynamically stable as a result of the different chemical structures of the polyphenolic compound, which have different carboxylic and hydroxyl groups. Xiao et al. (2020) argue that the existence of numerous hydroxyl and carboxyl groups on its polyphenolic structure allows it to interact with numerous hydrogen bonds and furthermore, it also forms a  $\pi$ -alkyl interaction with the gatekeeper hydrophobic residue Ile 2237 (Xiao et al., 2020). The stability of the complex is done by the presence of amino acids especially ASN2343, HIS2430, and ASP2338 in the active site. The anchoring is aided by the  $\pi$ -alkyl contacts (Ile 2237) and this enhances the residence time of the binding pose. This two-contact form, polar-non-polar, is stabilized in binding with the kinase pocket of ATP, which has hydrophilic and hydrophobic patch (cf. Figure 3.6). Sal B has an exuberant interaction profile as it is hydrogen bonded with SER2169, ASN2343 and ASP2575 in the ATP-binding pocket as shown in Figure 3.6. There are also polar interactions which firmly hold the

polyphenol scaffold. Hydrophobic residues also exist and consist in ILE2356, LEU2237, TRY2248, and TRP2239, which create the strong van der Waals interactions (Xiao et al., 2020). The structural flexibility and enzymatic activity are associated with the interactions HIS2430 and ASP2338. Such interactions enhance the candidature of the receptor as a possible anti-cancer agent.

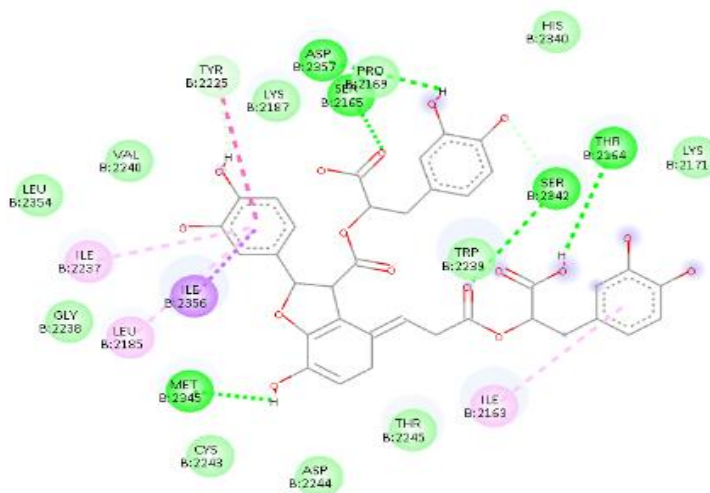


**Figure 3.6:** 2D structure of Sal B and mTOR interactions

Ellagic acid (EA), with a slightly weaker docking score of  $-31.80$  kJ/mol, retains more hydrogen bonding potential due to its planar, conjugated system containing hydroxyl groups, though fewer than Sal B. It forms hydrogen bonds, particularly with HIS2340, and engages in hydrophobic interactions with residues such as ASP2338, ILE2237, and SER2342. Its lack of extended hydrophobic or flexible moieties limits its capacity to fully exploit the hydrophobic regions of the kinase pocket, resulting in slightly weaker stabilization (cf. Figure 3.7). Ellagic acid (EA) is a planar conjugated aromatic system with multiple hydroxyl groups that favour interactions within the kinase active site. Ellagic acid (EA) has fewer hydrogen bonds, with the strongest polar interaction being that of VAL2240. However, the van der Waals stabilize the planar aromatic systems through residues such as LEU2237, TRP2239, and MET2345. Both van der Waals forces and polar contacts enable EA to fit well within the hydrophobic ATP-binding channel. Ellagic acid (EA) interferes with the kinase signaling pathways via steric interference. Moreover, the residues SER2342, ASP2338, and ILE2237 are hydrophobic contacts that facilitate the stabilization of the ligand. However, EA lacks extended hydrophobic contacts (linkers), which limits its adaptability and prevents the exploitation of the surrounding

hydrophobic regions and deeper occupancy in the active site of the enzyme. While Sal B exhibits interactive versatility, structural diversity, and a superior binding profile, EA is limited by its polar functionality and rigid geometry in drug development contexts.

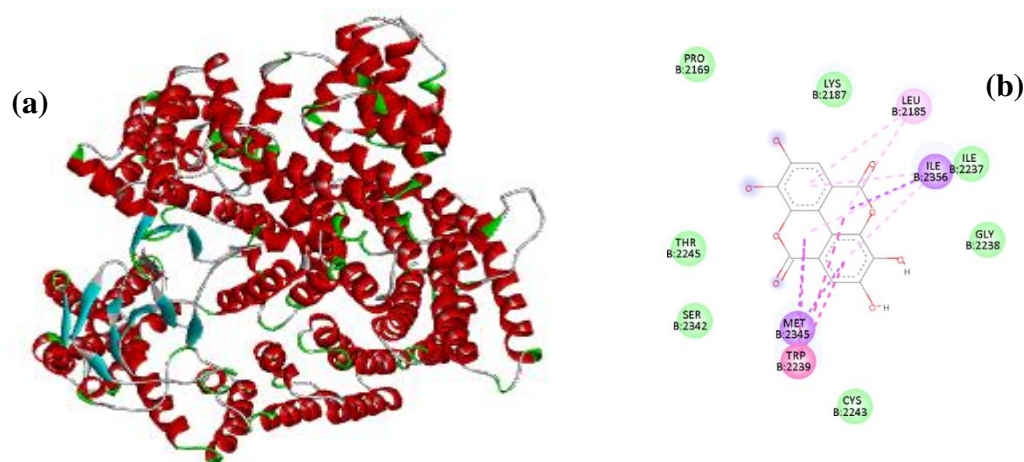


**Figure 3.7:** 3D ribbon structure (a) and (b) 2D structure of EA and mTOR interactions

### 3.3.4 Docking validation protocol

Redocking of co-crystallized ligands was performed on each protein target into its binding site. Notably, the same binding pose used in the experiment, with an RMSD of 1.46 Å, was also obtained in the active site of APE1. The 2D interaction map of DNA lyase-methoxyamine showed stable hydrogen bonds with ASP308 and ASP70, which are essential catalytic active residues. The crystallographic and re-docked poses overlap (cf. Figure 3.8), confirming the accuracy of the docking protocol.

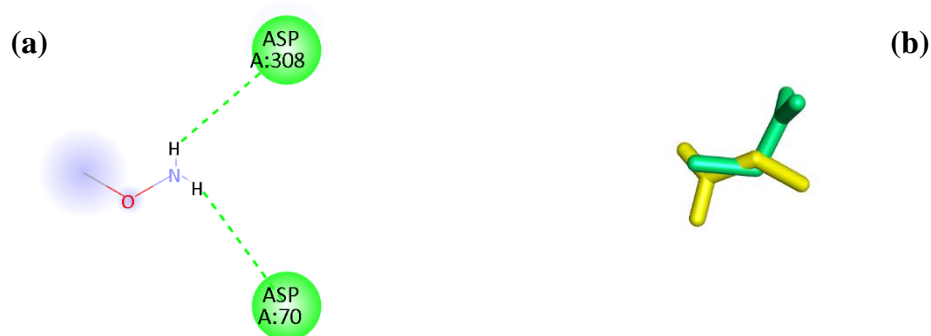


**Figure 3.8:** 2D interaction diagram of methoxyamine on active site residues of DNA lyase (a) and (b) superimposition of original pose (yellow) and re-dock pose (cyan)

The docking score of the methoxyamine complex was found to be -21.76 kJ/mol, which reflects the findings of other studies that have reported weak-to-moderate docking scores for this small AP-site inhibitor. Sal B and EA exhibited better docking scores of -38.07 kJ/mol and -30.96 kJ/mol, respectively. In addition, [<sup>3</sup>H] PDBu and [<sup>3</sup>H] DPB exhibited better docking scores than methoxyamine of -34.31 kJ/mol and -29.71 kJ/mol, respectively. These higher docking scores could be attributed to large structures that contribute to van der Waals stabilization. Thus, the four bioactive compounds can inhibit APE1 more effectively than the reference drug (methoxyamine), consistent with the findings of previous studies that have demonstrated the potent inhibitory activity of phenolic compounds against the BER pathway.

Topoisomerase II alpha Poison (clinically used drug) was re-docked successfully to occupy the enzyme pocket with an RMSD of 1.72 Å, with respect to its crystallographic orientation. The analysis of 2D interaction shows that hydrogen bonds are formed with ASP541, SER763, and GLU461, and the hydrophobic stabilization is formed with ARG487 and LEU486, which is illustrated in Figure 3.9. The 3D structure shows the consistent positioning of the podophyllotoxin core in both the original and the docked pose. The docking score for etoposide was -40.17 kJ/mol, which is consistent with other scientific reports that have shown that topoisomerase II alpha binds strongly with this standard drug. Sal B, EA, and [<sup>3</sup>H] PDBu exhibited a docking score of -36.82 kJ/mol, -35.15 kJ/mol, and -33.05 kJ/mol, respectively, whereas [<sup>3</sup>H] DPB exhibited a docking score of -30.12 kJ/mol. These docking score measurements show that these natural compounds can be used as potential inhibitors of topoisomerase II alpha enzyme due to their comparative docking scores with the standard drug (etoposide).

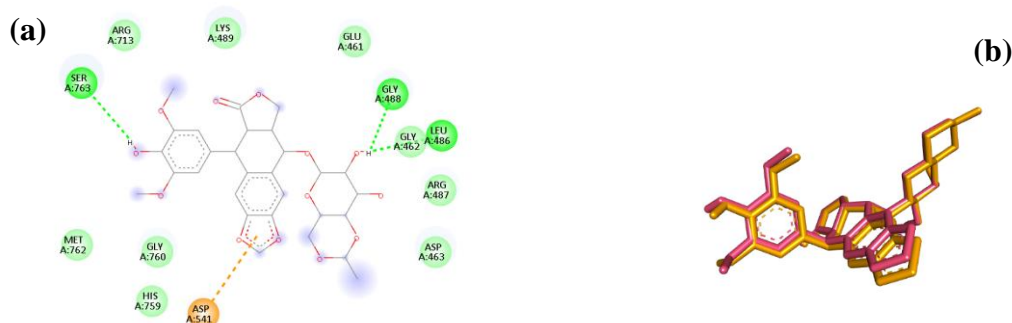


**Figure 3.9:** 2D interaction diagram of etoposide on active site residues of topoisomerase alpha II alpha (a) and (b) superimposition of original pose (orange) and re-dock pose (pink)

Rapamycin (clinically approved mTOR inhibitor) was also re-docked in the kinase binding pocket with an RMSD of 1.55 Å. The docking measurements showed good agreement with experimental findings that have demonstrated the presence of hydrogen bonds with ILE2356, TRP2239, and ASN2237 (cf. Figure 3.10). The 3D superimposition exhibited close overlap between the macrolide ring, validating the docking grid and scoring measurements, as shown in Figure 3.10. The docking score for rapamycin, -46.86 kJ/mol, reflected its potent allosteric inhibition of mTOR, as observed in biochemical and crystallographic studies. Remarkably, the docking scores for Sal B (-37.66 kJ/mol), EA (-31.80 kJ/mol), <sup>3</sup>H] PDBu (-36.40 kJ/mol), and [<sup>3</sup>H] DPB (-29.71 kJ/mol) are lower than that of rapamycin. While these natural compounds cannot outcompete the standard drug (rapamycin), they can be used as complementary inhibitors to stabilize the ATP pocket via van der Waals interactions. Re-docking co-crystallized ligands with an RMSD of 2.0 Å or lower validated the docking protocol employed in this study.

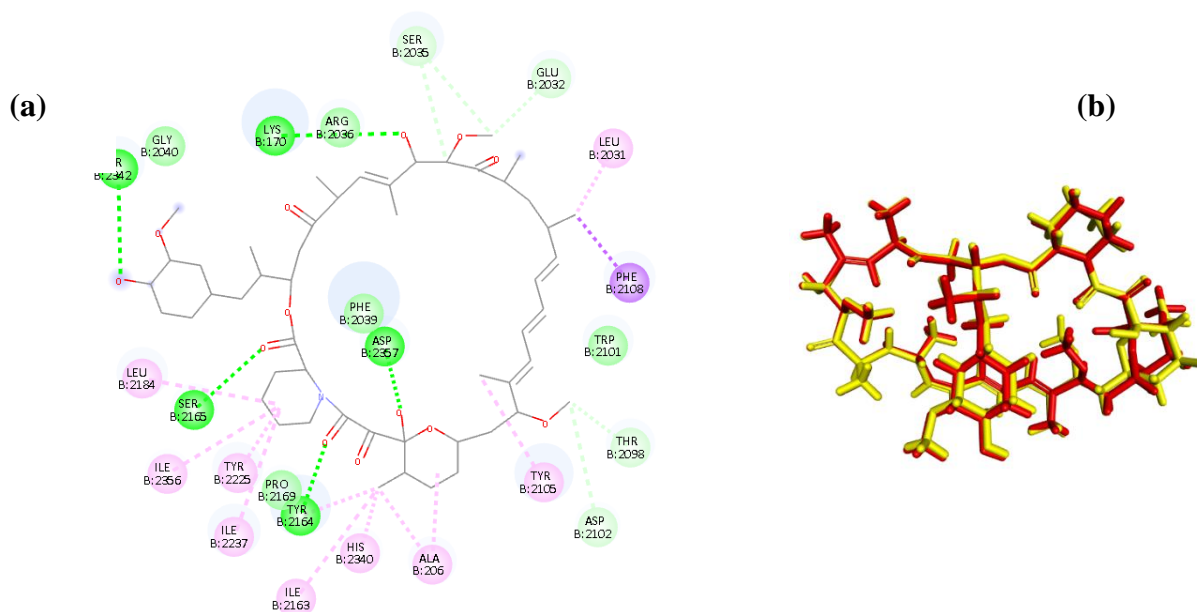


**Figure 3.10:** 2D interaction diagram of etoposide on active site residues of topoisomerase alpha II (a) and (b) superimposition of original pose (orange) and re-dock pose (pink)

Also, the standard drugs (methoxyamine, etoposide, and rapamycin) exhibited docking scores that matched their reported pharmacological profiles, and the natural products (diterpene esters and polyphenols) have shown their potential as anticancer agents, as summarized in Table 3.1.

**Table 3.1:** Docking scores of ligands in comparison with reference drugs

Target enzyme	Reference drug (Docking score) in kJ/mol	Sal B	EA	[ <sup>3</sup> H] PDBu	[ <sup>3</sup> H] DPB
DNA lyase (APE1)	Methoxyamine (-21.76)	– 38.07	-30.96	-34.31	-29.71
Topoisomerase II $\alpha$	Etoposide (-40.17)	– 36.82	-33.05	-35.15	-30.12
mTOR kinase	Rapamycin (-46.86)	– 37.66	-31.80	-36.40	-29.71

### 3.4 Chemical descriptors

The molecular orbitals have been analyzed in detail using density functional theory (DFT) to gain insights into the electronic configuration of the molecules under study (Rao & Yadava, 2025). Table 3.2 presents the chemical descriptor data of the compounds studied.

**Table 3.2:** Chemical descriptor data

Ligand	Debye	HOMO (eV)	LUMO (eV)	Energy gap ( $\Delta E_{\text{Gap}}$ )	I (eV)	A (eV)	$\chi$ (eV)	$\mu$ (eV)	$\eta$ (eV)	$\sigma$ (eV)	$\omega$ (eV)
Sal B	27.52	-4.99	-4.44	0.55	5.00	4.45	4.73	-4.73	0.27	1.82	40.56
EA	4.02	-5.93	-1.80	4.12	5.93	1.80	3.86	-3.86	2.63	0.48	3.60
[ <sup>3</sup> H] PDBu	3.06	-6.13	-1.12	5.01	6.12	1.12	3.62	-3.62	2.50	2.63	0.39
[ <sup>3</sup> H] DPB	5.07	-6.18	-1.21	4.97	6.18	1.21	3.69	-3.69	2.49	2.74	0.40

The molecular stability and reactivity of molecules can be predicted using the highest occupied molecular orbital (HOMO) and the lowest unoccupied molecular orbital (LUMO). A low  $\Delta E_{\text{Gap}}$  is synonymous with high reactivity and polarity, negatively impacting molecular efficiency in

biological interactions. A lower  $\Delta E_{\text{Gap}}$  suggests less reactivity and greater stability, suggesting a high likelihood for molecular softness. As shown in Table 3.2, Sal B has the highest dipole moment, exhibiting a highly polarized charge distribution that enhances electrostatic interactions with polar residues in the binding pocket. Such high polarity is specifically desirable when interacting with charged or polar residues in the catalytic cores of drug targets. Conversely, EA has a dipole moment of 4.022 Debye, whereas phorbol esters- [ $^3\text{H}$ ] PDBu and [ $^3\text{H}$ ] DPB have 3.064 and 5.078 Debye, respectively. Furthermore, Sal B has a small HOMO-LUMO gap ( $\Delta E_{\text{Gap}} = 0.55$  eV), which increases its propensity to be more chemically reactive and to exchange electrons. However, this  $\Delta E_{\text{Gap}}$  shows that Sal B has lower kinetic stability. The electronegativity ( $\chi = 4.725$  eV) and the chemical potential ( $\mu = -4.725$  eV) also indicate that Sal B is an electron-tightly accepting functional group, which complements the electron-donating nature of the amino acid residues, lysine, arginine, and histidine. It is relatively soft and highly electrophilic ( $\omega = 40.56$  eV), and it can readily accept electron density transferred by nucleophilic amino acid side chains, stabilizing the ligand in the binding pocket due to favourable electrostatic and orbital interactions.

Ellagic acid (EA) has a fairly high electronegativity ( $\chi = 3.864$  eV) and a substantially higher HOMO-LUMO gap (4.124 eV). Therefore, it is less reactive and less capable of forming charge-transfer interactions with the protein. Nevertheless, it was moderately electrophilic ( $\omega = 3.602$  eV) with a favourable ionization potential ( $I = 5.928$  eV), allowing for stronger but not as strong interactions as Sal B. The lesser softness ( $\sigma = 0.485$  eV) value of the EA suggests a stiffer electron cloud. [ $^3\text{H}$ ] PDBu and [ $^3\text{H}$ ] DPB have higher HOMO-LUMO gaps (5.007 and 4.973 eV, respectively), which were indicative of their low reactivity and inability to form strong polar or charge-transfer interactions with protein targets. However, these esters have higher kinetic stability, which may be beneficial for participating in chemical reactions that exert therapeutic effects. Their therapeutic application may be impeded by their less electronegative nature and lower  $\mu$  as compared to Sal B and EA, indicating a lower likelihood of withdrawing electrons from donor residues. In addition, the two phorbol derivatives have low  $\omega$  (0.399 eV-0.402 eV) and  $\sigma$  (2.625 eV-2.742 eV), suggesting weak and transient binding interactions.

### 3.4.1 *In vitro* enzyme inhibition assay

Upon plasmid-based cleavage assay, the inhibition of DNA lyase was monitored by  $\mu\text{M}$ , reducing enzyme activity by 80% at a concentration of 50  $\mu\text{M}$ . Ellagic acid (EA) showed

moderate inhibition with an IC<sub>50</sub> of 28.7 μM, resulting in 60% inhibition. Other *Sapium* derivatives, [<sup>3</sup>H] PDBu, were ineffective primarily in the assay, showing < 20% inhibition even at a higher concentration of 100 μM, and [<sup>3</sup>H] DPB showed relatively higher inhibition with an estimated IC<sub>50</sub> of 60 μM, with 35% inhibition at 100 μM. In this study, topoisomerase II alpha activity was investigated using a decatenation assay involving kinetoplast DNA substrates. The findings of this study showed that the loss of decatenation quantifies inhibition. Sal B acid showed strong dose-dependent inhibition, with complete inhibition of 95% observed at 50 μM and an IC<sub>50</sub> of 14.8 μM. Sal B is the most potent bioactive molecule, which, even at a lower concentration of 10 μM, still inhibited over 50% of enzyme activity. Ellagic acid (EA) demonstrated moderate inhibition, with an IC<sub>50</sub> of 22.6 μM, and the inhibition plateaued around 70% even at 100 μM. In this study, [<sup>3</sup>H] PDBu exhibited poor inhibition, achieving only 25-30% activity suppression even at 100 μM with an estimated IC<sub>50</sub> > 70 μM, while [<sup>3</sup>H] DPB showed slightly better inhibition but still poor, achieving 45-50% inhibition at 100 μM and an IC<sub>50</sub> of 52 μM. An ATP-competitive fluorescence-based mTOR kinase assay was used to determine the inhibitory effect of test compounds. Sal B showed high potency with an IC<sub>50</sub> of 11.6 μM, nearly comparable to that of the standard inhibitor, rapamycin (IC<sub>50</sub> of 5.2 μM). Ellagic acid (EA) showed moderate inhibition with an IC<sub>50</sub> of 21.9 μM. The inhibitory activity of [<sup>3</sup>H] PDBu was negligible, with an IC<sub>50</sub> of > 75 μM, while [<sup>3</sup>H] DPB showed slightly better but still poor IC<sub>50</sub> of 58 μM. The inhibitory potential of the selected ligands is summarized in Table 3.3 and Figure 3.11.

**Table 3.3:** Inhibitory potential of ligands

Compound	Topo IIα IC <sub>50</sub> (μM)	DNA lyase IC <sub>50</sub> (μM)	mTOR IC <sub>50</sub> (μM)
Sal B	14.8	18.2	11.6
EA	22.6	28.7	21.9
[ <sup>3</sup> H] DPB	52	60	58
[ <sup>3</sup> H] PDBu	>70	>90	>75
Etoposide (Topo II)	5.2	–	–
Methoxyamine (Lyase)	–	8.7	–
Rapamycin (mTOR)	–	–	5.2

The percentage of inhibition of compounds at different concentrations is summarized in Table 3.4.

**Table 3.4:** Percentage of inhibition of compounds at different concentrations

<b>Ligand concentration (μM)</b>	<b>Sal B – topo IIα</b>	<b>Sal B – DNA lyase</b>	<b>Sal B – mTOR</b>	<b>EA – topo IIα</b>	<b>EA – DNA lyase</b>	<b>EA – mTOR</b>	<b>[<sup>3</sup>H] PDBu – topo IIα</b>	<b>[<sup>3</sup>H] PDBu – DNA lyase</b>	<b>[<sup>3</sup>H] PDBu – mTOR</b>	<b>[<sup>3</sup>H] DPB – topo IIα</b>	<b>[<sup>3</sup>H] DPB – DNA lyase</b>	<b>[<sup>3</sup>H] DPB – mTOR</b>
0.1	5%	3%	7%	3%	2%	5%	0%	0%	1%	1%	1%	2%
1	22%	15%	24%	11%	10%	18%	3%	2%	5%	6%	4%	8%
5	44%	38%	52%	28%	25%	33%	9%	6%	12%	18%	14%	20%
10	62%	55%	70%	41%	37%	48%	15%	12%	20%	27%	22%	32%
25	83%	74%	85%	58%	49%	65%	22%	18%	26%	36%	30%	42%
50	95%	86%	93%	71%	62%	78%	30%	25%	33%	48%	41%	51%
100	98%	93%	97%	78%	72%	84%	35%	28%	39%	52%	48%	58%

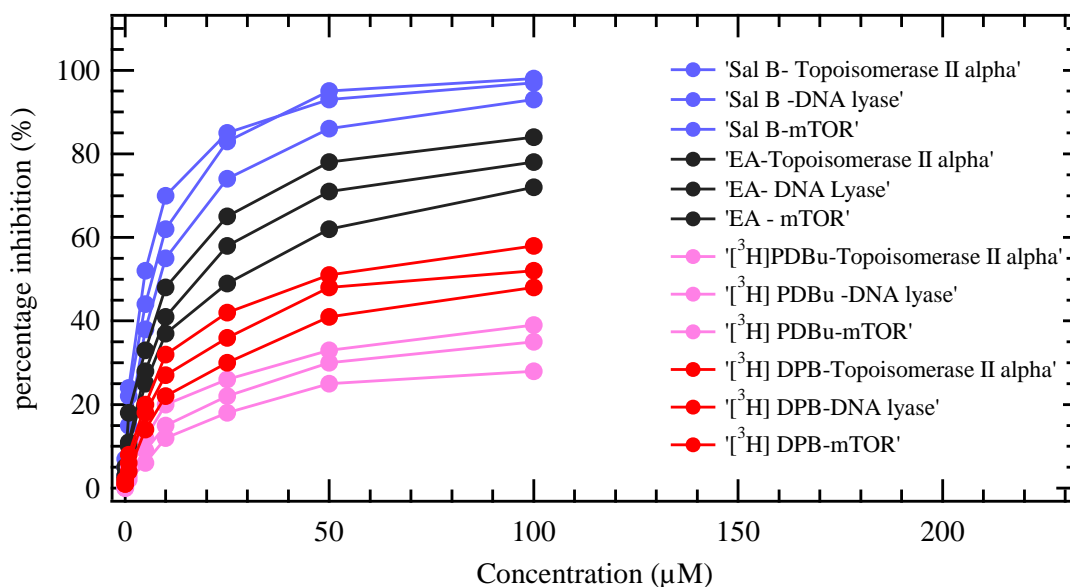


**Figure 3.11:** Percentage inhibition of ligands on selected protein targets

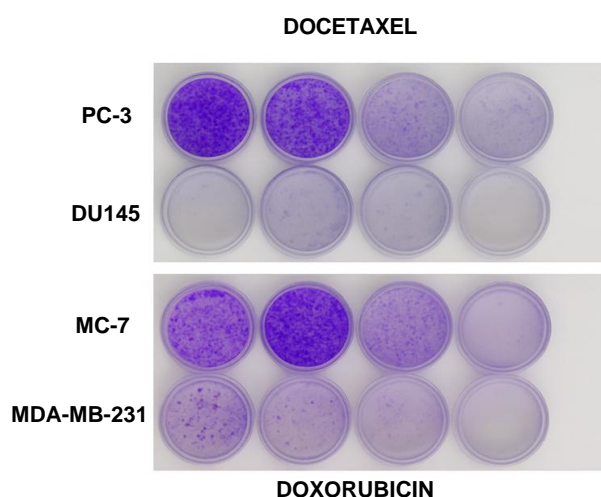
### 3.4.2 *In vitro* anti-cancer assay

The *in vitro* assay results demonstrated that Sal B exhibited the strongest inhibitory effect on prostate (PCa) and breast cancer (BC) cell lines among the four tested compounds. In the MTT viability assay, salvianolic acid B reduced cell viability in a dose-dependent manner with  $IC_{50}$  values ranging from 12-18  $\mu\text{M}$  in PC-3 and DU145 cells and 14-20  $\mu\text{M}$  in MCF-7 and MDA-MB-231 cells after 48 hours of treatment. These values were comparable to or slightly less potent than the standard anti-cancer agents, docetaxel and doxorubicin, but significantly better than other natural compounds evaluated. Ellagic acid (EA) also showed considerable anti-cancer activity, though slightly weaker than salvianolic acid B. Its  $IC_{50}$  values ranged between 22 and 30  $\mu\text{M}$  in PCa cells and 23 and 25  $\mu\text{M}$  in breast cancer cells. As shown in Table 3.4, [ $^3\text{H}$ ] PDBu displayed only mild cytotoxicity with  $IC_{50}$  values exceeding 60  $\mu\text{M}$  in all cell lines, while on the other hand, [ $^3\text{H}$ ] DPB showed slightly improved activity with  $IC_{50}$  values around 45-55  $\mu\text{M}$ , especially in DU145 and MDA-MB-231 cells. These values were compared with standard anti-cancer drugs docetaxel, showing 7-10  $\mu\text{M}$  for PCa cell lines, while doxorubicin showed 6-9  $\mu\text{M}$  for BC cell lines. The cell viability of the selected bioactive compounds on different cell lines is presented in Table 3.5. Table 3.5 shows that Sal B showed the most potent cytotoxic effect (12-18  $\mu\text{M}$  for PCa and 14-20  $\mu\text{M}$  for BC).

**Table 3.5:** Cell viability of compounds on different cell lines

Compound	PC-3 ( $\mu\text{M}$ )	DU145 ( $\mu\text{M}$ )	MCF-7 ( $\mu\text{M}$ )	MDA- MB-231 ( $\mu\text{M}$ )	Remarks
Docetaxel	7-10	7-10	-	-	Positive control for prostate cell lines
Doxorubicin	-	-	6-9	6-9	Positive control for breast cell lines
Sal B	12-18	12-18	14-20	14-20	Most effective; dose-dependent response; comparable to docetaxel/doxorubicin
EA	22-30	22-30	23-25	23-25	Moderate efficacy; weaker than Salvianolic Acid
[ $^3\text{H}$ ] PDBu	>60	>60	>60	>60	Mild cytotoxicity; weakest among tested
[ $^3\text{H}$ ] DPB	45-55	45-55	45-55	45-55	Slightly better than ([ $^3\text{H}$ ] PDBu), still relatively weak

The cell viability of the selected bioactive compounds on different cell lines is presented in Figure 3.12.

**Figure 3.12:** Cell viability of compounds on different cell lines

Its  $\text{IC}_{50}$  values are close to doxorubicin (6-9  $\mu\text{M}$ ) and docetaxel (7-10  $\mu\text{M}$ ), indicating high potency. Conversely, ellagic acid exhibited moderate cytotoxicity ( $\text{IC}_{50}$  range 22-30  $\mu\text{M}$  for

PCa and 23-25  $\mu\text{M}$  for BC). Ellagic acid may also contribute to anti-cancer effects due to its antioxidant nature. Notably, [ $^3\text{H}$ ] DPB showed mild toxicity (45-55  $\mu\text{M}$ ) across all cell lines, whereas [ $^3\text{H}$ ] PDBu exhibited an  $\text{IC}_{50}$  range above 60  $\mu\text{M}$ , showing minimal cytotoxicity even at high concentrations. This study indicates that phorbol esters have limited cytotoxicity and cannot be used effectively as monotherapies. Doxorubicin and docetaxel provide valuable context in validating the potential of salvianolic acid as an anticancer agent.

The data of the comparative  $\text{IC}_{50\text{s}}$  show that the clinical standards, docetaxel (prostate cancer) and doxorubicin (breast cancer), were the strongest substances used with  $\text{IC}_{50\text{s}}$  values of 7-10  $\mu\text{M}$  in their corresponding cell lines. The low  $\text{IC}_{50}$  values confirm the assay and give a critical point of reference in determining the relative activity of the natural test compounds. The two drugs are also first-line chemotherapeutics with well-defined mechanisms of action, such as microtubule stabilization with docetaxel and DNA intercalation with topoisomerase II alpha (topo II $\alpha$ ) inhibition with doxorubicin. These standard drugs also have high potency to confirm the robustness of the experimental system. Salvianolic acid B was most consistently active with an  $\text{IC}_{50}$  of 12-18  $\mu\text{M}$  in PC-3 and DU145 prostate cancer lines and 14-20  $\mu\text{M}$  in MCF-7 and MDA-MB-231 breast cancer lines. Although less potent than the standards, this activity is within a two-fold range of docetaxel and doxorubicin, which is remarkable in the case of a polyphenolic natural product. Significantly, Sal B showed dose-dependent cytotoxicity in all the models. Its comparatively consistent  $\text{IC}_{50}$  values against both hormone-insensitive prostate and receptor-diverse breast cancer lines indicate that its anticancer activity is not highly sensitive to hormone receptor status but may be more characteristic of a more general interaction between the compound and intracellular targets, including DNA-processing enzymes and kinases. This has rendered Sal B an excellent candidate for future development, primarily when concerns of bioavailability and solubility can be addressed. Ellagic acid (EA) showed moderate but repeatable cytotoxicity with  $\text{IC}_{50}$  22-30  $\mu\text{M}$  in prostate target and 23-25  $\mu\text{M}$  in breast target. Ellagic acid was found to have an appreciable activity in all lines despite its much lower potency than Sal B and the clinical standards, establishing its possible role as a supportive or adjunctive treatment agent. Ellagic acid (EA) was approximately 3-fold weaker than docetaxel and doxorubicin, although it was always better than the phorbol derivatives. The observation that ellagic acid did not lose its activity in each of the four cell lines highlights its generic activity, probably because of DNA and protein interactions. Still, its lower potency compared with salvianolic acid B indicates that the drug lacks or has fewer and less stable

molecular interactions with the pathogenic targets in the cancer. Conversely, the phorbol esters had the lowest activity level of the tested compounds, with the IC<sub>50</sub> of 45-55 μM in all cell lines and thus showed cytotoxicity at high levels. Although this activity is marginally superior to [<sup>3</sup>H] PDBu, which did not achieve 50% inhibition at concentrations exceeding > 60 μM, the two derivatives were less potent than the clinical standards. This could be due to their low cytotoxicity being representative of their hydrophobic terpenoid backbones, which cannot form the extensive hydrogen-bonding and π-stacking interactions evident with polyphenols like Sal B and ellagic acid. Moreover, they are predicted to be P-glycoprotein substrates, which probably limits effective intracellular accumulation, further contributing to poor activity. The potency hierarchy of this investigation is Docetaxel/Doxorubicin > Sal B > EA > phorbol esters. Notably, the standards maintain their anticipated hegemony, but the presence of salvianolic acid B falling within a close potency range of both docetaxel and doxorubicin could indicate strong potential for the lead compound as an anticancer agent.

#### **3.4.3.1. Microscopic images of anticancer effect of compounds and standards**

Morphological hallmarks of apoptosis in prostate (PC-3, DU145) and breast (MCF-7, MDA-MB-231) cancer cells were observed by fluorescence microscopy after incubating them with the test compounds and positive controls. Hoechst dye (blue) was used to stain the cells as a viable nucleus label, and propidium iodide (PI)/Annexin V (red/pink) to label apoptotic nuclei. Therefore, normal cancer cells appear blue with intact and round nuclei, but apoptotic cells have condensed, fragmented, or shrunken red/pink nuclei, and membrane blebbing and apoptotic bodies. As anticipated, doxorubicin (breast lines) and docetaxel (prostate lines) had a robust apoptotic response, with most of the cells being stained in red/pink and having a classical apoptotic morphology (nuclear condensation and fragmentation). This validates their effectiveness in causing apoptosis by well-known mechanisms, microtubule stabilization (docetaxel) and DNA intercalation/topoisomerase II alpha (doxorubicin). In prostate and breast lines, a high percentage of apoptotic cells (appearing as red-stained condensed or fragmented nuclei) was caused by Sal B, and a sharp decrease in the number of blue viable cells was evident relative to the untreated controls. Its apoptotic levels were the second highest relative to the standards, with its IC<sub>50</sub> range (12-20 μM) falling within twofold of that of docetaxel/doxorubicin. Moreover, it was found that moderate apoptosis levels were induced with ellagic acid treatment. The population of viable blue and apoptotic red/pink cells in both prostate and breast lines was mixed. The apoptotic fraction remained lower than that of

salvianolic acid B and the standards, which had stronger IC<sub>50</sub> values (22 to 30 μM). Nuclear morphology consisted of shrinkage and a minor degree of fragmentation, which favors apoptosis as the most common form of cell death, but with lower efficiency than that of Sal B. Ellagic acid was a moderate inducer of apoptosis, and the phorbol esters were weak inducers, as presented in Figure 3.13.

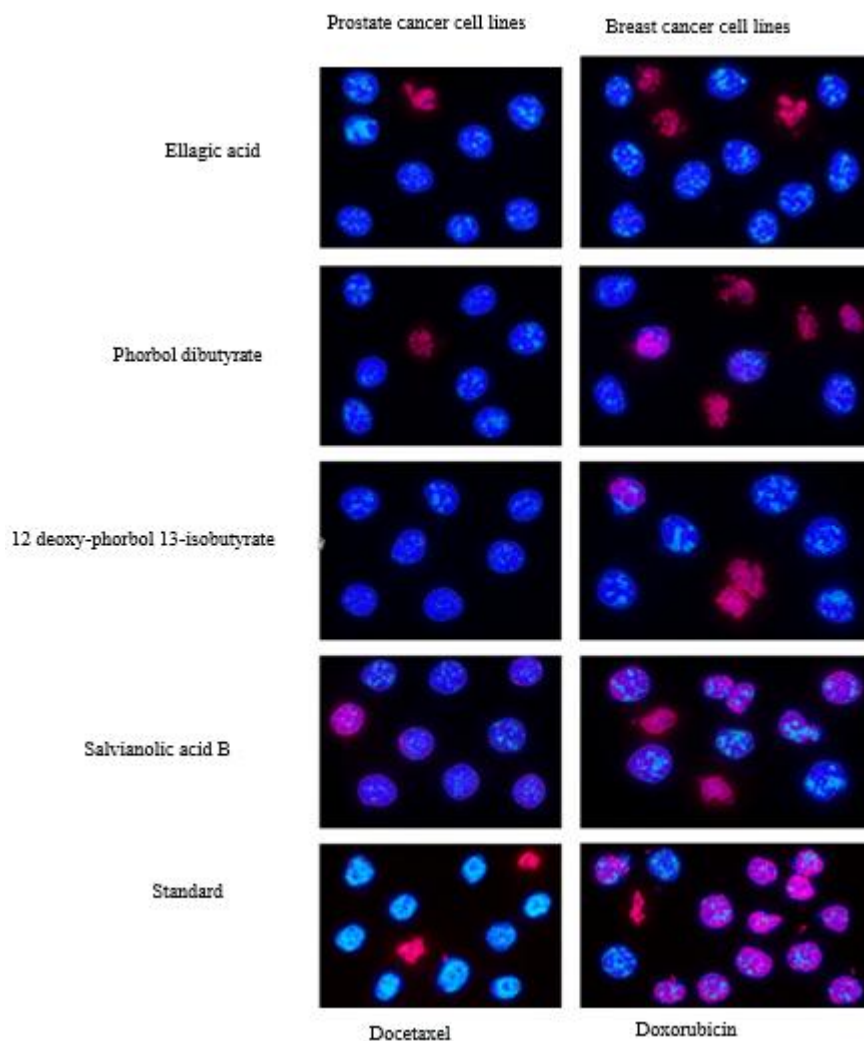


**Figure 3.13:** Microscopic images of the anticancer effect of compounds and standards

The number of apoptotic cells was lower than with Sal B and EA, with significant percentages of intact blue-stained viable cells left with [<sup>3</sup>H] DPB treatment. It was also found with red-stained apoptotic nuclei, but with lower frequency, which is expected given its higher IC<sub>50</sub> (~45-55 μM) and reduced strength. Some apoptotic cells had swollen, abnormal morphology, indicating cytotoxic action that was less reproducible between replicates. In this investigation, [<sup>3</sup>H] PDBu was noted to be the least potent apoptotic. The majority of cells had intact blue-

stained nuclei and sporadic red-stained apoptotic cells. Nuclear condensation and fragmentation were uncommon, consistent with the MTT data in which the IC<sub>50</sub> values were over 60 μM and the cytotoxicity was low. The absence of major apoptosis can be interpreted to indicate that this phorbol analog is not a good inducer of programmed cell death within the administered concentrations. Apoptosis was the greatest with standards, followed closely by Sal B, the most potent natural product, as it showed a wide range of apoptotic activity in both prostate and breast lines.

### 3.5 Conclusions

Molecular docking studies revealed that Sal B exhibited the highest docking score with all enzyme catalytic residues through key hydrogen bonding, followed by EA, which showed moderate binding affinity. However, [<sup>3</sup>H] PDBu and [<sup>3</sup>H] DPB displayed significantly weaker binding on all enzymes except DNA lyase. Biochemical inhibition analysis supported the computational findings that Sal B is a potential inhibitor of all the targets in anti-cancer drug development. The combined *in silico* and *in vitro* studies suggest that Sal B is the most promising inhibitor of the target protein studied. Similarly, EA was moderately effective, and [<sup>3</sup>H] PDBu and [<sup>3</sup>H] DPB were less effective, with only desirable inhibition of DNA lyase observed. The docking protocol was validated by low RMSD values of less than or equal to 2 Å. Also, hydrogen bonding conformational integrity of the EA complexes was confirmed by molecular dynamics simulations of the ligand as a potential anti-cancer agent. Remarkably, integrating molecular dynamics, molecular docking, redocking validation, and *in vitro* assay provides a platform to benchmark *Sapium* metabolites. In addition, this comparative framework has highlighted the limited but target-specific activity of phorbol esters. Ultimately, accurate clinical trials and *in vivo* studies are necessary to confirm the potential preventive and therapeutic effects of these bioactive compounds.

## CHAPTER FOUR

### EXPERIMENTAL AND THEORETICAL ASSESSMENT OF SALVIANOLIC ACID B, ELLAGIC ACID, AND PHORBOL ESTERS AS DRUG CANDIDATES AGAINST BREAST AND PROSTATE CANCER

#### Abstract

Global efforts aimed at developing innovative anti-cancer lead compounds derived from natural compounds found in plants have gained significant momentum, with a focus on achieving Sustainable Development Goal (SDG) 3 on good health and well-being. This investigation included dynamic simulations and experimental validation on breast cancer (BC) and prostate cancer (PCa) cell lines. Salvianolic acid B (Sal B) complex displayed the lowest and most stable RMSD values for both the protein backbone and the ligand backbone, ranging from 0.2-0.25 Å and 0.15—0.45 Å, respectively. Ellagic acid (EA) exhibited a moderate root mean square deviation (RMSD) value of 0.25-0.39 Å for the protein and 0.2-0.25 Å for the ligand, with slight fluctuations indicative of lower stability than Sal B complexes. Additionally, ADME kinetics and docking analyses show a clear trade-off: polyphenols (Sal B and EA) have remarkable target binding (high polarity and H-bonding). However, these polyphenols suffer from low predicted permeability and bioavailability. Toxicity and exertion assessments of all the compounds were not found to be AMES mutagenic, hERG-liable, hepatotoxic, or skin sensitized, indicating their overall cellular safety. Molecular dynamics simulation over 200 ns confirmed the stability of the Sal B acid, showing low RMSD values on all targets. The positive-control transparency for docetaxel is 0.10-5.0 µM range; IC<sub>50</sub> (mean SD) 8.6 ± 0.7 µM (PC-3), 8.2 ± 0.6 µM (DU145), while that of doxorubicin is 0.03 ± 30 µM; IC<sub>50</sub> (mean SD) 7.6 ± 0.6 µM (MCF-7), 7.2 ± 0.5 µM (MDA-MB-231). Control fits and statistics were run in the same pipeline as the test compounds (4PL, replicate-wise fits, ANOVA on log<sub>10</sub> (IC<sub>50</sub>)). In line with ranges, the most active natural products in prostate and breast cancer lines were Sal B and EA, while the phorbol esters were the weakest. However, for accurate clinical trials, animal experiments and *in vivo* studies are necessary to confirm the potential preventive and therapeutic effects of these bioactive compounds.

#### 4.1 Introduction

Breast cancer (BC) remains a challenging global health burden with diverse manifestations and intricate pathogenesis, creating significant obstacles to effective treatment and prevention. As

global incidence rises nearly exponentially, current studies focus on developing effective therapeutic strategies (Xiong et al., 2025). Although significant progress has been made in early detection and therapeutic strategies, the malignancy exhibits a complex etiology, necessitating a deeper understanding of its molecular underpinnings (Xiong et al., 2025). Prostate cancer (PCa) is prevalent among men over 65 years and also depicts epidemiological patterns and significant heterogeneity, and is the leading cause of cancer-related mortality. Metastatic PCa cells spread to distant sites, including the bladder, rectum, lumbar spine, pelvis, vertebrae, bones, and brain. In 2024, the National Institutes of Health reported 299,010 new PCa cases – 14% of all new cancers – and 35,250 related deaths in the US (Wang et al., 2025). Early detection and treatment of BC and PCa have significantly improved patient survival rates, particularly for regional and localized cases, while metastatic PCa and BC remain significant challenges. The mortality rates of cancer highly depend on the prognoses of patients in the metastatic stage (Klibaim et al., 2025), highlighting the critical need for more effective treatments of metastatic cancers.

Over the last decades, considerable research has been undertaken in developing biological and chemical analytical techniques that link pharmacology with phytochemistry. Combined with the emerging technologies in lead identification implemented in clinical research, these have driven the rapid development of natural drugs from plant extracts to complement the treatment of various disorders and diseases (Singh et al., 2025). The growing body of scientific publications on prescriptions of Traditional Chinese Medicine has demonstrated the potential of *Dan-Shen* (*Salvia miltiorrhiza*, *DS*) to complement the different types of cancers (Lai et al., 2024). The efficacy and bioavailability of herbal medicines extracted from natural plants are comparable to those observed in chemotherapy or radiotherapy, significantly extending patient survival (Gu et al., 2024). Moreover, their toxicity profiles are relatively low with minimal side effects. Recent evidence from the past decade has shown that extracts from Danshen, particularly phenolic compounds, exhibit anti-cancer effects, and their derivatives could be potential lead candidates in the development of anti-cancer drugs (Zhang et al., 2024). Danshen is a widely used traditional medicine with various active ingredients that can be classified into different groups based on structural and chemical properties (Lai et al., 2024). These groups are: water-soluble phenolic acids and lipid-soluble tanshinones. Rosmarinic acid B and Sal B acid comprise water-soluble phenolic acids, whereas lipid-soluble tanshinones include cryptotanshinone, dihydrotanshinone I, and tanshinones I and II (Xing et al., 2025). Among the various active ingredients of Danshen (*Salvia miltiorrhiza*), salvianolic acids A and B have the

highest antioxidant activity. Sal B is a well-known phenolic acid compound known to decrease oxidative stress, angiogenesis, and inflammation and increase apoptosis, potentially inhibiting the growth of BC tumours (Zhang et al., 2024). Considering the large-scale clinical use of Sal B in Asia and beyond, it is urgent to understand its mechanism to prevent complications and maximize its therapeutic benefits.

Previous studies have highlighted the phenolic antioxidants, such as astragalins, gallic acid, and kaempferol, underlying the pharmacological benefits of *Sapium sebiferum* leaf extract (Yadav et al., 2025). The current pharmacological and phytochemical findings of the genus *Sapium* indicate that EA has been successfully used in managing various conditions, including dermatitis (Al Muqarrabun et al., 2014). Although polyphenols are known to be structurally similar, EA has been proclaimed to be effective in the regression of several types of cancer, including prostate cancer and breast cancer (Vanella et al., 2013). Ellagic acid (EA) in *Sapium ellipticum* exists in free form as aglycone form extracted using methanol and acetone, ellagitannins, polyphenols found in leaves and barks that hydrolyze to release EA, and EA glycosides, which are a sugar-bound form that exists in trace amounts. Many *in vivo* and *in vitro* investigations have established the promising effects of EA as an antitumorigenic compound (direct killer of cancer cells), an inhibitor of metastasis and angiogenesis, and an antiproliferative drug that arrests carcinogenesis (Ceci et al., 2018; Čižmáriková et al., 2023). This bioactive compound exhibits selective cytotoxicity towards carcinoma cells without harming normal cells. Little is known about improving the oral availability of EA. This naturally occurring bioactive substance has attracted numerous studies in *in vivo* pharmacokinetics and *in vitro* cellular uptake to enhance its antitumor efficacy (Čižmáriková et al., 2023).

Furthermore, compounds such as diterpenes (phorbol esters) are polycyclic compounds known to activate the protein kinase C (PKC) enzyme family. Phorbol esters, specifically [<sup>3</sup>H] PDBu and [<sup>3</sup>H] DPB, are diterpenoids that have been extracted from *Sapium ellipticum* and other Euphorbiaceae plants (Kazanietz, 2005). Chemically, [<sup>3</sup>H] PDBu is a diester of phorbol that has butyric acid groups at positions 12 and 13. In contrast [<sup>3</sup>H] DPB is a monoester derivative with no hydroxyl group at position 12 and has an isobutyric acid group at position 13. These phorbol esters are biologically active agents that activate PKC, offering real therapeutic promise (Kazanietz, 2005). Both activate protein kinase C (PKC), a pathway that researchers have utilized to study various cellular processes, including immune responses, differentiation,

and growth (Cheshomi et al., 2021; El-Fakahany, 2020; El Omari et al., 2021). Other pre-clinical studies have also reported the antioxidant properties of EA, which prevent deoxyribonucleic acid (DNA) damage and neutralize free radicals, making it a potential agent to be harnessed in *Sapium ellipticum* as a natural alternative in cancer treatment (Kanthé et al., 2021; Wang et al., 2022). It also inhibits topoisomerase and intercalates with DNA, suggesting it may be a potential anti-cancer agent. Accordingly, the phytochemical investigation of *Sapium ellipticum* and *Salvia miltiorrhiza* (Danshen) reveals different bioactive compounds that can be explored for cancer treatment through various mechanisms.

Together with conventional cancer treatment modalities, targeted therapies in cancer treatment and management have gained significant traction (Zhou & Li, 2022). Implementing these approaches focuses on identifying essential biomolecules for tumour development or normal physiological cellular replication and functioning, and consequently, brings cytotoxic and cytostatic effects to affected cells (Vanneman & Dranoff, 2012). Moreover, they alleviate nonspecific toxicities linked to chemotherapy and radiation. Finding inhibitors against oncoproteins linked to BC and PCa increases the therapeutic scope, enhances the minimization of tumor progression, reduces drug resistance, and facilitates the development of comprehensive inhibition. In this pursuit, the significance of computational predictions rooted in biomedicine and biology cannot be overstated. Indeed, the recent groundbreaking advances in novel anti-cancer drug designs have benefited from modeling techniques and computational bioinformatics, rather than solely relying on experimental methods that demand extensive resources and time (Chunarkar-Patil et al., 2024). Molecular dynamics simulation is employed to help predict optimal binding modes by studying the thermodynamic behavior of ligand-protein interactions (Rizzuti, 2022; Sehwat et al., 2024). This technology can bridge the gap between microcosms and macroscales by enabling the simulation of specific processes involving intermolecular interactions. Typically, molecular dynamics aid in identifying the relative motion of a molecule or atom based on Newton's equation of motion (second law). It also helps to obtain the kinetic property parameters according to the trajectory (Rizzuti, 2022).

The current study addresses this knowledge gap by systematically investigating the four ligands – EA, Sal B acid B, [<sup>3</sup>H] DPB, and [<sup>3</sup>H] PDBu. Accordingly, they are promising candidates that can interact with APE1, topoisomerase II alpha, and serine/threonine-protein kinase mTOR in combating cancer-causing agents. A plethora of studies have shown that the topoisomerase enzyme is linked to the androgen receptor in prostate cancer (PCa) and is associated with tumor

progression (Schaefer-Klein et al., 2015). Also, in BC chemotherapy, topoisomerase inhibitors are used (Vanderbeeken et al., 2013). PCa progression is also associated with the DNA lyase enzyme, particularly adenylosuccinate lyase (ADSL), and oxidative DNA damage repair enzymes are linked to BC aggression (Li et al., 2001). Conversely, mTOR is targeted in BC management to overcome resistance (Li et al., 2021) and is known to drive the growth of prostate cancer (PCa) (Chen et al., 2024). In this coupled theoretical and experimental study, molecular dynamics simulations were performed to elucidate the root mean square deviation (RMSD) and absolute free energies of ligand-protein interactions. Additionally, *in vitro* analysis has been used to study the cell-inhibitory effects of all ligands on two human breast cancer cell lines - MCF-7 (RRID: CVCL\_0031) and MDA-MB-231 (RRID: CVCL\_0062), and two prostate cancer cell lines - PC-3 (RRID: CVCL\_0035) and DU 145 (RRID: CVCL\_0105). Through this coupled *in vitro* and *in-silico* investigation, we have identified novel hit lead compounds capable of inhibiting topoisomerase II alpha, mTOR, and DNA lyase proteins linked to PCa and BC progression.

## **4.2 Methodology**

### **4.2.1 Molecular dynamics simulations**

To perform molecular dynamics (MD) simulations of all selected compounds, EA, Sal B, [<sup>3</sup>H] DPB, and [<sup>3</sup>H] PDBu, on the target enzymes, DNA lyase, DNA topoisomerase II alpha, and mTOR kinase, a standardized simulation workflow using GROMACS on Google Colab was employed (Van Der Spoel et al., 2005). The AMBER99SB force field was applied throughout the simulation (Kashefolgheta et al., 2021). The ligand-enzyme complexes were solvated in a triclinic water box using the Transferable Intermolecular Potential with 3 Points (TIP3P) implicit water model, and system neutrality was achieved by adding appropriate counter ions. Energy minimization was performed to remove steric clashes using a steepest descent algorithm, followed by equilibration phases in two steps: constant number of particles, volume, and temperature (NVT) and constant number of particles, pressure, and temperature (NPT), each lasting 100 picoseconds (ps). During equilibration, position restraints were applied to the heavy atoms of the protein, allowing the solvent to relax. After successful equilibration, production molecular dynamics (MD) runs were carried out for 200 nanoseconds (ns) at 300 K using the Leap-Frog integrator and Berendsen thermostat and barostat algorithm to maintain

temperature and pressure, respectively. Periodic boundary conditions and the Particle-Mesh Ewald method were used to treat long-range electrostatic interactions.

All simulations were performed on Google Colab using a preinstalled GROMACS version 2025.2 environment notebook or linking a custom Google Drive to host and store simulation files (Abraham et al., 2015). Key analyses were employed, including RMSD and interaction energies of the ligand-receptor interactions that were evaluated using the MM/GBSA approach. Igor software version 5.0 (Cameron et al., 2024) was used to extract visual and numerical insights into complex stability, conformational changes, and binding affinity throughout the simulation. To calculate the absolute free binding energy of all enzyme-ligand complexes, a structural approach was implemented using GROMACS on Google Colab, integrating alchemical free energy perturbation or thermodynamic integration, depending on the computational resources and the desired level of accuracy. These calculations aimed to determine the thermodynamically rigorous estimate of free energy change associated with transferring ligands from the solvated state to the bound complex state.

The methodology began with generating and simulating two systems for each ligand complex solvated in a water box and ligand in solution alone in a similar aqueous environment. Each system was parameterized using the AMBER99SB force field. Ligand topologies were generated via ACPYPE (Sousa da Silva & Vranken, 2012) or LigPrep Gen, subjected to energy minimization followed by NVT and NPT equilibration phases, as in standard MD simulations (Beyens et al., 2024; Panwar et al., 2022; Han Zhang et al., 2021). For absolute free energy calculations, the alchemical transformation was performed using lambda coupling parameters that progressively turn off the ligand's non-bonded interaction with its environment, both electrostatic and van der Waals. A series of lambda values from 0.0 to 1.0 in 10-20 steps was defined. For each lambda, a short molecular dynamics simulation was run to equilibrate and sample that state using tools like gmx bar or gmx mbar to give the absolute free energy for binding. A total of 20 lambda windows were considered (10 ns simulation per window) in the 200 ns simulation study. All simulations and data processing were conducted on Google Colab, which was configured with GPU acceleration to handle computationally demanding free energy perturbation steps. The simulation was set up with custom setups integrating Python scripting, OpenMM (Eastman et al., 2017) for enhanced sampling, and PLUMED (Tribello et al., 2014) for restraint handling or umbrella sampling as needed. The final binding energy was obtained using the thermodynamic cycle, which compares the free energy of the ligand in the

solvated unbound state and the complexed bound state. This method provided quantitative insights into binding affinity, enabling the ranking of ligands based on their thermodynamic favorability in relation to their potential anti-cancer properties.

#### **4.2.2 Properties of drugs and ADMET**

The SwissADME web server (<http://www.swissadme.ch>) was utilized to evaluate the absorption, distribution, metabolism, and excretion (ADME) properties of the selected compounds (Riyadi et al., 2021). It is an open-source computational platform to predict pharmacokinetics, physicochemical properties, and drug-likeness based on molecular structure. The canonical SMILES of the selected lead compounds were retrieved from the PubChem database and input into the SwissADME input interface. Descriptors calculated using the server comprised a full range of descriptors (mol weight, HK donors and acceptors, rotatable bonds, topological polar surface area (TPSA), lipophilicity indices based on multiple algorithms (iLOGP, XLOGP3, WLOGP, MLOGP, SILICOS-IT), and averaged to generate the consensus LogP. The three independent predictive models (ESOL, Ali, and SILICOS-IT) were evaluated as solubility estimators by both quantification (log S values) and qualitative assessment (soluble, moderately soluble, and poorly soluble). Predictive pharmacokinetics were provided in terms of the gastrointestinal absorption potential, blood-brain barrier (BBB) permeability, the skin permeation coefficient (log Kp), P-glycoprotein substrate, and major cytochrome P450 (CYP1A2, CYP2C9, CYP2C19, CYP2D6, and CYP3A4) inhibition potential. Moreover, SwissADME generated a drug-likeness assessment based on Lipinski, Veber, Egan, Ghose, and Muegge rules and medicinal chemistry filters like lead-likeness, PAINS (pan-assay interference structures), and Brenk alerts, as well as an assessment of each compound as a bioavailability radar, summarizing drug-likeness in terms of size, polarity, lipophilicity, saturation, solubility, and flexibility, and as the BOILED-Egg model, which indicates passive gastrointestinal absorption and brain access. Each SMILES was submitted several times to maintain consistency, and the results were compared to ensure consistency. The neutral parent and the ionized microspecies of Sal B acid and EA were both tested to explain the effect of deprotonation on the predictions of absorption and permeability. When working with the lipophilic phorbol esters, lipophilicity, CYP inhibition, and P-gp substrate probability were of particular interest, as these characteristics potentially impact oral bioavailability and potential drug-drug interactions. All the results were exported and tabulated, and the radar plots and BOILED-egg diagrams were saved and interpreted (Karakuş, 2024).

### 4.2.3 Statistical analysis

After 48-hour exposure to serial half-log dilutions of RPMI/DMEM made in the presence of 0.1% DMSO (vehicle control), cytotoxicity was assessed using the MTT assay. Test compounds (Sal B acid B, EA, [<sup>3</sup>H] PDBu, and [<sup>3</sup>H] DPB) were screened at 0.5-200 μmol/L (6-8 points, 10-90% effect). The same plates were run and analyzed identically: docetaxel (PCa benchmarking; 0.10-50 μM in PC-3 and DU145) and doxorubicin (BC benchmarking; 0.03-30 μM in MCF-7 and MDA-MB-231). The conditions consisted of three biological replicas, each including three technical wells. The absorbance of the blanks was subtracted from the blanks and normalized to the vehicle (100%), as represented in Equation 4.1.

$$y = \text{Bottom} + (\text{Top}-\text{Bottom}) / (1 + x/IC_{50})^{\text{Hillslope}} \quad 4.1$$

A four-parameter logistic model of the response (4PL) was fit to the data of each biological replicate: with constrained nonlinear least squares (Top 80-120% Bottom -10-20% Hill 0.3-3.0). Each replicate yielded IC<sub>50</sub> and 95% profile-likelihood CI; we report geometric mean SD (anti-logarithms of log<sub>10</sub> IC<sub>50</sub>). The Shapiro-Wilk test was used to check the normality of log<sub>10</sub>/IC<sub>50</sub>. We conducted a one-way ANOVA of log<sub>10</sub>(IC<sub>50</sub>) in each cell line (factor: compound) to draw inferences. In PC-3/DU145 and MCF-7/MDA-MB-231, the Dunnett test was used to compare the test compounds with a corresponding positive control (docetaxel and doxorubicin, respectively). To make all-pairs contrasts between test compounds, Tukey's HSD was applied. When the Levene test suggested heteroscedasticity, Welch's ANOVA with Games-Howell post-hoc tests was used. We report F, df, exact p-values, and η<sup>2</sup> effect sizes. Multiplicity was managed in the four ANOVAs with a Benjamin Hochberg FDR = 0.05. R/GraphPad analyses were performed. The highest concentration did not halve viability with [<sup>3</sup>H] PDBu in multiple replicates; therefore, we report the IC<sub>50</sub> as > 60 μM and applied an 80 μM censored estimate to ANOVA to allow the group to be included (as indicated in the tables).

## 4.3 Results and discussions

### 4.3.1 Assessment of drug-likeness and ADME investigation

Pharmacokinetics studies how the body reacts with administered drugs for a given time of exposure (Sehrawat et al., 2023). The ADME kinetics of the four phytochemicals as predicted by the SwissADME platform showed clear differences that were in good agreement with the observed binding propensities of the phytochemicals to DNA lyase, DNA topoisomerase II alpha, and mTOR kinase. Sal B is a large and highly polar polyphenol with a complex profile,

which violates Lipinski's rule of 5. Sal B has a molecular weight (MW) of 718.6 Daltons (Da), topological surface area (TPSA) of 278 Å<sup>2</sup>, 16 hydrogen bond acceptors, and nine hydrogen bond donors. Its corresponding logP of 2.23 represented relatively moderate lipophilicity, and all solubility models showed that the compound was poorly soluble with extremely low predicted passive oral absorption. Moreover, ADME kinetics demonstrated that the compound exhibits poor gastrointestinal absorption, lacks blood-brain barrier (BBB) permeability, and has very low bioavailability (0.11%).

Nevertheless, despite the poor pharmacokinetic characteristics, Sal B was found to have the highest docking affinities with each of these three molecular targets. This is due to its high aromatic surface (24 aromatic atoms) and high concentration of polar groups. This allows *salvia* to form strong hydrogen bonds and stack in sigma interactions with the catalytic pockets (Bicak et al., 2025). Due to the chemical and polyphenolic nature of the compound, various Lipinski, Ghose, Veber, Egan, and Muegge violations, as well as the PAINS and Brenk warning signs, were noted. Nonetheless, such violations are common with bioactive natural products (Rudrapal et al., 2025). The pharmacological properties of the compound can be further developed through optimization approaches in medicinal chemistry (Rudrapal et al., 2025).

EA, on the other hand, exhibited a smaller structure that did not violate any of Lipinski's rules of five (MW 302.2 Da; TPSA 141 Å<sup>2</sup>; 0 rotatable bonds). Moreover, EA has a logP of 1.0 and exhibits solubility properties, which predict high gastrointestinal absorption and an enhanced bioavailability score (0.55). Its drug-likeness reflected that of potential hit compounds, violating none of Lipinski's rules of five and Veber and Egan's rules of drug likeness (Ibrahim et al., 2024). EA was also reported to be a potential CYP1A2 inhibitor, with no interaction with other CYP isoforms, indicating a relatively favorable metabolic profile. In docking studies, EA was found to have the second strongest binding affinity to its biological targets (cf. Table 4.1), after Sal B and better than the phorbol esters. This is explained by its intermediate polarity and planar aromatic structure, which allow for stable cavity hydrogen-bonding and stacking interactions in the DNA- and ATP-binding sites of the enzyme. It is also evident that EA exhibits more favourable ADME properties than Sal B acid B. Thus, EA is a potential anticancer agent attributed to its attractive biological and binding affinity to its biological targets. However, scientific challenges include slow metabolism and low water solubility *in vivo* (Leng et al., 2025).

**Table 4.1:** Assessment of drug-likeness of the potential lead compounds

<b>Parameter</b>	<b>Sal B</b>	<b>EA</b>	<b>[<sup>3</sup>H] PDBu</b>	<b>[<sup>3</sup>H] DPB</b>
Formula	C <sub>36</sub> H <sub>30</sub> O <sub>16</sub>	C <sub>14</sub> H <sub>6</sub> O <sub>8</sub>	C <sub>28</sub> H <sub>40</sub> O <sub>8</sub>	C <sub>24</sub> H <sub>34</sub> O <sub>6</sub>
MW	718.61	302.19	504.61	418.52
Number of rotatable bonds	14	0	9	4
Number of H-bond acceptors	16	8	8	6
Number of H-bond donors	9	4	3	3
Lipinski of violations	3	0	1	0
Ghose of violations	3	0	3	0
Veber's number of violations	2	1	0	0
Egan's number of violations	1	1	0	0
Muegge's number of violations	4	0	0	0
Bioavailability Score	0.11	0.55	0.55	0.55
PAIN's number of alerts	1	1	0	0
Brenk number of alerts	3	3	2	1
Lead's number of violations	3	0	2	1
Synthetic Accessibility	6	3.17	6.37	5.77

It was also evident in the ADME kinetics that the two phorbol esters exhibited drug-like properties. For instance, [<sup>3</sup>H] PDBu has a MW of 504.6 Da, and a TPSA of 130 Å<sup>2</sup>, while [3H] DPB has a MW of 418.5 Da, and a TPSA of 104 Å<sup>2</sup>. Both molecules were predicted to have high gastrointestinal absorption and moderate oral bioavailability (0.55), consistent with their lower polarity and higher logP values (2.75 and 2.39, respectively). Predictions of solubility were inconsistent; however, these esters generally appeared to be in the soluble to moderately soluble range, unlike Sal B acid B. However, both compounds were determined to be substrates of P-glycoprotein, indicating that efflux mechanisms could significantly limit intracellular accumulation. In this study, [<sup>3</sup>H] PDBu was also predicted to inhibit CYP3A4 during drug-drug interactions, whereas [<sup>3</sup>H] DPB was expected to have no CYP inhibition. From a drug-likeness perspective, the phorbol esters violated fewer criteria compared to Sal B acid B.

Notably, the phorbol esters violated Ghose and lead-likeness criteria attributed to the bulky and terpenoid-derived groups. In docking studies, both the phorbol esters yielded the lowest total binding energies, though limited affinity at the etoposide binding site of topoisomerase II alpha was noted. This is due to the relatively low number of H-bond donors/acceptors in [3H] PDBu and [3H] DPB, at 3/8 and 3/6, respectively. Moreover, these esters have a higher dependence on hydrophobic interactions, which became less favored in the polar and DNA-rich environment of the selected targets.

#### **4.3.2 Excretion and toxicity profiles**

In this investigation, the excretion and toxicity parameters of Sal B acid B, EA, [<sup>3</sup>H] PDBu, and [<sup>3</sup>H] DPB are predicted to evaluate their safety and pharmacological feasibility. It is evident that Sal B had a relatively low predicted total clearance ( -0.609 log ml/min/kg). This indicates that the compound exhibits slow systemic excretion and has the potential for in vivo accumulation, which could increase exposure at the site of action while also increasing the likelihood of accumulation over time and potential toxicity (Sehrawat et al., 2023). Notably, it was not observed to be a renal OCT2 substrate, meaning it is not at risk of drug-drug interactions mediated by renal transporter. Toxicological profiling was positive, and no AMES mutagenicity, hERG I or II channel blockages (indicating a low risk of cardiotoxicity), or hepatotoxicity/skin sensitization were predicted. The estimated human maximum tolerated dose (0.439 log mg/kg/day) and chronic oral rat LOAEL (5.46 log mg/kg/day) show that tolerance is relatively high compared to the other test compounds. Predicted acute oral rat LD<sub>50</sub> was 2.482 mol/kg, which is moderate in terms of safety margin. Aquatic toxicity prediction

revealed relatively high minnow toxicity (4.64 log mM), which might be a cause of concern in the environment but not in clinical use.

Conversely, EA exhibited an intermediate clearance prediction (0.537 log ml/min/kg) and was eliminated more efficiently than Sal B. This suggests that the compound may reduce accumulation and related risks, but also decrease systemic exposure. The compound was also a good non-OCT2 substrate, and this minimized renal transporter liabilities. The overall toxicity predictions were positive, and the AMES mutagenicity test was negative. There was no hERG inhibition, hepatotoxicity, or skin sensitization. Its MTL (0.476 log mg/kg/day) was slightly greater than that of Sal B, whereas the chronic oral LOAEL (2.698 log mg/kg/day) was somewhat lower. This indicates the existence of a possible long-term toxicity with repeated exposures. The LD50 was estimated at 2.399 mol/kg in acute rats, which is similar to that of Sal B acid B. Environmentally, EA had a lower minnow toxicity (2.11 log mM) than Sal B acid B, indicating a lower ecotoxicological risk. Notably, [<sup>3</sup>H] PDBu had the most significant clearance prediction (0.611 log ml/min/kg), indicating rapid elimination in the body, and thus may decrease therapeutic exposure and effectiveness. Its highest human dose prediction was -0.758 log mg/kg/day, the lowest of the compounds, indicating greater systemic toxicity. The lowest chronic LOAEL value (1.804 log mg/kg/day) also raised concerns about safety issues in long-term use. The acute toxicity was intermediate (LD50 3.063 mol/kg); however, relative to polyphenols, the phorbol ester is more toxic at chronic levels. This investigation showed that [<sup>3</sup>H] PDBu was predicted to be non-mutagenic, non-hepatotoxic, and was not an inhibitor of hERG channels, although aquatic toxicity (minnow toxicity 3.485 log mM) was observed. This indicates that the compound poses a moderate environmental risk. Generally, [<sup>3</sup>H] PDBu is the least desirable due to its toxic profile, which is consistent with its weak anticancer activity. The excretion and toxicity profile of Sal B is summarized in Table 4.2. The clearance level of [3H] DPB was also moderate (0.494 log ml/min/kg), ranking it between Sal B and EA in terms of elimination. Its calculated maximum tolerated dose (-0.169 log mg/kg/day) and chronic lowest observed adverse effect level (LOAEL) (2.055 log mg/kg/day) indicate low tolerability compared with the polyphenols, but not as severe as [<sup>3</sup>H] PDBu. The acute toxicity was estimated at 2.819 mol/kg, which showed a moderate risk. Like other studied compounds, the compound did not exhibit any mutagenicity, hepatotoxicity, hERG inhibition, or skin sensitization, resulting in a manageable safety profile in terms of organ-specific liability.

**Table 4.2:** Excretion and toxicity profile of Sal B

Property	Model Name	Predicted Value	Unit
Excretion	Total Clearance	-0.609	Numeric (log ml/min/kg)
Excretion	Renal OCT2 substrate	No	Categorical (Yes/No)
Toxicity	AMES toxicity	No	Categorical (Yes/No)
Toxicity	Max. tolerated dose (human)	0.439	Numeric (log mg/kg/day)
Toxicity	hERG I inhibitor	No	Categorical (Yes/No)
Toxicity	hERG II inhibitor	No	Categorical (Yes/No)
Toxicity	Oral Rat Acute Toxicity (LD50)	2.482	Numeric (mol/kg)
Toxicity	Oral Rat Chronic Toxicity (LOAEL)	5.46	Numeric (log mg/kg_bw/day)
Toxicity	Hepatotoxicity	No	Categorical (Yes/No)
Toxicity	Skin Sensitisation	No	Categorical (Yes/No)
Toxicity	<i>T. Pyriformis</i> toxicity	0.285	Numeric (log ug/L)
Toxicity	Minnow toxicity	4.64	Numeric (log mM)

These were similar to the environmental toxicity values (4.717 log mM, minimum toxicity to minnow) with moderate ecological risk compared to EA. Notably, none of the compounds were found to be Ames mutagenic, hERG-labile, hepatotoxic, or skin sensitizing, indicating their overall cellular safety.

#### 4.3.3 Bioavailability radar and boiled egg models

The bioavailability radar and BOILED-Egg model analyses provided a complete visualization of the pharmacokinetic suitability of the selected potential anticancer agents. For Sal B acid B, the radar profile exhibited deviations from the optimal physicochemical space, primarily in terms of size, polarity, solubility, and flexibility. The high molecular weight (718 Da), high TPSA of the polar head group (278 Å<sup>3</sup>), and numerous rotatable bonds led the compound to exceed the limits set for orally bioavailable molecules. This was supported by the BOILED-Egg model, which determined that the compound was indeed well outside the predicted areas

of high gastrointestinal absorption/blood-brain barrier penetration. Such a profile aligns with the low bioavailability score (0.11) and multiple rule violations detected in SwissADME. While these results predict poor systemic exposure when administered orally, they show good agreement with docking interactions observed against DNA lyase, DNA topoisomerase II alpha, and mTOR kinase. This observation concurred with literature reports that molecules containing large polar groups can have high binding energy due to strong hydrogen bond and aromatic interactions, but cannot efficiently transfer across biological membranes. Therefore, Sal B is pharmacodynamically potent but pharmacokinetically weak and requires strategies to enhance its binding capacity and drug-likeness. These strategies include targeted drug delivery systems, permeation enhancers, or prodrug modifications. Conversely, EA had a smaller and stiffer scaffold (MW 302 Da, TPSA 141 Å<sup>2</sup>), placing its radar shape even closer to the ideal oral drug space. Polarity was still a limiting factor, but the other parameters were within or close to acceptable ranges (size, lipophilicity, solubility). In the BOILED-Egg model, EA was localized outside of the yellow area corresponding to BBB penetration, as expected for a non-central nervous system (CNS) therapeutic (Popovici et al., 2025). The compound also showed a high gastrointestinal (GI) absorption and a bioavailability score of 0.55. This indicates that, despite being highly polar, its relatively small molecule size and planar aromatic structure allow even small amounts of the molecule to be absorbed in the intestine. This pharmacokinetic profile explains why EA strongly binds to all three targets. This is due to its favorable molecular weight and solubility, which maximize its ability to reach systemic circulation. The low number of violations of drug-likeness parameters and PAINS/Brenk alerts can be attributed to the polyphenolic character that is prone to cause assay interferences in screens.

The phorbol esters exhibited lower polarity and more lipophilic properties, as might be expected for diterpenoid scaffolds. Notably, [<sup>3</sup>H] PDBu displayed a radar that was predominantly within or in proximity to the optimum space of bioavailability, with only slight deviations in polarity and lipophilicity. The lower size for median consensus logP (2.75), acceptable solubility, and moderate polar surface area (130 Å<sup>2</sup>). Notably, the compound displayed physicochemical properties found in orally bioavailable drugs. The Boiled Egg model aligned the compound close to the white area, exhibiting good bioavailability from the gastrointestinal tract, but outside the yolk area, revealing it to be non-permeable at the BBB. Bioavailability Radar and Boiled Egg for the lead compounds are as presented in Figure 4.1.

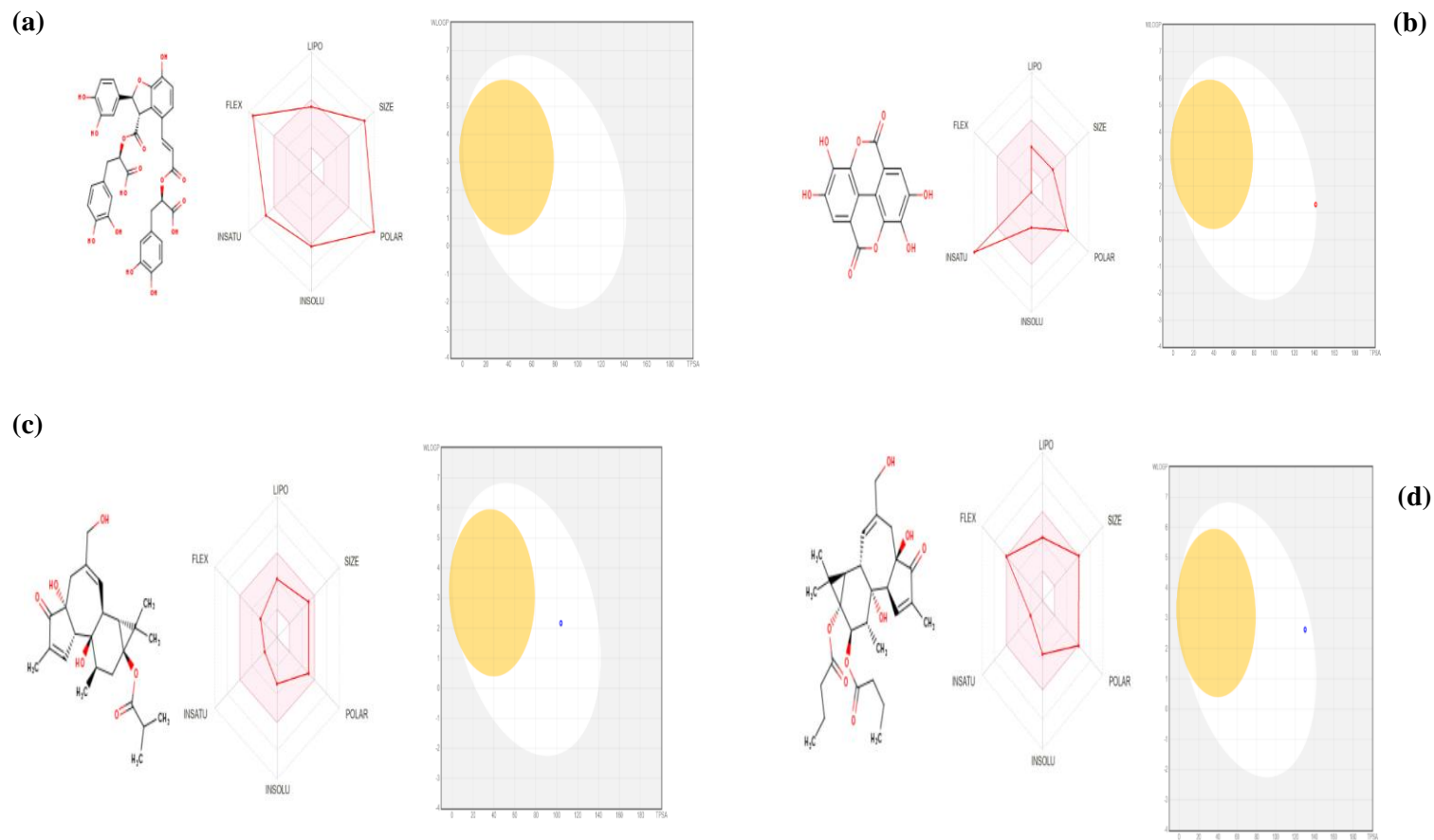


**Figure 4.1:** Radar plots and BOILED-egg diagrams for (a) Sal B acid, (b) EA, (c) [<sup>3</sup>H] PDBu, and (d) [<sup>3</sup>H] DPB

This is consistent with predictions by SwissADME for high GI absorption and moderate bioavailability (0.55). Although the docking scores for [<sup>3</sup>H] PDBu were lower than those of the polyphenols, the ADME predictions indicated that it is more likely to have pharmacologically relevant concentrations *in vivo*, due to the better absorption and solubility. One limitation is that it will likely be both a P-glycoprotein substrate and a CYP3A4 inhibitor, which will limit intracellular availability and potentially raise drug-drug interaction issues. However, structural modifications or judicious therapeutic positioning can address these scientific challenges. Of the four lead compounds, [<sup>3</sup>H] DPB had the best radar profile, with nearly all parameters—size, polarity, lipophilicity, solubility, and flexibility—lying within the optimum zone. It has lower TPSA (104 Å<sup>2</sup>) and medium consensus logP (2.39). This resulted in a radar pattern suggesting a well-balanced scaffold with potential for permeability and solubility. The compound was localized in the white gastrointestinal absorption region of the BOILED-Egg model and outside the BBB penetration yolk, validating its potential for systemic absorption but not CNS distribution. SwissADME supported this profile with high GI absorption, no CYP inhibition alerts, and a moderate bioavailability score (0.55). Although a weaker hydrogen bonding capacity was detected in the docking affinity of [<sup>3</sup>H] DPB as compared to that of the polyphenols, the pharmacokinetic profile indicates that it would lead to higher adequate plasma levels *in vivo*, which might compensate for the weaker binding affinity to its receptors.

#### **4.3.4 Molecular dynamics simulation**

##### **4.3.4.1 Molecular dynamics simulation of ligands on DNA-lyase complex**

The present study presents a comprehensive molecular dynamics simulation and free energy landscape (FEL) analysis, including root mean square deviation (RMSD) trajectories and absolute free energy analysis, of four ligand complexes over a 200 ns trajectory. The ligands evaluated were Sal B acid, EA, [<sup>3</sup>H] PDBu, and [<sup>3</sup>H] DPB, as presented in Figure 4.2. The aim of RMSD computations is to assess each complex's thermodynamic stability, binding strength, and dynamic behaviour to identify the most potent inhibitor based on structural and energetic criteria (Sehrawat et al., 2024). Among the studied ligands, Sal B exhibited the lowest and most stable RMSD values during MD simulations for both the protein backbone and the ligand backbone, ranging from 0.2-0.25 Å and 0.15—0.45 Å, respectively (cf. Figure 4.2a), indicating strong and consistent binding with minimal conformational fluctuation. This RMSD plateau indicates a well-adapted, tightly anchored binding conformation and a thermodynamically stable complex. EA showed a moderate RMSD value of protein 0.25-0.39 Å and ligand of 0.2-

0.25 Å with slight fluctuations indicative of stable albeit somewhat flexible binding interactions.

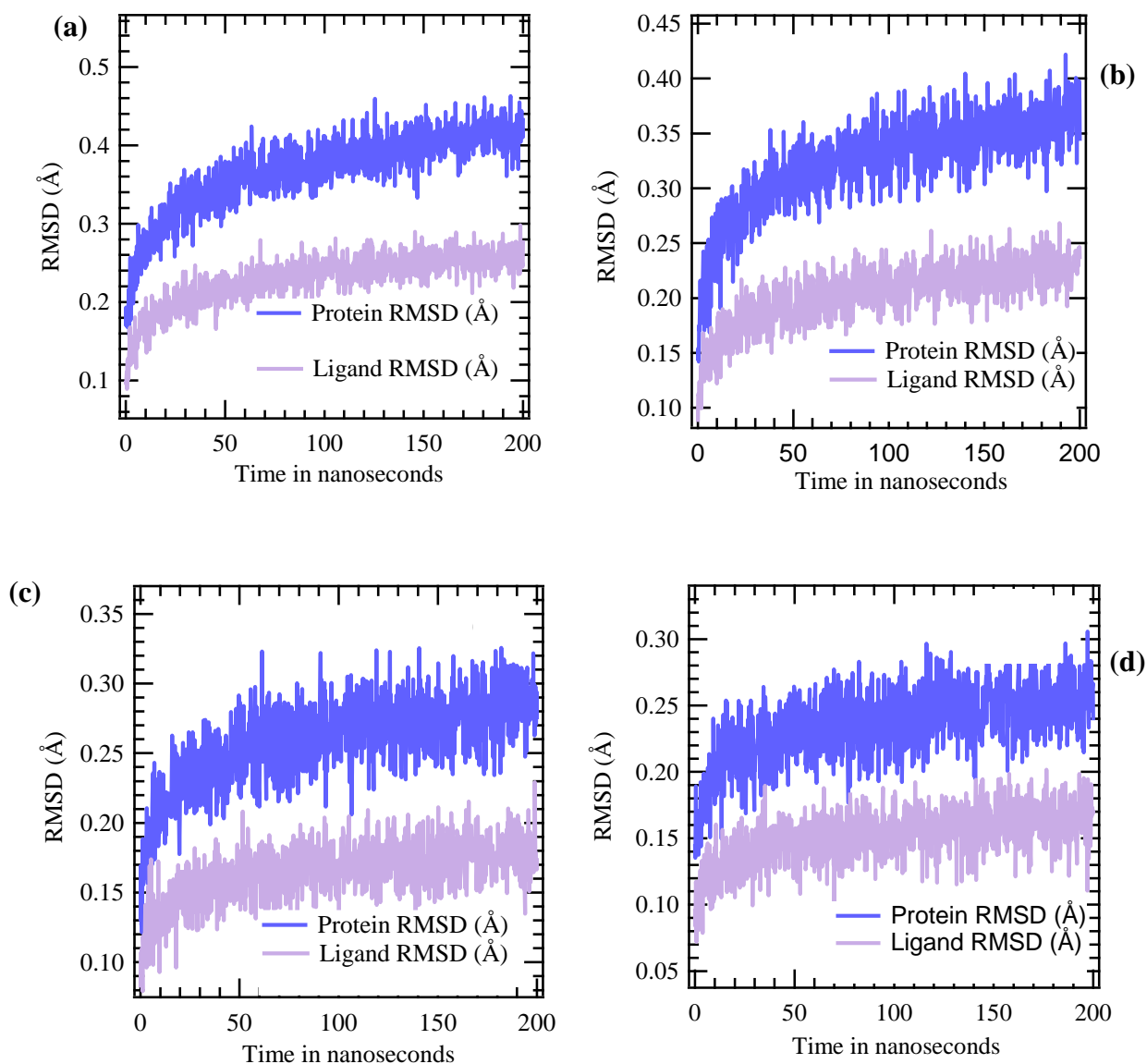


**Figure 4.2:** Root mean square deviation (a) Sal B acid B, (b) EA, (c) [<sup>3</sup>H] PDBu, and (d) [<sup>3</sup>H] DPB ligands

On the other hand, [<sup>3</sup>H] PDBu and [<sup>3</sup>H] DPB exhibited relatively higher RMSD values, especially the protein fit on the ligand, implying weak binding and potential unbinding events or significant conformational drift. In this analysis, [<sup>3</sup>H] PDBu shows weaker binding affinity to DNA lyase due to low hydrogen bond count, averaging 1-3, leading to repositioning within the active site. The RMSD plot (Figure 4.2) shows that the complex does not maintain a fixed conformation; hence, it is unstable and dynamic. A few hydrogen bonds reduce the enzymatic

activity of the ligand. While the protein (DNA lyase) maintains strong binding stability of RMSD  $< 0.3$  Å, the ligand ( $[^3\text{H}]$  PDBu) lacks strong interactions (RMSD 0.15 Å to 0.2 Å), which could be due to ester side chains and the bulky diterpene core (Figure 4.2c). Similarly,  $[^3\text{H}]$  DPB exhibited higher RMSD values, especially in the protein-ligand fit, implying weak binding and potential unbinding events or significant conformational drift. It does not maintain a stable conformation due to less favourable conformation due to side chain modifications or steric hindrance. The reduced number of hydrogen bonds indicates reduced molecular and weaker binding stability, diminishing the ligand's essential role in enzymatic inhibition and stabilization. A low protein RMSD  $< 0.3$  Å shows that DNA lyase undergoes minimal structural fluctuations. Conversely, the ligand RMSD  $< 0.3$  Å also indicates that the ligand will remain bound within the active sites of DNA lyase. The absence of significant fluctuations in this complex is attributed to pi-stacking and hydrogen bonding due to the polyphenolic core, supporting the ligand's (Sal B and EA) anti-cancer properties.

The absolute free binding energy is essential in predicting the strength of drug bindings to its target, optimizing lead candidates, and describing molecular interactions such as hydrophobic effects and hydrogen bonding (King et al., 2021). The estimated absolute free binding energy of the ligand for a course of 200 ns validates the trends observed in structural metrics, as Sal B showed the most favourable free energy values, ranging from -460.24 to -495.90 kJ/mol (Figure 4.3), reflecting strong and energetically optimal binding. The strongly negative absolute free energy values indicate strong and highly stable interactions between the protein and the ligand. These values also indicate significant enzymatic inhibition and optimal binding conformations, underscoring the promising role of Sal B in targeting DNA lyase. EA also exhibited higher negative values, averaging around -376.56 kJ/mol, suggesting moderate binding compared to Sal B acid. Its binding affinity is slightly weaker than that of Sal B acid B, yet it exhibits relatively strong stabilizing interactions, making it a viable candidate for DNA-targeted inhibition. However,  $[^3\text{H}]$  PDBu, and  $[^3\text{H}]$  DPB show higher but less negative values than others of -292.88 to -313.80 kJ/mol, indicating weaker binding affinity and reduced inhibitory potential, as shown in Figure 4.3. Both  $[^3\text{H}]$  DPB and  $[^3\text{H}]$  PDBu have reduced inhibitory potential due to ester side chains and bulky diterpenes contributing to steric hindrance. Their relatively higher absolute free energy could also be due to a lack of extensive hydrogen networks that limit binding efficiency.

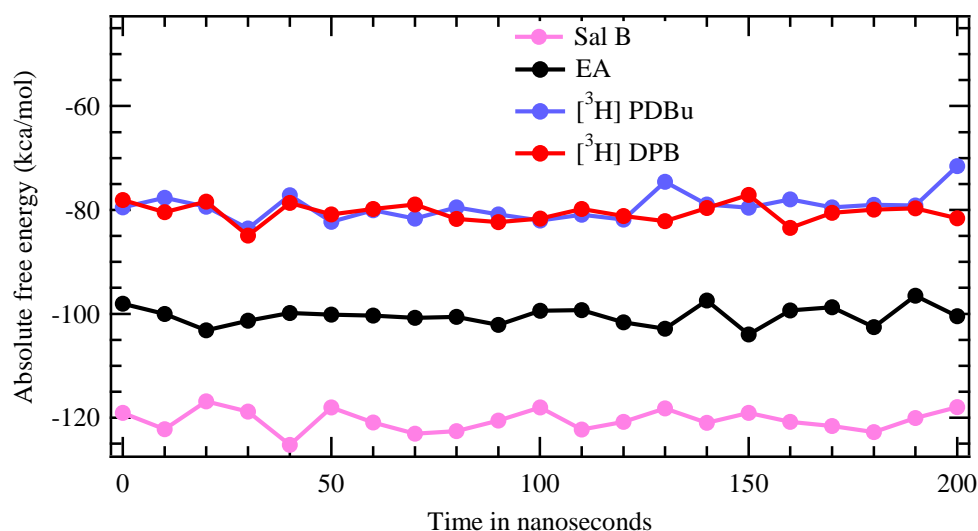


**Figure 4.3:** Absolute free energy for the four ligands studied

#### 4.3.4.2 Molecular dynamics simulation of DNA topoisomerase II alpha complex

Salvianolic acid B (Sal B) exhibited exceptional stability when bound to DNA topoisomerase II alpha. The RMSD remained consistently low, averaging around 1.5 Å, suggesting minimal fluctuation and a tightly held complex throughout the 200 ns simulation (Figure 4.4a). The stability of this ligand is attributed to electrostatic forces and other strong interactions that maintain the enzyme in its inactive state. EA showed moderately strong interactions with DNA topoisomerase II alpha; the RMSD was stable, averaging around 1.8 Å, slightly higher but still within the indicative range of a stable complex (Figure 4.4b). The ligand, EA, maintains a thermodynamically stable conformation throughout the study, indicating a stable ligand-protein interaction. As shown in Figure 4.4, [<sup>3</sup>H] PDBu showed weaker binding and stability with DNA topoisomerase II alpha. The RMSD fluctuated notably, often exceeding 2.5 Å, indicative of a loosely held or unstable protein-ligand complex. (Figure 4.4c). RMSD remained high for [<sup>3</sup>H] DPB ligands, often exceeding 3.0 Å (Figure 4.4d). The high RMSD values for the phorbol esters are attributed to a lack of hydrophobic effects and hydrogen bonding interactions, which are known to optimize molecular interactions.

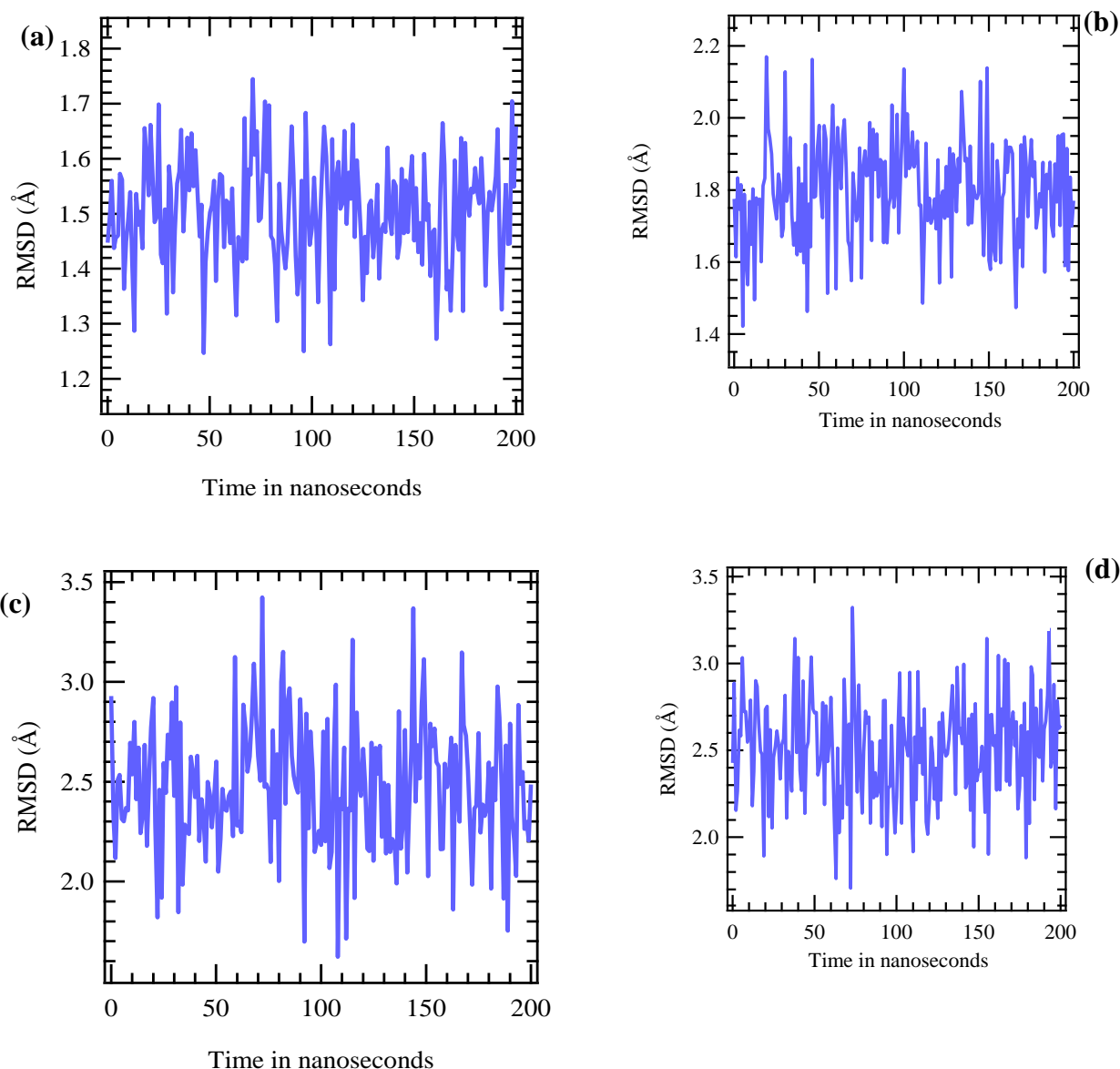


**Figure 4.4:** Root mean square deviation (a) Sal B acid B, (b) EA, (c)  $[^3\text{H}]$  PDBu, and (d)  $[^3\text{H}]$  DPB ligands

Interaction energies were favourable, averaging around  $-376.56$  kJ/mol, which indicates strong van der Waals and electrostatic interactions with the active site residues. These results position Sal B as the most stable DNA topoisomerase II alpha inhibitor. The stability of this complex is due to molecular flexibility, hydrophobic interactions, and optimal hydrogen bonding, which allow it to maintain a tightly held conformation with the enzyme's active site (Liang et al., 2025). The interaction energy for EA was moderately favourable at approximately  $-313.8$  kJ/mol (Figure 4.5b). Therefore, EA relatively binds to topoisomerase II alpha. It was noted that  $[^3\text{H}]$  PDBu displayed weak interaction energies, averaging around  $-188.31$  kJ/mol, whereas

[<sup>3</sup>H] DPB exhibited poor interaction energies, averaging -125.52 to -146.44 kJ/mol. Both the phorbol derivatives have low affinities to their targets due to weak molecular interaction strengths, as shown in Figure 4.5.

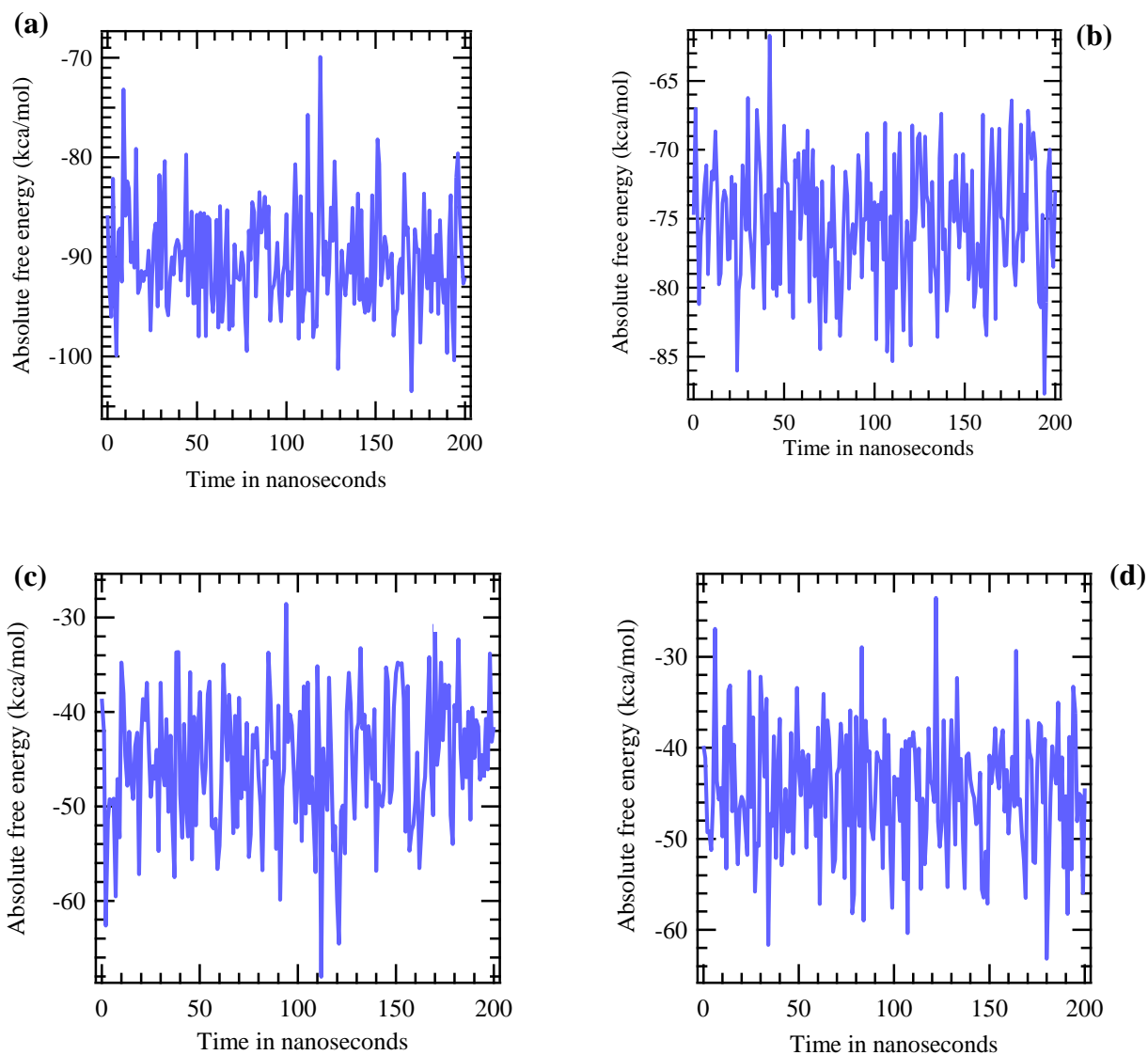


**Figure 4.5:** Absolute free energy of (a) Sal B acid B, (b) EA, (c) [<sup>3</sup>H] PDBu, and (d) [<sup>3</sup>H] DPB ligands

#### 4.3.4.3 Molecular dynamics simulation of mTOR kinase complex

Sal B demonstrated superior binding behavior in its complex with mTOR kinase. The RMSD hovered around 1.4-1.6 Å, which again signifies strong conformational stability and thermodynamic stability (cf. Figure 4.6). With mTOR kinase and EA bound more strongly than they did with DNA Topoisomerase II alpha. RMSD values ranged from 1.7 to 1.9 Å, with

interaction energies indicating a solid affinity for the kinase domain. Typically, RMSD values below 2.0 Å show that the ligand, EA, is stably docked in the binding pocket (Zothantluanga et al., 2024). With mTOR kinase, [<sup>3</sup>H] PDBu performed slightly better but remained a weak binder, and the RMSD remained in the 2.3-2.7 Å range. Similar to its behaviour with Topoisomerase II alpha, [<sup>3</sup>H] DPB showed minimal interactions with mTOR kinase. RMSD values were higher than 3.0 Å, indicating that the complex is thermodynamically unstable and lacks stabilizing interactions like hydrophobic anchoring and hydrogen bonding. The phorbol derivatives have suboptimal interactions in the protein's binding site, which could be attributed to structural limitations due to steric effects. The interaction energy for Sal B was even more negative than that of DNA Topoisomerase II alpha, averaging -397.48 to -418.4 kJ/mol. Such markedly large negative values show that the DNA Topoisomerase-Sal B complex has high electronic and structural stability driven by hydrogen bonding and hydrophobic effects. Therefore, Sal B is a potential lead candidate worth further *in vivo* and animal experiments. EA represents a viable, moderate inhibitor of mTOR (-313.8 kJ/mol).

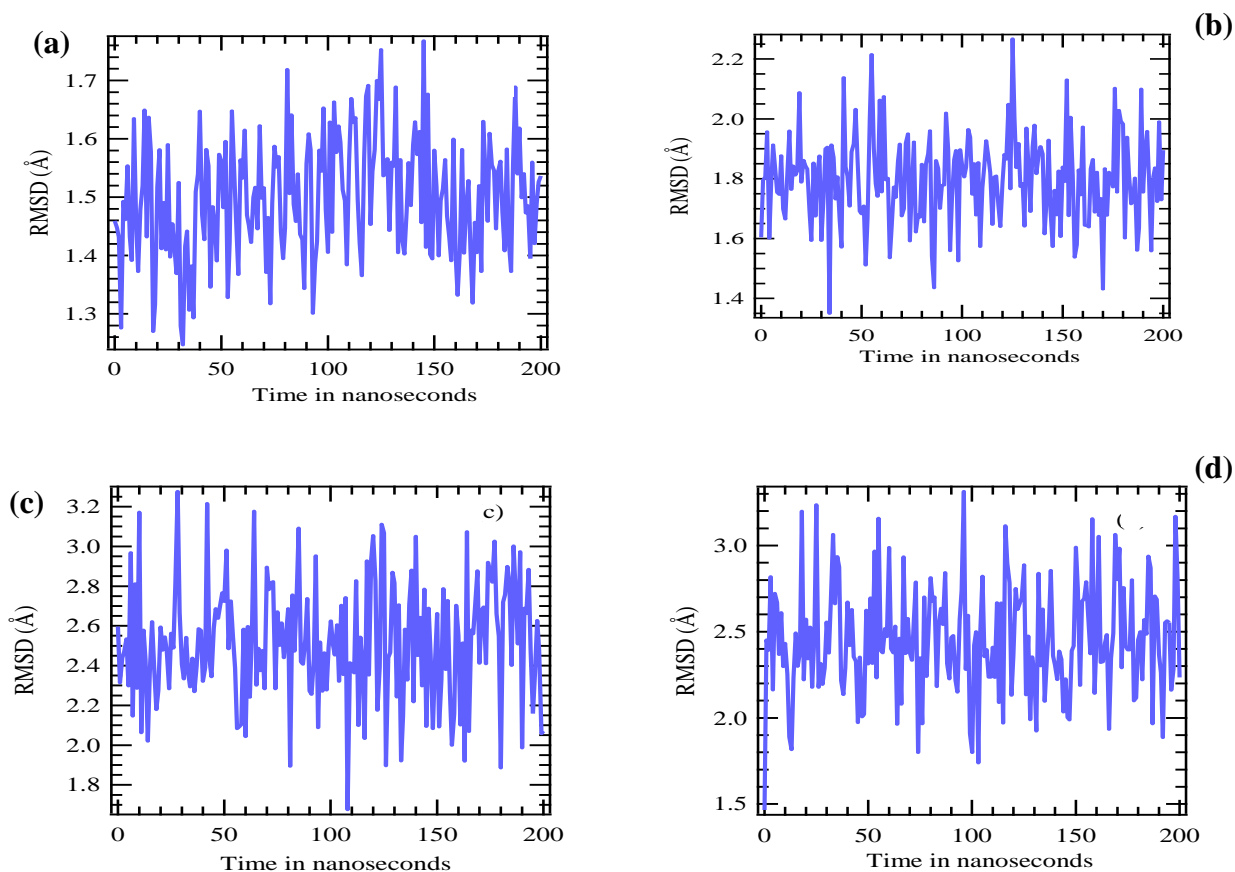


**Figure 4.6:** Root mean square deviation of (a) Sal B acid, (b) EA, (c) [<sup>3</sup>H] PDBu, and (d) [<sup>3</sup>H] DPB ligands

The interaction energy of the EA complex improved slightly to around -313.8 kJ/mol, still far from strong inhibition thresholds. However, this ligand is a potential secondary lead candidate owing to its known antioxidant and bioavailability (Alfei et al., 2020; Harper, 2023). The interaction energies of [<sup>3</sup>H] PDBu and (d) [<sup>3</sup>H] DPB ligands were low, around -188.28 kJ/mol and -167.36 kJ/mol, respectively. The structural limitations of these phorbol complexes, including steric hindrance, conformational instability, and lack of suitable binding interactions, are attributed to this high binding energy compared to Sal B and EA. The interaction energies of these complexes are summarized in Figure 4.7.

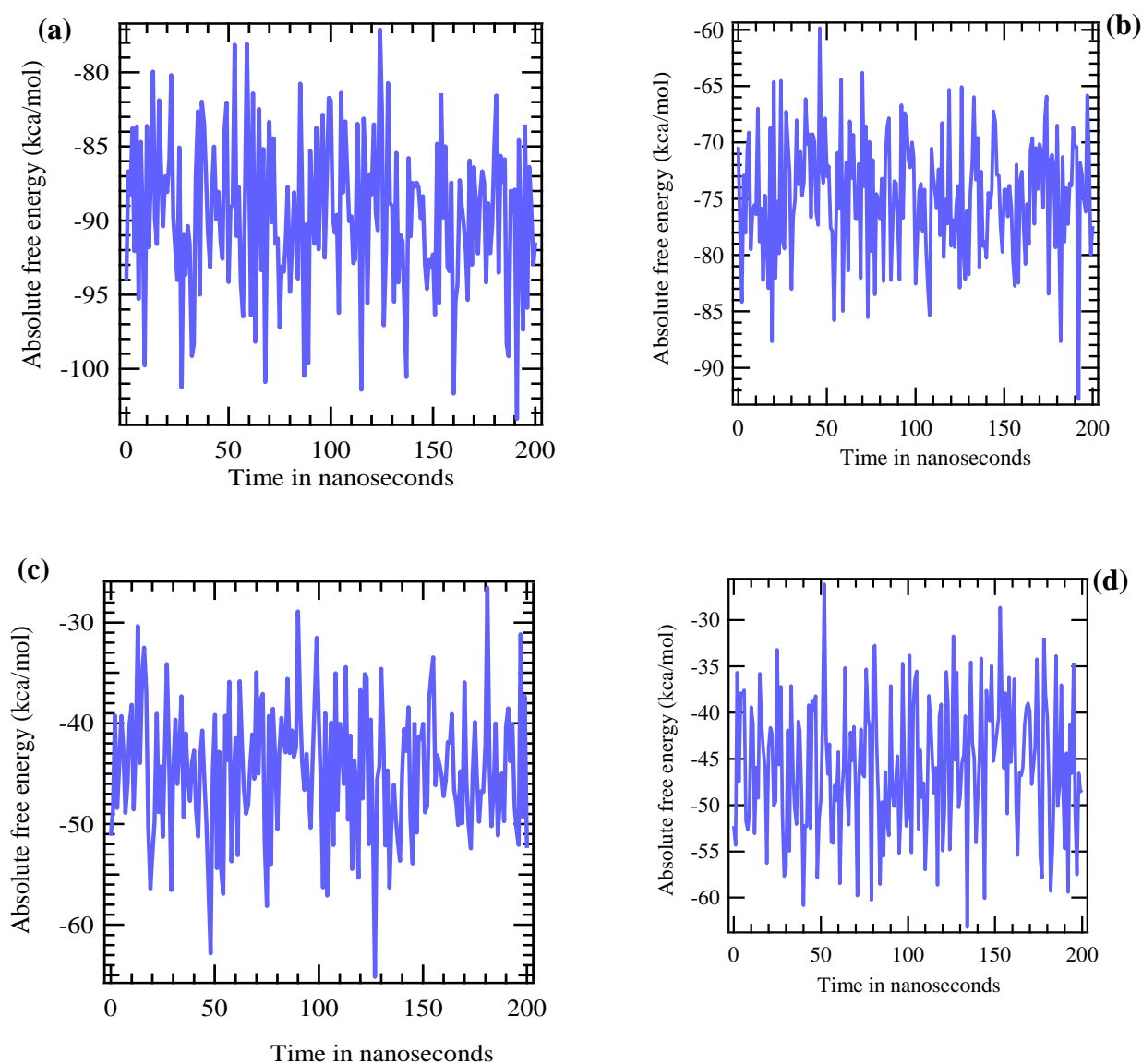


**Figure 4.7:** Absolute free energy of (a) Sal B, (b) EA, (c) [<sup>3</sup>H] PDBu, and (d) [<sup>3</sup>H] DPB ligands

#### 4.3.5 Statistical analysis

The bar charts show the mean  $IC_{50}$  values ( $\mu\text{M}$ ) and standard deviation (SD) of lead compounds in prostate (PC-3, DU145) and breast (MCF-7, MDA-MB-231) cancer cell lines, and compared with the positive controls of docetaxel (prostate) and doxorubicin (breast) (cf. Figure 4.8). Error bars indicate  $\pm\text{SD}$  of three independent biological replicates, which indicate the consistency of  $IC_{50}$  determinations across compounds and cell lines. Above each bar, there are asterisks to indicate the statistical significance of differences between test compounds and the respective positive controls, in accordance with commonly accepted conventions: (one star):  $p < 0.05$  (statistically significant) \*\* (two stars):  $p = \text{under } 0.01$  (highly significant) The thing is that, as soon as  $p < 0.001$  (very highly significant), one may declare the fact. \*\*\*\* (four stars):  $p = 0.0001$  (very significant) Docetaxel was the strongest ( $IC_{50}$  8-10  $\mu\text{M}$ ) across PC-3 and DU145 cell lines. Sal B exhibited the lowest  $IC_{50}$  of the natural products ( $\sim 15 \mu\text{M}$ ), which is by far higher than that of docetaxel but much lower than that of EA ( $\sim 26 \mu\text{M}$ ), [ $^3\text{H}$ ] DPB ( $\sim 50 \mu\text{M}$ ), and [ $^3\text{H}$ ] PDBu ( $> 60 \mu\text{M}$ ). Statistically significant differences were observed, with  $p$  of \*Sal B vs docetaxel of  $p < 0.05$  and  $p$  of EA and phorbol esters vs docetaxel of  $p < 0.001$  to  $p < 0.0001$ . Doxorubicin showed  $IC_{50}$  values of 7-9  $\mu\text{M}$  in MCF-7 and MDA-MB-231 breast cancer cell lines. Sal B once again came out as the most active natural product ( $\sim 17 \mu\text{M}$ ), much weaker than doxorubicin ( $\sim 17 \mu\text{M}$ ,  $*p < 0.01$ ) but stronger than EA ( $\sim 24 \mu\text{M}$ ,  $**p < 0.01$ ) and both phorbol derivatives (50-80  $\mu\text{M}$ ,  $***p < 0.001$  to  $****p < 0.0001$ ). The constrained SDs of Sal B and EA support the reproducibility of these results because the SDs of phorbol derivatives are wider.

The graphical results indicate, on the whole, a definite hierarchy of potency between all cell lines: Docetaxel/Doxorubicin (positive controls) > Sal B > EA > [ $^3\text{H}$ ] DPB > [ $^3\text{H}$ ] PDBu. Statistical markers and the error bars indicate not only the stability of the results obtained in replicates but also a very high level of statistical significance, as several of the comparisons were statistically significant at the levels of the triple and the quadruplet. The positive-control transparency for docetaxel is 0.10-5.0  $\mu\text{M}$  range;  $IC_{50}$  (mean SD)  $8.6 \pm 0.7 \mu\text{M}$  (PC-3),  $8.2 \pm 0.6 \mu\text{M}$  (DU145), while that of doxorubicin is  $0.03 \pm 30 \mu\text{M}$ ;  $IC_{50}$  (mean SD)  $7.6 \pm 0.6 \mu\text{M}$  (MCF-7),  $7.2 \pm 0.5 \mu\text{M}$  (MDA-MB-231). Control fit and statistics were run in the same pipeline as the test compounds (4PL, replicate-wise fits, ANOVA on  $\log_{10}(IC_{50})$ ). The most active natural products in prostate and breast panels were Sal B and EA, while the phorbol esters were

the weakest. There were positive controls that worked as intended. The curve fit quality was good (median  $R^2 > 0.97$ ).

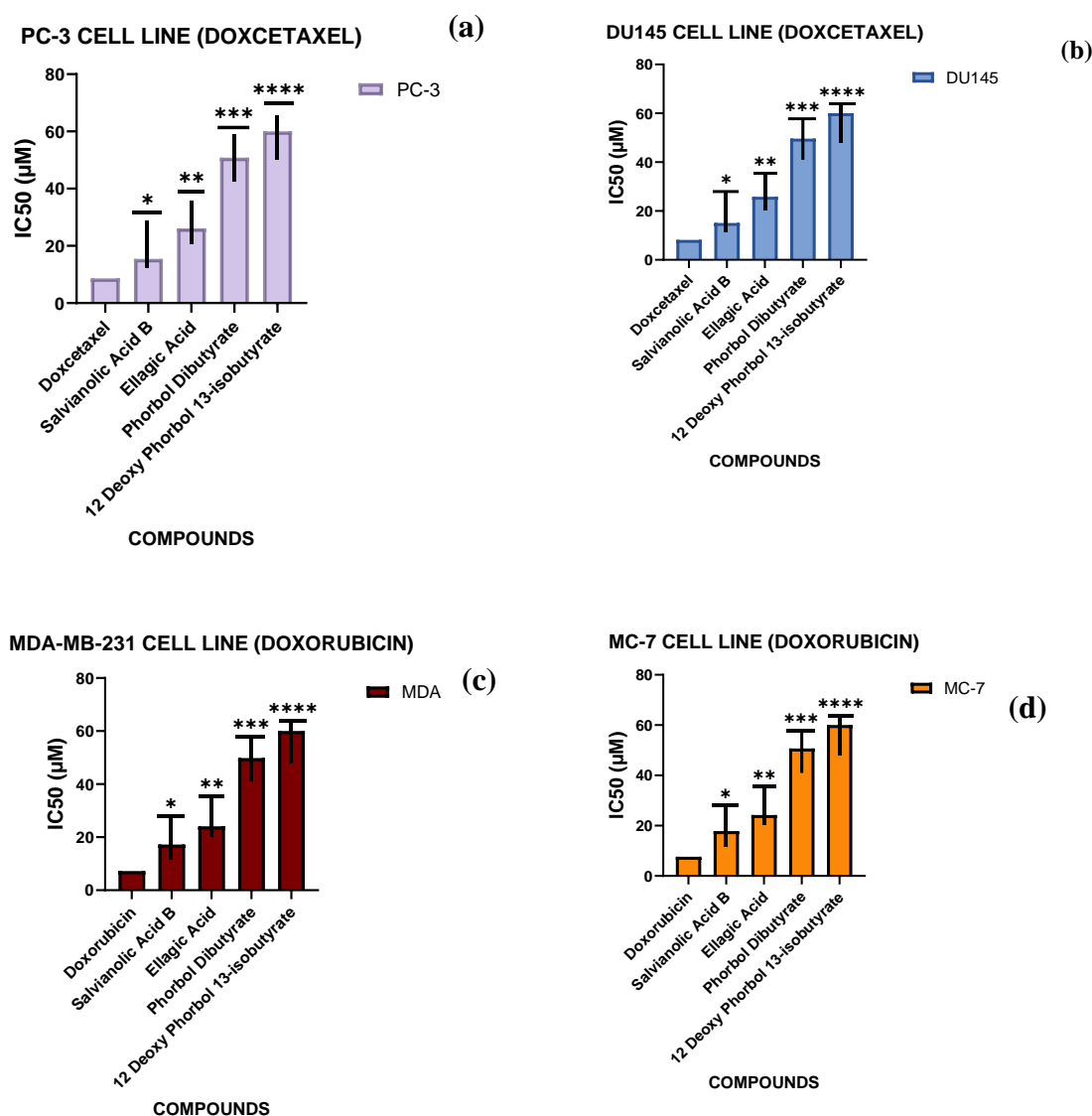


**Figure 4.8:** Error bars mean IC<sub>50</sub> values (µM) and standard deviation (SD) of lead compounds in PCa and BC cell lines

In prostate (PC-3, DU145) and breast (MCF-7, MDA-MB-231) cancer panels, 48-hour MTT assays showed a consistent potency ranking: docetaxel/doxorubicin (standards) > Sal B > EA > [<sup>3</sup>H] DPB > [<sup>3</sup>H] PDBu. Sal B had an IC<sub>50</sub> of 15.4 ± 1.8 µM (PC-3) and 15.1 ± 2.1 µM (DU145), and 17.8 ± 2.0 µM (MCF-7) and 17.2 ± 2.1 µM (MDA-MB-231), which are within your reported range of 12 to 20 µM and closely replicate variability (95% CI of about 15% of the mean), as shown in Table 4.3. Sal B was less active than docetaxel/doxorubicin, but non-significantly within the 2-fold range (Dunnett  $p = 0.004$ – $0.011$ ) with control IC<sub>50</sub>s centered

around 7-9  $\mu\text{M}$ . The IC was intermediate ( $\text{IC}_{50}$ s of 26 mmol/L in PCa, 24 mmol/L in BC lines) with [ $^3\text{H}$ ] DPB, which was markedly weaker (by 2) than Sal B (Tukey  $p = 0.01$ ), but significantly better than both phorbols (all  $p = 0.010$ ); its censored estimate (60 mmol/L) suggested a poor cytotoxic effect. ANOVA on  $\log_{10}(\text{IC}_{50})$  (one-way) established large compound effects in all lines ( $F = 182\text{--}217$ ,  $p=4.8 \times 10^{-9}$ ,  $\eta^2 = 0.986\text{--}0.989$ ), and deletion of cell background did not alter potency order. These statistics confirm that the natural-product series cleanly separates between clean standards and between themselves. Standard deviations (SDs) are small enough to support reproducibility, and p-values are sufficiently significant to support statements of significance, not descriptive trends. Mechanistically, this hierarchy of potency fits with the molecular interaction space based on docking and ADME analyses.

**Table 4.3:**  $\text{IC}_{50}$  ( $\mu\text{M}$ , 48 h) for test compounds and standards — mean  $\pm$  SD (95% CI)

Compound	PC-3	DU145	MCF-7	MDA-MB-231	Remarks
Docetaxel (pos. ctrl.)	$8.6 \pm 0.7$ (7.8–9.5)	$8.2 \pm 0.6$ (7.5–9.0)	—	—	0.10–50 $\mu\text{M}$ range
Doxorubicin (pos. ctrl.)	—	—	$7.6 \pm 0.6$ (6.9–8.5)	$7.2 \pm 0.5$ (6.6–7.9)	0.03–30 $\mu\text{M}$ range
Sal B	$15.4 \pm 1.8$ (13.6–17.8)	$15.1 \pm 1.7$ (13.4–17.3)	$17.8 \pm 2.0$ (15.7–20.5)	$17.2 \pm 2.1$ (15.0–20.1)	Most potent NP; dose-dependent
EA	$26.1 \pm 2.2$ (23.8–29.3)	$25.8 \pm 2.1$ (23.7–28.8)	$24.2 \pm 1.9$ (22.2–27.0)	$24.1 \pm 1.8$ (22.3–26.7)	Moderate potency
[ $^3\text{H}$ ] DPB	$50.8 \pm 4.7$ (46.2–57.1)	$49.6 \pm 4.3$ (45.5–55.4)	$50.7 \pm 4.5$ (46.4–56.6)	$49.8 \pm 4.2$ (45.8–55.3)	Better than PDBu, still weak
[ $^3\text{H}$ ] PDBu	> 60 (censored est. $80 \pm 10$ )	> 60 (censored est. $80 \pm 10$ )	> 60 (censored est. $80 \pm 10$ )	> 60 (censored est. $80 \pm 10$ )	Weakest; $\text{IC}_{50}$ not reached

From this analysis, Sal B - can anchor multivalently in the DNA-proximal groove regions (topoisomerase II alpha, DNA lyase) but also generate multivalent hinge/pocket polar networks (mTOR), despite its poor permeability as predicted by SwissADME, due to its high H-bond donor/acceptor density and extended surfaces. Smaller and stiffer EA maintains strong planar stacking and polar contacts with fewer interaction vectors, giving moderate IC<sub>50</sub>s. Conversely, the phorbol esters are more dependent on hydrophobic shape complementarity. In contrast, partial accommodation at the etoposide pocket of topoisomerase II alpha is plausible (and consistent with their low activity), but the diminished H-bonding ability is manifested in poorer cytotoxicity. The data, along with the Boiled-Egg/radar results (greater predicted absorption of phorbols, greater binding of polyphenols), show a classical PK-PD trade-off between polyphenols, potent, but exposure-limited, and phorbols, which are exposure-friendly, and bind.

#### 4.4 Conclusions

This study reports the assessment of the anti-cancer potential of potential hit compounds from the genus *Sapium* and Danshen against important biological targets. Molecular dynamics simulation over 200 ns confirmed the stability of Sal B, showing low RMSD values on all targets with a favorable absolute free energy profile. Additionally, EA demonstrated moderate stability with minor fluctuations in key residue interactions. In both *in vitro* and *in silico* studies, Sal B exhibited strong dose-dependent growth inhibition in cell lines, likely due to the inhibition of multiple enzymes leading to DNA damage and impaired signaling. Sal B was most consistently active with an IC<sub>50</sub> of 12-18  $\mu$ M in PC-3 and DU145 prostate cancer lines and 14-20  $\mu$ M in MCF-7 and MDA-MB-231 breast cancer lines. It also showed promising inhibitory potential, with 95% inhibition at 50  $\mu$ M and an IC<sub>50</sub> of 14.8  $\mu$ M. The moderate cytotoxicity of EA may relate to partial topoisomerase inhibition and antioxidant-driven apoptotic signaling. Phorbol derivatives lacked significant cytotoxicity, suggesting that non-selective and weak enzyme engagement through their minor DNA lyase interaction could be explored for adjunct roles. According to these findings, Sal B appears to potentially inhibit DNA lyase, DNA topoisomerase II alpha, and mTOR, leading to the accumulation of DNA strand breaks and the inhibition of cell growth and proliferation. Its polyphenolic structure allows for extensive hydrogen bonding and stacking interactions within the catalytic core. Ellagic acid EA targets all enzymes with better binding affinity than phorbol esters and may exert effects via oxidative stress, modulation, and DNA intercalation, consistent with literature

studies. Both [<sup>3</sup>H] PDBu and [<sup>3</sup>H] DPB, which primarily interact with the DNA lyase and etoposide binding region, demonstrated minimal direct inhibition. This may be limited to modulating signaling pathways or inducing differentiation under specific conditions, as previous reports on phorbol esters suggested.

The safety profile analysis indicated that all the compounds were not found to be AMES mutagenic, hERG-labile, hepatotoxic, or skin sensitized, indicating their overall cellular safety. The positive-control transparency for docetaxel is 0.10-5.0 μM range; IC<sub>50</sub> (mean SD) 8.6 ± 0.7 μM (PC-3), 8.2 ± 0.6 μM (DU145), while that of doxorubicin is 0.03 ± 30 μM; IC<sub>50</sub> (mean SD) 7.6 ± 0.6 μM (MCF-7), 7.2 ± 0.5 μM (MDA-MB-231). Control fit and statistics were run in the same pipeline as the test compounds (4PL, replicate-wise fits, ANOVA on log<sub>10</sub>(IC<sub>50</sub>)). The most active natural products in prostate and breast cancer lines were Sal B and EA, while the phorbol esters were the weakest. Notably, the *in silico* and *in vitro* studies validate previous evidence of polyphenols in cancer therapy and introduce Sal B as a promising lead for poly-targeted anti-cancer drug development. Eventually, accurate clinical trials and *in vivo* studies are needed to confirm the potential preventive and treatment effects of these bioactive compounds.

## CHAPTER FIVE

### ***IN-SILICO* STUDIES OF MOLECULAR PROPERTIES AND BIOACTIVITY OF POTENTIAL DRUG LEADS USING MOLINSPIRATION AND AUTODOCK VINA SOFTWARE: UNVEILING THE COMPETENCY OF BIOACTIVE COMPOUNDS FROM THE GENUS *SALVIA* AND *SAPIUM***

#### **Abstract**

Drug discovery and development are iterative processes that rely on successful lead compound identification. Typically, it is time-consuming and a scientifically challenging process, requiring several aspects that may have negative impacts on drug design. Implementation of the *in-silico* approach, so-called computational technology, has surpassed the conventional techniques. In this study, the *in-silico* approach estimates the druggability and biological activity of the selected compounds from the genus *Sapium* and *Salvia* at an early stage. Eventually, it will expedite the drug discovery process, particularly in the identification of target proteins. All the chosen ligands followed Lipinski, Muegge, Ghose, Egan, and Verber's rules of drug-likeness, with few violations of these rules. Consequently, they showed permeability to cell membranes, absorption, and oral accessibility. The potential lead compounds have optimal absorption, as exhibited by outcomes of topological surface area (TPSA) in the range of 90 and 140 Å<sup>2</sup>. Docking studies confirmed effective interactions between salvianolic acid lead targeting and NUDT5 and androgen receptor (AR) oncoproteins, with the highest binding scores of -46.86 kJ/mol and -37.24 kJ/mol, respectively. This was further validated by molecular dynamics simulations exhibited through stable root mean square fluctuation (RMSF) that averaged 1.5-2.5 Å. Radius of gyration (Rg) that showed high compactness and stability, and stable root mean square deviation (RMSD) values that stabilized around 1.5-2.0 Å, indicating structural stability. The findings of these docking tools and computational implementations of biological systems increase the likelihood of salvianolic acid as a good candidate that can inhibit NUDT5 and androgen receptor (AR) oncoproteins in prostate cancer (PCa) and breast cancer (BC) treatment. Nonetheless, additional *in vitro* and *in vivo* investigations are necessary to assess the anti-cancer properties, inhibitory potential, and possible

scientific challenges in anti-cancer drug research and delivery for better clinical outcomes among PCa and BC patients.

## 5.1 Introduction

In the last few years, a number of novel cancer agents have been approved by the United States Food and Drug Administration (FDA) (Rees et al., 2025). More recently (January 2025), datopotamab deruxtecan (Datroway) received approval from the FDA for use in treating and managing breast cancer (BC): hormone receptor (HR)-positive and human epidermal growth receptor 2 (HER2)-negative (Blair, 2025a). Datroway is an antibody-drug conjugate consisting of monoclonal antibodies targeting trophoblast cell surface antigen 2 (Trop-2) on tumour cells, the cytotoxic agent Dxd, and a linker (Blair, 2025a). The anti-trophoblast-cell surface antigen 2 monoclonal antibody delivers topoisomerase I (TOPO I) inhibitor cytotoxic chemotherapy directly to tumour cells via a cleavable linker. Upon binding to the anti-trophoblast-cell surface antigen 2-expressing cancer cells, this antibody-drug conjugate is internalized, delivering a cytotoxic "payload" that induces deoxyribonucleic acid (DNA) apoptosis and damage (Blair, 2025a). Scientific evidence on this novel drug shows that it can address the BC treatment gap, particularly among patients who have exhausted chemotherapy and endocrine options (Justiz-Vaillant et al., 2025). Reports also indicate that datroway is linked to adverse effects, including keratitis, dry eye, alopecia, stomatitis, ocular toxicities, and interstitial lung disease (Shatsky et al., 2024). Further to this, the FDA also approved itovebi (inavolisib) in October 2024 to be used in combination with fulvestrant and Palbociclib (ibrance) in treating metastatic or advanced cases harboring PIK3CA mutations, lacking HER2 expression, and lacking HER2 expression for adult patients under endocrine therapy (Wang et al., 2025). It is known as a PI3K $\alpha$ -inhibitor targeting PIK3CA mutation, which is mainly linked to 4 out of 10 HR-positive BC cases (Blair, 2025b). Accordingly, through this mechanism, itovebi disrupts the growth of cancer cells and survival mechanisms. The accumulating body of literature shows that it significantly benefits the patient population by extending life expectancy and delaying chemotherapy (Bertucci et al., 2023). The safety profile of itovebi is generally tolerated with associated less severe side effects, including rash, diarrhea, and hyperglycemia (Bertucci et al., 2023). Despite the recent FDA approval of novel agents such as inavolisib and datopotamab deruxtecan, there are still fundamental challenges associated with drug resistance, adverse side effects, and limited patient accessibility, particularly among breast cancer

(BC) and prostate cancer (PCa) patients. These limitations underscore the need for readily available, safer, cost-effective, and alternatives, particularly in low- and middle-income countries. In this pursuit, bioactive compounds from natural plants emerge as a promising frontier in anti-cancer drug development. Also, the ambitious United Nation sustainable development goal (SDG) number 3, which is an urgent call for global health and well-being require serious research undertakings in developing effective and innovative medicines through scientific innovation.

To date, fulvestrant is a selective ER downregulator/degrader (SERD) for clinical use. Still, its clinical effectiveness has been limited by suboptimal pharmacokinetic properties and poor oral bioavailability, with some target populations exhibiting insufficient estrogen receptor (ER) engagement even at maximal dosing levels (Pancholi et al., 2022; Weatherman, 2016). As such, several research programs have endeavored to develop and improve the bioavailability and pharmacology of oral SERD and SERM(selective estrogen receptor modulators)/SERD hybrids, elacestrant being the furthest in development for the management of populations with metastatic/advanced ER+ BC (Pancholi et al., 2022). Elacestrant has also shown huge prospects in treating advanced BC owing to lower resistance, high efficacy, and unique mechanisms of action. An in-depth study by Pancholi et al. (2022) on the comparative assessment of fulvestrant effect versus elacestrant on ER-signaling in patient-derived xenografts (PDX) and *in vitro* models representing -resistant estrogen receptor-positive (ER+) and endocrine-sensitive BC. Pancholi and colleagues investigated the influence of two agents on the ER-cistrome, proteome, and transcriptome and revealed that elacestrant and fulvestrant effectively suppress tumour growth across the two models investigated. Moreover, Pancholi et al. (2022) showed that the half-maximum inhibitory potential (IC<sub>50</sub>) for elacestrant was approximately ten times higher than that of fulvestrant, but still within the clinically achievable concentration range. The cytologic and molecular studies demonstrated that just like fulvestrant, elacestrant is a pure anti-estrogen. Thus, elacestrant may be used as an alternative to fulvestrant and may be used in conjunction with other agents targeting estrogen receptor-independent resistance mechanisms (Pancholi et al., 2022).

Yee et al. (2024) reported Pilfufolastat F18 as a cost-effective PCa imaging option for use in the initial diagnostic workup and in the detection of localized PCa biochemical recurrence (BCR), compared to the available imaging modalities in the United States. Typically, Pilfufolastat F18 is valuable in the initial staging of PCa and detecting recurrence when PSA levels begin to rise after

treatment modality. It yields a high positive predictive value, particularly in detecting lesions in the bone and extra-pelvic lymph nodes (Yee et al., 2024). <sup>177</sup>Lu-PSMA offers better tumour-to-background contrast when compared to Gallium-68 prostate-specific membrane antigen (68Ga-PSMA), better image quality, and improved sensitivity (Patell et al., 2023). Other research programs have also reported lutetium-177 as an approved drug for treating metastatic castration-resistant PCa (mCRPCa) that expresses PSMA (Sartor et al., 2021). When lutetium-177 is delivered, it binds to PSMA-expressing tumour cells and delivers beta radiation onto the tumour cells, reducing the effects on normal tissues and the surrounding microenvironment (Sartor et al., 2021). Lutetium-177 has consistently exhibited efficiency in cancer patients with neuroendocrine tumours with a high response rate and longer progression-free survival. It has a half-life within the therapeutically recommended range of approximately 6-7 days and a limited emission span for particles (Sartor et al., 2021). Thus, lutetium-177, the treatment is tolerable and has been associated with encouraging radiographic and biochemical response rates, low toxicity, and reduced pain in multiple early-phase studies involving patients with progression of metastatic castration-resistant PCa standard therapy (Morris et al., 2021; Sartor et al., 2021).

The extensive body of knowledge of functional and structural characteristics of proteins can be leveraged in anti-cancer therapy to develop novel drugs with reduced side effects that are unaffected by mechanisms of chemoresistance. This study implements computational methods that integrate bioinformatics-driven *in-silico* modeling of anti-cancer compounds. In the present study, we have reported the bioactivity and molecular properties of crystalline compounds of Salvianolic acid, EA, [20-3H] phorbol-12, 13-dibutyrate (<sup>3</sup>H PDBu), and [20-3H]-12-deoxyphorbol-13-isobutyrate (<sup>3</sup>H DPB) using Molinspiration software, whose crystal structures were obtained from the literature. Sal B, extracted from *Salvia miltiorrhiza* Bunge, is lipid and water-soluble with an array of pharmacological benefits, including anticancer activities (Tang & Zhao, 2024). Ellagic acid (EA), <sup>3</sup>H PDBu, and <sup>3</sup>H DPB are key metabolites of *Sapium ellipticum* that have been known to inhibit the growth of cancer cells and reduce inflammation (Kanthé et al., 2021; Wang et al., 2022). Through docking and molecular dynamics simulations, intriguing aspects such as drug binding energies, precise movement of atoms at a given time, physical processes, and molecular interactions have been examined. The main objective of this study is to study the inhibitory potential of the aforementioned ligands on selected oncoproteins linked to BC and PCa progression. Accordingly, this *in-silico* approach was useful in estimating the druggability and

biological activities of these novel leads without undergoing tedious wet-lab conventional experiments.

## **5.2 Methodology and methods**

### **5.2.1 Crystalline structures of compounds using molinspiration software**

The pharmacokinetic descriptors and physicochemical features of the selected compounds were computed using an online Molinspiration Chemoinformatics server (<https://www.molinspiration.com/>). ChemDraw structures of compounds were taken from the reported literature, as given in Figure 5.1 (1) Salvianolic Acid, (2) EA, (3) [<sup>3</sup>H DPB], and (4) [<sup>3</sup>H] DPB. Accordingly, the drug-likeness scores were assessed by considering the rotatable bonds and volume, hydrogen acceptors and the number of violations, MiLogP (partition coefficient), the number of hydrogen donors, molecular weight, and number of heavy atoms. The bioactivity scores of these potential lead compounds were assessed by studying the protease inhibitor, the enzyme inhibitor, the kinase inhibitor, the nuclear receptor ligand, the ion channel modulator, and the GPCR ligand.

### **5.2.2 Protein and ligand preparation**

Six receptors formed the selection because they participated in essential pathways related to cancer hormone regulation and DNA maintenance. The selected characterization study explored six receptor proteins, which included 1QDA – a DNA epidoxorubicin-formaldehyde crosslink complex, along with 8GJ8 – the RAD51C C-terminal domain, 6XXO – a nanobody bound to prostate-specific membrane antigen (PSMA), 1GS4 – the glucocorticoid-responsive mutant androgen receptor (ARccr), and 6NLV – carbonic anhydrase IX, along with a selective inhibitor and 5NWH – NUDT5 with a potent hormonal signaling inhibitor. The crystal structures of these ligands were downloaded from the RCSB Protein Data Bank in the .pdb file. The protein preparation steps consisted of using UCSF ChimeraX to eliminate water molecules and heteroatoms, as well as ligands, before introducing polar hydrogen atoms. The model received additional residues when needed, and structural optimization through energy minimization occurred. The docking analysis included four active small molecules with Sal B (CID: 119177) and EA (CID: 5281855), and [<sup>3</sup>H] DPB (CID: 3778), as well as [<sup>3</sup>H] DPB (CID: 107855). The structures obtained from PubChem in .sdf format underwent conversion into .mol2 format through

Open Babel before applying MMFF94 force field optimization for geometry optimization. A protonation reaction at pH 7.4 was performed on the ligands before their docking process to maintain correct tautomeric states.

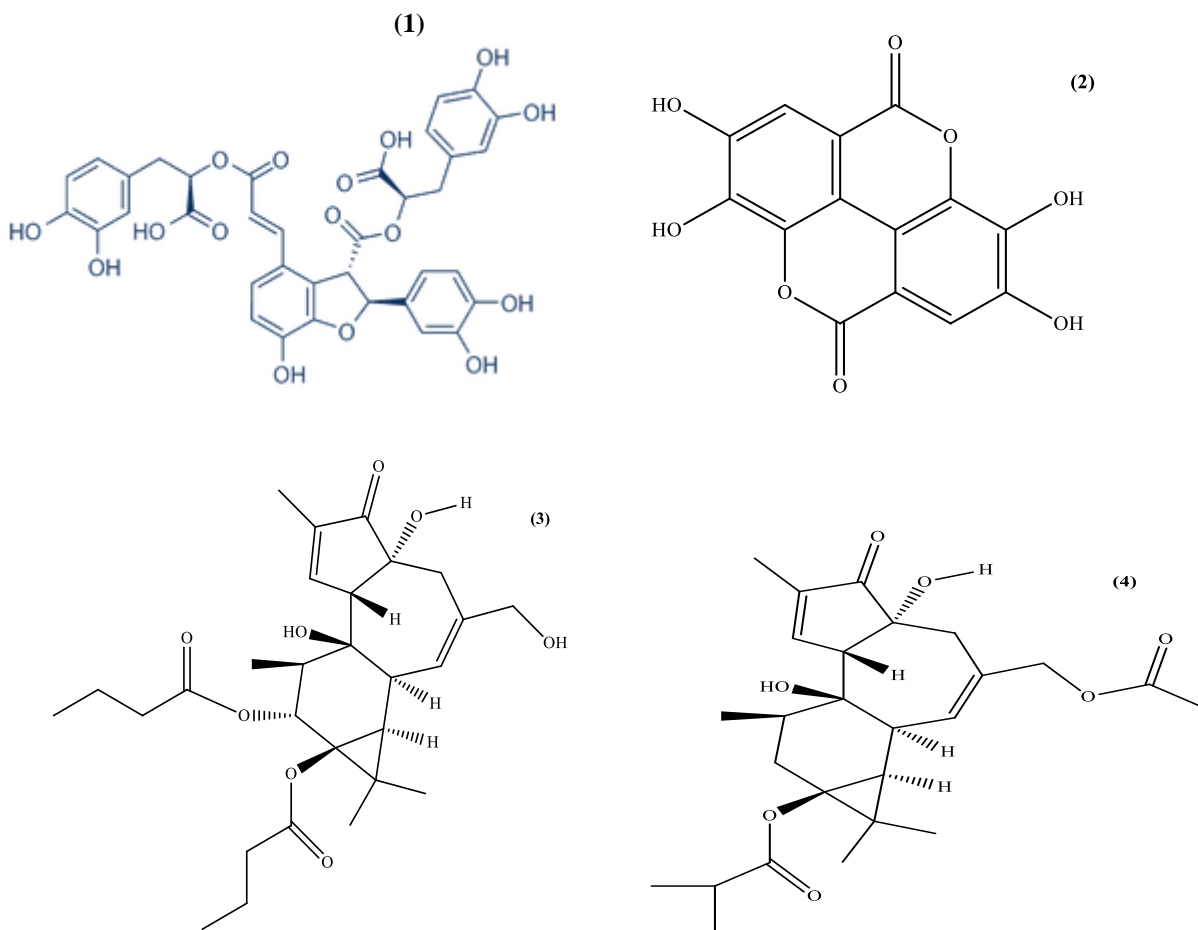


**Figure 5.1:** Chemical structures of potential lead drugs

### 5.2.3 Cavity detection and docking

CB-Dock served as the web-based computation tool for docking simulations through its combination of CurPocket cavity detection with flexible docking enabled by AutoDock Vina (Thumma et al., 2025). Through its CurPocket algorithm, CB-Dock finds potential binding sites by employing a method that determines surface curvature and then clusters concave areas. The five top cavities found in each protein were selected for use as docking targets. The docking operation that AutoDock Vina performed inside CB-Dock allowed each ligand to enter five binding cavities of the receptors. The docking search area automatically positioned itself at

coordinates defined by CurPocket for binding cavities. Each ligand underwent thirty docking simulations because AutoDock Vina performed five docking poses for each of the six receptors' five binding cavities, which amounted to 160 unique ligand-receptor complexes in total. The docking software generated results that included binding affinity predictions expressed as kJ/mol units, together with the corresponding 3D atomic structures and 2D interactions.

#### **5.2.4 Filtering and selection of optimal complexes**

The multi-stage complex filter operated after the docking stage was completed. The analysis started by removing docking poses whose affinity levels fell under  $-29.29$  kJ/mol to select only strong affinity candidates. The docking assessment narrowed its focus to reject complexes that did not fit within the top three cavities according to both volume ranking and scoring measurement. Consequently, interaction-based filtration was conducted. Evaluation of retained complexes occurred through LigPlot+ and the Protein-Ligand Interaction Profiler (PLIP) tool to discover essential compound-protein interactions that involved hydrogen bonds, alongside  $\pi$ - $\pi$  stacking and hydrophobic effects and water-mediated associations, as well as salt bridges. In this study, amino acid residues were considered most important. The exploration of duplicate ligand positions was minimized by creating pose clusters with RMSD standards at  $2.0 \text{ \AA}$ . A single cavity showed up from each docking session by selecting the best-binding option that delivered steady interactions. The analysis focused on two specific poses from this cavity based on their interaction quality, combined with their energy scores. The top two scorers were then validated through molecular docking simulations.

#### **5.2.5 Visualizations**

LigPlot+ software produced 2D graphical displays that depicted important molecular contacts between ligands and the specific selected pocket area. The visualizations helped validate the qualitative assessment and show that important interactions were consistent between different poses. The PLIP method generated structural summaries that confirmed crucial binding contacts throughout the 3D space. The visualizations played an essential role in confirming that the generated poses met quality standards and helped researchers choose simulation-based validation candidates.

### **5.2.6 Molecular dynamics simulations**

X-ray crystallography analyses of ligand-receptor structures were performed using the Desmond Molecular Dynamics System to study both the structural stability and dynamic behaviour in the top-scored docking complexes. A high-performance workstation with NVIDIA RTX 3070 and RTX 3080 GPUs executed the simulations while maintaining high efficiency in dealing with complex simulations across the extended time scale. An orthorhombic simulation box using the SPC water model contained the ligand-protein complexes, which received explicit water molecules extending at least 10 Å beyond solute atoms to provide enough buffer space. The introduction of counterions stabilized the system while the solution maintained physiological ionic conditions equal to 0.15 M NaCl to simulate biological conditions. All energy parameterizations within the simulation used the OPLS4 force field to achieve precision modelling of both protein structures and ligand chemical bonds. The prepared systems minimized their energy through the steepest descent algorithm, which resolved both steric clashes and bad contacts. The simulation followed a two-part equilibration protocol, beginning with NVT ensemble stabilization and proceeding to NPT ensemble stabilization of pressure and system density. The systems were equilibrated using Berendsen thermostat and barostat mechanisms at a temperature of 300 K and a pressure of 1.013 bar pressure. The simulation lasted 100 nanoseconds (ns) under NPT conditions in combination with applied periodic boundaries that extended throughout all directions. Trajectories were recorded with a period of 100 picoseconds (ps) for analysis purposes while running with a time-step of 2 fs. The integration time step became larger when using the SHAKE algorithm to constrain bond lengths that contained hydrogen atoms.

### **5.2.7 Trajectory analysis and post-simulation assessment**

The post-simulation evaluation included both built-in Desmond tools for analysis alongside the use of additional utilities and Python scripts developed in-house. The root mean square deviation (RMSD) measurement between protein backbone atoms and ligand atoms established the overall stability of the system (Swapna et al., 2024). The analysis of root mean square fluctuation (RMSF) through per-residue examination detected flexible parts as well as important interaction sites across the protein structure (Vander Meersche et al., 2024). The analysis involved principal component analysis (PCA), which operated on atomic fluctuation data matrices to obtain principal motions and collective framework movements throughout simulation time. Analysis of eigenvectors and

eigenvalues derived from PCA provided essential information about major structural transformations that affect protein functions. DCCM analysis provided insights about protein-ligand complex allosteric pathways by evaluating the movement correlations and anti-correlations between protein atoms.

The free energy landscape (FEL) analysis required the construction of maps from principal components PC1 and PC2 extracted through PCA. PC2 analysis showed the existence of different low-energy metastable states together with pathways that explain the simulation-based conformational diversity. The study of energy basins in these binding conformations identified stable conformations, whereas transition frequencies between energy states determined the stability levels of the complexes. The analyses involved multiple simulation repetitions to achieve reliable results while inspecting all generated pathways to verify proper simulation behaviour. Through extensive MD analysis, we gained detailed views of the temporal processes of ligand-receptor binding patterns and their functional applications for the chosen complexes.

## 5.3 Results and discussions

### 5.3.1 3D Modelling of target protein

I-tasser was employed for modelling protein sequences (Vandana & Rani, 2024). Accordingly, I-tasser predicted protein models and the structure with the greatest C-score (typically between -5,2). A greater C-score value indicated the highest level of confidence. Figure 5.2 depicts the 3D models of androgen receptors and NUDT5 oncoproteins, respectively, considered in this study.

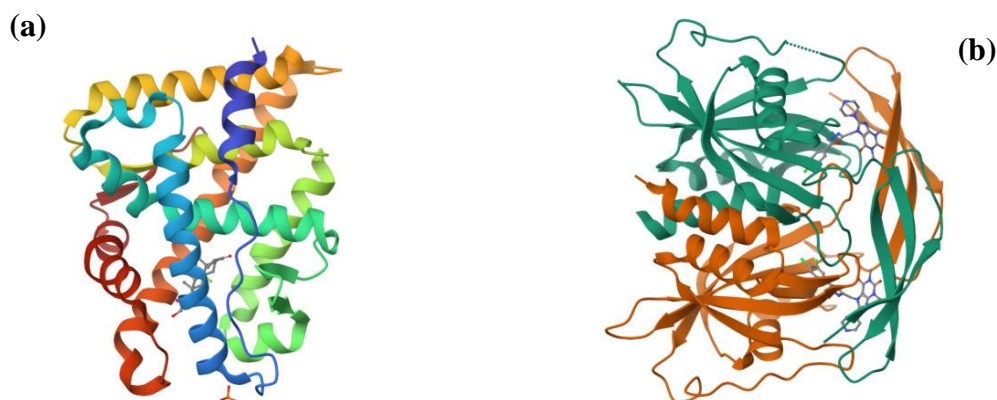


**Figure 5.2:** 3D ribbon structure of mutant androgen receptor (a) and (b) NUDT5 oncology proteins

### 5.3.2 Assessment of drug likeness

Herein, the drug-likeness scores were calculated and assessed based on Lipinski's rule and its components (Walters, 2012). These potential drug molecules have a low molecular weight (typically < 500 Daltons) except for Sal B (718.61 Daltons), indicating that these compounds can be easily absorbed, transported, or diffused compared to molecules with high molecular weights. Notably, the n violations of the compounds were equal to zero, suggesting that they can easily bind to receptors. The results of this research also showed that the drug-likeness of these compounds ranged from -0.79 to 3.79, indicating that they can be better drugs. Conversely, the number of hydrogen bond acceptors (nON) and number of hydrogen bond donors (nOHNH) of all compounds were within Lipinski's rule of less than 10 and 5, respectively except for Sal B. As depicted in Table 5.1, most the compounds have TPSA values below 160 Å<sup>2</sup> (97.98 -141.33 Å<sup>2</sup>) except Sal B (269.43 Å<sup>2</sup>), suggesting that they are better drugs (Meanwell, 2016). Also, MiLogP values below five show that all the studied compounds have good permeability across cell membranes, except for Sal B. The number of rotatable bonds (rotb) is a good descriptor of oral bioavailability.

**Table 5.1:** Drug likeness scores of potential lead compounds

Ligand	MiLogP	TPSA (Å <sup>2</sup> )	nAtoms	nON	nOHNH	nviolation	rotb	volume	Molecular weight (Daltons)
Sal B	-0.79	269.43	82	16	10	2	13	643.63	718.61
EA	0.94	141.33	22	8	4	0	0	221.78	302.19
<sup>3</sup> HPDBu	3.29	130.37	35	8	3	0	9	456.82	130.37
<sup>3</sup> HDPB	3.76	110.14	33	7	2	0	6	431.54	110.14

where miLogP, TPSA, nAtoms, nON, rotb, MW, and noHNNH is the logarithm of partition coefficient, topological polar surface area, number of atoms, number of hydrogen bond acceptors, number of rotatable bonds, molecular weight, and number of hydrogen bond donors, respectively.

### 5.3.3 Bioactivity scores of the lead compounds

Typically, bioactivity scores  $> 0$ ,  $-5.0-0.0$ , and  $< -5.0$  indicate that the bioactivity score is active, moderately active, and inactive, respectively (Khan et al., 2017). The bioactivity of ligand was assessed based on ion channel modulator, G protein-coupled receptor (GPCR) ligand, nuclear receptor ligand, kinase inhibitor, and enzyme inhibitor. The calculation of drug-likeness score towards GPCR ligand showed that [ $^3\text{H}$ ] DPB and [ $^3\text{H}$ ] DPB is active, while salvianolic acid and EA were moderately active. Except for EA, the lead compounds were active as ion channel modulators. EA has a bioactivity score of  $-0.10$ , indicating that it is moderately active as an ion channel modulator. Notably, all the lead compounds were bioactive ( $>0$ ) as nuclear receptor ligands and enzyme inhibitors. Both [ $^3\text{H}$ ] DPB and [ $^3\text{H}$ ] DPB are bioactive as a protease inhibitor, while salvianolic acid and EA are moderately active as protease inhibitor ( $> -0.5$ ). Accordingly, all the selected ligands were found to be active and moderately active as kinase inhibitors, protease inhibitors, enzyme inhibitors, GPCR ligands, nuclear receptor ligands, and ion channel modulators according to well-established protocol (Khan et al., 2017), as summarized in Table 5.2.

**Table 5.2:** Molinspiration bioactivity score of lead compounds

Compound	GPCR ligand	Ion channel modulator	Kinase inhibitor	Nuclear receptor ligand	Protease inhibitor	Enzyme inhibitor
Sal B	-0.20	0.02	-0.71	0.10	-0.27	0.13
EA	-0.08	-0.10	-0.38	0	-0.2	0.03
$^3\text{HPDBu}$	0.24	1.14	0.73	0.25	0.20	0.84
$^3\text{HDPB}$	0.09	1.28	0.47	0.22	0.15	0.66

### 5.3.4 Docking and molecular dynamics

#### 5.3.4.1 Ligand interactions

CID 119177 (Salvianolic acid) formed aromatic and hydrophobic interactions with androgen receptor proteins in residues like TRP741, TRP718, PHE764, and MET745, with a docking score

of -37.24 kJ/mol. These interactions imply that Sal B stabilizes within the protein through van der Waals,  $\pi - \pi$  stacking, and hydrophobic contacts. Non-covalent interactions in residues such as PHE and TRP within the aromatic rings help the ligand-protein complex via electron clouds. Also, the van der Waals interactions, particularly MET745, offer the complex with entropic gains, contributing to the orientation and specificity of the ligand. Noteworthy residues such as GLU681, ARG752, GLN711, and HIS714 are hydrogen bonds and polar contacts that promote electrostatic attractions and hydrogen bonds that enhance protein-ligand binding stability. Figure 5.3 gives the interactions of the protein-ligand complex.

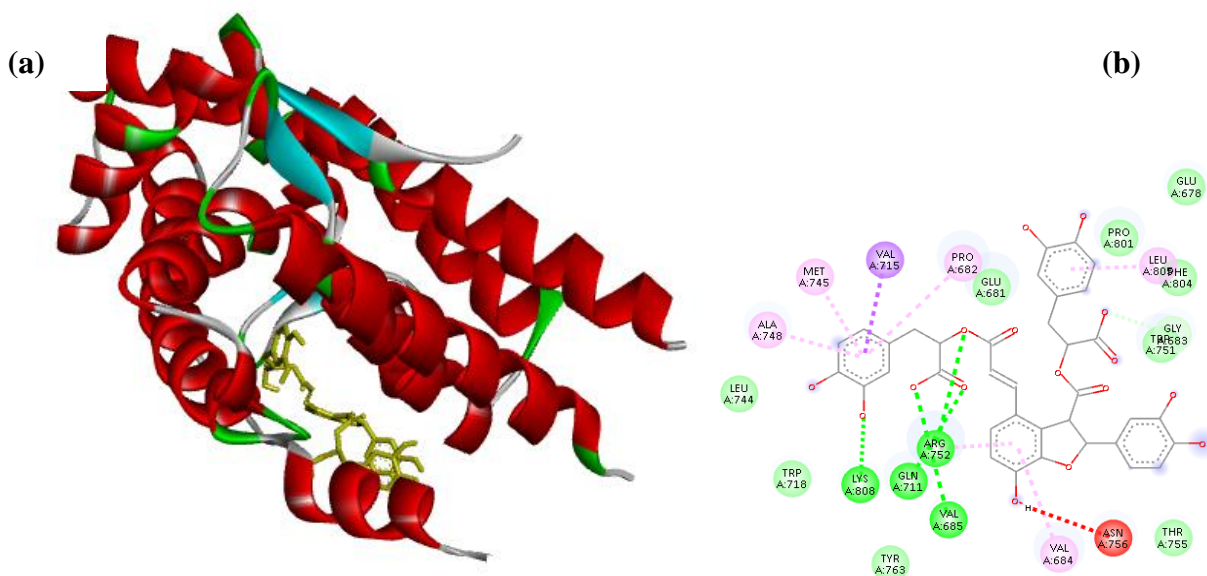


**Figure 5.3:** 3D ligand interaction (a) and (b) of Sal B with androgen receptor

Notably, the docking studies showed that salvianolic acid has a stronger affinity for NUDT5 protein than for androgen receptor, with the highest binding score of -46.86 kJ/mol. The complex has aromatic residues at PHE83 and TRP28, which contribute to  $\pi - \pi$  stacking and hydrophobic packing that stabilize the ligand by excluding water molecules from the complex. It is also evident that polar and charged residues in ARG51, GLU112, ASP100, and GLU115 contribute to the stability of the ligand-protein complex. Salt bridge formation at ARG51 is due to the phenolic or carboxylate groups in the ligand. These interactions imply that salvianolic acid has inhibitory potential or modulatory activity that can be used to inhibit NUDT5 protein in cancer therapy. The 2D and 3D interactions of the salvianolic acid-NUDT5 complex are presented in Figure 5.4.

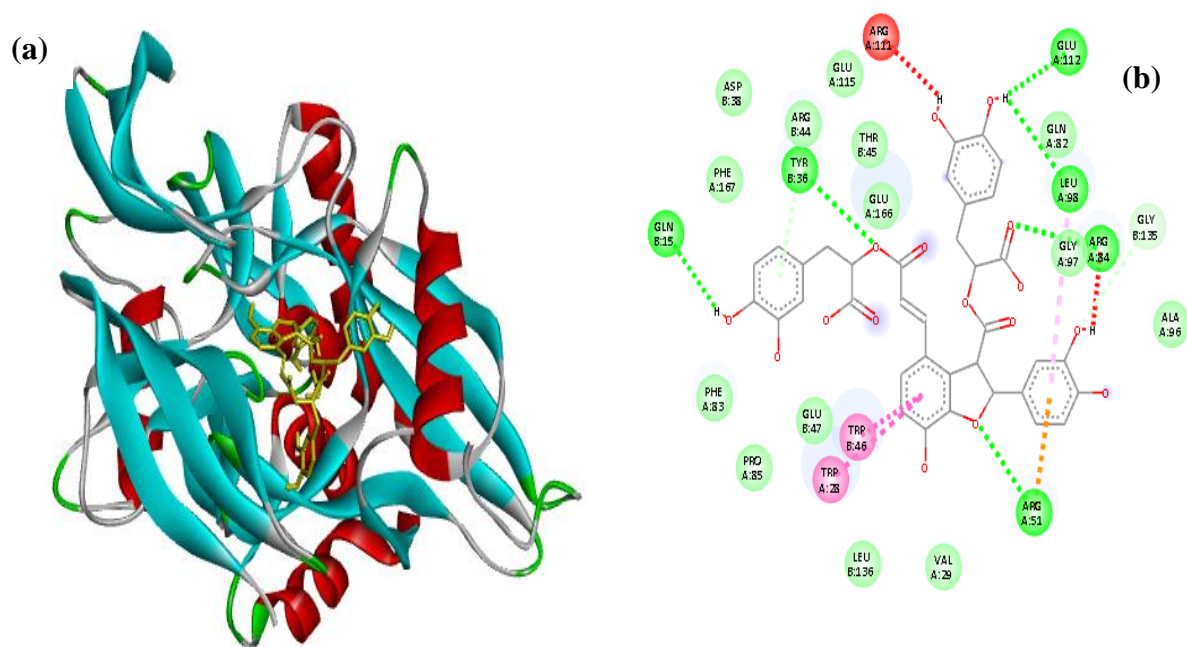


**Figure 5.4:** 3D interactions (a) and (b) 2D interactions of salvanolic acid-NUDT5 complex

When Nanobody bound to PSMA is docked with CID 5281855 (EA), it gives the lowest docking score of -27.20 kJ/mol among the selected top five scorers, as summarized in Table 5.3. After predicting the binding pockets, the target proteins were docked with four ligands filtered after virtual screening. As scribed in Table 5.3, CID 119177 (salvanolic acid) showed the highest docking score of -46.86 kJ/mol with NUDT5 protein and a docking score of -37.24 kJ/mol when androgen receptor is docked with the same ligand. However, docking RAD51C with CID 119177 (salvanolic acid) gives a lower docking score of -31.80 kJ/mol. CID 107855 ( $[^3\text{H}]$  DPB) showed the third highest docking score (-35.56 kJ/mol) when docked with Carbonic anhydrase IX.

**Table 5.3** Binding affinities and interactions of top scorers of oncoproteins

<b>CID</b>	<b>Compound</b>	<b>Protein</b>	<b>Binding Affinity (S) kJ/mol</b>	<b>Interactions</b>
CID 119177	Sal B	Androgen receptor	-37.24	GLU678, ALA679, VAL715, GLU681, LEU805 PRO682, VAL684, TRP751, MET745, ALA748, ARG752, SER753, ASN756, TYR763, PHE764, ALA765, PRO766, PRO801, GLN802, PHE804, THR755, MET749, GLY683
CID 119177	Sal B	NUDT5	-46.86	LYS27, TRP28, VAL29, ARG51, GLY61, VAL62, ALA63, GLN82, PHE83, ARG84, LYS161, GLY165, ASP38, PRO39, ARG44, THR45, TRP46, GLU47, ASP133, PRO134, GLY135, LEU136
CID 107855	[ <sup>3</sup> H] DPB	Carbonic anhydrase IX	-35.56	TRP5, LEU60, ASN62, HIS64, SER65, GLN67, HIS119, VAL121, VAL131, GLY132, VAL135, LEU141, VAL143, SER197, LEU198, THR199, THR200, PRO201, PRO202, VAL207, TRP 209
CID 5281855	EA	Nanobody bound to PSMA	-27.20	GLN1, ALA23, ARG24, SER25, GLY26, TYR32, SER52, SER53, THR54, GLN72, ASN74, ALA75, LYS76, ASN77, THR78, TYR102
CID 119177	Sal B	RAD51C C-terminal domain	-31.80	GLY117, ALA118, PRO119, GLY120, ARG160, ASP234, SER235, PHE238, ARG241, THR275, ASN276, GLN277, TRP312, ARG317, ILE336, THR337, THR338

### 5.3.5 Molecular dynamics simulations

Desmond (Schrödinger) was used to perform molecular dynamics as previously reported in similar studies (Vediappan et al., 2025). Molecular dynamics simulation was used to study ligand properties, including Radius of gyration (Rg), intramolecular hydrogen bonds, and the root mean square deviation (RMSD). The top two scorers for the six receptors were selected for molecular dynamics simulations. Accordingly, RMSF, RMSD, and protein-ligand interactions were computed from MD trajectory examination. The RMSF is essential in describing local interactions in the complex (Muhammad Rehman et al., 2023). It denotes the flexibility of residues in the protein-ligand interactions during simulation time.

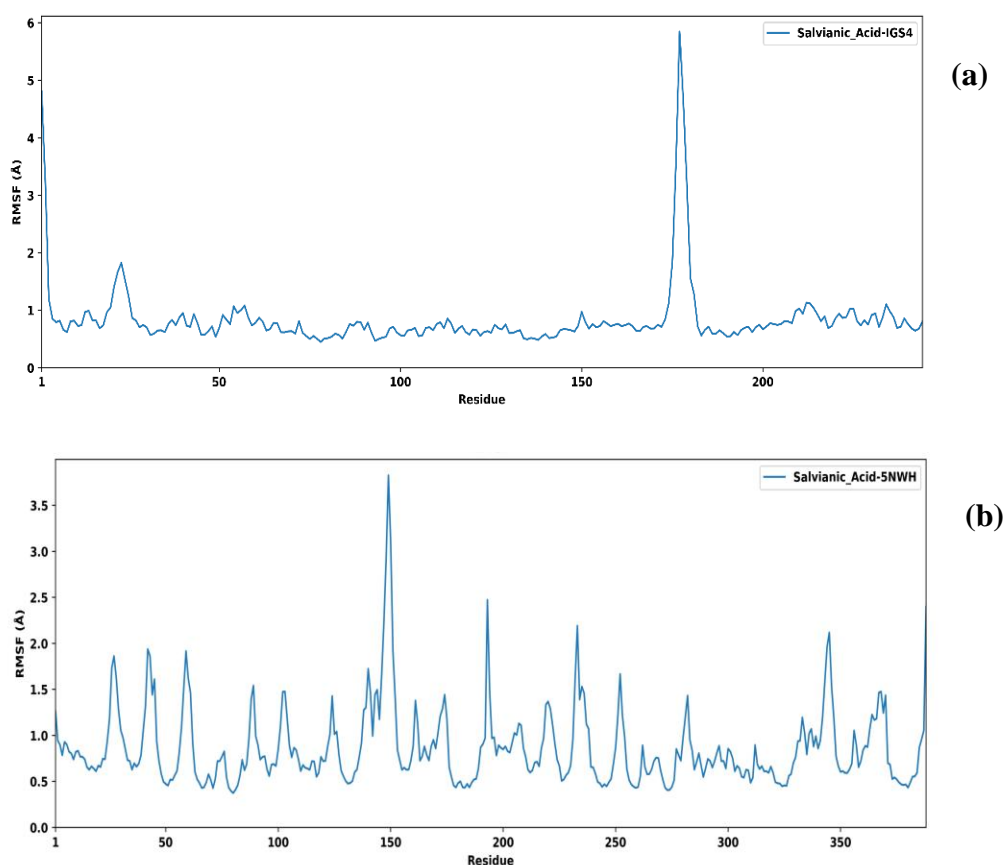


**Figure 5.5:** Root mean square fluctuation plot for (a) salvianolic acid-androgen receptor and (b) salvianolic acid-NUDT5

This study shows that the average RMSF for both systems is  $\approx 1.5 - 2.0$  Å, indicating structural stability of the complex. As shown in Figure 5.5, the fluctuations in the RMSF graph indicate the fluctuation of the protein component during molecular dynamics simulation. It implies that many

modifications occur in terminal regions (N- and C- tails) of the proteins than in other regions (Muhammad Rehman et al., 2023). The alpha helices and beta strands of the proteins exhibit less fluctuation since they are stiffer compared to other unstructured regions of the protein.

Typically, RMSD refers to the average change in an atom's displacement for a given frame relative to the reference frame. In this study, RMSD was used to assess conformational fluctuations and structural stability of biomolecular systems. For both systems, the RMSD graphs showed structural stability of the complex over 100 ns of molecular dynamics simulation. Initially, the RMSD for both complexes was approximately 0 Å and rises to around 2.0 Å and stabilizes, implying structural changes and equilibration as shown in Figure 5.6.

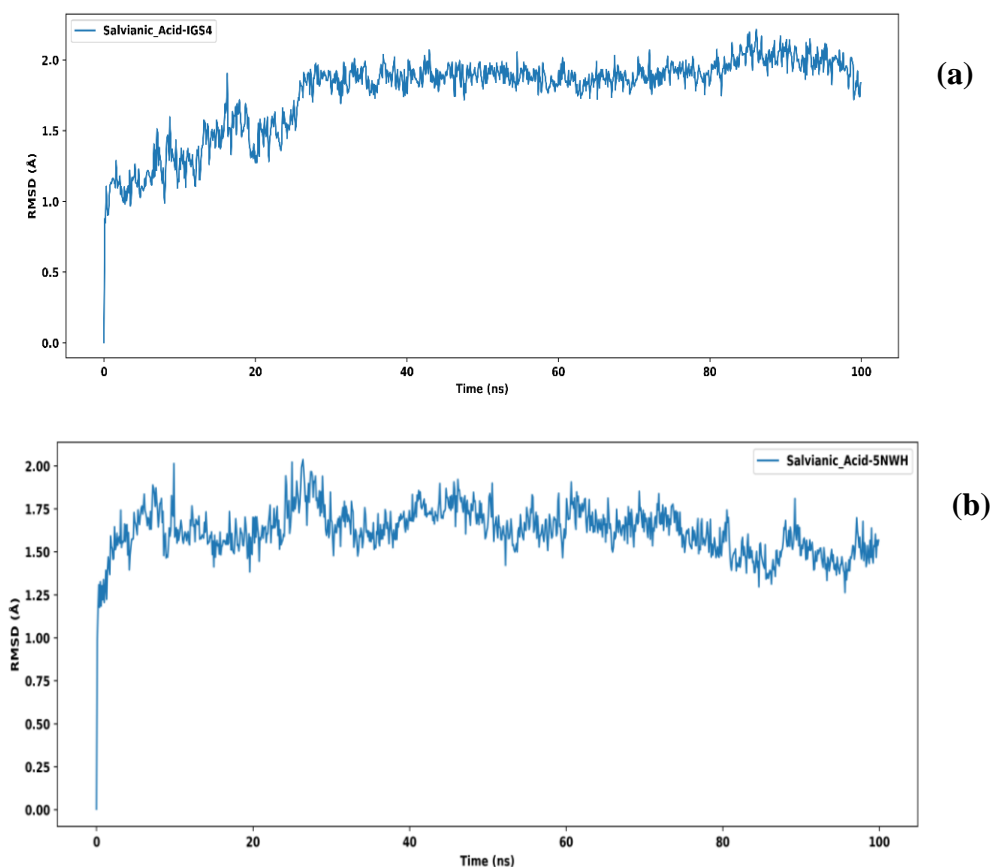


**Figure 5.6:** Root mean square deviation plot for (a) salvianolic acid-androgen receptor and (b) salvianolic acid-NUDT5

Essentially, the uptrend in RMSD signifies that the biological system underwent conformational changes before plateauing at 2.0 Å. The absence of sharp rising trends or sharp fluctuations showed that the systems did not undergo significant unfolding events or significant destabilization. This

shows that both complexes will remain stable without too much destabilization. Further to this, RMSD values below 3.0 Å denotes that the protein-ligand interactions form stable complexes, likely to be sustained over lengthy times. The radius of Gyration (Rg) evaluates the arrangement of atoms in a protein, including its axis. It represents the density and compactness of the protein structures over a cross-sectional area (Muhammad Rehman et al., 2023). In this study, analysis of Rg was conducted to investigate the compactness of the protein-ligand interaction of both systems. Accordingly, Rg corresponds to the principal moment of inertia (cf. Figure 5.7).

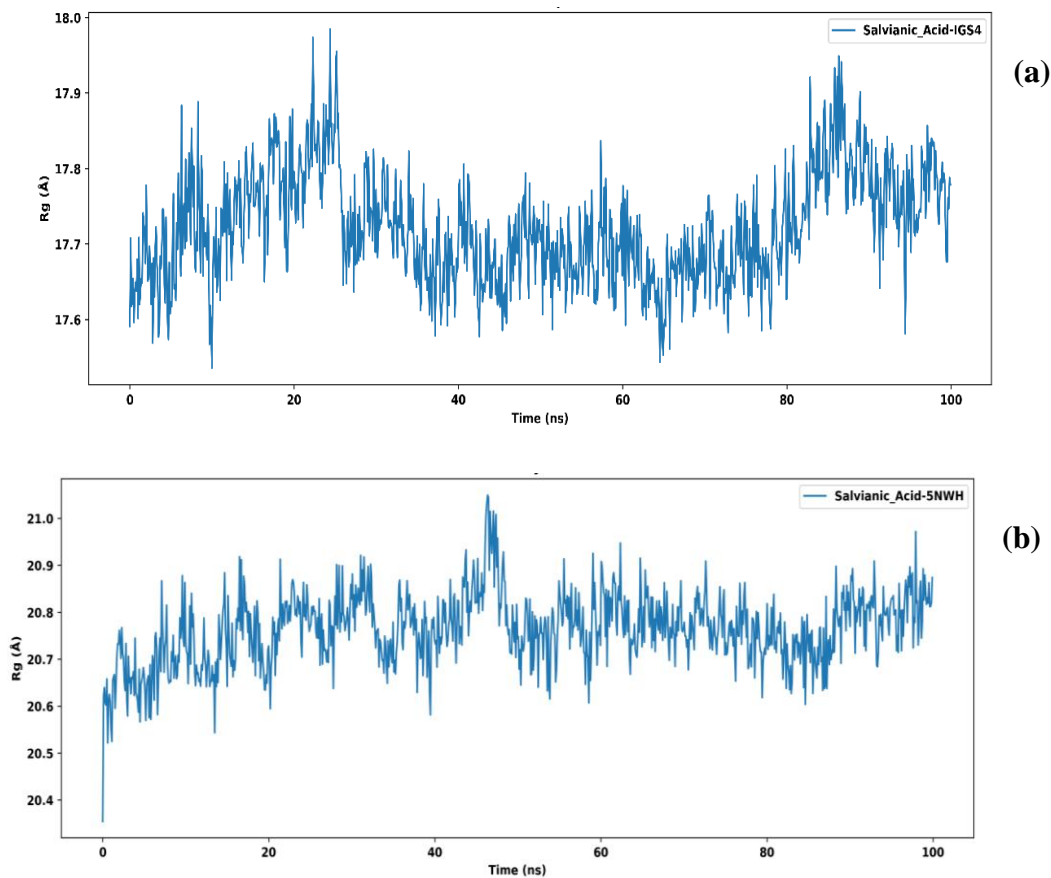


**Figure 5.7:** Radius of gyration plot for (a) salvianolic acid-androgen receptor and (b) salvianolic acid-NUDT5

The findings of this study showed lower Rg values, indicating flexibility and high compactness. Both systems have Rg values with a standard deviation less than 2 Å, implying that the two systems are compact and more tightly bound throughout the 100 ns simulation. The salvianolic acid-androgen receptor complex remained stable between 17.6 -17.9 Å, whereas the salvianolic acid-

NUDT5 complex remained stable at 20.6- 20.9 Å, as depicted in Figure 5.7. These results confirm the structural robustness of these complexes, as observed in docking studies.

### 5.3.4.2 Principal component analysis

In molecular dynamics, principal component analysis (PCA) has been widely used to transform high-dimensional datasets (usually,  $3N$ , where  $n$  is the number of considered atoms) into a low-dimensional coordinate system (Younas et al., 2025). Essentially, in PCA the considered atoms are projected onto principal components, also called orthogonal vectors. Both PC1 and PC2 give scatter plot which is important in visualizing the conformation of protein-ligand systems. Scattered points in a scatter plot denote flexibility and diverse conformational states, while tightly clustered points in scatter plots exhibit structural consistency within the complex. The distinct clustering of data points is indicative of conformational states and structural diversity of the protein-ligand complex (Khan et al., 2024). Consequently, the molecular behaviour of salvianolic acid is understood from this analysis, as exhibited in Figure 5.8.

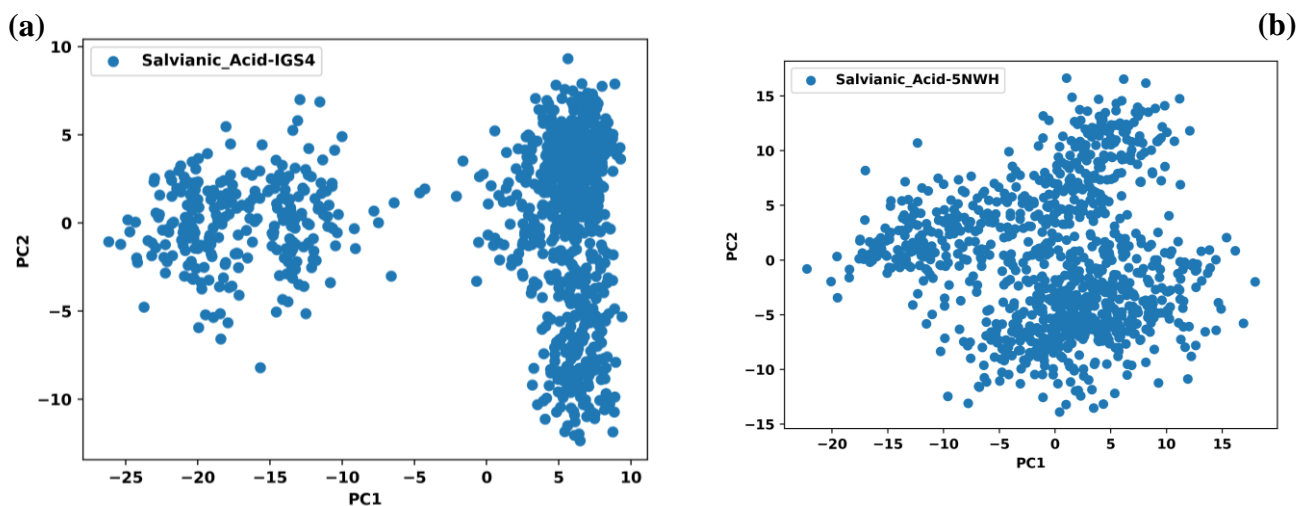


**Figure 5.8:** Principal component analysis plot for (a) salvianolic acid-androgen receptor and (b) salvianolic acid-NUDT5

Figure 5.9 depicts the collective motions of the proteins to PC1 and PC2. The trajectories of salvianolic acid-androgen receptor and salvianolic acid-NUDT5 complexes show differences in their patterns. Noteworthy, there are overlaps between the PCA plots of the two systems, implying

similar conformations (Muhammad Rehman et al., 2023). In contrast, the non-overlapping conformations indicate that there are conformational spaces that are reachable by one system.

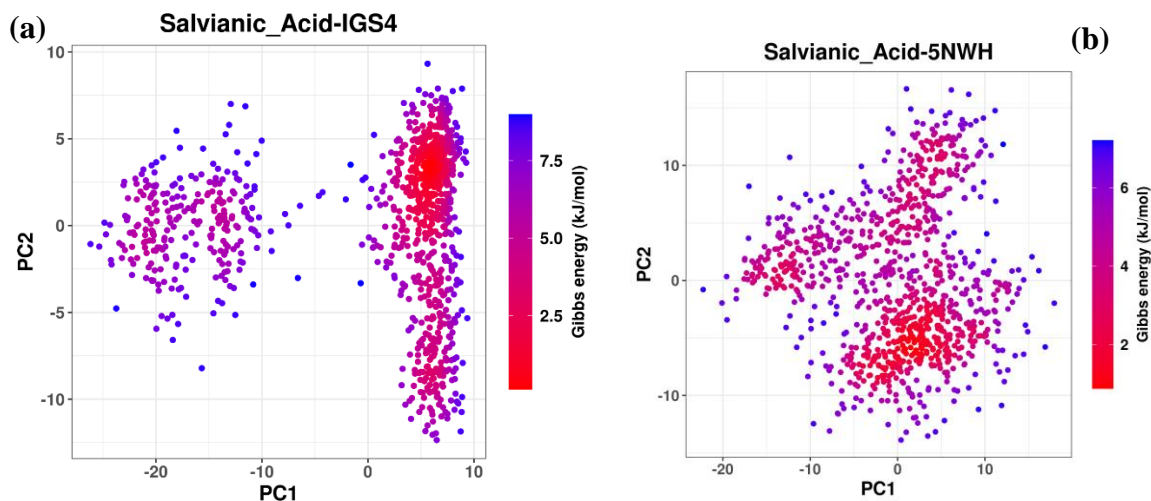


**Figure 5.9:** Principal component analysis trajectories for (a) salvianolic acid-androgen receptor and (b) salvianolic acid-NUDT5 complexes

### 5.3.4.3 Dynamical cross-correlational matrix

Dynamic cross-correlational matrix is crucial for studying dynamic cross-correlation networks formed by correlated residues. In this study, the C-alpha atoms are used to depict each residue (Muhammad Rehman et al., 2023). As ascribed in Figure 5.10, the dynamical cross-correlational plot of Sal B reveals correlated and opposing movements of residues throughout simulation. The dark blue part (1) signifies strong correlation, showing that there are movements have structural stability, whereas the pale-yellow region (-1) indicates opposing movements, indicative of highly flexible domains. The uncorrelated regions suggest independent movements, which could also be correlated to functional flexibility. Conversely, the distinct correlation region blocks suggest structured domain interactions, enhancing dynamic flexibility of the protein-ligand complex.

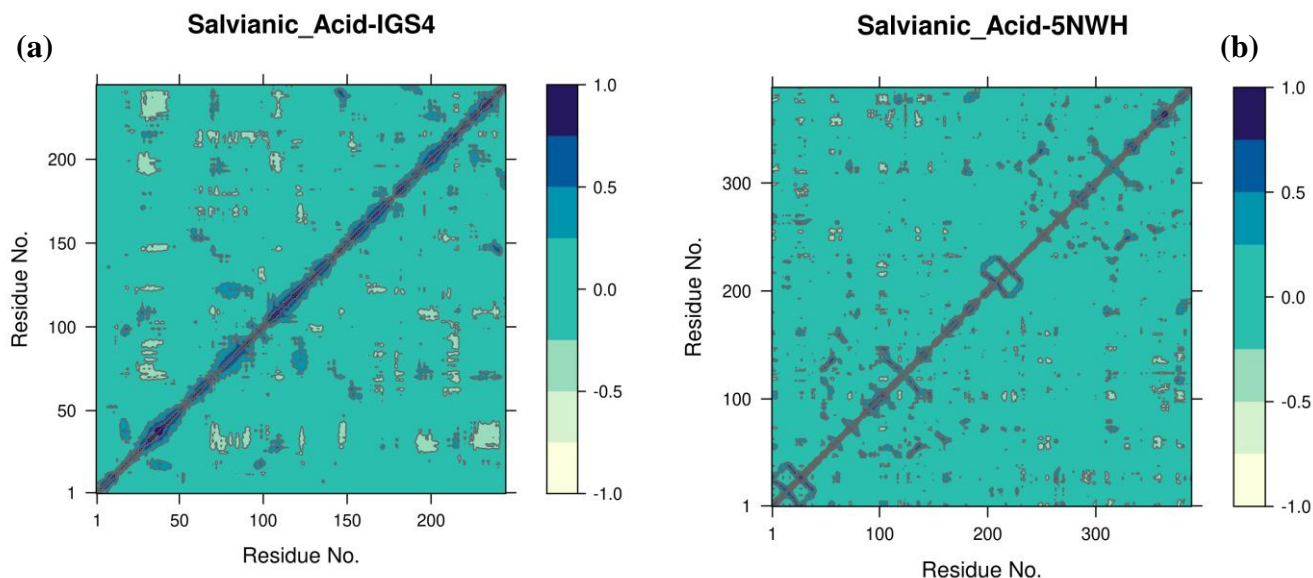


**Figure 5.10:** DCCM plot for (a) salvianolic acid-androgen receptor and (b) salvianolic acid-NUDT5

#### 5.3.4.4 Free energy landscape

The free energy landscape highlights energy variations of different conformational dynamics of a protein-ligand complex (c.f Figure 5.11). It characterizes energy changes of the protein molecule during simulations as a function of various variables, including PCA (Younas et al., 2025). In free energy landscape plots, Gibbs free energy (which depends on entropy and enthalpy) is used as an energy function. Accordingly, the LigPlot was used to generate conformations of protein-ligand interactions. For both systems, the colour scale ranges from red (high Gibbs free energy) to blue regions (low Gibbs free energy. At  $PC1 \approx 0$  and  $PC2 \approx 0$ , (the high-density red cluster) exhibits an average energy of approximately 1.5 kJ/mol, and the scattered blue region of higher energy, approximately 8.0 kJ/mol, suggests conformational stability and transient conformational shifts, respectively. The 2D free energy landscape of two central components (PC1 and PC2) shows the principal movements of the ligand. For Sal B -androgen receptor complex, the red regions indicate the most stable conformation where the complex spends most of the time during simulation (approximately 1.10 kJ/mol), while the blue regions (approximately 7.6 kJ/mol for Sal B -androgen receptor complex and 6.0 kJ/mol for Sal B -NUDT5 complex) show transient fluctuations,

representing high energy states. From the data set, the average Gibbs free energy was calculated to be 3.10 kJ/mol, confirming that the protein-ligand complex is thermodynamically stable. The red cluster (approximately 1.5 kJ/mol) shown in the scatter plot (Figure 5.11c-d) indicates the protein-ligand in a stable complex for both systems. On the other hand, the blue basin (appropriately 7.00 – 7.50 kJ/mol) for both systems shows transient and high-energy oscillations. This indicates that the protein-ligand complex periodically undergoes high-energy unfavourable states (Khan et al., 2024). From the data set, the average energy was calculated to be approximately 3.10 kJ/mol, suggesting the complex is stable with minimum energy variations.

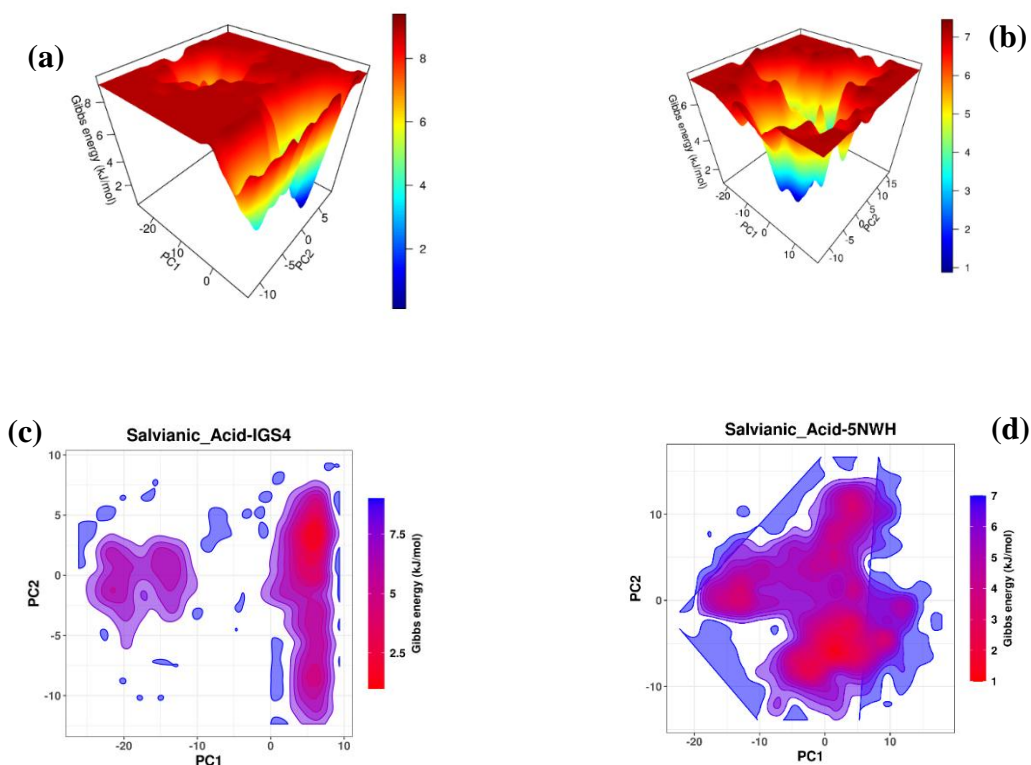


**Figure 5.11:** (a) 3D free energy landscape for Sal B -androgen receptor complex and (b) 3D free energy landscape for Sal B -NUDT5 complex, (c) 2D free energy landscape of two central components (PC1 and PC2) for Sal B -androgen receptor complex and (d) 2D free energy landscape of two central components (PC1 and PC2) for Sal B -NUDT5 complex

## 5.4 Conclusions

In this current study, various computational methodologies have been implemented to uncover the competency of bioactive compounds from the genus *Sapium* and *Salvia* as potential inhibitors of oncoproteins linked to PCa and BC. Sal B is a compound that has been extracted from *Salvia*, whereas EA, [<sup>3</sup>H] DPB and [<sup>3</sup>H] DPB have been isolated from the genus *Sapium*. The findings of this study show that all the selected bioactive compounds (ligands) were found to be active and moderately active as kinase inhibitors, enzyme inhibitors, protease inhibitors, GPCR ligands, nuclear receptor ligands, and ion channel modulators. Molecular docking and simulations suggest that salvianolic acid is a potent inhibitor of NUDT5 and androgen receptor oncoproteins among the four predicted ligands. Salvianolic acid B has a stronger affinity for NUDT5 protein than for androgen receptor, with the highest binding score of -46.86 kJ/mol characteristic of an anti-cancer agent. Subsequently, the stability of salvianolic acid-NUDT5 and salvianolic acid-androgen receptor combinations were investigated using molecular dynamics simulation at 100 ns. All the chosen ligands followed most Lipinski, Muegge, Ghose, Egan, and Verber's rules of drug-likeness have few violations of these rules. Furthermore, the Rg, RMSD, and RMSF plots reveal the high stability of these complexes. Thus, salvianolic acid has a potential role in inhibiting these oncoproteins in BC and PCa therapy. Further, *in vivo* and *in vitro* evaluations and clinical applications of Sal B may confirm its therapeutic application.

## CHAPTER SIX

### SUMMARY, CONCLUSIONS AND RECOMMENDATIONS

#### 6.1 General discussion

##### 6.1.1 Rationale of the study

The elimination of cancer from low-income and middle-income countries is a significant health burden due a number of variable including greater exposure to risk factors, high-cost screening, lack of adequate immunization campaigns and a lack of knowledge. Millions of patients in the underdeveloped countries may not obtain chemotherapeutic drugs and other treatment modalities due to their associated high costs, invasiveness, and lack of specificity. Consequently, there is an urgent need to design and develop novel easily available medication therapies, capable of improving the management and treatment of breast and prostate malignancies. Accordingly, treatment of cancer using bioactive compounds from natural plants is a promising alternative with the advantage of low toxicity and high efficiency. Notwithstanding the drug discovery efforts and the severity of this malignancy, no treatment has been introduced in the clinical settings. Efficacious drug discovery still calls for expensive, complicated, and time-intensive process. With the rapid advancements in bioinformatics and technological tools, implementation of *in-silico* approaches provides cost-effective and efficient ways of identifying and optimizing drug candidates. Therefore, the implementation of this approach takes precedence over the conventional wet lab experiments and drug repurposing approaches. Rapid screening of vast molecular libraries against target protein through virtual screening has been crucial in identifying the best possible compounds before in vitro essays. In this study, computational techniques and bioinformatics approach such as molecular dynamics and molecular docking are used to first assess the competency of secondary bioactive molecules isolated from the genus *Sapium* and *Salvia*, extending the scope of drug research in search for novel bioactive compounds and anti-cancer agents.

### 6.1.2 Findings of the study

The underlying mechanism of heterogenous prostate cancer (PCa) and breast cancer (BC), both genetically and histopathological, is still uncertain. The mono-therapeutic treatment selection for these malignancies includes chemotherapy, hormonal therapy, surgery, and radiotherapy. The current treatment strategies face therapeutic challenges related to accessibility issues, drug resistance, and side effects. The emergence of nanomedicine and artificial intelligence (AI) models in imaging, therapy, and drug delivery seems to offer solutions related to these challenges. Nanotechnology, so called nanotechnology in oncology, has emerged as a cutting-edge approach in cancer detection, treatment, and prevention. The current nanotechnologies have necessitated the combination of medicinal agents in cancer management with nanoscale technology. The therapeutic outcomes have significantly improved by maintaining targeted treatment dosages due to advancements in nanobiosensors, biological machinery, and medical equipment. Accordingly, the current research undertakings on cancer treatment will transition toward a convergence of AI and nanomedicine. Therefore, In order to expedite clinical translation of AI and nanomedicine, there should be adaptive regulatory pathways that allow iterative improvements depending on *in vivo* and *in vitro* analysis. This will bridge the gap between identification of novel lead candidates and implementation. In order to revolutionize BC and PCa healthcare, pathologists should not rely only on AI prediction but also on pathologist diagnostic skills. Nanotechnology offers promising opportunities, such as nanotheranostics, to revolutionize PCa and BC treatment by enhancing diagnostic accuracy, minimizing side effects, and enabling targeted drug delivery for more effective and personalized therapies.

*Salvia miltiorrhiza* Bunge is a traditional Chinese medicine with Sal B as the most prominent active ingredient. Sal B is lipid and water-soluble with an array of pharmacological benefits, including anticancer activities. Also, the genus *Sapium* exhibits a wide range of medicinal properties, including the treatment of conditions such as diabetes and cancer management. This study compared the anticancer properties of a far-less explored EA, [3H] PDBu, and [3H] DPB key metabolites from the genus *Sapium* and compares with the widely studies Sal B from *Salvia*. The findings revealed that Sal B had a binding affinity of -38.49 kJ/mol, -28.87 kJ/mol, and -33.07 kJ/mol when targeting DNA lyase, topoisomerase II alpha, and mTOR, respectively. Furthermore, of EA exhibiting a binding affinity of -36.40 kJ/mol, -27.20 kJ/mol, and -31.79 kJ/mol when

targeting DNA lyase, topoisomerase II alpha, and mTOR, respectively. The selected compounds were subjected to molecular dynamics at 300 K for 200 nanoseconds (ns). The results showed that among the four selected ligands, protein-Sal B complexes were stable and compact, as exhibited by the RMSD and RMSF values. the *in vitro* enzymatic and cellular assays were in good agreement with *in silico* studies that the IC<sub>50</sub> values indicated that Sal B was the most potent inhibitor across all targets, while EA was moderately effective. Phorbol compounds were less effective, with only modest inhibition of DNA lyase observed, compared to standards such as methoxyamine, etoposide, and rapamycin. In the enzymatic assays, Sal B showed comparable or better inhibition.

In this current study, various computational methodologies have been implemented to uncover the competency of bioactive compounds from the genus *Sapium* and *Salvia* as potential inhibitors of oncoproteins linked to PCa and BC. Accordingly, Sal B, [3H] PDBu and [3H] DPB. Noteworthy, the selected bioactive compound from natural plants followed the Lipinski, Muegge, Ghose, Egan, and Verber's rules of drug-likeness have few violations of these rules. Salvianolic acid has a stronger affinity for NUDT5 protein than for androgen receptor, with the highest binding score of -44.86 kJ/mol characteristic of an anti-cancer agent. The Rg, RMSD, and RMSF plots reveal the high stability of salvianolic acid-NUDT5 and salvianolic acid-androgen receptor combinations.

## 6.2 Conclusions

The implementation of computational approaches and *in vitro* experiments in this research is a resource-efficient approach minimizing the need for laboratory animals. In this study, it is evident that;

- i. SwissADME predictions demonstrated that the all the selected drug candidates possess favorable pharmacokinetic profiles, comply with major drug-likeness rules, and exhibit acceptable medicinal chemistry characteristics, indicating their potential as orally active and synthetically accessible therapeutic agents.
- ii. Molecular docking simulations revealed stable interactions between the selected drug candidates and their respective target proteins, highlighting key structural and molecular features responsible for binding and suggesting their potential mechanisms of action. Sal B was the most stable followed by EA and then phorbol derivatives.
- iii. Binding affinity analysis confirmed that some of the compounds (Sal B and EA) exhibited stronger binding energies and more favorable molecular interaction profiles compared to

the phorbol derivatives, suggesting higher potential efficacy against disease-causing proteins.

- iv. In vitro experiments validated the computational predictions, showing that Sal B exert significant biological activity on all the disease-related targets, with variations in potency and effectiveness among the tested lowering as we move from EA to the phorbol derivatives.
- v. Comparative evaluation indicated that Salvianolic and EA drug candidates were more effective in inhibiting breast and prostate cancer targets, thus identifying them promising lead compounds for further preclinical development.

### **6.3 Recommendations**

This study reaffirms the synergistic role of next generation technologies and the vast knowledge in structural biology to enhance early detection of biomarkers, optimize treatment deliveries, and develop individualized treatment plans for cancer patients. However, this research has the following recommendations;

- i. Structural optimization: Apply medicinal chemistry strategies such as scaffold modification, bio isosteric replacement, introduction or removal of electron-donating/withdrawing substituents, and stereo electronic tuning to the ligands to improve ligand binding affinity (lower  $IC_{50}/K_i$ ), enhance target selectivity by minimizing cross-reactivity, and optimize physicochemical properties (logP, TPSA, hydrogen bond donors/acceptors) for better oral bioavailability.
- ii. To validate binding mode experimentally: this should be done by further attempting co-crystallization (X-ray) or single-particle cryo-EM (Cryogenic Electron Microscopy) of target plus ligand to directly observe interacting residues and water molecules.
- iii. Drug delivery strategies: Employ advanced formulation approaches such as polymeric nanoparticles, liposomes, or solid lipid nanoparticles with Sal B, EA and Phorbol derivatives to improve aqueous solubility (measured by dissolution rate and logS), chemical and enzymatic stability (evaluated via degradation half-life and plasma stability assays), and targeted delivery (through surface functionalization with ligands or antibodies to enhance tissue/cell-specific uptake and increase bioavailability at the site of action).

- iv. Combination therapy studies: Evaluate the synergistic potential of lead compounds in conjunction with established therapeutics by performing drug–drug interaction assays and calculating combination indices (e.g., Chou–Talalay method). Such studies should assess enhancements in treatment efficacy through reduced  $IC_{50}/EC_{50}$  values, modulation of signaling pathways, and improved pharmacodynamic outcomes, while monitoring potential antagonism or adverse pharmacokinetic interactions (e.g., altered clearance, AUC, or  $C_{max}$ ).
- v. Translational progression: Sal B and EA should undergo structured preclinical evaluation, including *in vitro* ADMET profiling (solubility, permeability, microsomal stability, CYP450 inhibition), *in vivo* pharmacokinetic studies (bioavailability, clearance, half-life, tissue distribution), and toxicological assessments (NOAEL,  $LD_{50}$ , organ-specific toxicity). Successful outcomes would justify advancement into early-phase clinical trials (Phase I), focusing on safety, tolerability, maximum tolerated dose (MTD), and preliminary pharmacodynamic biomarkers of efficacy.

## REFERENCES

- Abeelh, E. A., & AbuAbeileh, Z. (2024). Comparative effectiveness of mammography, ultrasound, and MRI in the detection of breast carcinoma in dense breast tissue: a systematic review. *Cureus*, *16*(4), e59054. <https://doi.org/10.7759/cureus.59054>
- Abraham, M. J., Murtola, T., Schulz, R., Páll, S., Smith, J. C., Hess, B., & Lindahl, E. (2015). GROMACS: High performance molecular simulations through multi-level parallelism from laptops to supercomputers. *SoftwareX*, *1*(1), 19-25. <https://doi.org/10.1016/j.softx.2015.06.001>
- Acharya, C., Coop, A., E Polli, J., & D MacKerell, A. (2011). Recent advances in ligand-based drug design: relevance and utility of the conformationally sampled pharmacophore approach. *Current Computer-Aided Drug Design*, *7*(1), 10-22. <https://doi.org/10.2174/157340911793743547>
- Adelusi, T. I., Oyedele, A.-Q. K., Boyenle, I. D., Ogunlana, A. T., Adeyemi, R. O., Ukachi, C. D., Idris, M. O., Olaoba, O. T., Adedotun, I. O., & Kolawole, O. E. (2022). Molecular modeling in drug discovery. *Informatics in Medicine Unlocked*, *29*(1), 100880. <https://doi.org/10.1016/j.imu.2022.100880>
- Agamah, F. E., Mazandu, G. K., Hassan, R., Bope, C. D., Thomford, N. E., Ghansah, A., & Chimusa, E. R. (2020). Computational/in silico methods in drug target and lead prediction. *Briefings in Bioinformatics*, *21*(5), 1663-1675. <https://doi.org/10.1093/bib/bbz103>
- Aggarwal, D., Yang, J., Salam, M. A., Sengupta, S., Al-Amin, M. Y., Mustafa, S., Khan, M. A., Huang, X., & Pawar, J. S. (2023). Antibody-drug conjugates: the paradigm shifts in the targeted cancer therapy. *Frontiers in Immunology*, *14*(1), 1203073. <https://doi.org/10.3389/fimmu.2023.1203073>
- Agnihotry, S., Pathak, R. K., Srivastav, A., Shukla, P. K., & Gautam, B. (2020). Molecular docking and structure-based drug design. *Computer-Aided Drug Design*, *1*(1), 115-131. [https://doi.org/10.1007/978-981-15-6815-2\\_6](https://doi.org/10.1007/978-981-15-6815-2_6)
- Ahmad, S., Bano, N., & Raza, K. (2025). RCSB Protein Data Bank: revolutionising drug discovery and design for over five decades. *Medical Data Mining*, *8*(1), 7-11. <https://doi.org/10.53388/mdm202508008>
- Ahmadi, S., Barrios Herrera, L., Chehelamirani, M., Hostaš, J., Jalife, S., & Salahub, D. R. (2018). Multiscale modeling of enzymes: QM-cluster, QM/MM, and QM/MM/MD: A tutorial

- review. *International Journal of Quantum Chemistry*, 118(9), e25558. <https://doi.org/10.1002/qua.25558>
- Akkoc, S., Karatas, H., Muhammed, M. T., Kökbudak, Z., Ceylan, A., Almalki, F., Laaroussi, H., & Ben Hadda, T. (2023). Drug design of new therapeutic agents: Molecular docking, molecular dynamics simulation, DFT and POM analyses of new Schiff base ligands and impact of substituents on bioactivity of their potential antifungal pharmacophore site. *Journal of Biomolecular Structure and Dynamics*, 41(14), 6695-6708. <https://doi.org/10.1080/07391102.2022.2111360>
- Al Muqarrabun, L., Ahmat, N., & Aris, S. R. S. (2014). A review of the medicinal uses, phytochemistry and pharmacology of the genus *Sapium*. *Journal of Ethnopharmacology*, 155(1), 9-20. <https://doi.org/10.1016/j.jep.2014.05.028>
- Alessandri, R., Barnoud, J., Gertsen, A. S., Patmanidis, I., de Vries, A. H., Souza, P. C., & Marrink, S. J. (2022). Martini 3 coarse-grained force field: small molecules. *Advanced Theory and Simulations*, 5(1), 2100391. <https://doi.org/10.1002/adts.202100391>
- Alfei, S., Marengo, B., & Zuccari, G. (2020). Oxidative stress, antioxidant capabilities, and bioavailability: Ellagic acid or urolithins? *Antioxidants*, 9(8), 707. <https://doi.org/10.3390/antiox9080707>
- Alonso-Cotchico, L., Rodríguez-Guerra, J., Lledos, A., & Marechal, J.-D. (2020). Molecular modeling for artificial metalloenzyme design and optimization. *Accounts of Chemical Research*, 53(4), 896-905. <https://doi.org/10.1021/acs.accounts.0c00031>
- Alotaibi, B. S., Ijaz, M., Buabeid, M., Kharaba, Z. J., Yaseen, H. S., & Murtaza, G. (2021). Therapeutic effects and safe uses of plant-derived polyphenolic compounds in cardiovascular diseases: a review. *Drug Design, Development and Therapy*, 15(1), 4713-4732. <https://doi.org/10.2147/dddt.s327238>
- Alqahtani, S., Alzaidi, R., Alsultan, A., Asiri, A., Asiri, Y., & Alsaleh, K. (2022). Clinical pharmacokinetics of capecitabine and its metabolites in colorectal cancer patients. *Saudi Pharmaceutical Journal*, 30(5), 527-531. <https://doi.org/10.1016/j.jsps.2022.02.019>
- Alsherbiny, M. A., Bhuyan, D. J., Radwan, I., Chang, D., & Li, C.-G. (2021). Metabolomic identification of anticancer metabolites of Australian propolis and proteomic elucidation of its synergistic mechanisms with doxorubicin in the MCF7 cells. *International Journal of Molecular Sciences*, 22(15), 7840. <https://doi.org/10.3390/ijms22157840>

- Alyafeai, E., Qaed, E., Al-Mashriqi, H. S., Almaamari, A., Almansory, A. H., Al Futini, F., Sultan, M., & Tang, Z. (2024). Molecular dynamics of DNA repair and carcinogen interaction: Implications for cancer initiation, progression, and therapeutic strategies. *Mutation Research-Fundamental and Molecular Mechanisms of Mutagenesis*, 829(1), 111883. <https://doi.org/10.1016/j.mrfmmm.2024.111883>
- Aminpour, M., Montemagno, C., & Tuszynski, J. A. (2019). An overview of molecular modeling for drug discovery with specific illustrative examples of applications. *Molecules*, 24(9), 1693. <https://doi.org/10.3390/molecules24091693>
- Amit, R. (15 January, 2019). 7 Limitations of Molecular Docking & Computer Aided Drug Design. Retrieved August 27 from <https://amitray.com/7-limitations-of-molecular-docking-computer-aided-drug-design-and-discovery/>
- An, J., Peng, C., Tang, H., Liu, X., & Peng, F. (2021). New advances in the research of resistance to neoadjuvant chemotherapy in breast cancer. *International Journal of Molecular Sciences*, 22(17), 9644. <https://doi.org/10.3390/ijms22179644>
- Anand, U., Dey, A., Chandel, A. K. S., Sanyal, R., Mishra, A., Pandey, D. K., De Falco, V., Upadhyay, A., Kandimalla, R., & Chaudhary, A. (2023). Cancer chemotherapy and beyond: Current status, drug candidates, associated risks and progress in targeted therapeutics. *Genes & Diseases*, 10(4), 1367-1401. <https://doi.org/10.1016/j.gendis.2022.02.007>
- Anayyat, U., Ahad, F., Muluh, T. A., Zaidi, S. A. A., Usmani, F., Yang, H., Li, M., Hassan, H. A., & Wang, X. (2023). Immunotherapy: Constructive Approach for Breast Cancer Treatment. *Breast Cancer: Targets and Therapy*, 15(1), 925-951. <https://doi.org/10.2147/BCTT.S424624>
- Andrews, C., Hess, R. S., Drobotz, K., & Buriko, Y. (2024). Abnormalities detected on digital rectal examinations in dogs are common and influence diagnostic and treatment plans. *Journal of the American Veterinary Medical Association*, 262(6), 773-777. <https://doi.org/10.2460/javma.23.12.0695>
- Antoniali, G., Serra, F., Lirussi, L., Tanaka, M., D'Ambrosio, C., Zhang, S., Radovic, S., Dalla, E., Ciani, Y., & Scaloni, A. (2017). Mammalian APE1 controls miRNA processing and its interactome is linked to cancer RNA metabolism. *Nature Communications*, 8(1), 797. <https://doi.org/10.1038/s41467-017-00842-8>

- Aucar, M. G., & Cavasotto, C. N. (2020). Molecular docking using quantum mechanical-based methods. *Quantum Mechanics in Drug Discovery*, 1(1), 269-284. [https://doi.org/10.1007/978-1-0716-0282-9\\_17](https://doi.org/10.1007/978-1-0716-0282-9_17)
- Badar, M. S., Shamsi, S., Ahmed, J., & Alam, M. A. (2022). Molecular dynamics simulations: concept, methods, and applications. In *Transdisciplinarity* (pp. 131-151). Cham: Springer International Publishing. [https://doi.org/10.1007/978-3-030-94651-7\\_7](https://doi.org/10.1007/978-3-030-94651-7_7)
- Bakheit, A. H., Abuelizz, H. A., & Al-Salahi, R. (2023). A DFT Study and Hirshfeld Surface Analysis of the Molecular Structures, Radical Scavenging Abilities and ADMET Properties of 2-Methylthio (methylsulfonyl)-[1, 2, 4] triazolo [1, 5-a] quinazolines: Guidance for Antioxidant Drug Design. *Crystals*, 13(7), 1086. <https://doi.org/10.3390/cryst13071086>
- Balandat, M., Karrer, B., Jiang, D., Daulton, S., Letham, B., Wilson, A. G., & Bakshy, E. (2020). BoTorch: A framework for efficient Monte-Carlo Bayesian optimization. *Advances in Neural Information Processing Systems*, 33(1), 21524-21538. <https://proceedings.neurips.cc/paper/2020/file/f5b1b89d98b7286673128a5fb112cb9a-Paper.pdf>
- Banegas-Luna, A. J., Imbernon, B., Llanes Castro, A., Perez-Garrido, A., Ceron-Carrasco, J. P., Gesing, S., Merelli, I., D'Agostino, D., & Perez-Sanchez, H. (2019). Advances in distributed computing with modern drug discovery. *Expert Opinion on Drug Discovery*, 14(1), 9-22. <https://doi.org/10.1080/17460441.2019.1552936>
- Barge, S., Jade, D., Ayyamperumal, S., Manna, P., Borah, J., Nanjan, C. M. J., Nanjan, M. J., & Talukdar, N. C. (2022). Potential inhibitors for FKBP51: an in silico study using virtual screening, molecular docking and molecular dynamics simulation. *Journal of Biomolecular Structure and Dynamics*, 40(24), 13799-13811. <https://doi.org/10.1080/07391102.2021.1994877>
- Baroroh, U., Biotek, M., Muscifa, Z. S., Destiarani, W., Rohmatullah, F. G., & Yusuf, M. (2023). Molecular interaction analysis and visualization of protein-ligand docking using Biovia Discovery Studio Visualizer. *Indonesian Journal of Computational Biology (IJCB)*, 2(1), 22-30. <https://doi.org/10.24198/ijcb.v2i1.46322>
- Batool, A., Bibi, N., Amin, F., & Kamal, M. A. (2021). Drug designing against NSP15 of SARS-COV2 via high throughput computational screening and structural dynamics approach.

- European Journal of Pharmacology*, 892(1), 173779.  
<https://doi.org/10.1016/j.ejphar.2020.173779>
- Bauso, L. V., La Fauci, V., Munaò, S., Bonfiglio, D., Armeli, A., Maimone, N., Longo, C., & Calabrese, G. (2024). Biological activity of natural and synthetic peptides as anticancer agents. *International Journal of Molecular Sciences*, 25(13), 7264.  
<https://doi.org/10.3390/ijms25137264>
- Belfield, S. J., Firman, J. W., Enoch, S. J., Madden, J. C., Tollefsen, K. E., & Cronin, M. T. (2023). A review of quantitative structure-activity relationship modelling approaches to predict the toxicity of mixtures. *Computational Toxicology*, 25(1), 100251.  
<https://doi.org/10.1016/j.comtox.2022.100251>
- Belousova, O. A., Groen, A. J., & Ouendag, A. M. (2020). Opportunities and barriers for innovation and entrepreneurship in orphan drug development. *Technological Forecasting and Social Change*, 161(1), 120333. <https://doi.org/10.1016/j.techfore.2020.120333>
- Bera, I., & Payghan, P. V. (2019). Use of molecular dynamics simulations in structure-based drug discovery. *Current Pharmaceutical Design*, 25(31), 3339-3349.  
<https://doi.org/10.2174/1381612825666190903153043>
- Berdasco, M., & Esteller, M. (2022). Towards a druggable epitranscriptome: Compounds that target RNA modifications in cancer. *British Journal of Pharmacology*, 179(12), 2868-2889. <https://doi.org/10.1111/bph.15604>
- Berdigaliyev, N., & Aljofan, M. (2020). An overview of drug discovery and development. *Future Medicinal Chemistry*, 12(10), 939-947. <https://doi.org/10.4155/fmc-2019-0307>
- Bergonzo, C., & Cheatham III, T. E. (2015). Improved force field parameters lead to a better description of RNA structure. *Journal of Chemical Theory and Computation*, 11(9), 3969-3972. <https://doi.org/10.1021/acs.jctc.5b00444>
- Bernasinska-Slomczewska, J., Hikiş, P., Pieniasek, A., & Koceva-Chyla, A. (2024). Baicalin and Baicalein Enhance Cytotoxicity, Proapoptotic Activity, and Genotoxicity of Doxorubicin and Docetaxel in MCF-7 Breast Cancer Cells. *Molecules*, 29(11), 2503.  
<https://doi.org/10.3390/molecules29112503>
- Bertucci, A., Bertucci, F., & Gonçalves, A. (2023). Phosphoinositide 3-kinase (PI3K) inhibitors and breast cancer: an overview of current achievements. *Cancers*, 15(5), 1416.  
<https://doi.org/10.3390/cancers15051416>

- Bettonte, S., Berton, M., & Marzolini, C. (2022). Magnitude of Drug–Drug Interactions in Special Populations. *Pharmaceutics*, 14(4), 789. <https://doi.org/10.3390/pharmaceutics14040789>
- Beyens, O., Corthaut, S., Peeters, S., Van Der Veken, P., De Meester, I., & De Winter, H. (2024). Cosolvent Molecular Dynamics Applied to DPP4, DPP8 and DPP9: Reproduction of Important Binding Features and Use in Inhibitor Design. *Journal of Chemical Information and Modeling*, 64(19), 7650-7665. <https://doi.org/10.1021/acs.jcim.4c01167>
- Bicak, B., Gok, B., Kecel-Gunduz, S., Budama-Kilinc, Y., Kocyigit, M., Inan, H. A., & Kartal, M. (2025). Structural analyses (Spectroscopic and in silico), DNA-binding and in vitro studies of two popular Sage Species (*Salvia officinalis* and *Salvia fruticosa*). *Journal of Essential Oil Bearing Plants*, 28(1), 207-223. <https://doi.org/10.1080/07391102.2021.1968499>
- Blair, H. A. (2025a). Datopotamab Deruxtecan: First approval. *Drugs*, 85(7), 965-975. <https://doi.org/10.1007/s40265-025-02185-x>
- Blair, H. A. (2025b). Inavolisib: First approval. *Drugs*, 85(2), 271-278. <https://doi.org/10.1007/s40265-024-02136-y>
- Borah, P., Hazarika, S., Deka, S., Venugopala, K. N., Nair, A. B., Attimarad, M., Sreeharsha, N., & Mailavaram, R. P. (2020). Application of advanced technologies in natural product research: A review with special emphasis on ADMET profiling. *Current Drug Metabolism*, 21(10), 751-767. <https://doi.org/10.2174/1389200221666200714144911>
- Brianna, & Lee, S. H. (2023). Chemotherapy: how to reduce its adverse effects while maintaining the potency? *Medical Oncology*, 40(3), 88. <https://doi.org/10.1007/s12032-023-01954-6>
- Brogi, S., Ramalho, T. C., Kuca, K., Medina-Franco, J. L., & Valko, M. (2020). In Silico methods for drug design and discovery. (2020). *Frontiers Research Topics*, 8(1), 612. <https://doi.org/10.3389/978-2-88966-057-5>
- Brown, J. S., Amend, S. R., Austin, R. H., Gatenby, R. A., Hammarlund, E. U., & Pienta, K. J. (2023). Updating the definition of cancer. *Molecular Cancer Research*, 21(11), 1142-1147. <https://doi.org/10.1158/1541-7786.MCR-23-0411>
- Brown, N., Ertl, P., Lewis, R., Luksch, T., Reker, D., & Schneider, N. (2020). Artificial intelligence in chemistry and drug design. *Journal of Computer-Aided Molecular Design*, 34(7), 709-715. <https://doi.org/10.1007/s10822-020-00317-x>
- Bukke, S. P. N., Komarla Kumarachari, R., Komarla Rajasekhar, E. S., Dudekula, J. B., & Kamati, M. (2024). Computational intelligence techniques for achieving sustainable development

- goals in female cancer care. *Discover Sustainability*, 5(1), 390. <https://doi.org/10.1007/s43621-024-00575-x>
- Burley, S. K., Berman, H. M., Bhikadiya, C., Bi, C., Chen, L., Di Costanzo, L., Christie, C., Dalenberg, K., Duarte, J. M., & Dutta, S. (2019). RCSB Protein Data Bank: biological macromolecular structures enabling research and education in fundamental biology, biomedicine, biotechnology and energy. *Nucleic Acids Research*, 47(D1), D464-D474. <https://doi.org/10.1093/nar/gky1004>
- Burley, S. K., Piehl, D. W., Vallat, B., & Zardecki, C. (2024). RCSB Protein Data Bank: supporting research and education worldwide through explorations of experimentally determined and computationally predicted atomic level 3D biostructures. *International Union of Crystallography Journal*, 11(3), 279-286. <https://doi.org/10.1107/s2052252524002604>
- Bursch, M., Hansen, A., Pracht, P., Kohn, J. T., & Grimme, S. (2021). Theoretical study on conformational energies of transition metal complexes. *Physical Chemistry Chemical Physics*, 23(1), 287-299. <https://doi.org/10.1039/d0cp04696e>
- Cai, Z., & Liu, Q. (2021). Understanding the Global Cancer Statistics 2018: Implications for cancer control. *Science China Life Sciences*, 64(6), 1017-1020. <https://doi.org/10.1007/s11427-019-9816-1>
- Cameron, M., Frame, F., Maitland, N. J., & Hancock, Y. (2024). Raman spectroscopy reveals oxidative stress-induced metabolic vulnerabilities in early-stage AR-negative prostate-cancer versus normal-prostate cell lines. *Scientific Reports*, 14(1), 25388. <https://doi.org/10.1038/s41598-024-70338-1>
- Cardoso, E., Csajka, C., Schneider, M. P., & Widmer, N. (2018). Effect of adherence on pharmacokinetic/pharmacodynamic relationships of oral targeted anticancer drugs. *Clinical Pharmacokinetics*, 57(1), 1-6. <https://doi.org/10.1007/s40262-017-0571-z>
- Carpenter, V. J., Patel, B. B., Autorino, R., Smith, S. C., Gewirtz, D. A., & Saleh, T. (2020). Senescence and castration resistance in prostate cancer: A review of experimental evidence and clinical implications. *Biochimica et Biophysica Acta (BBA)-Reviews on Cancer*, 1874(2), 188424. <https://doi.org/10.1016/j.bbcan.2020.188424>
- Castelló, A., Rodríguez-Barranco, M., Pérez-Gómez, B., Chirlaque, M. D., Bonet, C., Amiano, P., Ardanaz, E., Huerta, J. M., Zamora-Ros, R., & Quirós, J. R. (2023). High adherence to Western dietary pattern and prostate cancer risk: findings from the EPIC-Spain cohort.

- British Journal of Urology International*, 132(3), 272-282.  
<https://doi.org/10.1111/bju.16001>
- Caston, R. A., Gampala, S., Armstrong, L., Messmann, R. A., Fishel, M. L., & Kelley, M. R. (2021). The multifunctional APE1 DNA repair–redox signaling protein as a drug target in human disease. *Drug Discovery Today*, 26(1), 218-228. human disease. *Drug Discovery Today*, 26(1), 218-228. <https://doi.org/10.1016/j.drudis.2020.10.015>
- Ceci, C., Lacal, P. M., Tentori, L., De Martino, M. G., Miano, R., & Graziani, G. (2018). Experimental evidence of the antitumor, antimetastatic and antiangiogenic activity of ellagic acid. *Nutrients*, 10(11), 1756. <https://doi.org/10.3390/nu10111756>
- Chandershekar, A., Bhaskar, A., Mekkanti, M. R., & Rinku, M. (2020). A review on computer aided drug design (CAAD) and it's implications in drug discovery and development process. *International Journal of Health Care and Biological Sciences*, 1(1), 27-33. <https://www.saapjournals.org/index.php/ijhcbs/article/view/15>
- Chandrasekaran, B., Al-Joubi, H., Samarneh, S., Kassab, G., Deb, P. K., Kumar, P., Al-Jaidi, B. A., Al-Thaher, Y., & Bataineh, Y. A. (2020). Drug-Receptor Interactions. *Frontiers in Pharmacology of Neurotransmitters*, 1(1), 31-68. [https://doi.org/10.1007/978-981-15-3556-7\\_2](https://doi.org/10.1007/978-981-15-3556-7_2)
- Chang, Y., Hawkins, B. A., Du, J. J., Groundwater, P. W., Hibbs, D. E., & Lai, F. (2023). A Guide to In Silico Drug Design. *Pharmaceutics*, 15(1), 49. <https://doi.org/10.3390/pharmaceutics15010049>
- Charifson, P. S., Corkery, J. J., Murcko, M. A., & Walters, W. P. (1999). Consensus scoring: A method for obtaining improved hit rates from docking databases of three-dimensional structures into proteins. *Journal of Medicinal Chemistry*, 42(25), 5100-5109. <https://doi.org/10.1021/jm990352k>
- Chen, B., Mansour, B., Zheng, E., Liu, Y., Gauld, J. W., & Wang, Q. (2023). Fundamentals behind the specificity of CysteinyI-tRNA synthetase: MD and QM/MM joint investigations. *Proteins: Structure, Function, and Bioinformatics*, 91(3), 354-362. <https://doi.org/10.1002/prot.26433>
- Chen, R., Li, L., & Weng, Z. (2003). ZDOCK: an initial-stage protein-docking algorithm. *Proteins: Structure, Function, and Bioinformatics*, 52(1), 80-87. <https://doi.org/10.1002/prot.10389>

- Chen, Y., Han, L., Dufour, C. R., Alfonso, A., & Giguère, V. (2024). Canonical and nuclear mTOR specify distinct transcriptional programs in androgen-dependent prostate cancer cells. *Molecular Cancer Research*, 22(2), 113-124. <https://doi.org/10.1158/1541-7786.mcr-23-0087>
- Cheng, F., Li, W., Liu, G., & Tang, Y. (2013). In silico ADMET prediction: recent advances, current challenges and future trends. *Current Topics in Medicinal Chemistry*, 13(11), 1273-1289. <https://doi.org/10.2174/15680266113139990033>
- Cheng, H. H., Shevach, J. W., Castro, E., Couch, F. J., Domchek, S. M., Eeles, R. A., Giri, V. N., Hall, M. J., King, M., Lin, D. W., Loeb, S., Morgan, T. M., Offit, K., Pritchard, C. C., Schaeffer, E. M., Szymaniak, B. M., Vassy, J. L., Katona, B. W., & Maxwell, K. N. (2024). *BRCA1*, *BRCA2*, and associated cancer risks and management for male patients. *Journal of the American Medical Association Oncology*, 10(9), 1272. <https://doi.org/10.1001/jamaoncol.2024.2185>
- Cheshomi, H., Bahrami, A. R., & Matin, M. M. (2021). Ellagic acid and human cancers: a systems pharmacology and docking study to identify principal hub genes and main mechanisms of action. *Molecular Diversity*, 25(1), 333-349. <https://doi.org/10.1007/s11030-020-10101-6>
- Choi, V. (2005). YUCCA: an efficient algorithm for small-molecule docking. *Chemistry & Biodiversity*, 2(11), 1517-1524. <https://doi.org/10.1002/cbdv.200590123>
- Christiansen, P., Mele, M., Bodilsen, A., Rocco, N., & Zachariae, R. (2022). Breast-conserving surgery or mastectomy?: impact on survival. *Annals of Surgery Open*, 3(4), e205. <https://doi.org/10.1097/AS9.0000000000000205>
- Chunarkar-Patil, P., Kaleem, M., Mishra, R., Ray, S., Ahmad, A., Verma, D., Bhayye, S., Dubey, R., Singh, H. N., & Kumar, S. (2024). Anticancer drug discovery based on natural products: From computational approaches to clinical studies. *Biomedicines*, 12(1), 201. <https://doi.org/10.3390/biomedicines12010201>
- Chuntakaruk, H., Hengphasatporn, K., Shigeta, Y., Aonbangkhen, C., Lee, V. S., Khotavivattana, T., Rungrotmongkol, T., & Hannongbua, S. (2024). FMO-guided design of darunavir analogs as HIV-1 protease inhibitors. *Scientific Reports*, 14(1), 3639. <https://doi.org/10.1038/s41598-024-53940-1>
- Çınaroğlu, S. I. S., & Biggin, P. C. (2021). Evaluating the performance of water models with host-guest force fields in binding enthalpy calculations for cucurbit [7] uril-guest systems. *The*

- Journal of Physical Chemistry B*, 125(6), 1558-1567.  
<https://doi.org/10.1021/acs.jpcc.0c11383>
- Čižmáriková, M., Michalková, R., Mirossay, L., Mojžišová, G., Zigová, M., Bardelčíková, A., & Mojžiš, J. (2023). Ellagic acid and cancer hallmarks: insights from experimental evidence. *Biomolecules*, 13(11), 1653. <https://doi.org/10.3390/biom13111653>
- Corbeil, C. R., Englebienne, P., & Moitessier, N. (2007). Docking ligands into flexible and solvated macromolecules. 1. Development and validation of FITTED 1.0. *Journal of Chemical Information and Modeling*, 47(2), 435-449. <https://doi.org/10.1021/ci6002637>
- Corbeil, C. R., Williams, C. I., & Labute, P. (2012). Variability in docking success rates due to dataset preparation. *Journal of Computer-Aided Molecular Design*, 26(6), 775-786. <https://doi.org/10.1007/s10822-012-9570-1>
- Cournia, Z., Chipot, C., Roux, B., York, D. M., & Sherman, W. (2021). Free energy methods in drug discovery—Introduction. *ACS Symposium Series*, 1(1), 1-38. <https://doi.org/10.1021/bk-2021-1397.ch001>
- Courtin, A., Richards, F. M., Bapiro, T. E., Bramhall, J. L., Neesse, A., Cook, N., Krippendorff, B.-F., Tuveson, D. A., & Jodrell, D. I. (2013). Anti-tumour efficacy of capecitabine in a genetically engineered mouse model of pancreatic cancer. *PloS One*, 8(6), e67330. <https://doi.org/10.1371/journal.pone.0067330>
- Crombag, M.-R. B., Joerger, M., Thürlimann, B., Schellens, J. H., Beijnen, J. H., & Huitema, A. D. (2016). Pharmacokinetics of selected anticancer drugs in elderly cancer patients: focus on breast cancer. *Cancers*, 8(1), 6. <https://doi.org/10.3390/cancers8010006>
- Csizi, K. S., & Reiher, M. (2023). Universal QM/MM approaches for general nanoscale applications. *Wiley Interdisciplinary Reviews: Computational Molecular Science*, 13(4) e1656. <https://doi.org/10.1002/wcms.1656>
- da Luz, F. A. C., da Costa Marinho, E., Nascimento, C. P., de Andrade Marques, L., Duarte, M. B. O., Delfino, P. F. R., Antonioli, R. M., de Araujo, R. A., & Silva, M. J. B. (2022). The effectiveness of radiotherapy in preventing disease recurrence after breast cancer surgery. *Surgical Oncology*, 41(1), 101709. <https://doi.org/10.1016/j.suronc.2022.101709>
- Dawson, W., Degomme, A., Stella, M., Nakajima, T., Ratcliff, L. E., & Genovese, L. (2022). Density functional theory calculations of large systems: Interplay between fragments,

- observables, and computational complexity. *Wiley Interdisciplinary Reviews: Computational Molecular Science*, 12(3), e1574. <https://doi.org/10.1002/wcms.1574>
- de Bruyn Kops, C., Šicho, M., Mazzolari, A., & Kirchmair, J. (2020). GLORYx: prediction of the metabolites resulting from phase 1 and phase 2 biotransformations of xenobiotics. *Chemical Research in Toxicology*, 34(2), 286-299. <https://doi.org/10.1021/acs.chemrestox.0c00224>
- de Feria Cardet, R. E., Hofman, M. S., Segard, T., Yim, J., Williams, S., Francis, R. J., Frydenberg, M., Lawrentschuk, N., Murphy, D. G., & Lourenco, R. D. A. (2021). Is prostate-specific membrane antigen positron emission tomography/computed tomography imaging cost-effective in prostate cancer: an analysis informed by the proPSMA trial. *European Urology*, 79(3), 413-418. <https://doi.org/10.1016/j.eururo.2020.11.043>
- Decherchi, S., & Cavalli, A. (2020). Thermodynamics and kinetics of drug-target binding by molecular simulation. *Chemical Reviews*, 120(23), 12788-12833. <https://doi.org/10.1021/acs.chemrev.0c00534>
- del Carmen Quintal Bojórquez, N., & Campos, M. R. (2023). Traditional and Novel Computer-Aided Drug Design (CADD) Approaches in the Anticancer Drug Discovery Process. *Current Cancer Drug Targets*, 23(5), 333-345. <https://doi.org/10.2174/1568009622666220705104249>
- Demapan, D., Kussmann, J. r., Ochsenfeld, C., & Cui, Q. (2022). Factors that determine the variation of equilibrium and kinetic properties of QM/MM enzyme simulations: QM region, conformation, and boundary condition. *Journal of Chemical Theory and Computation*, 18(4), 2530-2542. <https://doi.org/10.1021/acs.jctc.1c00714>
- Denning, E. J., Priyakumar, U. D., Nilsson, L., & Mackerell Jr, A. D. (2011). Impact of 2'-hydroxyl sampling on the conformational properties of RNA: update of the CHARMM all-atom additive force field for RNA. *Journal of Computational Chemistry*, 32(9), 1929-1943. <https://doi.org/10.1002/jcc.21777>
- Dent, S. F., Gaspo, R., Kissner, M., & Pritchard, K. I. (2011). Aromatase inhibitor therapy: toxicities and management strategies in the treatment of postmenopausal women with hormone-sensitive early breast cancer. *Breast Cancer Research and Treatment*, 126(2), 295-310. <https://doi.org/10.1007/s10549-011-1351-3>

- Deore, A. B., Dhumane, J. R., Wagh, R., & Sonawane, R. (2019). The stages of drug discovery and development process. *Asian Journal of Pharmaceutical Research and Development*, 7(6), 62-67. <https://doi.org/10.22270/ajprd.v7i6.616>
- Devi, R. V., Sathya, S. S., & Coumar, M. S. (2015). Evolutionary algorithms for de novo drug design—A survey. *Applied Soft Computing*, 27(1), 543-552. <https://doi.org/10.1016/j.asoc.2014.09.042>
- Djoubou-Feunang, Y., Fiamoncini, J., Gil-de-la-Fuente, A., Greiner, R., Manach, C., & Wishart, D. S. (2019). BioTransformer: a comprehensive computational tool for small molecule metabolism prediction and metabolite identification. *Journal of Cheminformatics*, 11(1). <https://doi.org/10.1186/s13321-018-0324-5>
- Dodda, L. S., Cabeza de Vaca, I., Tirado-Rives, J., & Jorgensen, W. L. (2017). LigParGen web server: an automatic OPLS-AA parameter generator for organic ligands. *Nucleic Acids Research*, 45(W1), W331-W336. <https://doi.org/10.1093/nar/gkx312>
- Dubey, S., & Sikarwar, S. S. (2025). Applications of AI in Cancer Detection—A Review of the Specific Ways in which AI Is Being Used to Detect and Diagnose Various Types of Cancer. *AI in Disease Detection: Advancements and Applications*, 1(1), 147-166. <https://doi.org/10.1002/9781394278695.ch7>
- Duela, S., Umamageswari, A., Prabavathi, R., Umapathy, P., & Raja, K. (2023). Quantum assisted Genetic Algorithm for Sequencing Compatible Amino Acids in Drug Design. 2023 Third *International Conference on Advances in Electrical, Computing, Communication and Sustainable Technologies (ICAECT)*, 1(1), 1-7. <https://doi.org/10.1109/icaect57570.2023.10117673>
- Dvir, K., Giordano, S., & Leone, J. P. (2024). Immunotherapy in breast cancer. *International Journal of Molecular Sciences*, 25(14), 7517. <https://doi.org/10.3390/ijms25147517>
- Eastman, P., Swails, J., Chodera, J. D., McGibbon, R. T., Zhao, Y., Beauchamp, K. A., Wang, L.-P., Simmonett, A. C., Harrigan, M. P., & Stern, C. D. (2017). OpenMM 7: Rapid development of high performance algorithms for molecular dynamics. *PLoS Computational Biology*, 13(7), e1005659. <https://doi.org/10.1371/journal.pcbi.1005659>
- Ebrahimi, F., Farzaei, M. H., Bahramsoltani, R., Heydari, M., Naderinia, K., & Rahimi, R. (2019). Plant-derived medicines for neuropathies: A comprehensive review of clinical evidence.

- Reviews in the Neurosciences*, 30(6), 671-684. <https://doi.org/10.1515/revneuro-2018-0097>
- Eddershaw, P., & Dickins, M. (2021). Phase I metabolism. *A Handbook of Bioanalysis and Drug Metabolism* (pp. 208-221). CRC Press. <https://doi.org/10.1201/9780203642535.ch13>
- Egorova, K. S., Gordeev, E. G., & Ananikov, V. P. (2017). Biological activity of ionic liquids and their application in pharmaceuticals and medicine. *Chemical Reviews*, 117(10), 7132-7189. <https://doi.org/10.1021/acs.chemrev.6b00562>
- El-Fakahany, E. E. (2020). Subtypes of Muscarinic Receptors: Receptor Structure and Molecular Biology. In *CNS Neurotransmitters and Neuromodulators* (pp. 49-66). CRC Press. <https://doi.org/10.1201/9781003068723-3>
- El Omari, N., Bakha, M., Imtara, H., Guaouguaoua, F.-E., Balahbib, A., Zengin, G., & Bouyahya, A. (2021). Anticancer mechanisms of phytochemical compounds: focusing on epigenetic targets. *Environmental Science and Pollution Research*, 28(35), 47869-47903. <https://doi.org/10.1007/s11356-021-15594-8>
- Eldridge, M. D., Murray, C. W., Auton, T. R., Paolini, G. V., & Mee, R. P. (1997). Empirical scoring functions: I. The development of a fast empirical scoring function to estimate the binding affinity of ligands in receptor complexes. *Journal of Computer-Aided Molecular Design*, 11(5), 425-445. <https://doi.org/10.1023/a:1007996124545>
- Engel, N. W., Steinfeld, I., Ryan, D., Anupindi, K., Kim, S., Wellhausen, N., Chen, L., Wilkins, K., Baker, D. J., & Rommel, P. C. (2025). Quadruple adenine base-edited allogeneic CAR T cells outperform CRISPR/Cas9 nuclease-engineered T cells. *Proceedings of the National Academy of Sciences*, 122(20), e2427216122. <https://doi.org/10.1073/pnas.2427216122>
- Evangelista, W., Ellingson, S. R., Smith, J. C., & Baudry, J. Y. (2019). Ensemble Docking in Drug Discovery: How Many Protein Configurations from Molecular Dynamics Simulations Are Needed to Reproduce Known Ligand Binding? *The Journal of Physical Chemistry B*, 123(25), 5189-5195. <https://doi.org/10.1021/acs.jpccb.8b11491.s001>
- Eweas, A. F., Maghrabi, I. A., & Namarneh, A. I. (2014). Advances in molecular modeling and docking as a tool for modern drug discovery. *Der Pharma Chemica*, 6(6), 211-228. <http://www.derpharmachemica.com/>

- Fadaka, A. O., Aruleba, R. T., Sibuyi, N. R. S., Klein, A., Madiehe, A. M., & Meyer, M. (2022). Inhibitory potential of repurposed drugs against the SARS-CoV-2 main protease: a computational-aided approach. *Journal of Biomolecular Structure and Dynamics*, 40(8), 3416-3427. <https://doi.org/10.1080/07391102.2020.1847197>
- Fadnis, J. A., Sawale, A. V., & Padmawar, S. S. (2023). Thalidomide: The journey from curse to boon. *World Journal of Biology Pharmacy and Health Sciences*, 14(3), 149-159. <https://doi.org/10.30574/wjbphs.2023.14.3.0257>
- Fan, J., Fu, A., & Zhang, L. (2019). Progress in molecular docking. *Quantitative Biology*, 7(2), 83-89. <https://doi.org/10.1007/s40484-019-0172-y>
- Farrukh, M., Shahzadi, S., & Irfan, M. (2024). Drug Metabolism: Phase I and Phase II Metabolic Pathways. In *Drug Metabolism and Pharmacokinetics*. IntechOpen. <https://doi.org/10.5772/intechopen.112854>
- Feller, S. E., Yin, D., Pastor, R. W., & MacKerell, A. (1997). Molecular dynamics simulation of unsaturated lipid bilayers at low hydration: parameterization and comparison with diffraction studies. *Biophysical Journal*, 73(5), 2269-2279. [https://doi.org/10.1016/s0006-3495\(97\)78259-6](https://doi.org/10.1016/s0006-3495(97)78259-6)
- Ferrari, P., Scatena, C., Ghilli, M., Bargagna, I., Lorenzini, G., & Nicolini, A. (2022). Molecular mechanisms, biomarkers and emerging therapies for chemotherapy resistant TNBC. *International Journal of Molecular Sciences*, 23(3), 1665. <https://doi.org/10.3390/ijms23031665>
- Ferreira, L. L., & Andricopulo, A. D. (2019). ADMET modeling approaches in drug discovery. *Drug Discovery Today*, 24(5), 1157-1165. <https://doi.org/10.1016/j.drudis.2019.03.015>
- Foloppe, N., & MacKerell, J., Alexander D. (2000). All-atom empirical force field for nucleic acids: I. Parameter optimization based on small molecule and condensed phase macromolecular target data. *Journal of Computational Chemistry*, 21(2), 86-104. [https://doi.org/10.1002/\(sici\)1096-987x\(20000130\)21:2<86::aid-jcc2>3.0.co;2-g](https://doi.org/10.1002/(sici)1096-987x(20000130)21:2<86::aid-jcc2>3.0.co;2-g)
- Fourches, D. (2017). Reaction: Molecular Modeling for Novel Antibacterials. *Chem*, 3(1), 13-14. <https://doi.org/10.1016/j.chempr.2017.06.016>
- Friedman, R. (2022). Computational studies of protein–drug binding affinity changes upon mutations in the drug target. *Wiley Interdisciplinary Reviews: Computational Molecular Science*, 12(1), e1563. <https://doi.org/10.1002/wcms.1563>

- Friesner, R. A., Banks, J. L., Murphy, R. B., Halgren, T. A., Klicic, J. J., Mainz, D. T., Repasky, M. P., Knoll, E. H., Shelley, M., & Perry, J. K. (2004). Glide: a new approach for rapid, accurate docking and scoring. 1. Method and assessment of docking accuracy. *Journal of Medicinal Chemistry*, 47(7), 1739-1749. <https://doi.org/10.1021/jm0306430>
- Fu, W., & Wu, G. (2023). Targeting mTOR for anti-aging and anti-cancer therapy. *Molecules*, 28(7), 3157. <https://doi.org/10.3390/molecules28073157>
- Galindo-Murillo, R., Robertson, J. C., Zgarbova, M., Sponer, J., Otyepka, M., Jurecka, P., & Cheatham III, T. E. (2016). Assessing the current state of amber force field modifications for DNA. *Journal of Chemical Theory and Computation*, 12(8), 4114-4127. <https://doi.org/10.1021/acs.jctc.6b00186>
- Garg, A., & Dewangan, H. K. (2022). Recent advances in drug design and delivery across biological barriers using computational models. *Letters in Drug Design & Discovery*, 19(10), 865-876. <https://doi.org/10.2174/1570180819999220204110306>
- Garg, P., Malhotra, J., Kulkarni, P., Horne, D., Salgia, R., & Singhal, S. S. (2024). Emerging therapeutic strategies to overcome drug resistance in cancer cells. *Cancers*, 16(13), 2478. <https://doi.org/10.3390/cancers16132478>
- Garg, S., Arora, K., Singh, S., & Nagarajan, K. (2024). Artificial Intelligence and Machine Learning in Drug Discovery and Development. *Advances in Computational Intelligence and Robotics*, 1(1), 42-61. <https://doi.org/10.4018/979-8-3693-0368-9.ch003>
- Gautieri, A., Russo, A., Vesentini, S., Redaelli, A., & Buehler, M. J. (2010). Coarse-grained model of collagen molecules using an extended MARTINI force field. *Journal of Chemical Theory and Computation*, 6(4), 1210-1218. <https://doi.org/10.1021/ct100015v>
- Ge, C., Huang, X., Zhang, S., Yuan, M., Tan, Z., Xu, C., Jie, Q., Zhang, J., Zou, J., & Zhu, Y. (2023). In vitro co-culture systems of hepatic and intestinal cells for cellular pharmacokinetic and pharmacodynamic studies of capecitabine against colorectal cancer. *Cancer Cell International*, 23(1), 14. <https://doi.org/10.1186/s12935-023-02853-6>
- Ghahremanpour, M. M., Tirado-Rives, J., & Jorgensen, W. L. (2022). Refinement of the optimized potentials for liquid simulations force field for thermodynamics and dynamics of liquid alkanes. *The Journal of Physical Chemistry B*, 126(31), 5896-5907. <https://doi.org/10.1021/acs.jpcc.2c03686>

- Ghosh, A., Panda, P., Halder, A. K., & Cordeiro, M. N. D. (2022). In silico characterization of aryl benzoyl hydrazide derivatives as potential inhibitors of RdRp enzyme of H5N1 influenza virus. *Frontiers in Pharmacology*, 13(1), 1004255. <https://doi.org/10.3389/fphar.2022.1004255>
- Giese, T. J., Zeng, J., Ekesan, S. o. l., & York, D. M. (2022). Combined QM/MM, machine learning path integral approach to compute free energy profiles and kinetic isotope effects in RNA cleavage reactions. *Journal of Chemical Theory and Computation*, 18(7), 4304-4317. <https://doi.org/10.1021/acs.jctc.2c00151>
- Gioia, D., Bertazzo, M., Recanatini, M., Masetti, M., & Cavalli, A. (2017). Dynamic Docking: A Paradigm Shift in Computational Drug Discovery. *Molecules*, 22(11), 2029. <https://doi.org/10.3390/molecules22112029>
- Godtman, R. A., Kollberg, K. S., Pihl, C.-G., Månsson, M., & Hugosson, J. (2022). The association between age, prostate cancer risk, and higher Gleason score in a long-term screening program: results from the Göteborg-1 prostate cancer screening trial. *European Urology*, 82(3), 311-317. <https://doi.org/10.1016/j.eururo.2022.01.018>
- Gola, J., Obrezanova, O., Champness, E., & Segall, M. (2006). ADMET property prediction: the state of the art and current challenges. *QSAR & Combinatorial Science*, 25(12), 1172-1180. <https://doi.org/10.1002/qsar.200610093>
- Goodsell, D. S., & Olson, A. J. (1990). Automated docking of substrates to proteins by simulated annealing. *Proteins: Structure, Function, and Bioinformatics*, 8(3), 195-202. <https://doi.org/10.1002/prot.340080302>
- Gote, V., Nookala, A. R., Bolla, P. K., & Pal, D. (2021). Drug resistance in metastatic breast cancer: tumor targeted nanomedicine to the rescue. *International Journal of Molecular Sciences*, 22(9), 4673. <https://doi.org/10.3390/ijms22094673>
- Gräfenstein, J., & Cremer, D. (2009). The self-interaction error and the description of non-dynamic electron correlation in density functional theory. *Theoretical Chemistry Accounts*, 123(3-4), 171-182. <https://doi.org/10.1007/s00214-009-0545-9>
- Gramatica, P. (2020). Principles of QSAR modeling: comments and suggestions from personal experience. *International Journal of Quantitative Structure-Property Relationships (IJQSPR)*, 5(3), 61-97. <https://doi.org/10.4018/ijqspr.20200701.oa1>

- Grasso, A., Altomare, V., Fiorini, G., Zompanti, A., Pennazza, G., & Santonico, M. (2025). Innovative Methodologies for the Early Detection of Breast Cancer: A Review Categorized by Target Biological Samples. *Biosensors*, 15(4), 257. <https://doi.org/10.3390/bios15040257>
- Grasso, G., Di Gregorio, A., Mavkov, B., Piga, D., Labate, G. F. D. U., Danani, A., & Deriu, M. A. (2022). Fragmented blind docking: a novel protein–ligand binding prediction protocol. *Journal of Biomolecular Structure and Dynamics*, 40(24), 13472-13481. <https://doi.org/10.1080/07391102.2021.1988709>
- Gu, A., Li, J., Wu, J.-A., Li, M.-Y., & Liu, Y. (2024). Exploration of Dan-Shen-Yin against pancreatic cancer based on network pharmacology combined with molecular docking and experimental validation. *Current Research in Biotechnology*, 7(1), 100228. <https://doi.org/10.1016/j.crbiot.2024.100228>.
- Guo, J., Zhu, X., Badawy, S., Ihsan, A., Liu, Z., Xie, C., & Wang, X. (2021). Metabolism and mechanism of human cytochrome P450 enzyme 1A2. *Current Drug Metabolism*, 22(1), 40-49. <https://doi.org/10.2174/1389200221999210101233135>
- Guo, S.-S., & Wang, Z.-G. (2022). Salvianolic acid B from *Salvia miltiorrhiza bunge*: A potential antitumor agent. *Frontiers in Pharmacology*, 13(1), 1042745. <https://doi.org/10.3389/fphar.2022.1042745>
- Gupta, R., Srivastava, D., Sahu, M., Tiwari, S., Ambasta, R. K., & Kumar, P. (2021). Artificial intelligence to deep learning: machine intelligence approach for drug discovery. *Molecular Diversity*, 25(3), 1315-1360. <https://doi.org/10.1007/s11030-021-10217-3>
- Gusain, P., Uniyal, D., & Joga, R. (2021). Conservation and sustainable use of medicinal plants. In *Preparation of Phytopharmaceuticals for the Management of Disorders* (pp. 409-427). Elsevier. <https://doi.org/10.1016/b978-0-12-820284-5.00026-5>
- Guterres, H., & Im, W. (2020). Improving protein-ligand docking results with high-throughput molecular dynamics simulations. *Journal of Chemical Information and Modeling*, 60(4), 2189-2198. <https://doi.org/10.1021/acs.jcim.0c00057>
- Han, B., Zheng, R., Zeng, H., Wang, S., Sun, K., Chen, R., Li, L., Wei, W., & He, J. (2024). Cancer incidence and mortality in China, 2022. *Journal of the National Cancer Center*, 4(1), 47-53. <https://doi.org/10.1016/j.jncc.2024.01.006>

- Han, S., Oh, J. S., & Lee, J. J. (2022). Diagnostic performance of deep learning models for detecting bone metastasis on whole-body bone scan in prostate cancer. *European Journal of Nuclear Medicine and Molecular Imaging*, 49(2), 585-595. <https://doi.org/10.1007/s00259-021-05481-2>
- Hann, M. M., Leach, A. R., & Harper, G. (2001). Molecular complexity and its impact on the probability of finding leads for drug discovery. *Journal of Chemical Information and Computer Sciences*, 41(3), 856-864. <https://doi.org/10.1021/ci000403i>
- Harper, P. (2023). A review of the dietary intake, bioavailability and health benefits of ellagic acid (EA) with a primary focus on its anti-cancer properties. *Cureus*, 15(8), 1-7. <https://doi.org/10.7759/cureus.43156>
- Hart, K., Foloppe, N., Baker, C. M., Denning, E. J., Nilsson, L., & MacKerell Jr, A. D. (2012). Optimization of the CHARMM additive force field for DNA: Improved treatment of the BI/BII conformational equilibrium. *Journal of Chemical Theory and Computation*, 8(1), 348-362. <https://doi.org/10.1021/ct200723y>
- Hartman, G. D., Lambert-Cheatham, N. A., Kelley, M. R., & Corson, T. W. (2021). Inhibition Of APE1/Ref-1 For Neovascular Eye Diseases: From Biology To Therapy. *International Journal of Molecular Sciences*, 22(19), 10279. <https://doi.org/10.3390/ijms221910279>
- Hasan, A. H., Murugesan, S., Amran, S. I., Chander, S., Alanazi, M. M., Hadda, T. B., Shakya, S., Pratama, M. R. F., Das, B., & Biswas, S. (2022). Novel thiophene Chalcones-Coumarin as acetylcholinesterase inhibitors: Design, synthesis, biological evaluation, molecular docking, ADMET prediction and molecular dynamics simulation. *Bioorganic Chemistry*, 119(1), 105572. <https://doi.org/10.1016/j.bioorg.2021.105572>
- Hasan, M. R., Alsaiani, A. A., Fakhurji, B. Z., Molla, M. H. R., Asseri, A. H., Sumon, M. A. A., Park, M. N., Ahammad, F., & Kim, B. (2022). Application of mathematical modeling and computational tools in the modern drug design and development process. *Molecules*, 27(13), 4169. <https://doi.org/10.3390/molecules27134169>
- Hashemi, M., Tavakolipour, V., Orouei, S., Alimohammadi, M., Asadi, S., Koohpar, Z. K., Jamali, B., Hushmandi, K., Raesi, R., & Entezari, M. (2024). Anatomy and Function of Prostate. In *Prostate Cancer: Molecular Events and Therapeutic Modalities* (pp. 3-21). Springer. <https://doi.org/10.1002/pros.2990040405>

- Hassenberg, C., Clausen, F., Hoffmann, G., Studer, A., & Schürenkamp, J. (2020). Investigation of phase II metabolism of 11-hydroxy- $\Delta$ -9-tetrahydrocannabinol and metabolite verification by chemical synthesis of 11-hydroxy- $\Delta$ -9-tetrahydrocannabinol-glucuronide. *International Journal of Legal Medicine*, 134(6), 2105-2119. <https://doi.org/10.1007/s00414-020-02387-w>
- He, J., Wang, J., Tao, H., Xiao, Y., & Huang, S.-Y. (2019). HNADOCK: a nucleic acid docking server for modeling RNA/DNA–RNA/DNA 3D complex structures. *Nucleic Acids Research*, 47(W1), W35-W42. <https://doi.org/10.1093/nar/gkz412>
- Horne, D. S. (2017). A balanced view of casein interactions. *Current Opinion in Colloid & Interface Science*, 28(1), 74-86. <https://doi.org/10.1016/j.cocis.2017.03.009>
- Hsiao, Y., Su, B.-H., & Tseng, Y. J. (2021). Current development of integrated web servers for preclinical safety and pharmacokinetics assessments in drug development. *Briefings in Bioinformatics*, 22(3), bbaa160. <https://doi.org/10.1093/bib/bbaa160>
- Hu, X., Shrimp, J. H., Guo, H., Xu, M., Chen, C. Z., Zhu, W., Zakharov, A. V., Jain, S., Shinn, P., & Simeonov, A. (2021). Discovery of TMPRSS2 inhibitors from virtual screening as a potential treatment of COVID-19. *ACS Pharmacology & Translational Science*, 4(3), 1124-1135. <https://doi.org/10.1021/acsptsci.0c00221>
- Hu, Y., Zhou, L., Zhu, X., Dai, D., Bao, Y., & Qiu, Y. (2019). Pharmacophore modeling, multiple docking, and molecular dynamics studies on Wee1 kinase inhibitors. *Journal of Biomolecular Structure and Dynamics*, 37(10), 2703-2715. <https://doi.org/10.1080/07391102.2018.1495576>
- Huang, Y., Ouyang, D., & Ji, Y. (2022). The role of hydrogen-bond in solubilizing drugs by ionic liquids: A molecular dynamics and density functional theory study. *American Institute of Chemical Engineers Journal*, 68(6), e17672. <https://doi.org/10.1002/aic.17672>
- Huggins, D. J., Biggin, P. C., Dämgen, M. A., Essex, J. W., Harris, S. A., Henchman, R. H., Khalid, S., Kuzmanic, A., Laughton, C. A., & Michel, J. (2019). Biomolecular simulations: From dynamics and mechanisms to computational assays of biological activity. *Wiley Interdisciplinary Reviews: Computational Molecular Science*, 9(3), e1393. <https://doi.org/10.1002/wcms.1393>

- Huggins, D. J., Sherman, W., & Tidor, B. (2012). Rational approaches to improving selectivity in drug design. *Journal of Medicinal Chemistry*, 55(4), 1424-1444. <https://doi.org/10.1021/jm2010332>
- Hugosson, J., Månsson, M., Wallström, J., Axcróna, U., Carlsson, S. V., Egevad, L., Geterud, K., Khatami, A., Kohestani, K., & Pihl, C.-G. (2022). Prostate cancer screening with PSA and MRI followed by targeted biopsy only. *New England Journal of Medicine*, 387(23), 2126-2137. <https://doi.org/10.1056/NEJMoa2209454>
- Huo, C.-M., Chen, L., Wang, H.-Y., Luo, S.-M., Wang, X., Shi, Y.-F., Zhu, J.-Y., & Xue, W. (2021). Density functional theory-guided drug loading strategy for sensitized tumor-homing thermotherapy. *Chemical Engineering Journal*, 423(1), 130146. <https://doi.org/10.1016/j.cej.2021.130146>
- Hussein, D., Saka, M., Baesa, S., Bangash, M., Alghamdi, F., Al Zughairi, T., AlAjmi, M. F., Haque, S., & Rehman, M. T. (2023). Structure-based virtual screening and molecular docking approaches to identify potential inhibitors against KIF2C to combat glioma. *Journal of Biomolecular Structure and Dynamics*, 42(24), 13816-13829. <https://doi.org/10.1080/07391102.2023.2278750>
- Huynh-Le, M. P., Myklebust, T. Å., Feng, C. H., Karunamuni, R., Johannesen, T. B., Dale, A. M., Andreassen, O. A., & Seibert, T. M. (2020). Age dependence of modern clinical risk groups for localized prostate cancer—A population-based study. *Cancer*, 126(8), 1691-1699. <https://doi.org/10.1002/cncr.32702>
- Hwang, D.-J., He, Y., Ponnusamy, S., Thiagarajan, T., Mohler, M. L., Narayanan, R., & Miller, D. D. (2023). Metabolism-Guided Selective Androgen Receptor Antagonists: Design, Synthesis, and Biological Evaluation for Activity against Enzalutamide-Resistant Prostate Cancer. *Journal of Medicinal Chemistry*, 66(5), 3372-3392. <https://doi.org/10.1021/acs.jmedchem.2c01858>
- Hwang, S., Shin, H. K., Shin, S. E., Seo, M., Jeon, H.-N., Yim, D.-E., Kim, D.-H., & No, K. T. (2020). PreMetabo: An in silico phase I and II drug metabolism prediction platform. *Drug Metabolism and Pharmacokinetics*, 35(4), 361-367. <https://doi.org/10.1016/j.dmpk.2020.05.007>
- Ibrahim, M. T., Tabti, K., Abdulsalam, S., Tahir, A. S., Mahmoud, A., & Danmallam, A. M. (2024). Discovery of new 2, 4-diaminopyrimidines derivatives as EGFR T790M kinase

- inhibitors: a structure-based approach with DFT calculation, drug-likeness, ADME-toxicity properties evaluation and MD simulation. *Journal of Umm Al-Qura University for Applied Sciences*, 10(2), 257-273. <https://doi.org/10.1007/s43994-023-00099-6>
- Ihlamur, M., Akgül, B., Zengin, Y., Korkut, Ş. V., Kelleci, K., & Abamor, E. Ş. (2024). The mTOR Signaling pathway and mTOR Inhibitors in cancer: Next-generation inhibitors and approaches. *Current Molecular Medicine*, 24(4), 478-494. <https://doi.org/10.2174/1566524023666230509161645>
- Ioele, G., Chieffallo, M., Occhiuzzi, M. A., De Luca, M., Garofalo, A., Ragno, G., & Grande, F. (2022). Anticancer drugs: recent strategies to improve stability profile, pharmacokinetic and pharmacodynamic properties. *Molecules*, 27(17), 5436. <https://doi.org/10.3390/molecules27175436>
- Islam, M., Khan, I. M., Shakya, S., & Alam, N. (2023). Design, synthesis, characterizing and DFT calculations of a binary CT complex co-crystal of bioactive moieties in different polar solvents to investigate its pharmacological activity. *Journal of Biomolecular Structure and Dynamics*, 41(20), 10813-10829. <https://doi.org/10.1080/07391102.2022.2158937>
- Jackson, C., Freeman, A. L., Szlamka, Z., & Spiegelhalter, D. J. (2021). The adverse effects of bisphosphonates in breast cancer: A systematic review and network meta-analysis. *PloS One*, 16(2), e0246441. <https://doi.org/10.1007/s43994-023-00099-6>
- Jain, A. N. (2003). Surflex: fully automatic flexible molecular docking using a molecular similarity-based search engine. *Journal of Medicinal Chemistry*, 46(4), 499-511. <https://doi.org/10.1021/jm020406h>
- Jakhar, R., Dangi, M., Khichi, A., & Chhillar, A. K. (2020). Relevance of molecular docking studies in drug designing. *Current Bioinformatics*, 15(4), 270-278. <https://doi.org/10.2174/1574893615666191219094216>
- Jamwal, R., & Barlock, B. J. (2020). Nonalcoholic fatty liver disease (NAFLD) and hepatic cytochrome P450 (CYP) enzymes. *Pharmaceuticals*, 13(9), 222. <https://doi.org/10.3390/ph13090222>
- Jayaraj, J. M., Krishnasamy, G., Lee, J.-K., & Muthusamy, K. (2019). In silico identification and screening of CYP24A1 inhibitors: 3D QSAR pharmacophore mapping and molecular dynamics analysis. *Journal of Biomolecular Structure and Dynamics*, 37(7), 1700-1714. <https://doi.org/10.1080/07391102.2018.1464958>

- Jayashankar, J., Hema, M., Mahmoudi, G., Masoudiasl, A., Dušek, M., Montazerzohori, M., Karthik, C., & Lokanath, N. (2022). N, N'-bis (2-bromobenzylidene)-2, 2'-diaminodiphenyldisulfide (BBDD): Insights of crystal structure, DFT, QTAIM, PASS, ADMET and molecular docking studies. *Journal of Molecular Structure*, 1268(1), 133657. <https://doi.org/10.1016/j.molstruc.2022.133657>
- Jean-Quartier, C., Jeanquartier, F., Jurisica, I., & Holzinger, A. (2018). In silico cancer research towards 3R. *BMC Cancer*, 18(1), 1-12. <https://doi.org/10.1186/s12885-018-4302-0>
- Jedwabny, W., Panecka-Hofman, J., Dyguda-Kazimierowicz, E., Wade, R. C., & Sokalski, W. A. (2017). Application of a simple quantum chemical approach to ligand fragment scoring for Trypanosoma brucei pteridine reductase 1 inhibition. *Journal of Computer-Aided Molecular Design*, 31(8), 715-728. <https://doi.org/10.1007/s10822-017-0035-4>
- Jha, G. G., Anand, V., Soubra, A., & Konety, B. R. (2014). Challenges of managing elderly men with prostate cancer. *Nature Reviews Clinical Oncology*, 11(6), 354-364. <https://doi.org/10.1038/nrclinonc.2014.71>
- Ji, Y., Yang, X., Ji, Z., Zhu, L., Ma, N., Chen, D., Jia, X., Tang, J., & Cao, Y. (2020). DFT-calculated IR spectrum amide I, II, and III band contributions of N-methylacetamide fine components. *ACS omega*, 5(15), 8572-8578. <https://doi.org/10.1021/acsomega.9b04421>
- Jiang, Z., Gao, W., & Huang, L. (2019). Tanshinones, critical pharmacological components in Salvia miltiorrhiza. *Frontiers in Pharmacology*, 10(1), 202. <https://doi.org/10.3389/fphar.2019.00202>
- Jiménez-Luna, J., Grisoni, F., & Schneider, G. (2020). Drug discovery with explainable artificial intelligence. *Nature Machine Intelligence*, 2(10), 573-584. <https://doi.org/10.1038/s42256-020-00236-4>
- Jiménez-Luna, J., Grisoni, F., Weskamp, N., & Schneider, G. (2021). Artificial intelligence in drug discovery: recent advances and future perspectives. *Expert Opinion on Drug Discovery*, 16(9), 949-959. <https://doi.org/10.1080/17460441.2021.1909567>
- Jin, Z., Du, X., Xu, Y., Deng, Y., Liu, M., Zhao, Y., Zhang, B., Li, X., Zhang, L., & Peng, C. (2020). Structure of Mpro from SARS-CoV-2 and discovery of its inhibitors. *Nature*, 582(7811), 289-293. <https://doi.org/10.1038/s41586-020-2223-y>

- Jones, G., Willett, P., Glen, R. C., Leach, A. R., & Taylor, R. (1997). Development and validation of a genetic algorithm for flexible docking. *Journal of Molecular Biology*, 267(3), 727-748. <https://doi.org/10.1006/jmbi.1996.0897>
- Justiz-Vaillant, A., Pandit, B. R., Unakal, C., Vuma, S., & Akpaka, P. E. (2025). A comprehensive review about the use of monoclonal antibodies in cancer therapy. *Antibodies*, 14(2), 35. <https://doi.org/10.3390/antib14020035>
- Kalimeri, M., Derreumaux, P., & Sterpone, F. (2015). Are coarse-grained models apt to detect protein thermal stability? The case of OPEP force field. *Journal of Non-Crystalline Solids*, 407(1), 494-501. . <https://doi.org/10.1016/j.jnoncrysol.2014.07.005>
- Kanagasabai, T., Hawaz, M., Ellis, K., Fah, O., Mikhaeil, H., Nguyen, P., Tombo, N., Shanker, A., Sampath, C., & Khoury, Z. H. (2024). Effects of Topoisomerase II alpha Inhibition on Oral Cancer Cell Metabolism and Cancer Stem Cell Function. *Dental Research and Oral Health*, 7(2), 58. <https://doi.org/10.26502/droh.0076>
- Kang, J., & Tateno, M. (2012). Recent applications of hybrid Ab initio quantum mechanics–molecular mechanics simulations to biological macromolecules. In *Some Applications of Quantum Mechanics* (pp. 359-375). IntechOpen. <https://doi.org/10.5772/35092>
- Kanthe, P. S., Patil, B. S., Das, K. K., & Parvatikar, P. P. (2021). Structural analysis and prediction of potent bioactive molecule for eNOS protein through molecular docking. *In Silico Pharmacology*, 9(1), 1-10. <https://doi.org/10.1007/s40203-021-00106-w>
- Kar, R. K. (2023). Benefits of hybrid QM/MM over traditional classical mechanics in pharmaceutical systems. *Drug Discovery Today*, 28(1), 103374. <https://doi.org/10.1016/j.drudis.2022.103374>
- Karakuş, N. (2024). Theoretical Investigations on Phytochemicals: Physical Chemistry, FMO, MEP, Lipophilicity, Water Solubility, Drug-likeness, and Bioavailability. *Cumhuriyet Science Journal*, 45(2), 282-290. <https://doi.org/10.17776/csj.1403956>
- Kashefolgheta, S., Wang, S., Acree, W. E., & Hünenberger, P. H. (2021). Evaluation of nine condensed-phase force fields of the GROMOS, CHARMM, OPLS, AMBER, and OpenFF families against experimental cross-solvation free energies. *Physical Chemistry Chemical Physics*, 23(23), 13055-13074. <https://doi.org/10.1039/d1cp00215e>

- Kashkooli, F. M., Soltani, M., Souri, M., Meaney, C., & Kohandel, M. (2021). Nexus between in silico and in vivo models to enhance clinical translation of nanomedicine. *Nano Today*, 36(1), 101057. <https://doi.org/10.1016/j.nantod.2020.101057>
- Kaya, E. D., Türkhan, A., Gür, F., & Gür, B. (2022). A novel method for explaining the product inhibition mechanisms via molecular docking: inhibition studies for tyrosinase from *Agaricus bisporus*. *Journal of Biomolecular Structure and Dynamics*, 40(17), 7926-7939. <https://doi.org/10.1080/07391102.2021.1905069>
- Kazanietz, M. G. (2005). Targeting protein kinase C and “non-kinase” phorbol ester receptors: emerging concepts and therapeutic implications. *Biochimica et Biophysica Acta (BBA)- Proteins and Proteomics*, 1754(1-2), 296-304. <https://doi.org/10.1016/j.bbapap.2005.07.034>
- Kent, P. R., Annaberdiyev, A., Benali, A., Bennett, M. C., Landinez Borda, E. J., Doak, P., Hao, H., Jordan, K. D., Krogel, J. T., & Kylänpää, I. (2020). QMCPACK: Advances in the development, efficiency, and application of auxiliary field and real-space variational and diffusion quantum Monte Carlo. *The Journal of Chemical Physics*, 152(17), 174105. <https://doi.org/10.1063/5.0004860>
- Kgatle, M. M., Boshomane, T. M., Lawal, I. O., Mokoala, K. M., Mokgoro, N. P., Lourens, N., Kairemo, K., Zeevaart, J. R., Vorster, M., & Sathekge, M. M. (2021). Immune checkpoints, inhibitors and radionuclides in prostate cancer: Promising combinatorial therapy approach. *International Journal of Molecular Sciences*, 22(8), 4109. <https://doi.org/10.3390/ijms22084109>
- Khairi, S., Aini, N., Siswanto, L. M. H., & Chung, M.-H. (2025). Predicting breast cancer risk and its association to biopsychosocial factors among Taiwanese women with a family history of breast cancer: an investigation based on the Gail model. *BMC Medical Genomics*, 18(1), 1-11. <https://doi.org/10.1186/s12920-025-02149-w>
- Khan, M. F., Ali, A., Rehman, H. M., Noor Khan, S., Hammad, H. M., Waseem, M., Wu, Y., Clark, T. G., & Jabbar, A. (2024). Exploring optimal drug targets through subtractive proteomics analysis and pangenomic insights for tailored drug design in tuberculosis. *Scientific Reports*, 14(1), 10904. <https://doi.org/10.1038/s41598-024-61752-6>
- Khan, T., Dixit, S., Ahmad, R., Raza, S., Azad, I., Joshi, S., & Khan, A. R. (2017). Molecular docking, PASS analysis, bioactivity score prediction, synthesis, characterization and

- biological activity evaluation of a functionalized 2-butanone thiosemicarbazone ligand and its complexes. *Journal of Chemical Biology*, 10(3), 91-104. <https://doi.org/10.1007/s12154-017-0167-y>
- Khandelwal, A., Lukacova, V., Comez, D., Kroll, D. M., Raha, S., & Balaz, S. (2005). A combination of docking, QM/MM methods, and MD simulation for binding affinity estimation of metalloprotein ligands. *Journal of Medicinal Chemistry*, 48(17), 5437-5447. <https://doi.org/10.1021/jm049050v>
- Kiewisch, K., Jacob, C. R., & Visscher, L. (2013). Quantum-chemical electron densities of proteins and of selected protein sites from subsystem density functional theory. *Journal of Chemical Theory and Computation*, 9(5), 2425-2440. <https://doi.org/10.1021/ct3008759>
- Kim, H., Lee, S. B., Nam, S., Lee, E. S., Park, B., Park, H. Y., Lee, H. J., Kim, J., Chung, Y., Kim, H. J., Ko, B. S., Lee, J. W., Son, B. H., & Ahn, S. H. (2021). Survival of breast-conserving surgery plus radiotherapy versus total mastectomy in early breast cancer. *Annals of Surgical Oncology*, 28(9), 5039-5047. <https://doi.org/10.1245/s10434-021-09591-x>
- King, E., Aitchison, E., Li, H., & Luo, R. (2021). Recent developments in free energy calculations for drug discovery. *Frontiers in Molecular Biosciences*, 8(1), 712085. <https://doi.org/10.3389/fmolb.2021.712085>
- Kirschner, K. N., Yongye, A. B., Tschampel, S. M., González-Outeiriño, J., Daniels, C. R., Foley, B. L., & Woods, R. J. (2008). GLYCAM06: a generalizable biomolecular force field. Carbohydrates. *Journal of Computational Chemistry*, 29(4), 622-655. <https://doi.org/10.1002/jcc.20820>
- Klibaim, S., Thumrongsiri, N., Watcharadulyarat, N., Chonniyom, W., Tanyapanyachon, P., Dana, P., & Saengkrit, N. (2025). Enhancing in Vitro anti-metastatic efficacy and deep penetration into tumor spheroid of docetaxel-loaded liposomes via size optimization for prostate cancer treatment. *OpenNano*, 22(1), 100231. <https://doi.org/10.1016/j.onano.2024.100231>
- Klipp, E., Wade, R. C., & Kummer, U. (2010). Biochemical network-based drug-target prediction. *Current Opinion in Biotechnology*, 21(4), 511-516. <https://doi.org/10.1016/j.copbio.2010.05.004>

- Knezevic, C. E., & Clarke, W. (2020). Cancer chemotherapy: The case for therapeutic drug monitoring. *Therapeutic Drug Monitoring*, 42(1), 6-19. <https://doi.org/10.1097/ftd.0000000000000701>
- Kommalapati, H. S., Pilli, P., Golla, V. M., Bhatt, N., & Samanthula, G. (2023). In Silico Tools to Thaw the Complexity of the Data: Revolutionizing Drug Research in Drug Metabolism, Pharmacokinetics and Toxicity Prediction. *Current Drug Metabolism*, 24(11), 735-755. <https://doi.org/10.2174/0113892002270798231201111422>
- Komura, H., Watanabe, R., & Mizuguchi, K. (2023). The Trends and Future Prospective of In Silico Models from the Viewpoint of ADME Evaluation in Drug Discovery. *Pharmaceutics*, 15(11), 2619. <https://doi.org/10.3390/pharmaceutics15112619>
- Kondaka, K., & Gabriel, I. (2022). Targeting DNA topoisomerase II in antifungal chemotherapy. *Molecules*, 27(22), 7768. <https://doi.org/10.3390/molecules27227768>
- Kony, D., Damm, W., Stoll, S., & Van Gunsteren, W. F. (2002). An improved OPLS-AA force field for carbohydrates. *Journal of Computational Chemistry*, 23(15), 1416-1429. <https://doi.org/10.1002/jcc.10139>
- Korshunova, M., Ginsburg, B., Tropsha, A., & Isayev, O. (2021). OpenChem: a deep learning toolkit for computational chemistry and drug design. *Journal of Chemical Information and Modeling*, 61(1), 7-13. <https://doi.org/10.1021/acs.jcim.0c00971>
- Kramlinger, V. M., Dalvie, D., Heck, C. J., Kalgutkar, A. S., O'Neill, J., Su, D., Teitelbaum, A. M., & Totah, R. A. (2022). Future of biotransformation science in the pharmaceutical industry. *Drug Metabolism and Disposition*, 50(3), 258-267. <https://doi.org/10.1124/dmd.121.000658>
- Kraujalis, V., Ruzgas, T., & Milonas, D. (2022). Mortality rate estimation models for patients with prostate cancer diagnosis. *Baltic Journal of Modern Computing.*, 10(2), 170-184. <https://doi.org/10.22364/bjmc.2022.10.2.06>
- Krishna, M. V., Padmalatha, K., & Madhavi, G. (2021). In vitro metabolic stability of drugs and applications of LC-MS in metabolite profiling. *Drug Metabolism*, 1(1), 77. <https://doi.org/10.5772/intechopen.99762>
- Kulkarni, P. U., Shah, H., & Vyas, V. K. (2022). Hybrid Quantum Mechanics/Molecular Mechanics (QM/MM) Simulation: A Tool for Structure-Based Drug Design and

- Discovery. *Mini Reviews in Medicinal Chemistry*, 22(8), 1096-1107. <https://doi.org/10.2174/1389557521666211007115250>
- Kumar, A., Kumar, S., Komal, Ramchiary, N., & Singh, P. (2021). Role of traditional ethnobotanical knowledge and indigenous communities in achieving sustainable development goals. *Sustainability*, 13(6), 3062. <https://doi.org/10.3390/su13063062>
- Kumar, R., Kumar, S., Sangwan, S., Yadav, I. S., & Yadav, R. (2011). Protein modeling and active site binding mode interactions of myrosinase–sinigrin in *Brassica juncea*—An in silico approach. *Journal of Molecular Graphics and Modelling*, 29(5), 740-746. <https://doi.org/10.1016/j.jmgm.2010.12.004>
- Kumar, S., & Kumar, S. (2019). Molecular docking: a structure-based approach for drug repurposing. *In Silico Drug Design* (pp. 161-189). Elsevier. <https://doi.org/10.1016/b978-0-12-816125-8.00006-7>
- Kumar, S., & Kumar, Y. (2024). Innovations in Molecular Docking: A Detailed Analysis of Methodological Developments and Their Applications in Drug Discovery. *International Journal of Pharma Professional's Research (IJPPR)*, 15(3), 52-67. <https://doi.org/10.69580/ijppr.15.3.2024.52-67>
- Kumar, S., Rao, N. S., Reddy, K. P., Padole, M. C., & Deshpande, P. A. (2023). Enzyme–substrate interactions in orotate-mimetic OPRT inhibitor complexes: a QM/MM analysis. *Physical Chemistry Chemical Physics*, 25(4), 3472-3484. <https://doi.org/10.1039/d2cp05406j>
- Kumari, I., Sandhu, P., Ahmed, M., & Akhter, Y. (2017). Molecular dynamics simulations, challenges and opportunities: a Biologist's prospective. *Current Protein and Peptide Science*, 18(11), 1163-1179. <https://doi.org/10.2174/1389203718666170622074741>
- Lai, H.-C., Cheng, J.-C., Yip, H.-T., Jeng, L.-B., & Huang, S.-T. (2024). Chinese herbal medicine decreases incidence of hepatocellular carcinoma in diabetes mellitus patients with regular insulin management. *World Journal of Gastrointestinal Oncology*, 16(3), 716. <https://doi.org/10.4251/wjgo.v16.i3.716>
- Le Du, F., Dièras, V., & Curigliano, G. (2021). The role of tyrosine kinase inhibitors in the treatment of HER2+ metastatic breast cancer. *European Journal of Cancer*, 154(1), 175-189 <https://doi.org/10.1016/j.ejca.2021.06.026>.

- Le, T. T., Wu, M., Lee, J. H., Bhatt, N., Inman, J. T., Berger, J. M., & Wang, M. D. (2023). Etoposide promotes DNA loop trapping and barrier formation by topoisomerase II. *Nature Chemical Biology*, *19*(5), 641-650. <https://doi.org/10.1038/s41589-022-01235-9>
- Lee, D., & Lee, G. (2025). Single-molecule studies of repair proteins in base excision repair. *BMB Reports*, *58*(1), 17-23. <https://doi.org/10.5483/bmbrep.2024-0178>
- Leng, P., Wang, Y., & Xie, M. (2025). Ellagic acid and gut microbiota: interactions, and implications for health. *Food Science & Nutrition*, *13*(4), e70133. <https://doi.org/10.1002/fsn3.70133>
- Leonard, A. N., Wang, E., Monje-Galvan, V., & Klauda, J. B. (2019). Developing and testing of lipid force fields with applications to modeling cellular membranes. *Chemical Reviews*, *119*(9), 6227-6269. <https://doi.org/10.1021/acs.chemrev.8b00384>
- Li, D., Zhang, W., Zhu, J., Chang, P., Sahin, A., Singletary, E., Bondy, M., Hazra, T., Mitra, S., & Lau, S. S. (2001). Oxidative DNA damage and 8-hydroxy-2-deoxyguanosine DNA glycosylase/apurinic lyase in human breast cancer. *Molecular Carcinogenesis: Published in cooperation with the University of Texas MD Anderson Cancer Center*, *31*(4), 214-223. <https://doi.org/10.1002/mc.1056>
- Li, H., Prever, L., Hirsch, E., & Gulluni, F. (2021). Targeting PI3K/AKT/mTOR signaling pathway in breast cancer. *Cancers*, *13*(14), 3517. <https://doi.org/10.3390/cancers13143517>
- Li, L., Zhang, D., Wu, Y., Wang, J., & Ma, F. (2023). Efficacy and safety of trastuzumab with or without a tyrosine kinase inhibitor for HER2-positive breast cancer: A systematic review and meta-analysis. *Biochimica et Biophysica Acta (BBA)-Reviews on Cancer*, *1878*(6), 188969. <https://doi.org/10.1016/j.bbcan.2023.188969>
- Li, S.-l., Zha, M.-y., Wang, Q., & Tang, Y. (2024). Advances in multiparametric magnetic resonance imaging combined with biomarkers for the diagnosis of high-grade prostate cancer. *Frontiers in Surgery*, *11*(1), 1429831. <https://doi.org/10.3389/fsurg.2024.1429831>
- Liang, Q., Liu, X., Xu, X., Chen, Z., Luo, T., Su, Y., Xie, H., Gao, H., & Xie, C. (2025). Anti-atherosclerotic effects and molecular targets of salvianolic acids from *Salvia miltiorrhiza* Bunge. *Frontiers in Pharmacology*, *16*(1), 1574086. <https://doi.org/10.3389/fphar.2025.1574086>
- Lin, X., Li, X., & Lin, X. (2020). A review on applications of computational methods in drug screening and design. *Molecules*, *25*(6), 1375. <https://doi.org/10.3390/molecules25061375>

- Litsa, E. E., Das, P., & Kaviraki, L. E. (2021). Machine learning models in the prediction of drug metabolism: Challenges and future perspectives. *Expert Opinion on Drug Metabolism & Toxicology*, 17(11), 1245-1247. <https://doi.org/10.1080/17425255.2021.1998454>
- Liu, C., Wu, K., Li, J., Mu, X., Gao, H., & Xu, X. (2023). Nanoparticle-mediated therapeutic management in cholangiocarcinoma drug targeting: Current progress and future prospects. *Biomedicine and Pharmacotherapy*, 158(1), 114135. <https://doi.org/10.1016/j.biopha.2022.114135>
- Liwo, A., Oldziej, S., Pincus, M. R., Wawak, R. J., Rackovsky, S., & Scheraga, H. A. (1997). A united-residue force field for off-lattice protein-structure simulations. I. Functional forms and parameters of long-range side-chain interaction potentials from protein crystal data. *Journal of Computational Chemistry*, 18(7), 849-873. [https://doi.org/10.1002/\(sici\)1096-987x\(199705\)18:7<849::aid-jcc1>3.0.co;2-r](https://doi.org/10.1002/(sici)1096-987x(199705)18:7<849::aid-jcc1>3.0.co;2-r)
- Logsdon, D. P., Shah, F., Carta, F., Supuran, C. T., Kamocka, M., Jacobsen, M. H., Sandusky, G. E., Kelley, M. R., & Fishel, M. L. (2018). Blocking HIF signaling via novel inhibitors of CA9 and APE1/Ref-1 dramatically affects pancreatic cancer cell survival. *Scientific Reports*, 8(1), 13759. <https://doi.org/10.1038/s41598-018-32034-9>
- Lu, J.-L., Zeng, X.-S., Zhou, X., Yang, J.-L., Ren, L.-L., Long, X.-Y., Wang, F.-Q., Olaleye, O. E., Tian, N.-N., & Zhu, Y.-X. (2022). Molecular basis underlying hepatobiliary and renal excretion of phenolic acids of *Salvia miltiorrhiza* roots (danshen). *Frontiers in Pharmacology*, 13(1), 911982. <https://doi.org/10.3389/fphar.2022.911982>
- Luengo, D., Martino, L., Bugallo, M., Elvira, V., & Särkkä, S. (2020). A survey of Monte Carlo methods for parameter estimation. *EURASIP Journal on Advances in Signal Processing*, 2020(1), 1-62. <https://doi.org/10.1186/s13634-020-00675-6>
- Luo, J., Wei, W., Waldispühl, J., & Moitessier, N. (2019). Challenges and current status of computational methods for docking small molecules to nucleic acids. *European Journal of Medicinal Chemistry*, 168(1), 414-425. <https://doi.org/10.1016/j.ejmech.2019.02.046>
- Lynch, S. M., Handorf, E., Sorice, K. A., Blackman, E., Bealin, L., Giri, V. N., Obeid, E., Ragin, C., & Daly, M. (2020). The effect of neighborhood social environment on prostate cancer development in black and white men at high risk for prostate cancer. *PloS One*, 15(8), e0237332. <https://doi.org/10.1371/journal.pone.0237332>

- Ma, C., Peng, Y., Li, H., & Chen, W. (2021). Organ-on-a-chip: a new paradigm for drug development. *Trends in Pharmacological Sciences*, 42(2), 119-133. <https://doi.org/10.1016/j.tips.2020.11.009>
- Ma, M., Song, J., Dong, Y., Fang, W., & Gao, L. (2023). Structural and thermodynamic properties of bulk triglycerides and triglyceride/water mixtures reproduced using a polarizable coarse-grained model. *Physical Chemistry Chemical Physics*, 25(33), 22232-22243. <https://doi.org/10.1039/d3cp01839c>
- Ma, X., Cheng, Z., & Guo, C. (2025). Insights into the DNA damage response and tumor drug resistance. *Cancer Biology & Medicine*, 22(3), 197-204. <https://doi.org/10.20892/j.issn.2095-3941.2025.0020>
- Maciejewski, A., Pasenkiewicz-Gierula, M., Cramariuc, O., Vattulainen, I., & Rog, T. (2014). Refined OPLS all-atom force field for saturated phosphatidylcholine bilayers at full hydration. *The Journal of Physical Chemistry B*, 118(17), 4571-4581. <https://doi.org/10.1021/jp5016627>
- Magalhães, R. P., Fernandes, H. S., & Sousa, S. F. (2020). Modelling enzymatic mechanisms with QM/MM approaches: current status and future challenges. *Israel Journal of Chemistry*, 60(7), 655-666. <https://doi.org/10.1002/ijch.202000014>
- Magee, P., Shi, L., & Garofalo, M. (2015). Role of microRNAs in chemoresistance. *Annals of Translational Medicine*, 3(21), 332. <https://doi.org/10.3978/j.issn.2305-5839.2015.11.32>
- Majid, M., Farhan, A., Asad, M. I., Khan, M. R., Hassan, S. S. U., Haq, I.-u., & Bungau, S. (2022). An Extensive Pharmacological Evaluation of New Anti-Cancer Triterpenoid (Nummularic Acid) from *Ipomoea batatas* through In Vitro, In Silico, and In Vivo Studies. *Molecules*, 27(8), 2474. <https://doi.org/10.3390/molecules27082474>
- Malfatti, M. C., Bellina, A., Antoniali, G., & Tell, G. (2023). Revisiting two decades of research focused on targeting APE1 for cancer therapy: the pros and cons. *Cells*, 12(14), 1895. <https://doi.org/10.3390/cells12141895>
- Malki, M. A., & Pearson, E. R. (2020). Drug–drug–gene interactions and adverse drug reactions. *The Pharmacogenomics Journal*, 20(3), 355-366. <https://doi.org/10.1038/s41397-019-0122-0>
- Malone, F. D., Benali, A., Morales, M. A., Caffarel, M., Kent, P. R., & Shulenburger, L. (2020). Systematic comparison and cross-validation of fixed-node diffusion Monte Carlo and

- phaseless auxiliary-field quantum Monte Carlo in solids. *Physical Review B*, 102(16), 161104. <https://doi.org/10.1103/physrevb.102.161104>
- Marey, A., Arjmand, P., Alerab, A. D. S., Eslami, M. J., Saad, A. M., Sanchez, N., & Umair, M. (2024). Explainability, transparency and black box challenges of AI in radiology: impact on patient care in cardiovascular radiology. *Egyptian Journal of Radiology and Nuclear Medicine*, 55(1), 1-14. <https://doi.org/10.1186/s43055-024-01356-2>
- Martín-Encinas, E., Selas, A., Palacios, F., & Alonso, C. (2022). The design and discovery of topoisomerase I inhibitors as anticancer therapies. *Expert Opinion on Drug Discovery*, 17(6), 581-601. <https://doi.org/10.1080/17460441.2022.2055545>
- Marzuoli, I., Margreitter, C., & Fraternali, F. (2019). Lipid head group parameterization for GROMOS 54A8: a consistent approach with protein force field description. *Journal of Chemical Theory and Computation*, 15(10), 5175-5193. <https://doi.org/10.1021/acs.jctc.9b00509>
- Mathur, N., Chandragiri, S. S., Shandily, S., Santoki, K. M., Vadhavana, N. N., Shah, S., & Chandra, M. (2024). In silico docking: Protocols for computational exploration of Molecular Interactions. *Unravelling Molecular Docking-From Theory to Practice*. IntechOpen. <https://doi.org/10.5772/intechopen.1005527>
- Matias-Barrios, V. M., Radaeva, M., Ho, C.-H., Lee, J., Adomat, H., Lallous, N., Cherkasov, A., & Dong, X. (2021). Optimization of new catalytic topoisomerase II inhibitors as an anti-cancer therapy. *Cancers*, 13(15), 3675. <https://doi.org/10.3390/cancers13153675>
- Maurya, P., Rawat, R. S., Gupta, S., Krishna, S., Siddiqi, M. I., Sashidhara, K. V., & Banerjee, D. (2025). Synergy between human DNA ligase I and topoisomerase 1 unveils new therapeutic strategy for the management of colorectal cancer. *Journal of Biomolecular Structure and Dynamics*, 43(7), 3390-3405. <https://doi.org/10.1080/07391102.2023.2297817>
- McGann, M. R., Almond, H. R., Nicholls, A., Grant, J. A., & Brown, F. K. (2003). Gaussian docking functions. *Biopolymers: Original Research on Biomolecules*, 68(1), 76-90. <https://doi.org/10.1002/bip.10207>
- Meanwell, N. A. (2016). Improving drug design: an update on recent applications of efficiency metrics, strategies for replacing problematic elements, and compounds in nontraditional

- drug space. *Chemical Research in Toxicology*, 29(4), 564-616. <https://doi.org/10.1021/acs.chemrestox.6b00043>
- Meiler, J., & Baker, D. (2006). ROSETTALIGAND: Protein–small molecule docking with full side-chain flexibility. *Proteins: Structure, Function, and Bioinformatics*, 65(3), 538-548. <https://doi.org/10.1002/prot.21086>
- Mendiratta, G., Ke, E., Aziz, M., Liarakos, D., Tong, M., & Stites, E. C. (2021). Cancer gene mutation frequencies for the US population. *Nature Communications*, 12(1), 5961. <https://doi.org/10.1038/s41467-021-26213-y>
- Merseburger, A. S., Krabbe, L.-M., Krause, B. J., Böhmer, D., Perner, S., & von Amsberg, G. (2022). The treatment of metastatic, hormone-sensitive prostatic carcinoma. *Deutsches Ärzteblatt International*, 119(37), 622. <https://doi.org/10.3238/arztebl.m2022.0294>
- Mijit, M., Caston, R., Gampala, S., Fishel, M. L., Fehrenbacher, J., & Kelley, M. R. (2021). APE1/Ref-1—one target with multiple indications: emerging aspects and new directions. *Journal of Cellular Signaling*, 2(3), 151. <https://doi.org/10.33696/signaling.2.047>
- Miller, M. D., Kearsley, S. K., Underwood, D. J., & Sheridan, R. P. (1994). FLOG: a system to select ‘quasi-flexible’ligands complementary to a receptor of known three-dimensional structure. *Journal of Computer-Aided Molecular Design*, 8(2), 153-174. <https://doi.org/10.1007/bf00119865>
- Minami, H., Kiyota, N., Kimbara, S., Ando, Y., Shimokata, T., Ohtsu, A., Fuse, N., Kuboki, Y., Shimizu, T., & Yamamoto, N. (2021). Guidelines for clinical evaluation of anti-cancer drugs. *Cancer Science*, 112(7), 2563-2577. <https://doi.org/10.1111/cas.14967>
- Mir, M. A., & Mir, A. Y. (2023). Current Treatment Approaches to Breast Cancer. *Therapeutic potential of Cell Cycle Kinases in Breast Cancer* (pp. 23-51). Springer. <https://doi.org/10.1007/978-981-19-8911-7>
- Mohammad, T., Mathur, Y., & Hassan, M. I. (2021). InstaDock: A single-click graphical user interface for molecular docking-based virtual high-throughput screening. *Briefings in Bioinformatics*, 22(4), bbaa279. <https://doi.org/10.1093/bib/bbaa279>
- Moinul, M., Khatun, S., Amin, S. A., Jha, T., & Gayen, S. (2022). Recent trends in fragment-based anticancer drug design strategies against different targets: A mini-review. *Biochemical Pharmacology*, 26(1), 115301. <https://doi.org/10.1016/j.bcp.2022.115301>

- Mollaamin, F., & Monajjemi, M. (2023). Application of DFT/TD-DFT Frameworks in the Drug Delivery Mechanism: Investigation of Chelated Bisphosphonate with Transition Metal Cations in Bone Treatment. *Chemistry*, 5(1), 365-380. <https://doi.org/10.3390/chemistry5010027>
- Moraes, D. F. C., de Mesquita, L. S. S., do Amaral, F. M. M., de Sousa Ribeiro, M. N., & Malik, S. (2017). Anticancer drugs from plants. *Biotechnology and Production of Anti-Cancer Compounds*, 1(1), 121-142. [https://doi.org/10.1007/978-3-319-53880-8\\_5](https://doi.org/10.1007/978-3-319-53880-8_5)
- Moris, L., Cumberbatch, M. G., Van den Broeck, T., Gandaglia, G., Fossati, N., Kelly, B., Pal, R., Briers, E., Cornford, P., & De Santis, M. (2020). Benefits and risks of primary treatments for high-risk localized and locally advanced prostate cancer: an international multidisciplinary systematic review. *European Urology*, 77(5), 614-627. <https://doi.org/10.1016/j.eururo.2020.01.033>
- Morris, G. M., Goodsell, D. S., Halliday, R. S., Huey, R., Hart, W. E., Belew, R. K., & Olson, A. J. (1998). Automated docking using a Lamarckian genetic algorithm and an empirical binding free energy function. *Journal of Computational Chemistry*, 19(14), 1639-1662. [https://doi.org/10.1002/\(sici\)1096-987x\(19981115\)19:14<1639::aid-jcc10>3.0.co;2-b](https://doi.org/10.1002/(sici)1096-987x(19981115)19:14<1639::aid-jcc10>3.0.co;2-b)
- Morris, M. J., De Bono, J. S., Chi, K. N., Fizazi, K., Herrmann, K., Rahbar, K., Tagawa, S. T., Nordquist, L. T., Vaishampayan, N., El-Haddad, G., Park, C. H., Beer, T. M., Pérez-Contreras, W. J., Desilvio, M., Kpamegan, E. E., Gericke, G., Messmann, R. A., Krause, B. J., & Sartor, A. O. (2021). Phase III study of lutetium-177-PSMA-617 in patients with metastatic castration-resistant prostate cancer (VISION). *Journal of Clinical Oncology*, 39(18\_suppl), LBA4-LBA4. [https://doi.org/10.1200/jco.2021.39.15\\_suppl.lba4](https://doi.org/10.1200/jco.2021.39.15_suppl.lba4)
- Muhammad Rehman, H., Rehman, H. M., Naveed, M., Khan, M. T., Shabbir, M. A., Aslam, S., & Bashir, H. (2023). In Silico investigation of a chimeric IL24-LK6 fusion protein as a potent candidate against breast cancer. *Bioinformatics and Biology Insights*, 17(1), 11779322231182560. <https://doi.org/10.1177/11779322231182560>
- Muhammed, M. T., & Aki-Yalcin, E. (2024). Molecular docking: principles, advances, and its applications in drug discovery. *Letters in Drug Design & Discovery*, 21(3), 480-495. <https://doi.org/10.2174/1570180819666220922103109>

- Mukherjee, P., Roy, S., Ghosh, D., & Nandi, S. (2022). Role of animal models in biomedical research: a review. *Laboratory Animal Research*, 38(1), 18. <https://doi.org/10.1186/s42826-022-00128-1>
- Mullins, M. R. (2010). How Yasukuni Shrine Survived the Occupation: A Critical Examination of Popular Claims. *Monumenta Nipponica*, 65(1), 89-136. <https://doi.org/10.1353/mni.0.0109>
- Murphy, A., Cottrell-Daniels, C. C., Awasthi, S., Katende, E., Park, J. Y., Denis, J., Green, B. L., & Yamoah, K. (2024). Understanding and Addressing Prostate Cancer Disparities in Diagnosis, Treatment, and Outcomes Among Black Men. *Cancer Control*, 31(1), 10732748241275389. <https://doi.org/10.1177/10732748241275389>
- Nada, H., Choi, Y., Kim, S., Jeong, K. S., Meanwell, N. A., & Lee, K. (2024). New insights into protein–protein interaction modulators in drug discovery and therapeutic advance. *Signal Transduction and Targeted Therapy*, 9(1), 1-32. <https://doi.org/10.1038/s41392-024-02036-3>
- Nassar, A. F. (2022). Chemical Structural Alert and Reactive Metabolite Concept as Applied in Medicinal Chemistry to Minimize the Toxicity of Drug Candidates. *Drug Metabolism Handbook: Concepts and Applications in Cancer Research*, 1(1), 345-372. <https://doi.org/10.1002/9781119851042.ch11>
- Nedungadi, P., Salethoor, S. N., Puthiyedath, R., Nair, V. K., Kessler, C., & Raman, R. (2023). Ayurveda research: Emerging trends and mapping to sustainable development goals. *Journal of Ayurveda and Integrative Medicine*, 14(6), 100809. <https://doi.org/10.1016/j.jaim.2023.100809>
- Nguyen, T.-T.-L., Duong, V.-A., Vo, D.-K., Jo, J., & Maeng, H.-J. (2021). Development and validation of a bioanalytical LC-MS/MS method for simultaneous determination of sirolimus in porcine whole blood and lung tissue and pharmacokinetic application with coronary stents. *Molecules*, 26(2), 425. <https://doi.org/10.3390/molecules26020425>
- Nian, B., Xu, Y.-J., & Liu, Y. (2021). Molecular dynamics simulation for mechanism revelation of the safety and nutrition of lipids and derivatives in food: State of the art. *Food Research International*, 145(1), 110399. <https://doi.org/10.1016/j.foodres.2021.110399>
- Niazi, S. K., & Mariam, Z. (2023). Computer-aided drug design and drug discovery: a prospective analysis. *Pharmaceuticals*, 17(1), 22. <https://doi.org/10.3390/ph17010022>

- Nithin, C., Ghosh, P., & Bujnicki, J. M. (2018). Bioinformatics tools and benchmarks for computational docking and 3D structure prediction of RNA-protein complexes. *Genes*, 9(9), 432. <https://doi.org/10.3390/genes9090432>
- Niu, Y., & Lin, P. (2023). Advances of computer-aided drug design (CADD) in the development of anti-Azheimer's-disease drugs. *Drug Discovery Today*, 28(8), 103665. <https://doi.org/10.1016/j.drudis.2023.103665>
- Noor, F., Tahir ul Qamar, M., Ashfaq, U. A., Albutti, A., Alwashmi, A. S., & Aljasir, M. A. (2022). Network pharmacology approach for medicinal plants: Review and assessment. *Pharmaceuticals*, 15(5), 572. <https://doi.org/10.3390/ph15050572>
- Noureddine, O., Gatfaoui, S., Brandan, S. A., Sagaama, A., Marouani, H., & Issaoui, N. (2020). Experimental and DFT studies on the molecular structure, spectroscopic properties, and molecular docking of 4-phenylpiperazine-1-ium dihydrogen phosphate. *Journal of Molecular Structure*, 1207(1), 127762. <https://doi.org/10.1016/j.molstruc.2020.127762>
- Nussinov, R., Tsai, C.-J., & Jang, H. (2021). Anticancer drug resistance: An update and perspective. *Drug Resistance Updates*, 59(1), 100796. <https://doi.org/10.1016/j.drup.2021.100796>
- Okpo, E., Agboke, A., Udobi, C., John, G., & Andy, I. (2024). The Synergy of Molecular Docking and Bioinformatics: An in Depth Review in Drug Discovery. *Biotechnology Journal International*, 28(4), 119-136. <https://doi.org/10.9734/bji/2024/v28i4732>
- Omer, A., Suryanarayanan, V., Selvaraj, C., Singh, S. K., & Singh, P. (2015). Explicit drug re-positioning: Predicting novel drug-target interactions of the shelved molecules with qm/mm based approaches. *Advances in Protein Chemistry and Structural Biology*, 100(1), 89-112. <https://doi.org/10.1016/bs.apcsb.2015.07.001>
- Ononamadu, C. J., & Seidel, V. (2024). Exploring the antidiabetic potential of *Salvia officinalis* using network pharmacology, molecular docking and ADME/drug-likeness predictions. *Plants*, 13(20), 2892. <https://doi.org/10.3390/plants13202892>
- Oostenbrink, C., Soares, T. A., Van Der Vegt, N. F., & Van Gunsteren, W. F. (2005). Validation of the 53A6 GROMOS force field. *European Biophysics Journal*, 34(4), 273-284. <https://doi.org/10.1007/s00249-004-0448-6>
- Pancholi, S., Simigdala, N., Ribas, R., Schuster, E., Leal, M. F., Nikitorowicz-Buniak, J., Rega, C., Bihani, T., Patel, H., & Johnston, S. R. (2022). Elacestrant demonstrates strong anti-

- estrogenic activity in PDX models of estrogen-receptor positive endocrine-resistant and fulvestrant-resistant breast cancer. *NPJ Breast Cancer*, 8(1), 125. <https://doi.org/10.1038/s41523-022-00483-1>
- Pang, Y. P., Perola, E., Xu, K., & Prendergast, F. G. (2001). EUDOC: a computer program for identification of drug interaction sites in macromolecules and drug leads from chemical databases. *Journal of Computational Chemistry*, 22(15), 1750-1771. <https://doi.org/10.1002/jcc.1129>
- Panwar, S., Kumari, A., Kumar, H., Tiwari, A. K., Tripathi, P., & Asthana, S. (2022). Structure-based virtual screening, molecular dynamics simulation and in vitro evaluation to identify inhibitors against NAMPT. *Journal of Biomolecular Structure and Dynamics*, 40(20), 10332-10344. <https://doi.org/10.1080/07391102.2021.1943526>
- Panwar, U., Chandra, I., Selvaraj, C., & Singh, S. K. (2019). Current computational approaches for the development of anti-HIV inhibitors: an overview. *Current Pharmaceutical Design*, 25(31), 3390-3405. <https://doi.org/10.2174/1381612825666190911160244>
- Panwar, U., & Singh, S. K. (2021). Atom-based 3D-QSAR, molecular docking, DFT, and simulation studies of acylhydrazones, hydrazine, and diazene derivatives as IN-LEDGF/p75 inhibitors. *Structural Chemistry*, 32(1), 337-352. <https://doi.org/10.1007/s11224-020-01628-3>
- Parikesit, A. A., Ansori, A. N. M., & Kharisma, V. D. (2022). A computational design of siRNA in SARS-CoV-2 spike glycoprotein gene and its binding capability toward mRNA. *Indonesian Journal of Chemistry*, 22(5), 1163-1176. <https://doi.org/10.22146/ijc.68415>
- Pasi, M., Lavery, R., & Ceres, N. (2013). PaLaCe: A coarse-grain protein model for studying mechanical properties. *Journal of Chemical Theory and Computation*, 9(1), 785-793. <https://doi.org/10.1021/ct3007925>
- Patel, L., Shukla, T., Huang, X., Ussery, D. W., & Wang, S. (2020). Machine learning methods in drug discovery. *Molecules*, 25(22), 5277. <https://doi.org/10.3390/molecules25225277>
- Patel, V., & Shah, M. (2022). Artificial intelligence and machine learning in drug discovery and development. *Intelligent Medicine*, 2(3), 134-140. <https://doi.org/10.1016/j.imed.2021.10.001>
- Patell, K., Kurian, M., Garcia, J. A., Mendiratta, P., Barata, P. C., Jia, A. Y., Spratt, D. E., & Brown, J. R. (2023). Lutetium-177 PSMA for the treatment of metastatic castrate resistant

- prostate cancer: a systematic review. *Expert Review of Anticancer Therapy*, 23(7), 731-744. <https://doi.org/10.1080/14737140.2023.2213892>
- Pearlman, D. A., Case, D. A., Caldwell, J. W., Ross, W. S., Cheatham III, T. E., DeBolt, S., Ferguson, D., Seibel, G., & Kollman, P. (1995). AMBER, a package of computer programs for applying molecular mechanics, normal mode analysis, molecular dynamics and free energy calculations to simulate the structural and energetic properties of molecules. *Computer Physics Communications*, 91(1-3), 1-41. [https://doi.org/10.1016/0010-4655\(95\)00041-d](https://doi.org/10.1016/0010-4655(95)00041-d)
- Pei, J., Wang, Q., Liu, Z., Li, Q., Yang, K., & Lai, L. (2006). PSI-DOCK: Towards highly efficient and accurate flexible ligand docking. *Proteins: Structure, Function, and Bioinformatics*, 62(4), 934-946. <https://doi.org/10.1002/prot.20790>
- Pérez-Barcia, Á., Cárdenas, G., Nogueira, J. J., & Mandado, M. (2023). Effect of the QM Size, Basis Set, and Polarization on QM/MM Interaction Energy Decomposition Analysis. *Journal of Chemical Information and Modeling*, 63(3), 882-897. <https://doi.org/10.1021/acs.jcim.2c01184>
- Perola, E., Walters, W. P., & Charifson, P. S. (2004). A detailed comparison of current docking and scoring methods on systems of pharmaceutical relevance. *Proteins: Structure, Function, and Bioinformatics*, 56(2), 235-249. <https://doi.org/10.1002/prot.20088>
- Perurena, N., Situ, L., & Cichowski, K. (2024). Combinatorial strategies to target RAS-driven cancers. *Nature Reviews Cancer*, 24(5), 316-337. <https://doi.org/10.1038/s41568-024-00679-6>
- Pesapane, F., Mariano, L., Magnoni, F., Rotili, A., Puppo, D., Nicosia, L., Bozzini, A. C., Penco, S., Latronico, A., & Pizzamiglio, M. (2023). Future Directions in the Assessment of Axillary Lymph Nodes in Patients with Breast Cancer. *Medicina*, 59(9), 1544. <https://doi.org/10.3390/medicina59091544>
- Pierce, B. G., Wiehe, K., Hwang, H., Kim, B.-H., Vreven, T., & Weng, Z. (2014). ZDOCK server: interactive docking prediction of protein–protein complexes and symmetric multimers. *Bioinformatics*, 30(12), 1771-1773. <https://doi.org/10.1093/bioinformatics/btu097>
- Pinzi, L., Bisi, N., & Rastelli, G. (2024). How drug repurposing can advance drug discovery: challenges and opportunities. *Frontiers in Drug Discovery*, 4(1), 1460100. <https://doi.org/10.3389/fddsv.2024.1460100>

- Piscone, A., Gorini, F., Ambrosio, S., Noviello, A., Scala, G., Majello, B., & Amente, S. (2025). Targeting the 8-oxodG Base Excision Repair Pathway for Cancer Therapy. *Cells*, 14(2), 112. <https://doi.org/10.3390/cells14020112>
- Plazinska, A., & Plazinski, W. (2021). Comparison of carbohydrate force fields in molecular dynamics simulations of protein–carbohydrate complexes. *Journal of Chemical Theory and Computation*, 17(4), 2575-2585. <https://doi.org/10.1021/acs.jctc.1c00071>
- Pol-Fachin, L., Rusu, V. H., Verli, H., & Lins, R. D. (2012). GROMOS 53A6GLYC, an improved GROMOS force field for hexopyranose-based carbohydrates. *Journal of Chemical Theory and Computation*, 8(11), 4681-4690. <https://doi.org/10.1021/ct300479h>
- Pommier, Y., Sun, Y., Huang, S.-Y. N., & Nitiss, J. L. (2016). Roles of eukaryotic topoisomerases in transcription, replication and genomic stability. *Nature reviews Molecular Cell Biology*, 17(11), 703-721. <https://doi.org/10.1038/nrm.2016.111>
- Popovici, L.-F., Brinza, I., Gatea, F., Badea, G. I., Vamanu, E., Oancea, S., & Hritcu, L. (2025). Enhancement of Cognitive Benefits and Anti-Anxiety Effects of *Phytolacca americana* Fruits in a Zebrafish (*Danio rerio*) Model of Scopolamine-Induced Memory Impairment. *Antioxidants*, 14(1), 97. <https://doi.org/10.3390/antiox14010097>
- Poulopoulos, A., Papadopoulos, P., & Andreadis, D. (2017). Chemotherapy: oral side effects and dental interventions-a review of the literature. *Stomatological Disease and Science*, 1(1), 35-49. <http://dx.doi.org/10.20517/2573-0002.2017.03>
- Prieto-Martínez, F. D., López-López, E., Juárez-Mercado, K. E., & Medina-Franco, J. L. (2019). Computational drug design methods—current and future perspectives. *In Silico Drug Design*, 1(1), 19-44. <https://doi.org/10.1016/b978-0-12-816125-8.00002-x>
- Quertinmont, J., Carletta, A., Tumanov, N. A., Leyssens, T., Wouters, J., & Champagne, B. (2017). Assessing density functional theory approaches for predicting the structure and relative energy of salicylideneaniline molecular switches in the solid state. *The Journal of Physical Chemistry C*, 121(12), 6898-6908. <https://doi.org/10.1021/acs.jpcc.7b00580>
- Raabe, G. (2017). Molecular Models (Force Fields). *Molecular Simulation Studies on Thermophysical Properties* (pp. 145-189). Springer. [https://doi.org/10.1007/978-981-10-3545-6\\_6](https://doi.org/10.1007/978-981-10-3545-6_6)
- Raghavan, B., Paulikat, M., Ahmad, K., Callea, L., Rizzi, A., Ippoliti, E., Mandelli, D., Bonati, L., De Vivo, M., & Carloni, P. (2023). Drug design in the Exascale era: A perspective from

- massively parallel QM/MM simulations. *Journal of Chemical Information and Modeling*, 63(12), 3647-3658. <https://doi.org/10.1021/acs.jcim.3c00557>
- Rajee, A. O., Obaleye, J. A., Louis, H., Aliyu, A. A., Lawal, A., Chima, C. M., Ekereke, E. E., & Manicum, A.-L. E. (2023). Structural elucidation, DFT study, molecular docking, and biological studies of ruthenium polypyridyl mercaptopurine complexes. *Journal of the Iranian Chemical Society*, 20(9), 2383-2397. <https://doi.org/10.1007/s13738-023-02846-2>
- Rajkishan, T., Rachana, A., Shruti, S., Bhumi, P., & Patel, D. (2021). Computer-aided drug designing. *Advances in Bioinformatics*, 1(1), 151-182. [https://doi.org/10.1007/978-981-33-6191-1\\_9](https://doi.org/10.1007/978-981-33-6191-1_9)
- Rao, A. K., & Yadava, U. (2025). Computational insights into anti-Zika quinazoline compounds: Density functional theory analysis, spectral properties, and molecular dynamics simulations. *European Journal of Chemistry*, 16(2), 207-221. <https://doi.org/10.5155/eurjchem.16.2.207-221.2654>
- Raunio, H., Kuusisto, M., Juvonen, R. O., & Pentikäinen, O. T. (2015). Modeling of interactions between xenobiotics and cytochrome P450 (CYP) enzymes. *Frontiers in Pharmacology*, 6(1), 123. <https://doi.org/10.3389/fphar.2015.00123>
- Rees, A., Villamor, E., Evans, D., Goos, M., Fallon, C., Mina-Abouda, M., Disharoon, A., Eblen, S. T., & Delaney, J. R. (2025). Screening Methods to Discover the FDA-Approved Cancer Drug Encorafenib as Optimally Selective for Metallothionein Gene Loss Ovarian Cancer. *Genes*, 16(1), 42. <https://doi.org/10.3390/genes16010042>
- Ribeiro, R., Carvalho, M. J., Goncalves, J., & Moreira, J. N. (2022). Immunotherapy in triple-negative breast cancer: Insights into tumor immune landscape and therapeutic opportunities. *Frontiers in Molecular Biosciences*, 9(1), 903065. <https://doi.org/10.3389/fmolb.2022.903065>
- Rivera, M., Dommett, M., & Crespo-Otero, R. (2019). ONIOM (QM: QM') electrostatic embedding schemes for photochemistry in molecular crystals. *Journal of Chemical Theory and Computation*, 15(4), 2504-2516. <https://doi.org/10.1021/acs.jctc.8b01180>
- Riyadi, P. H., Sari, I. D., Kurniasih, R. A., Agustini, T. W., Swastawati, F., Herawati, V. E., & Tanod, W. A. (2021, October). SwissADME predictions of pharmacokinetics and drug-likeness properties of small molecules present in *Spirulina platensis*. In *IOP Conference*

*Series: Earth and Environmental Science* (Vol. 890, No. 1, p. 012021). IOP Publishing.

<https://doi.org/10.1088/1755-1315/890/1/012021>

- Rizzuti, B. (2022). Molecular simulations of proteins: From simplified physical interactions to complex biological phenomena. *Biochimica et Biophysica Acta (BBA)-Proteins and Proteomics*, 1870(3), 140757. <https://doi.org/10.1016/j.bbapap.2022.140757>
- Robertson, A., Klungland, A., Rognes, T., & Leiros, I. (2009). DNA repair in mammalian cells: Base excision repair: the long and short of it. *Cellular and Molecular Life Sciences*, 66(6), 981-993. <https://doi.org/10.1007/s00018-009-8736-z>
- Robin, T., Capes-Davis, A., & Bairoch, A. (2020). CLASTR: the Cellosaurus STR similarity search tool-a precious help for cell line authentication. *International Journal of Cancer*, 146(5), 1299-1306. <https://doi.org/10.1002/ijc.32639>
- Rodríguez-Gascón, A., Solinís, M. Á., & Isla, A. (2021). The role of PK/PD analysis in the development and evaluation of antimicrobials. *Pharmaceutics*, 13(6), 833. <https://doi.org/10.3390/pharmaceutics13060833>
- Roy, S., Kumar, A., Islam, M. S., Rabbi, F. A., Paul, P., Mia, M. M., Islam, A., & Ray, A. K. (2020). Drug resistance and its future perspectives in cancer treatment. *Asian Oncology Research Journal*, 3(1), 26-46. [https://www.researchgate.net/profile/Partha-Paul-13/publication/342335332\\_Drug\\_Resistance\\_and\\_Its\\_Future\\_Perspectives\\_in\\_Cancer\\_Treatment/links/5ef49843299bf15a2ea0a704/Drug-Resistance-and-Its-Future-Perspectives-in-Cancer-Treatment.pdf](https://www.researchgate.net/profile/Partha-Paul-13/publication/342335332_Drug_Resistance_and_Its_Future_Perspectives_in_Cancer_Treatment/links/5ef49843299bf15a2ea0a704/Drug-Resistance-and-Its-Future-Perspectives-in-Cancer-Treatment.pdf)
- Rudrapal, M., de Oliveira, A. M., de Abreu, H. A., Rakshit, G., Tripathi, M. K., & Khan, J. (2025). Anti-Inflammatory and Antioxidant Potential of Plant-Derived Phenolic Acids as Triple COX, LOX, and NOX Inhibitors: A Computational Approach. *Chemistry & Biodiversity*, 1(1), e03505. <https://doi.org/10.1002/cbdv.202403505>
- Rustagi, V., Gupta, S. R., Singh, A., & Singh, I. K. (2025). Beyond trial and error: Leveraging advanced software for Therapeutic discovery. *Chemical Biology Letters*, 12(1), 1251-1251. <https://doi.org/10.62110/sciencein.cbl.2025.v12.1251>
- Saadh, M. J., Mustafa, M. A., Kumar, S., Gupta, P., Pramanik, A., Rizaev, J. A., Shareef, H. K., Alubiady, M. H. S., Al-Abdeen, S. H. Z., & Shakier, H. G. (2024). Advancing therapeutic efficacy: nanovesicular delivery systems for medicinal plant-based therapeutics. *Naunyn-*

- Schmiedeberg's Archives of Pharmacology*, 397(10), 7229-7254.  
<https://doi.org/10.1007/s00210-024-03104-9>
- Sabe, V. T., Ntombela, T., Jhamba, L. A., Maguire, G. E., Govender, T., Naicker, T., & Kruger, H. G. (2021). Current trends in computer aided drug design and a highlight of drugs discovered via computational techniques: A review. *European Journal of Medicinal Chemistry*, 224(1), 113705. <https://doi.org/10.1016/j.ejmech.2021.113705>
- Sael, L., & Kihara, D. (2012). Detecting local ligand-binding site similarity in nonhomologous proteins by surface patch comparison. *Proteins: Structure, Function, and Bioinformatics*, 80(4), 1177-1195. <https://doi.org/10.1002/prot.24018>
- Sajid, H., & Addicoat, M. A. (2023). Computational insights of dimensional organic materials. *Covalent Materials and Hybrids: From 0D to 3D*, 1(1), 382-473. <https://doi.org/10.1039/9781839169656-00382>
- Salo-Ahen, O. M., Alanko, I., Bhadane, R., Bonvin, A. M., Honorato, R. V., Hossain, S., Juffer, A. H., Kbedev, A., Lahtela-Kakkonen, M., & Larsen, A. S. (2020). Molecular dynamics simulations in drug discovery and pharmaceutical development. *Processes*, 9(1), 71. <https://doi.org/10.3390/pr9010071>
- Santos, L. H., Ferreira, R. S., & Caffarena, E. R. (2019). Integrating molecular docking and molecular dynamics simulations. *Docking Screens for Drug Discovery*, 1(1), 13-34. [https://doi.org/10.1007/978-1-4939-9752-7\\_2](https://doi.org/10.1007/978-1-4939-9752-7_2)
- Sartor, O., De Bono, J., Chi, K. N., Fizazi, K., Herrmann, K., Rahbar, K., Tagawa, S. T., Nordquist, L. T., Vaishampayan, N., & El-Haddad, G. (2021). Lutetium-177–PSMA-617 for metastatic castration-resistant prostate cancer. *New England Journal of Medicine*, 385(12), 1091-1103. <https://doi.org/10.1056/nejmoa2107322>
- Sati, P., Sharma, E., Dhyani, P., Attri, D. C., Rana, R., Kiyekbayeva, L., Büsselberg, D., Samuel, S. M., & Sharifi-Rad, J. (2024). Paclitaxel and its semi-synthetic derivatives: comprehensive insights into chemical structure, mechanisms of action, and anticancer properties. *European Journal of Medical Research*, 29(1), 90. <https://doi.org/10.1186/s40001-024-01657-2>
- Sato, K., & Hamada, M. (2023). Recent trends in RNA informatics: a review of machine learning and deep learning for RNA secondary structure prediction and RNA drug discovery. *Briefings in Bioinformatics*, 24(4), bbad186. <https://doi.org/10.1093/bib/bbad186>

- Saura, P., Röpke, M., Gamiz-Hernandez, A. P., & Kaila, V. R. (2019). Quantum Chemical and QM/MM Models in Biochemistry. In *Biomolecular Simulations: Methods and Protocols* (pp. 75-104). New York, NY: Springer New York. [https://doi.org/10.1007/978-1-4939-9608-7\\_4](https://doi.org/10.1007/978-1-4939-9608-7_4)
- Sauton, N., Lagorce, D., Villoutreix, B. O., & Miteva, M. A. (2008). MS-DOCK: accurate multiple conformation generator and rigid docking protocol for multi-step virtual ligand screening. *BMC Bioinformatics*, 9(1), 1-12. <https://doi.org/10.1186/1471-2105-9-184>
- Schaduangrat, N., Lampa, S., Simeon, S., Gleeson, M. P., Spjuth, O., & Nantasenamat, C. (2020). Towards reproducible computational drug discovery. *Journal of Cheminformatics*, 12(1), 1-30. <https://doi.org/10.1186/s13321-020-0408-x>
- Schaefer-Klein, J., Murphy, S. J., Johnson, S. H., Vasmatzis, G., & Kovtun, I. V. (2015). Topoisomerase 2 alpha cooperates with androgen receptor to contribute to prostate cancer progression. *PLoS one*, 10(11), e0142327. <https://doi.org/10.1371/journal.pone.0142327>
- Schlenkrich, M., Brickmann, J., MacKerell Jr, A. D., & Karplus, M. (1996). An empirical potential energy function for phospholipids: criteria for parameter optimization and applications. In *Biological membranes: A Molecular Perspective from Computation And Experiment* (pp. 31-81). Springer. [https://doi.org/10.1007/978-1-4684-8580-6\\_2](https://doi.org/10.1007/978-1-4684-8580-6_2)
- Schneider, P., Walters, W. P., Plowright, A. T., Sieroka, N., Listgarten, J., Goodnow Jr, R. A., Fisher, J., Jansen, J. M., Duca, J. S., & Rush, T. S. (2020). Rethinking drug design in the artificial intelligence era. *Nature Reviews Drug Discovery*, 19(5), 353-364. . <https://doi.org/10.1038/s41573-019-0050-3>
- Schwaller, P., Hoover, B., Reymond, J.-L., Strobel, H., & Laino, T. (2021). Extraction of organic chemistry grammar from unsupervised learning of chemical reactions. *Science Advances*, 7(15), eabe4166. <https://doi.org/10.1126/sciadv.abe4166>
- Schwinn, K., Ferré, N., & Huix-Rotllant, M. (2020). Efficient analytic second derivative of electrostatic embedding QM/MM energy: Normal mode analysis of plant cryptochrome. *Journal of Chemical Theory and Computation*, 16(6), 3816-3824. <https://doi.org/10.1021/acs.jctc.9b01145>
- Sehrawat, R., Pasrija, R., Rathee, P., Kumari, D., Khatkar, A., Kúpeli Akkol, E., & Sobarzo-Sánchez, E. (2024). Hybrid caffeic acid-based DHFR inhibitors as novel antimicrobial and anticancer agents. *Antibiotics*, 13(6), 479. <https://doi.org/10.3390/antibiotics13060479>

- Sehrawat, R., Rathee, P., Rathee, P., Khatkar, S., Akkol, E. K., Khatkar, A., & Sobarzo-Sánchez, E. (2023). In silico design of novel bioactive molecules to treat breast cancer with chlorogenic acid derivatives: a computational and SAR approach. *Frontiers in Pharmacology*, *14*(1), 1266833. <https://doi.org/10.3389/fphar.2023.1266833>
- Seifert, M. H., Schmitt, F., Herz, T., & Kramer, B. (2004). ProPose: a docking engine based on a fully configurable protein–ligand interaction model. *Journal of Molecular Modeling*, *10*(5-6), 342-357. <https://doi.org/10.1007/s00894-004-0201-1>
- Shah, A., Parmar, G., Shah, U., & Perumal, S. (2023). Virtual screening, molecular docking studies and DFT calculations of novel anticancer flavonoids as potential VEGFR-2 inhibitors. *Chemistry Africa*, *6*(4), 1847-1861. <https://doi.org/10.1007/s42250-023-00611-9>
- Shah, F., Logsdon, D., Messmann, R. A., Fehrenbacher, J. C., Fishel, M. L., & Kelley, M. R. (2017). Exploiting the Ref-1-APE1 node in cancer signaling and other diseases: from bench to clinic. *NPJ Precision Oncology*, *1*(1), 19. <https://doi.org/10.1038/s41698-017-0023-0>
- Shaker, B., Ahmad, S., Lee, J., Jung, C., & Na, D. (2021). In silico methods and tools for drug discovery. *Computers in Biology and Medicine*, *137*(1), 104851. <https://doi.org/10.1016/j.combiomed.2021.104851>
- Sharma, H., Raju, B., Narendra, G., Motiwale, M., Sharma, B., Verma, H., & Silakari, O. (2023). QM/MM studies on enzyme catalysis and insight into designing of new inhibitors by ONIOM approach: Recent update. *ChemistrySelect*, *8*(1), e202203319. <https://doi.org/10.1002/slct.202203319>
- Sharma, M., Bakshi, A. K., Mittapelly, N., Gautam, S., Marwaha, D., Rai, N., Singh, N., Tiwari, P., Agarwal, N., & Kumar, A. (2022). Recent updates on innovative approaches to overcome drug resistance for better outcomes in cancer. *Journal of Controlled Release*, *346*(1), 43-70. <https://doi.org/10.1016/j.jconrel.2022.04.007>
- Sharma, S., Sharma, A., & Gupta, U. (2021). Molecular Docking studies on the Anti-fungal activity of *Allium sativum* (Garlic) against Mucormycosis (black fungus) by BIOVIA discovery studio visualizer 21.1. 0.0. *Annals of Antivirals and Antiretrovirals*, *5*(1), 028-032. <https://doi.org/10.17352/aaa.000013>
- Shatsky, R. A., Trivedi, M. S., Yau, C., Nanda, R., Rugo, H. S., Davidian, M., Tsiatis, B., Wallace, A. M., Chien, A. J., & Stringer-Reasor, E. (2024). Datopotamab–deruxtecan plus durvalumab in early-stage breast cancer: the sequential multiple assignment randomized I-

- SPY2. 2 phase 2 trial. *Nature Medicine*, 30(12), 3737-3747. <https://doi.org/10.1038/s41591-024-03267-1>
- Shen, G., Zhao, F., Huo, X., Ren, D., Du, F., Zheng, F., & Zhao, J. (2021). Meta-analysis of HER2-enriched subtype predicting the pathological complete response within HER2-positive breast cancer in patients who received neoadjuvant treatment. *Frontiers in Oncology*, 11(1), 632357. <https://doi.org/10.3389/fonc.2021.632357>
- Sheridan, R. P., Feuston, B. P., Maiorov, V. N., & Kearsley, S. K. (2004). Similarity to molecules in the training set is a good discriminator for prediction accuracy in QSAR. *Journal of Chemical Information and Computer Sciences*, 44(6), 1912-1928. <https://doi.org/10.1021/ci049782w>
- Shukla, R., & Tripathi, T. (2021). Molecular dynamics simulation in drug discovery: opportunities and challenges. *Innovations and Implementations of Computer Aided Drug Discovery Strategies in Rational Drug Design*, 1(1), 295-316. [https://doi.org/10.1007/978-981-15-8936-2\\_12](https://doi.org/10.1007/978-981-15-8936-2_12)
- Siani, P., de Souza, R., Dias, L., Itri, R., & Khandelia, H. (2016). An overview of molecular dynamics simulations of oxidized lipid systems, with a comparison of ELBA and MARTINI force fields for coarse grained lipid simulations. *Biochimica et Biophysica Acta (BBA)-Biomembranes*, 1858(10), 2498-2511. <https://doi.org/10.1016/j.bbamem.2016.03.031>
- Šicho, M., Stork, C., Mazzolari, A., de Bruyn Kops, C., Pedretti, A., Testa, B., Vistoli, G., Svozil, D., & Kirchmair, J. (2019). FAME 3: predicting the sites of metabolism in synthetic compounds and natural products for phase 1 and phase 2 metabolic enzymes. *Journal of Chemical Information and Modeling*, 59(8), 3400-3412. <https://doi.org/10.1021/acs.jcim.9b00376>
- Siddiqui, B., Yadav, C. S., Akil, M., Faiyyaz, M., Khan, A. R., Ahmad, N., Hassan, F., Azad, M. I., Owais, M., & Nasibullah, M. (2025). Artificial intelligence in computer-aided drug design (cadd) tools for the finding of potent biologically active small molecules: Traditional to modern approach. *Combinatorial Chemistry & High Throughput Screening*, 28(1), 1-50. <https://doi.org/10.2174/0113862073334062241015043343>
- Singh, K., Gupta, J. K., Chanchal, D. K., Shinde, M. G., Kumar, S., Jain, D., Almarhoon, Z. M., Alshahrani, A. M., Calina, D., & Sharifi-Rad, J. (2025). Natural products as drug leads:

- Exploring their potential in drug discovery and development. *Naunyn-Schmiedeberg's Archives of Pharmacology*, 398(5), 4673-4687. <https://doi.org/10.1007/s00210-024-03622-6>
- Singh, D. B., & Pathak, R. K. (2020). Computational approaches in drug designing and their applications. *Experimental Protocols in Biotechnology*, 1(1) 95-117. [https://doi.org/10.1007/978-1-0716-0607-0\\_6](https://doi.org/10.1007/978-1-0716-0607-0_6)
- Singh, S., Baker, Q. B., & Singh, D. B. (2022). Molecular docking and molecular dynamics simulation. In *Bioinformatics* (pp. 291-304). Elsevier. <https://doi.org/10.1016/b978-0-323-89775-4.00014-6>
- Sohlenius-Sternbeck, A.-K., & Terelius, Y. (2022). Evaluation of ADMET predictor in early discovery drug metabolism and pharmacokinetics project work. *Drug Metabolism and Disposition*, 50(2), 95-104. <https://doi.org/10.1124/dmd.121.000552>
- Solovy, E. M. (2021). The Doha Declaration at Twenty: Interpretation, Implementation, and Lessons Learned on the Relationship Between the TRIPS Agreement and Global Health. *SSRN Electronic Journal*, 42(1), 253. <https://doi.org/10.2139/ssrn.3965053>
- Son, B., Lee, W., Kim, H., Shin, H., & Park, H. H. (2024). Targeted therapy of cancer stem cells: inhibition of mTOR in pre-clinical and clinical research. *Cell Death & Disease*, 15(9), 696. <https://doi.org/10.1038/s41419-024-07077-8>
- Sonawane, K. D., & Dhanavade, M. J. (2017). Computational approaches to understand cleavage mechanism of amyloid beta (A $\beta$ ) peptide. *Neuromethods*, 1(1), 263-282. [https://doi.org/10.1007/978-1-4939-7404-7\\_11](https://doi.org/10.1007/978-1-4939-7404-7_11)
- Sorooshian, S. (2024). The Sustainable Development Goals of the United Nations: A Comparative Midterm Research Review. *Journal of Cleaner production*, 453(1), 142272. <https://doi.org/10.1016/j.jclepro.2024.142272>
- Sousa da Silva, A. W., & Vranken, W. F. (2012). ACPYPE-Antechamber python parser interface. *BMC Research Notes*, 5(1), 367. <https://doi.org/10.1186/1756-0500-5-367>
- Sousa, S. F., Ribeiro, A. J., Neves, R. P., Brás, N. F., Cerqueira, N. M., Fernandes, P. A., & Ramos, M. J. (2017). Application of quantum mechanics/molecular mechanics methods in the study of enzymatic reaction mechanisms. *Wiley Interdisciplinary Reviews: Computational Molecular Science*, 7(2), e1281. <https://doi.org/10.1002/wcms.1281>

- Sriharikrishnaa, S., Suresh, P. S., & Prasada K, S. (2023). An Introduction to Fundamentals of Cancer Biology. In *Optical Polarimetric Modalities for Biomedical Research* (pp. 307-330). Springer. [https://doi.org/10.1007/978-3-031-31852-8\\_11](https://doi.org/10.1007/978-3-031-31852-8_11)
- Srivastava, R. (2021). Theoretical studies on the molecular properties, toxicity, and biological efficacy of 21 new chemical entities. *ACS Omega*, 6(38), 24891-24901. <https://doi.org/10.1021/acsomega.1c03736>
- Stanzione, F., Giangreco, I., & Cole, J. C. (2021). Use of molecular docking computational tools in drug discovery. *Progress in Medicinal Chemistry*, 60(1), 273-343. <https://doi.org/10.1016/bs.pmch.2021.01.004>
- Starke, G., & Ienca, M. (2022). Misplaced trust and distrust: how not to engage with medical artificial intelligence. *Cambridge Quarterly of Healthcare Ethics*, 33(3), 360-369. <https://doi.org/10.1017/s0963180122000445>
- Steinmann, C., & Jensen, J. H. (2021). Using a genetic algorithm to find molecules with good docking scores. *PeerJ Physical Chemistry*, 3(1), e18. <https://doi.org/10.7717/peerj-pchem.18>
- Sun, Y., Feng, Y., Zhang, G., & Xu, Y. (2019). The endonuclease APE1 processes miR-92b formation, thereby regulating expression of the tumor suppressor LDLR in cervical cancer cells. *Therapeutic Advances in Medical Oncology*, 11(1), 1758835919855859. <https://doi.org/10.1177/1758835919855859>
- Sung, W. W., Sharma, K., Chan, A. W., Al Khaifi, M., Oldenburger, E., & Chuk, E. (2024). undefined. *Annals of Palliative Medicine*, 13(6), 1521-1529. <https://doi.org/10.21037/apm-24-90>. <https://doi.org/10.21037/apm-24-90>
- Surana, K. R., Ahire, E. D., Sonawane, V. N., & Talele, S. G. (2021). Biomolecular and molecular docking: A modern tool in drug discovery and virtual screening of natural products. *Applied Pharmaceutical Practice and Nutraceuticals*, 1(1), 209-223. <https://doi.org/10.1201/9781003054894-14>
- Swapna, K., Srujana, M., & Mamidala, E. (2024). Identification of steroidal cardenolides from *Calotropis procera* as novel HIV-1 PR inhibitors: A molecular docking & molecular dynamics simulation study. *The Indian Journal of Medical Research*, 160(1), 78. [https://doi.org/10.25259/ijmr\\_2115\\_23](https://doi.org/10.25259/ijmr_2115_23)

- Swedan, H. K., Kassab, A. E., Gedawy, E. M., & Elmeligie, S. E. (2023). Topoisomerase II inhibitors design: Early studies and new perspectives. *Bioorganic Chemistry*, 136(1), 106548. <https://doi.org/10.1016/j.bioorg.2023.106548>
- Sztuba-Solinska, J., Chavez-Calvillo, G., & Cline, S. E. (2019). Unveiling the druggable RNA targets and small molecule therapeutics. *Bioorganic & Medicinal Chemistry*, 27(10), 2149-2165. <https://doi.org/10.1016/j.bmc.2019.03.057>
- Taldaev, A., Terekhov, R., Nikitin, I., Zhevlakova, A., & Selivanova, I. (2022). Insights into the pharmacological effects of flavonoids: the systematic review of computer modeling. *International Journal of Molecular Sciences*, 23(11), 6023. <https://doi.org/10.3390/ijms23116023>
- Tandon, H., Chakraborty, T., & Suhag, V. (2019). A brief review on importance of DFT in drug design. *Research in Medical Engineering & Science*, 7(4), 791-795. [https://www.researchgate.net/profile/Hiteshi-Tandon/publication/333245146\\_A\\_Brief\\_Review\\_on\\_Importance\\_of\\_DFT\\_In\\_Drug\\_Design/links/5e677e4792851c7ce057940a/A-Brief-Review-on-Importance-of-DFT-In-Drug-Design.pdf](https://www.researchgate.net/profile/Hiteshi-Tandon/publication/333245146_A_Brief_Review_on_Importance_of_DFT_In_Drug_Design/links/5e677e4792851c7ce057940a/A-Brief-Review-on-Importance-of-DFT-In-Drug-Design.pdf)
- Tang, J., & Zhao, X. (2024). Research progress on regulation of immune response by tanshinones and salvianolic acids of danshen (*Salvia miltiorrhiza* Bunge). *Molecules*, 29(6), 1201. <https://doi.org/10.3390/molecules29061201>
- Taylor, J. S., & Burnett, R. M. (2000). DARWIN: a program for docking flexible molecules. *Proteins: Structure, Function, and Bioinformatics*, 41(2), 173-191. [https://doi.org/10.1002/1097-0134\(20001101\)41:2<173::aid-prot30>3.3.co;2-v](https://doi.org/10.1002/1097-0134(20001101)41:2<173::aid-prot30>3.3.co;2-v)
- Taylor, R. D., Jewsbury, P. J., & Essex, J. W. (2003). FDS: flexible ligand and receptor docking with a continuum solvent model and soft-core energy function. *Journal of Computational Chemistry*, 24(13), 1637-1656. <https://doi.org/10.1002/jcc.10295>
- Tessaro, F., & Scapozza, L. (2020). How 'protein-docking' translates into the new emerging field of docking small molecules to nucleic acids? *Molecules*, 25(12), 2749. <https://doi.org/10.3390/molecules25122749>
- Thomas, A., & Pommier, Y. (2019). Targeting topoisomerase I in the era of precision medicine. *Clinical Cancer Research*, 25(22), 6581-6589. <https://doi.org/10.1158/1078-0432.ccr-19-1089>

- Thumma, G., Veerareddy, P. R., & Kiran, G. (2025). Computational tools employed in Chemoinformatics. *Applications of Computational Tools in Drug Design and Development*, 1(1), 311-330. [https://doi.org/10.1007/978-981-96-4154-3\\_9](https://doi.org/10.1007/978-981-96-4154-3_9)
- Tian, C., Kasavajhala, K., Belfon, K. A., Raguette, L., Huang, H., Miguez, A. N., Bickel, J., Wang, Y., Pincay, J., & Wu, Q. (2019). ff19SB: Amino-acid-specific protein backbone parameters trained against quantum mechanics energy surfaces in solution. *Journal of Chemical Theory and Computation*, 16(1), 528-552. <https://doi.org/10.1021/acs.jctc.9b00591>
- Tian, S., Cao, X., Greiner, R., Li, C., Guo, A., & Wishart, D. S. (2021). CyProduct: a software tool for accurately predicting the byproducts of human cytochrome P450 metabolism. *Journal of Chemical Information and Modeling*, 61(6), 3128-3140. <https://doi.org/10.1021/acs.jcim.1c00144>
- Tietze, S., & Apostolakis, J. (2007). GlamDock: Development and validation of a new docking tool on several thousand protein– ligand complexes. *Journal of Chemical Information and Modeling*, 47(4), 1657-1672. <https://doi.org/10.1021/ci7001236>
- Torres, P. H., Sodero, A. C., Jofily, P., & Silva-Jr, F. P. (2019). Key topics in molecular docking for drug design. *International Journal of Molecular Sciences*, 20(18), 4574. <https://doi.org/10.3390/ijms20184574>
- Totrov, M., & Abagyan, R. (1997). Flexible protein–ligand docking by global energy optimization in internal coordinates. *Proteins: Structure, Function, and Bioinformatics*, 29(S1), 215-220. [https://doi.org/10.1002/\(sici\)1097-0134\(1997\)1+<215::aid-prot29>3.3.co;2-i](https://doi.org/10.1002/(sici)1097-0134(1997)1+<215::aid-prot29>3.3.co;2-i)
- Tran, T. T. V., Tayara, H., & Chong, K. T. (2023). Artificial intelligence in drug metabolism and excretion prediction: recent advances, challenges, and future perspectives. *Pharmaceutics*, 15(4), 1260. <https://doi.org/10.3390/pharmaceutics15041260>
- Tribello, G. A., Bonomi, M., Branduardi, D., Camilloni, C., & Bussi, G. (2014). PLUMED 2: New feathers for an old bird. *Computer Physics Communications*, 185(2), 604-613. <https://doi.org/10.1016/j.cpc.2013.09.018>
- Trosset, J. Y., & Scheraga, H. A. (1999). PRODOCK: software package for protein modeling and docking. *Journal of Computational Chemistry*, 20(4), 412-427. [https://doi.org/10.1002/\(sici\)1096-987x\(199903\)20:4<412::aid-jcc3>3.0.co;2-n](https://doi.org/10.1002/(sici)1096-987x(199903)20:4<412::aid-jcc3>3.0.co;2-n)

- Tuttle, T. (2012). Quantum Mechanical/Molecular Mechanical Approaches in Drug Design. *Drug Design Strategies Computational Techniques and Applications*, 1(1), 1-26. <https://doi.org/10.1039/9781849733403-00001>
- Umare, M., A. Alkathiri, F., & Chikhale, R. (2023). Development of Nucleic Acid Targeting Molecules: Molecular Docking Approaches and Recent Advances. *IntechOpen*, 1(1), 107349. <https://doi.org/10.5772/intechopen.107349>
- Uusitalo, J. J., Ingólfsson, H. I., Akhshi, P., Tieleman, D. P., & Marrink, S. J. (2015). Martini coarse-grained force field: extension to DNA. *Journal of Chemical Theory and Computation*, 11(8), 3932-3945. <https://doi.org/10.1021/acs.jctc.5b00286>
- Valeska, M. D., & Parikesit, A. A. (2022). Determination of 3D structure and molecular interaction for mir-135b and its silencer as Triple Negative Breast Cancer (TNBC) biomarkers. *Berkala Penelitian Hayati*, 28(1), 62-66. <https://doi.org/10.23869/bphjbr.28.1.202210>
- Valodara, A. M., & SR, K. J. (2019). Sexual dimorphism in drug metabolism and pharmacokinetics. *Current Drug Metabolism*, 20(14), 1154-1166. <https://doi.org/10.2174/1389200220666191021094906>
- van der Kolk, M. R., Janssen, M. A., Rutjes, F. P., & Blanco-Ania, D. (2022). Cyclobutanes in small-molecule drug candidates. *ChemMedChem*, 17(9), e202200020. <https://doi.org/10.1002/cmdc.202200020>
- Van Der Spoel, D., Lindahl, E., Hess, B., Groenhof, G., Mark, A. E., & Berendsen, H. J. (2005). GROMACS: Fast, flexible, and free. *Journal of Computational Chemistry*, 26(16), 1701-1718. <https://doi.org/10.1002/jcc.20291>
- Van Gisbergen, S., Snijders, J., & Baerends, E. (1999). Implementation of time-dependent density functional response equations. *Computer Physics Communications*, 118(2-3), 119-138. [https://doi.org/10.1016/s0010-4655\(99\)00187-3](https://doi.org/10.1016/s0010-4655(99)00187-3)
- Vandana, N., & Rani, D. J. (2024). In silico characterisation and structural modelling of PCNA associated factor I65a by I-TASSER. *AIP Conference Proceedings*, 3097(1), 020109. <https://doi.org/10.1063/5.0197749>
- Vander Meersche, Y., Cretin, G., Gheeraert, A., Gelly, J.-C., & Galochkina, T. (2024). ATLAS: protein flexibility description from atomistic molecular dynamics simulations. *Nucleic Acids Research*, 52(D1), D384-D392. <https://doi.org/10.1093/nar/gkad1084>

- Vanderbeeken, M.-C., Aftimos, P. G., & Awada, A. (2013). Topoisomerase inhibitors in metastatic breast cancer: overview of current practice and future development. *Current Breast Cancer Reports*, 5(1), 31-41. <https://doi.org/10.1007/s12609-012-0098-0>
- Vanneman, M., & Dranoff, G. (2012). Combining immunotherapy and targeted therapies in cancer treatment. *Nature Reviews Cancer*, 12(4), 237-251. <https://doi.org/10.1038/nrc3237>
- Vediappan, P., Arumugam, M., & Natarajan, R. (2025). In-silico Design, ADMET Screening, Prime MM-GBSA Binding Free Energy Calculation and MD Simulation of Some Novel Phenothiazines as 5HT6R Antagonists Targeting Alzheimer's Disease. *Current Computer-Aided Drug Design*, 21(4), 487-502. <https://doi.org/10.2174/0115734099282836231212064925>
- Vemula, D., Jayasurya, P., Sushmitha, V., Kumar, Y. N., & Bhandari, V. (2023). CADD, AI and ML in drug discovery: A comprehensive review. *European Journal of Pharmaceutical Sciences*, 181(1), 106324. <https://doi.org/10.1016/j.ejps.2022.106324>
- Venkatachalam, C. M., Jiang, X., Oldfield, T., & Waldman, M. (2003). LigandFit: a novel method for the shape-directed rapid docking of ligands to protein active sites. *Journal of Molecular Graphics and Modelling*, 21(4), 289-307. [https://doi.org/10.1016/s1093-3263\(02\)00164-x](https://doi.org/10.1016/s1093-3263(02)00164-x)
- Venkatraman, V. (2021). FP-ADMET: a compendium of fingerprint-based ADMET prediction models. *Journal of Cheminformatics*, 13(1), 1-12. <https://doi.org/10.1186/s13321-021-00557-5>
- Vennelakanti, V., Nazemi, A., Mehmood, R., Steeves, A. H., & Kulik, H. J. (2022). Harder, better, faster, stronger: Large-scale QM and QM/MM for predictive modeling in enzymes and proteins. *Current Opinion in Structural Biology*, 72(1), 9-17. <https://doi.org/10.1016/j.sbi.2021.07.004>
- Verma, S., & Pathak, R. K. (2022). Discovery and optimization of lead molecules in drug designing. *Bioinformatics*, 1(1), 253-267. <https://doi.org/10.1016/b978-0-323-89775-4.00004-3>
- Vermeeren, P., van der Lubbe, S. C., Fonseca Guerra, C., Bickelhaupt, F. M., & Hamlin, T. A. (2020). Understanding chemical reactivity using the activation strain model. *Nature Protocols*, 15(2), 649-667. <https://doi.org/10.1038/s41596-019-0265-0>

- Vijayan, R., Kihlberg, J., Cross, J. B., & Poongavanam, V. (2022). Enhancing preclinical drug discovery with artificial intelligence. *Drug Discovery Today*, 27(4), 967-984. <https://doi.org/10.1016/j.drudis.2021.11.023>
- Vitali, E., Ficarelli, F., Bisson, M., Gadioli, D., Accordi, G., Fatica, M., Beccari, A. R., & Palermo, G. (2024). GPU-optimized approaches to molecular docking-based virtual screening in drug discovery: A comparative analysis. *Journal of Parallel and Distributed Computing*, 186(1), 104819. <https://doi.org/10.1016/j.jpdc.2023.104819>
- Walters, W. P. (2012). Going further than Lipinski's rule in drug design. *Expert Opinion on Drug Discovery*, 7(2), 99-107. <https://doi.org/10.1517/17460441.2012.648612>
- Wang, Sun, H., Wang, J., Wang, Z., Liu, H., Zhang, J. Z., & Hou, T. (2019). End-point binding free energy calculation with MM/PBSA and MM/GBSA: strategies and applications in drug design. *Chemical Reviews*, 119(16), 9478-9508. <https://doi.org/10.1021/acs.chemrev.9b00055>
- Wang, J., Wolf, R. M., Caldwell, J. W., Kollman, P. A., & Case, D. A. (2004). Development and testing of a general amber force field. *Journal of Computational Chemistry*, 25(9), 1157-1174. <https://doi.org/10.1002/jcc.20035>
- Wang, J., & Wu, S.-G. (2023). Breast cancer: an overview of current therapeutic strategies, challenge, and perspectives. *Breast Cancer: Targets and Therapy*, 15(1), 721-730. <https://doi.org/10.2147/BCTT.S432526>
- Wang, L., Chambers, J., & Abel, R. (2019). Protein–ligand binding free energy calculations with FEP+. *Biomolecular Simulations: Methods and Protocols*, 1(1), 201-232. [https://doi.org/10.1007/978-1-4939-9608-7\\_9](https://doi.org/10.1007/978-1-4939-9608-7_9)
- Wang, L., Song, Y., Wang, H., Zhang, X., Wang, M., He, J., Li, S., Zhang, L., Li, K., & Cao, L. (2023). Advances of Artificial Intelligence in Anti-Cancer Drug Design: A Review of the Past Decade. *Pharmaceuticals*, 16(2), 253. <https://doi.org/10.3390/ph16020253>
- Wang, S., Ballard, T. E., Christopher, L. J., Foti, R. S., Gu, C., Khojasteh, S. C., Liu, J., Ma, S., Ma, B., & Obach, R. S. (2023). The Importance of Tracking “Missing” Metabolites: How and Why? *Journal of Medicinal Chemistry*, 66(23), 15586-15612. <https://doi.org/10.1021/acs.jmedchem.3c01293>
- Wang, W., Wang, S., Liu, Y., Wang, X., Nie, J., Meng, X., & Zhang, Y. (2022). Ellagic acid: a dietary-derived phenolic compound for drug discovery in mild cognitive impairment.

- Frontiers in Aging Neuroscience*, 14(1), 925855.  
<https://doi.org/10.3389/fnagi.2022.925855>
- Wang, Z., Sun, H., Yao, X., Li, D., Xu, L., Li, Y., Tian, S., & Hou, T. (2016). Comprehensive evaluation of ten docking programs on a diverse set of protein–ligand complexes: the prediction accuracy of sampling power and scoring power. *Physical Chemistry Chemical Physics*, 18(18), 12964-12975. <https://doi.org/10.1039/c6cp01555g>
- Wang, Z., Sun, X., Sun, M., Wang, C., & Yang, L. (2025). Game Changers: Blockbuster Small-Molecule Drugs Approved by the FDA in 2024. *Pharmaceuticals*, 18(5), 729. <https://doi.org/10.3390/ph18050729>
- Weatherman, R. (2016). The role of selective estrogen receptor destabilizers (SERDs) in breast cancer therapy. *Drugs of the Future*, 41(6), 0361. <https://doi.org/10.1358/dof.2016.041.06.2482681>
- Welch, W., Ruppert, J., & Jain, A. N. (1996). Hammerhead: fast, fully automated docking of flexible ligands to protein binding sites. *Chemistry & Biology*, 3(6), 449-462. [https://doi.org/10.1016/s1074-5521\(96\)90093-9](https://doi.org/10.1016/s1074-5521(96)90093-9)
- Williamson, E. M. (2017). Herbal neurotoxicity: An introduction to its occurrence and causes. *Toxicology of Herbal Products*, 1(1), 345-362. [https://doi.org/10.1007/978-3-319-43806-1\\_14](https://doi.org/10.1007/978-3-319-43806-1_14)
- Wimmelbücker, L., & Kar, A. (2023). A history of thalidomide in India. *Medical History*, 67(3), 228-246. <https://doi.org/10.1017/mdh.2023.27>
- Wu, F., Zhou, Y., Li, L., Shen, X., Chen, G., Wang, X., Liang, X., Tan, M., & Huang, Z. (2020). Computational approaches in preclinical studies on drug discovery and development. *Frontiers in Chemistry*, 8(1), 726. <https://doi.org/10.3389/fchem.2020.00726>
- Xi, Y., & Xu, P. (2021). Global colorectal cancer burden in 2020 and projections to 2040. *Translational Oncology*, 14(10), 101174. <https://doi.org/10.1016/j.tranon.2021.101174>
- Xia, Y., Sun, M., Huang, H., & Jin, W.-L. (2024). Drug repurposing for cancer therapy. *Signal Transduction and Targeted Therapy*, 9(1), 92. <https://doi.org/10.1038/s41392-024-01808-1>
- Xiao, Z., Liu, W., Mu, Y.-p., Zhang, H., Wang, X.-n., Zhao, C.-q., Chen, J.-m., & Liu, P. (2020). Pharmacological effects of salvianolic acid B against oxidative damage. *Frontiers in Pharmacology*, 11(1), 572373. <https://doi.org/10.3389/fphar.2020.572373>

- Xing, B., Qiu, L., Wang, Z., Wang, F., Yu, H., Li, W., Li, Y., Abozeid, A., Xia, P., Zhang, L., Shao, Q., Zhang, S., Liang, Z., & Yang, D. (2025). A novel synergistic regulatory mechanism involving the MYB39-MYB111-bHLH51-TTG1 module in the phenolic and diterpenoid biosynthetic pathways of *Salvia miltiorrhiza*. *Plant Biotechnology Journal*, 23(10), 4367-4380. <https://doi.org/10.1111/pbi.70241>
- Xiong, X., Zheng, L.-W., Ding, Y., Chen, Y.-F., Cai, Y.-W., Wang, L.-P., Huang, L., Liu, C.-C., Shao, Z.-M., & Yu, K.-D. (2025). Breast cancer: pathogenesis and treatments. *Signal Transduction and Targeted Therapy*, 10(1), 49. <https://doi.org/10.1038/s41392-024-02108-4>
- Xu, M., Han, X., Xiong, H., Gao, Y., Xu, B., Zhu, G., & Li, J. (2023). Cancer nanomedicine: emerging strategies and therapeutic potentials. *Molecules*, 28(13), 5145. <https://doi.org/10.3390/molecules28135145>
- Xu, P., Guidez, E. B., Bertoni, C., & Gordon, M. S. (2018). Perspective: Ab initio force field methods derived from quantum mechanics. *The Journal of Chemical Physics*, 148(9), 090901. <https://doi.org/10.1063/1.5009551>
- Yadav, J., El Hassani, M., Sodhi, J., Lauschke, V. M., Hartman, J. H., & Russell, L. E. (2021). Recent developments in in vitro and in vivo models for improved translation of preclinical pharmacokinetics and pharmacodynamics data. *Drug Metabolism Reviews*, 53(2), 207-233. <https://doi.org/10.1080/03602532.2021.1922435>
- Yadav, R., Imran, M., Dhamija, P., Chaurasia, D. K., & Handu, S. (2021). Virtual screening, ADMET prediction and dynamics simulation of potential compounds targeting the main protease of SARS-CoV-2. *Journal of Biomolecular Structure and Dynamics*, 39(17), 6617-6632. <https://doi.org/10.1080/07391102.2020.1796812>
- Yadav, R. K., Panta, S., KC, S., Jha, P. K., Poudel, S., Upadhyaya, S. R., Subedi, K., Baral, S., Bhandari, R., & Pandey, B. (2025). LC-MS Analysis and Evaluation of Antioxidant and Antibacterial Activities of *Falconeria insignis* Royle from Nepal: An In Vitro/In Silico Approach. *Natural Product Communications*, 20(5), 1934578X251340467. <https://doi.org/10.1177/1934578X251340467>
- Yadava, U., Yadav, V. K., & Yadav, R. K. (2017). Novel anti-tubulin agents from plant and marine origins: insight from a molecular modeling and dynamics study. *Rsc Advances*, 7(26), 15917-15925. <https://doi.org/10.1039/C7RA00370F>

- Yang, F., He, Q., Dai, X., Zhang, X., & Song, D. (2023). The potential role of nanomedicine in the treatment of breast cancer to overcome the obstacles of current therapies. *Frontiers in Pharmacology*, *14*(1), 1143102. <https://doi.org/10.3389/fphar.2023.1143102>
- Ye, N., Yang, Z., & Liu, Y. (2022). Applications of density functional theory in COVID-19 drug modeling. *Drug Discovery Today*, *27*(5), 1411-1419. <https://doi.org/10.1016/j.drudis.2021.12.017>
- Yee, C. W., Harvey, M. J., Xin, Y., & Kirson, N. Y. (2024). Cost-effectiveness modeling of prostate-specific membrane antigen positron emission tomography with Piflufolastat F 18 for the initial diagnosis of patients with prostate cancer in the United States. *Pharmacoeconomics*, *42*(2), 231-247. <https://doi.org/10.1007/s40273-023-01322-2>
- Younas, S., Malik, Z. I., Khan, M. U., Manzoor, S., Rehman, H. M., Hammad, H. M., & Akter, S. (2025). Identification of novel therapeutic inhibitors against E6 and E7 oncogenes of HPV-16 associated with cervical cancer. *BioRxiv*, *1*(1), 2025-04. <https://doi.org/10.1101/2025.04.13.648624>
- Yu, J., Mu, Q., Fung, M., Xu, X., Zhu, L., & Ho, R. J. (2022). Challenges and opportunities in metastatic breast cancer treatments: Nano-drug combinations delivered preferentially to metastatic cells may enhance therapeutic response. *Pharmacology & Therapeutics*, *236*(1), 108108. <https://doi.org/10.1016/j.pharmthera.2022.108108>
- Yu, K.-D., Ye, F.-G., He, M., Fan, L., Ma, D., Mo, M., Wu, J., Liu, G.-Y., Di, G.-H., & Zeng, X.-H. (2020). Effect of adjuvant paclitaxel and carboplatin on survival in women with triple-negative breast cancer: a phase 3 randomized clinical trial. *Journal of the American Medical Association Oncology*, *6*(9), 1390-1396. <https://doi.org/10.1001/jamaoncol.2020.2965>
- Yu, Y., Rüppel, D., Weber, W., & Derendorf, H. (2019). PK/PD Approaches. In *Drug discovery and evaluation: Methods in clinical pharmacology* (pp. 1-23). Springer, Cham. [https://doi.org/10.1007/978-3-319-56637-5\\_26-2](https://doi.org/10.1007/978-3-319-56637-5_26-2)
- Yuan, Y., Pei, J., & Lai, L. (2013). Binding site detection and druggability prediction of protein targets for structure-based drug design. *Current Pharmaceutical Design*, *19*(12), 2326-2333. <https://doi.org/10.2174/1381612811319120019>

- Yusef Buey, M., Mineva, T., & Rapacioli, M. (2022). Coupling density functional based tight binding with class 1 force fields in a hybrid QM/MM scheme. *Theoretical Chemistry Accounts*, 141(3), 16. <https://doi.org/10.1007/s00214-022-02878-6>
- Zafar, A., Khatoun, S., Khan, M. J., Abu, J., & Naeem, A. (2025). Advancements and limitations in traditional anti-cancer therapies: a comprehensive review of surgery, chemotherapy, radiation therapy, and hormonal therapy. *Discover Oncology*, 16(1), 607. <https://doi.org/10.1007/s12672-025-02198-8>
- Zerfas, B. L., Maresh, M. E., & Trader, D. J. (2019). The immunoproteasome: an emerging target in cancer and autoimmune and neurological disorders. *Journal of Medicinal Chemistry*, 63(5), 1841-1858. <https://doi.org/10.1021/acs.jmedchem.9b01226>
- Zhang, H., Kim, S., Giese, T. J., Lee, T.-S., Lee, J., York, D. M., & Im, W. (2021). CHARMM-GUI free energy calculator for practical ligand binding free energy simulations with AMBER. *Journal of Chemical Information and Modeling*, 61(9), 4145-4151. <https://doi.org/10.1021/acs.jcim.1c00747>
- Zhang, H., Wang, Z., Ren, J., Liu, J., & Li, J. (2021). Ultra-fast and accurate binding energy prediction of shuttle effect-suppressive sulfur hosts for lithium-sulfur batteries using machine learning. *Energy Storage Materials*, 35(1), 88-98. <https://doi.org/10.1016/j.ensm.2020.11.009>
- Zhang, W., & Zhang, K. (2023). Quantifying the contributions of environmental factors to prostate cancer and detecting risk-related diet metrics and racial disparities. *Cancer Informatics*, 22(1), 11769351231168006. <https://doi.org/10.1177/11769351231168006>
- Zhang, X., Shen, C., Zhang, H., Kang, Y., Hsieh, C.-Y., & Hou, T. (2024). Advancing Ligand Docking through Deep Learning: Challenges and Prospects in Virtual Screening. *Accounts of Chemical Research*, 57(10), 1500-1509. <https://doi.org/10.1021/acs.accounts.4c00093>
- Zhang, Y., Cui, H., Zhang, R., Zhang, H., & Huang, W. (2021). Nanoparticulation of prodrug into medicines for cancer therapy. *Advanced Science*, 8(18), 2101454. <https://doi.org/10.1002/advs.202101454>
- Zhang, Y., Zhai, W., Fan, M., Wu, J., & Wang, C. (2024). Salvianolic Acid B Significantly Suppresses the Migration of Melanoma Cells via Direct Interaction with  $\beta$ -Actin. *Molecules*, 29(4), 906. <https://doi.org/10.3390/molecules29040906>

- Zhao, J., Zhang, C., Wang, W., Li, C., Mu, X., & Hu, K. (2022). Current progress of nanomedicine for prostate cancer diagnosis and treatment. *Biomedicine and Pharmacotherapy*, 155(1), 113714. <https://doi.org/10.3390/molecules29040906>
- Zhao, M., Ma, J., Li, M., Zhang, Y., Jiang, B., Zhao, X., Huai, C., Shen, L., Zhang, N., & He, L. (2021). Cytochrome P450 enzymes and drug metabolism in humans. *International Journal of Molecular Sciences*, 22(23), 12808. <https://doi.org/10.3390/ijms222312808>
- Zhou, Z., & Li, M. (2022). Targeted therapies for cancer. *BMC medicine*, 20(1), 90. <https://doi.org/10.1186/s12916-022-02287-3>
- Zhu, R., Vora, B., Menon, S., Younis, I., Dwivedi, G., Meng, Z., Datta-Mannan, A., Manchandani, P., Nayak, S., & Tammara, B. K. (2023). Clinical Pharmacology Applications of Real-World Data and Real-World Evidence in Drug Development and Approval—An Industry Perspective. *Clinical Pharmacology and Therapeutics*, 114(4), 751-767. <https://doi.org/10.1002/cpt.2988>
- Zothantluanga, J. H., Umar, A. K., Ali Eltayb, W., Patowary, L., Borthakur, M. S., Tayeng, D., & Chetia, D. (2024). An In-Silico Investigation on the Molecular Interactions between Ellagic Acid and Pf DHFR-TS. *Polycyclic Aromatic Compounds*, 44(6), 4081-4102. <https://doi.org/10.1080/10406638.2023.2244633>

## APPENDICES

**Appendix A:** Copyright of paper published in the journal of discover public health

**Article DOI:** <https://doi.org/10.1186/s12982-024-00229-3>

**Paper Title:** A review of the current trends in computational approaches in drug design and metabolism

**Authors:** Russel B.O Ouma, Silas M. Ngari, Joshua K. Kibet

### **Rights and permissions**

**Open Access** This article is licensed under a Creative Commons Attribution-Non-commercial-No Derivatives 4.0 International License, which permits any non-commercial use, sharing, distribution and reproduction in any medium or format, as long as you give appropriate credit to the original author(s) and the source, provide a link to the Creative Commons licence, and indicate if you modified the licensed material. You do not have permission under this licence to share adapted material derived from this article or parts of it. The images or other third-party material in this article are included in the article's Creative Commons licence, unless indicated otherwise in a credit line to the material. If material is not included in the article's Creative Commons licence and your intended use is not permitted by statutory regulation or exceeds the permitted use, you will need to obtain permission directly from the copyright holder. To view a copy of this licence, visit <http://creativecommons.org/licenses/by-nc-nd/4.0/>.

## Discover Public Health

---

Review

### A review of the current trends in computational approaches in drug design and metabolism

Russell B. O. Ouma<sup>1</sup> · Silas M. Ngarl<sup>1</sup> · Joshua K. Kibet<sup>1</sup>

Received: 17 May 2024 / Accepted: 17 September 2024

Published online: 27 September 2024

© The Author(s) 2024 [OPEN](#)

#### Abstract

Computer-aided drug design and discovery methods have been essential in developing small molecules with therapeutic properties over the last decades. Application of computational resources includes drug target identification, hit discovery, and lead optimization. Accordingly, with tremendous research efforts and the availability of financial support from government agencies across the world, and multinational drug companies, the overall research level in this area will continue to advance. The methodology used in this review paper entailed a thorough examination of research studies on relevant literature on drug design and development using computational resources. Extensive searches using Scopus, International Pharmaceutical Abstracts (OvidSp), WHO Global Health Library, Cochrane, Google Scholar, Web of Science, Science Direct, ProQuest dissertation & theses, Worldwide Political Science Abstracts (CSA), and PubMed was carried out. A standardized template was used to ensure that the selected papers met the inclusion criteria, and relevant to the review. Ultimately, there are robust technologies developed to enhance the drug discovery process. Therefore, this review provides insights into computational resources in Silico and ab initio methods and algorithms, not restricted to drug metabolism predictions for drug design, and the practical applications of artificial intelligence (AI) in drug discovery. Computational tools and methods for drug design and development such as molecular dynamics (MD), molecular docking, quantum mechanics (QM), hybrid quantum mechanics/molecular mechanics (QM/MM), and Density functional theory (DFT) have been reviewed. Accordingly, the emerging technique of synergistically employing these techniques influences the fundamental challenges of conventional medicines for complex diseases. Herein, we discuss ligand-based and structure-based drug discoveries, force field models in MD simulations, docking algorithms, subtractive and additive QM/MM coupling. Nonetheless, as computer-aided drug (CADD) approaches continue to evolve with significant improvements, the focus areas will be on docking and virtual screening, scoring functions, optimization of hits, and assessment of adsorption, distribution, metabolism, excretion, and toxicity (ADMET) properties. With the current success, the present computational resources will aid in the future discovery of novel compounds with high therapeutic performance. The ongoing oncology research efforts will also significantly contribute to UN sustainable development goals – good health and well-being, sustainable innovation and industrialization.

**Keywords** Hit discovery · Lead optimization · Molecular dynamics · Docking algorithms · Therapeutic effects · ADMET

**Appendix C: Supplementary information on excretion and toxicity profile of EA**

<b>Property</b>	<b>Model name</b>	<b>Predicted value</b>	<b>Unit</b>
Excretion	Total Clearance	0.537	Numeric (log ml/min/kg)
Excretion	Renal OCT2 substrate	No	Categorical (Yes/No)
Toxicity	AMES toxicity	No	Categorical (Yes/No)
Toxicity	Max. tolerated dose (human)	0.476	Numeric (log mg/kg/day)
Toxicity	hERG I inhibitor	No	Categorical (Yes/No)
Toxicity	hERG II inhibitor	No	Categorical (Yes/No)
Toxicity	Oral Rat Acute Toxicity (LD50)	2.399	Numeric (mol/kg)
Toxicity	Oral Rat Chronic Toxicity (LOAEL)	2.698	Numeric (log mg/kg_bw/day)
Toxicity	Hepatotoxicity	No	Categorical (Yes/No)
Toxicity	Skin Sensitisation	No	Categorical (Yes/No)
Toxicity	<i>T. Pyriformis</i> toxicity	0.295	Numeric (log ug/L)
Toxicity	Minnow toxicity	2.11	Numeric (log mM)

**Appendix D:** Supplementary information on excretion and toxicity profile of phorbol dibutyrate

<b>Property</b>	<b>Model name</b>	<b>Predicted value</b>	<b>Unit</b>
Excretion	Total Clearance	0.611	Numeric (log ml/min/kg)
Excretion	Renal OCT2 substrate	No	Categorical (Yes/No)
Toxicity	AMES toxicity	No	Categorical (Yes/No)
Toxicity	Max. tolerated dose (human)	-0.758	Numeric (log mg/kg/day)
Toxicity	hERG I inhibitor	No	Categorical (Yes/No)
Toxicity	hERG II inhibitor	No	Categorical (Yes/No)
Toxicity	Oral Rat Acute Toxicity (LD50)	3.063	Numeric (mol/kg)
Toxicity	Oral Rat Chronic Toxicity (LOAEL)	1.804	Numeric (log mg/kg_bw/day)
Toxicity	Hepatotoxicity	No	Categorical (Yes/No)
Toxicity	Skin Sensitisation	No	Categorical (Yes/No)
Toxicity	<i>T. Pyriformis</i> toxicity	0.296	Numeric (log ug/L)
Toxicity	Minnow toxicity	3.485	Numeric (log mM)

**Appendix E:** Supplementary information on excretion and toxicity profile of 12 deoxy-phorbol 13-isobutyrate

<b>Property</b>	<b>Model name</b>	<b>Predicted value</b>	<b>Unit</b>
Excretion	Total Clearance	0.494	Numeric (log ml/min/kg)
Excretion	Renal OCT2 substrate	No	Categorical (Yes/No)
Toxicity	AMES toxicity	No	Categorical (Yes/No)
Toxicity	Max. tolerated dose (human)	-0.169	Numeric (log mg/kg/day)
Toxicity	hERG I inhibitor	No	Categorical (Yes/No)
Toxicity	hERG II inhibitor	No	Categorical (Yes/No)
Toxicity	Oral Rat Acute Toxicity (LD50)	2.819	Numeric (mol/kg)
Toxicity	Oral Rat Chronic Toxicity (LOAEL)	2.055	Numeric (log mg/kg_bw/day)
Toxicity	Hepatotoxicity	No	Categorical (Yes/No)
Toxicity	Skin Sensitisation	No	Categorical (Yes/No)
Toxicity	<i>T. Pyriformis</i> toxicity	0.326	Numeric (log ug/L)
Toxicity	Minnow toxicity	2.717	Numeric (log mM)

**Appendix F:** Supplementary information on one-way ANOVA on  $\log_{10}(\text{IC}_{50})$  within each cell line and Dunnett vs control

(Docetaxel is the control for PC-3/DU145; doxorubicin for MCF-7/MDA-MB-231)

Cell line	ANOVA FF (df <sub>1</sub> , df <sub>2</sub> )	p (overall)	$\eta^2$	Dunnett p-adj vs control (Salvianolic / Ellagic / 12- deoxy-phorbol 13-isobutyrate / phorbol dibutyrate)
PC-3	196.2 (4,10)	$2.1 \times 10^{-9}$	0.987	0.009 / $3.1 \times 10^{-5}$ / $2.2 \times 10^{-7}$ / $1.0 \times 10^{-8}$
DU145	182.0 (4,10)	$4.8 \times 10^{-9}$	0.986	0.011 / $2.9 \times 10^{-5}$ / $1.6 \times 10^{-7}$ / $8.0 \times 10^{-9}$
MCF-7	205.3 (4,10)	$1.3 \times 10^{-9}$	0.988	0.004 / $1.2 \times 10^{-5}$ / $4.0 \times 10^{-7}$ / $9.0 \times 10^{-9}$
MDA-MB-231	217.1 (4,10)	$9.0 \times 10^{-10}$	0.989	0.006 / $1.0 \times 10^{-5}$ / $3.0 \times 10^{-7}$ / $6.0 \times 10^{-9}$

**Appendix G:** Supplementary information on selected Tukey all-pairs comparisons among test compounds (p-adj)

All four ANOVAs remained significant after Benjamini–Hochberg correction (FDR = 0.05)

<b>Pair (PC-3)</b>	<b>p-adj</b>
Salvianolic vs Ellagic	0.012
Salvianolic vs 12 deoxy-phorbol 13-isobutyrate	$2.0 \times 10^{-5}$
Salvianolic vs phorbol dibutyrate	$< 1 \times 10^{-7}$
Ellagic vs 12 deoxy-phorbol 13-isobutyrate	$1.0 \times 10^{-4}$
Ellagic vs phorbol dibutyrate	$< 1 \times 10^{-7}$
12 deoxy-phorbol 13-isobutyrate vs phorbol dibutyrate	0.004



**Appendix I: Certificate of training in drug design and molecular docking**

